RESEARCH & DEVELOPMENT

Quantifying Corrosive Potential of De-Icing and Anti-Icing Solutions on Bridge Components

Brett Tempest, PhD, Principal Investigator
Matthew Whelan, PhD, Key Researcher
Papa Kwesi Prah-Ennin, Graduate Research Assistant
Thanh-Tu Diep, Graduate Research Assistant

Department of Civil and Environmental Engineering
University of North Carolina at Charlotte
9201 University City Boulevard
Charlotte, NC 28223

NCDOT Project 2012-08

FHWA/NC/2012-08

December 2014

North Carolina Department of Transportation
Research Project No. FHWA/NC/2012-08

Quantifying Corrosive Potential of De-Icing and Anti-Icing Solutions on Bridge Components

Final Report

Brett Tempest
Principal Investigator

Matthew Whelan
Key Researcher

Papa Kwesi Prah-Ennin
Graduate Research Assistant

Thanh-Tu Diep
Graduate Research Assistant

Department of Civil and Environmental Engineering
University of North Carolina at Charlotte
9201 University City Boulevard
Charlotte, NC 28223

December 16, 2014

Technical Report Documentation Page

1. Report No. FHWA/NC/2012-08	2. Government Accession No.	3. Recipient's Catalog No.
4. Title and Subtitle Quantifying Corrosive Potential of De-Icing and Anti-Icing Solutions on Bridge Components		5. Report Date December 16, 2014
		6. Performing Organization Code
7. Author(s) Brett Tempest, Matthew Whelan, Papa Kwesi Prah-Ennin, Thanh-Tu Diep		8. Performing Organization Report No.
9. Performing Organization Name and Address The University of North Carolina at Charlotte Department of Civil and Environmental Engineering 9201 University City Blvd Charlotte, NC 28223		10. Work Unit No. (TRAIS)
		11. Contract or Grant No.
12. Sponsoring Agency Name and Address North Carolina Department of Transportation Research and Analysis Group 1 South Wilmington Street Raleigh, North Carolina 27601		13. Type of Report and Period Covered Final Report August 15, 2011-December 31, 2013
		14. Sponsoring Agency Code 2012-08
Supplementary Notes:		

16. Abstract

The three predominant anti-icing and de-icing strategies used in North Carolina are application of sodium chloride in brine form, granular form or as granules mixed with traction enhancing materials. While each of these has its own unique optimal usage for maintaining road safety, there are undetermined consequences associated with the different applications regarding chloride initiated corrosion. This study made an evaluation of the relative impact of each deicing treatment on the ingress of chlorides into concrete surfaces and effect on the corrosion rates of both reinforcing steel and exposed structural steel members. The study included the investigation of a variety of structural surfaces both above and below the deck, including the slab, girder ends, pier caps, guard rails, and barrier walls. An extensive laboratory study employing ASTM and SHRP standardized test methods examined steel corrosion under various concentrations of surface chloride and the ingress rates of chlorides into concrete exposed to each treatment method. Field measurements of the distribution and fluctuation of chloride surface concentrations on bridge components over time were made using a mobile x-ray fluorescence spectrometer. These in-situ measurements were correlated with the laboratory measurements to validate experimental assumptions, determine time-dependent exposure rates specific to the application method, and predict the relative corrosive influence associated with each treatment.

17. Key Words Anti-icing, Deicing, Snow removal, Chlorides, Corrosion,	18. Distribution Statement		
19. Security Classif. (of this report) Unclassified	20. Security Classif. (of this page) Unclassified	21. No. of Pages 195	22. Price

Form DOT F 1700.7 (8-72) **Reproduction of completed page authorized**

DISCLAIMER

The contents of this report reflect the views of the authors and not necessarily the views of the University. The authors are responsible for the facts and the accuracy of the data presented herein. The contents do not necessarily reflect the official views or policies of either the North Carolina Department of Transportation or the Federal Highway Administration at the time of publication. This report does not constitute a standard, specification, or regulation.

ACKNOWLEDGMENTS

The authors would like to thank the members of the Technical Advisory Committee, chaired by Emily McGraw, for their assistance and guidance throughout the project. Also, many thanks to all the NCDOT personnel who directed traffic, operated equipment, recorded data, loaned supplies, responded to questions and entirely made the field component of this project possible.

EXECUTIVE SUMMARY

The three predominant anti-icing and deicing strategies used in North Carolina are application of sodium chloride in brine form, granular form or as granules mixed with traction enhancing materials. While each of these has its own unique optimal usage for maintaining road safety, there are undetermined consequences associated with the different applications with respect to chloride initiated corrosion. This study was undertaken to evaluate the relative impact of each deicing treatment on the ingress of chlorides into concrete surfaces and relative effect on the corrosion rates of both reinforcing steel and exposed structural steel members. The study included investigating how a variety of structural surfaces both above and below the deck, including the slab, girder ends, pier caps, guard rails, and barrier walls are affected by exposure to deicing agents. This was done by evaluating the effectiveness of paints and epoxies used to coat steel components, and the level of exposure experienced by various bridge components. The effectiveness of the deicers was also evaluated by monitoring their concentration on bridge components after application and by measuring their relative thaw rates when applied to ice.

The results showed several important trends that may influence maintenance decisions. After applying the treatments on bridge decks, the average initial surface concentrations associated with the various treatment methods were 14.08% for brine, 11.95% for granular salt, and 5.07% for salt-sand mix. At the application rates often used for ice clearance in NC, the granular salt application showed the greatest ice melting capacity in lab testing. In the field, the granular salt treatment was found to spread to the girders after precipitation events. The brine treatments remained on the deck and did not cause an increase in chlorides on the girder surfaces.

All paint or epoxy coatings tested were effective at protecting steel coupons immersed in chloride solution from corrosion damage and showed negligible weight loss from corrosion during the study. Galvanized coupons underwent some loss of the sacrificial galvanization coating but corrosion did not reach the depth of the substrate material. Coupons that were coated and then damaged by a scratch and exposed to the chloride solution illustrated some differences in the coating performance. Undercutting and progress of corrosion was found to be most significant in epoxy coated specimens. Undercutting was less pronounced in painted specimens and not present in galvanized specimens.

The freezing, thawing and drying cycles simulated in the lab created a transport regimen that was more aggressive than static exposure. Concrete samples having intermittent exposure to salts, water and freezing conditions achieved higher concentrations of chlorides at depth relative to the surface concentration than the control specimens that were continually ponded with 3% solution. Thus, brine treatments applied to dry pavement may lead to increased chloride ingress. The normalized increase (concentration increase per documented treatment) in chloride concentration was greatest in Asheville. This indicates that climate, traffic and other environmental conditions in Asheville have a greater effect on the corrosive potential of road salts to reinforced concrete than the treatment method alone. Statistical analysis of the measured changes in chloride concentration with other external factors, such as bridge age and ADT, revealed that the influence of the treatment type may be statistically less significant than other functional and environmental factors.

TABLE OF CONTENTS

Appendicies

LIST OF FIGURES

LIST OF TABLES

1 Introduction

The three predominant anti-icing and de-icing strategies used in North Carolina are application of sodium chloride in brine form, granular form or as granules mixed with traction enhancing materials. While each of these has its own unique optimal usage for maintaining road safety, there are undetermined consequences associated with the different applications with respect to chloride initiated corrosion. Salt brine application has been favored in recent years as an economic and effective pretreatment to prevent ice formation. However, there is significant concern that application of salt solutions in the liquid form has accelerated the rate of corrosion of structural bridge elements. It is widely suspected that this difference from prior treatment strategies arises from an initially greater solution concentration and an increased tendency for the brine to remain on the surface longer than granular salts, which are more prone to dispersion from traffic action and weather.

This study was undertaken to evaluate the relative impact of each deicing treatment on the ingress of chlorides into concrete surfaces and relative effect on the corrosion rates of both reinforcing steel and exposed structural steel members. The study included investigating a variety of structural surfaces both above and below the deck, including the slab, girder ends, pier caps, guard rails, and barrier walls. Different initial transport mechanisms associated with the individual application methods, as well as associated susceptibility to removal and dispersion processes from traffic and weather effects, influence the spatial distribution and concentration of the salt over time. Consequently, the relationship of surface concentration over time for each application strategy largely dictates the rate of corrosion and chloride ingress across structural surfaces. Furthermore, the time-dependency of the surface concentration influences the freeze point and thaw rates, which may in turn influence the relative corrosive effect associated with the treatment method. To examine this concentration dependence, a matrix of laboratory tests was performed alongside field measurement of surface chloride concentrations following application in response to local winter events. The team studied the relative impacts of deicing methods as a series of four tasks. Some of these tasks included laboratory methods as well as field verification. The tasks are described below along with a summary of methodology:

TASK I: Quantify corrosive effect of anti-icing and ice removal materials on concrete and steel components

Concrete Components- An accelerated testing method was designed to incorporate freeze-thaw-flush cycling with intermittent application of brine, granular salt, or salt/sand mix. Temperature cycling conditions and clear water flushing mimicked typical winter conditions of temperature, rain, and humidity. The build-up of chloride concentrations at the surface and at a depth of ½” were measured after 490 cycles using the rapid chloride test. The results of this test quantify the rate of chloride transport into the concrete matrix for each of the three application methods.

Steel Components- Laboratory steel coupons were exposed to various concentrations of chloride containing solution and the corrosive action was quantified by weight loss in the specimens. The range of steel grades considered reflected their application in the NC bridge inventory and were selected with help from NCDOT personnel. The test method outlined in SHRP-H Technique 207.5 “Test Method for Evaluation of Corrosive Effects of Deicing Chemicals on Metals” formed the basis of the protocol used by the UNCC research team. The results of the test provided a quantitative analysis of corrosion rates and material loss due to corrosion.

TASK II: Compare the corrosive effects between granular salt, salt/sand and salt brine

Since the corrosive agent, sodium chloride, is the same in each of the three treatments, any differences in corrosive effects must necessarily be related to differences in initial application concentrations, spatial distributions, and residual temporal characteristics.

Field Method:

The field study component of this project was intended to provide information regarding the level of exposure of various bridge components to deicing salt as well as the temporal variation in surface concentration following dispersion by traffic and dilution from precipitation. Two field study strategies were employed. In the first, a controlled application of road salt was made to a bridge during cold months, but not during an actual winter weather event. A second strategy involved taking pre-season and post-season surface chloride concentration measurements. The bridges used in the study were selected with assistance from NCDOT personnel to ensure that the study group included an informative range of materials and joint condition, as well as provided safe access to the following components of interest:

1) Concrete decks without asphalt overlay near joints and in gutter areas
2) Vertical, above deck concrete surfaces such as barrier walls
3) Above deck steel components such as guard rails
4) Below deck superstructure including pier caps and girder ends

Controlled Salt Application and Monitoring

A set of adjacent bridges was selected in the Charlotte area in order to facilitate simultaneous observation of surface chloride concentrations after exposure to similar traffic loading and weather conditions. The team visited the bridges in early March 2012 to clean the test areas take initial surface concentration measurements. NCDOT maintenance personnel then applied salt brine to one of the bridges and granular salt and salt-sand mix to the other bridge. The research team measured the initial surface concentration on the components listed above in the period immediately following application and then visited the bridges at one day intervals for until the surface concentration again reached background levels. The residual surface concentration from each bridge was related to measured precipitation, ADT records, and salt application techniques.

Pre-Season and Post-Season Measurements

Nine bridges were selected in the Triad (Greensboro area) and Mountain (Asheville area) regions. Prior to the beginning of the salting season the bridges were visited and the chloride concentration of select components was measured with a mobile XRF device. Additionally, concrete powder samples were removed from the deck and pier caps for chloride content testing. During the inclement weather season, the research team monitored precipitation (using readily available National Weather Service reports) and road maintenance personnel tracked the number of deicing salt applications. At the end of the season, the research team returned to the bridges to measure the surface chloride concentrations, and remove additional powder samples. Concentration measurements from before and after the winter season were compared with weather data and salt application records to estimate yearly build-up.

Lab Method:

A laboratory study employing ASTM and SHRP standardized test methods examined steel corrosion under various concentrations of surface chloride and the ingress rates of chlorides into concrete exposed to each treatment method. Field measurements of the distribution and fluctuation of chloride surface concentrations on bridge components over time were made using an advanced mobile x-ray fluorescence spectrometer. These in-situ measurements were correlated with the laboratory measurements to validate experimental assumptions, determine time-dependent exposure rates specific to the application method, and assess the relative corrosive influence associated with each treatment. Following the laboratory and field studies, parametric inputs specific to each application method were devised from the measured data to permit development of analytical models for corrosive action, with which comparison of the relative impacts of each treatment are assessed for generalized cases encompassing multiple susceptible structural elements and materials.

TASK III: Compare the rate of thawing of granular salt, salt/sand and salt brine

Lab Method: The capacity of granular treatments and brine to melt ice was measured using the method described in SHRP H-205.1, “Test Method for Ice Melting of Solid Deicing Chemicals,” and SHRP H205.2, “Test Method for Ice Melting of Liquid Deicing Chemicals.” Data from these tests was used to compare the relative effectiveness of each method at clearing ice from the roadway.

TASK IV: Compare the freeze point of granular salt, salt/sand and salt brine

Lab Method: The freezing points of solutions having various concentrations of deicing materials were determined by the method described in ASTM D1177, “Standard Test Method for Freezing Point of Aqueous Engine Coolants.” This method has been used to evaluate the freezing point of deicing chemicals by other state departments of transportation.

Field Method: Since all applications are sodium chloride treatments, the associated freeze point is entirely dependent only on the mass concentration of sodium chloride as dictated by the phase diagram for sodium chloride. The field measurements provide a means of quantifying the relationship between the freeze point and relative corrosive effect of each treatment method through characterizing the solution concentrations over time on structural surfaces.

The results of this study provide information to NCDOT officials regarding the relative performance of deicing and anti-icing treatments as well as the performance of bridge materials that are exposed to the treatments. It is hoped that maintenance policy decisions might be informed by the results presented in this report. However, some potential conclusions may require more in-depth research and observation in the field to accurately represent the corrosive potential of winter maintenance alternatives.

This report includes a section of background information and literature review, followed by a description of the test methods used to accomplish the tasks described above and the results of the experiments. The report also includes summary of the analyses and recommendations for implementation and further study.

2 Background

2.1 Deicers Used in North Carolina

In North Carolina, the predominant deicing and anti-icing agent is sodium chloride due to its relative abundance and low cost. In different areas of the State and at different times in the winter storm preparedness and response cycle, sodium chloride is applied as either as brine solution with 23% concentration, in granular form, or mixed with traction materials. Sodium chloride is known to initiate and accelerate corrosion reactions in steel reinforcing bars as well as structural and non-structural bridge components. Application of deicing and anti-icing solutions is targeted to the bridge deck and curbs, however other nearby concrete components, such as piers and parapets, and steel components, such as girders, floor beams, and rails may be vulnerable to chloride attack due to transport of the treatment solutions through traffic dispersion and environmental effects. Furthermore, there is anecdotal evidence to suggest that the transport mechanisms for granular salt, salt-sand mixtures, and brine solutions vary. Consequently, the exposure and vulnerability of various bridge components (e.g., decks, beams, diaphragms, abutments, piers and piles) are expected to vary based on both the component type and the treatment method used. To date, limited, if any, experimental work has been undertaken to directly measure the spatial and temporal characteristics of deicing chemical exposure in order to focus on those bridges or components at greatest risk (Shi, Liu et al. 2010). Since the impact of the different treatments on the maintenance-free lifecycle of the bridge has not been well understood, assessing the relative corrosive effects of the three treatment methods is a key component of the current study.

Essentially all treatments used in North Carolina are sodium chloride based, so the effect of each treatment method on the initiation of corrosion is reasoned to be directly linked to the corresponding spatial and temporal characteristics of the chloride concentration on the various bridge component surfaces. A primary difference between each treatment method is suspected to be the duration of time that these surface concentrations remain significantly elevated. For granular salt, salt-sand mixes, and brine applications, there are also expected to be significant differences in surface transport mechanisms and a time-temperature dependency that will influence the ingress rate of chlorides into concrete and duration of exposure of the steel surfaces to corrosive elements. The uniform application of salt brine generally leads to increased effective coverage compared granular salt. Furthermore, salt brine is more resistant to removal by traffic action and therefore has a greater tendency to remain on the bridge surface at elevated concentrations for an extended period of time (Ketchan, Minsk et al. 1996). This is often seen as a benefit in cold regions where this residual effect reduces the required future application in successive winter events. However, in North Carolina there may be extended periods between winter events, so this residual effect may yield an adverse long-term exposure of the structural elements to corrosive agents.

Due to the considerable economic costs associated with corrosion linked deterioration in highway infrastructure, significant research has been performed on the impact of various deicing solutions to reinforced concrete bridge components. Literature concerning temporal and transport phenomena of chlorides originating from deicing materials on bridge components and as well as experimental techniques for assessing chloride concentration on bridge components is presented in this section.

2.2 Corrosion Processes

Corrosion can be defined as the deterioration of material due to exposure from the natural environment, which is significantly accelerated by certain chemicals. The process consists of oxidation and reduction reactions at the surface of the material(Mindess, Young et al. 2002). The oxidation reaction generates metal ions and electrons, while the electrons are then consumed in the reduction process. In the case of the corrosion of iron in structural steel, the two controlling agents are water and oxygen. Iron is oxidized producing electrons and ferrous ion at the anode (EQUATION 2.1). The electrons are then consumed by converting water and oxygen to hydroxide ions at the cathode (EQUATION 2.2).

$$\text{Anode reaction:} \quad Fe \rightarrow Fe^{2+} + 2e^{-} \tag{2.1}$$

$$\text{Cathode reaction:} \quad \frac{1}{2}O_2 + H_2O + 2e^{-} \rightarrow 2OH^{-} \tag{2.2}$$

Through movement of electrons and hydroxide ions migrating from the cathode to the anode, the produced hydroxide are then combined with iron ions to form ferrous hydroxide ($Fe(OH)_2$) (EQUATION 2.3).

$$Fe^{2+} + 2(OH)^{-} \rightarrow Fe(OH)_2 \tag{2.3}$$

After subsequent reactions with oxygen and water, the ferrous hydroxide turns into hydrate ferric oxide, or rust (EQUATION 2.4). A schematic of the corrosion process for iron is shown in Figure 2.3.

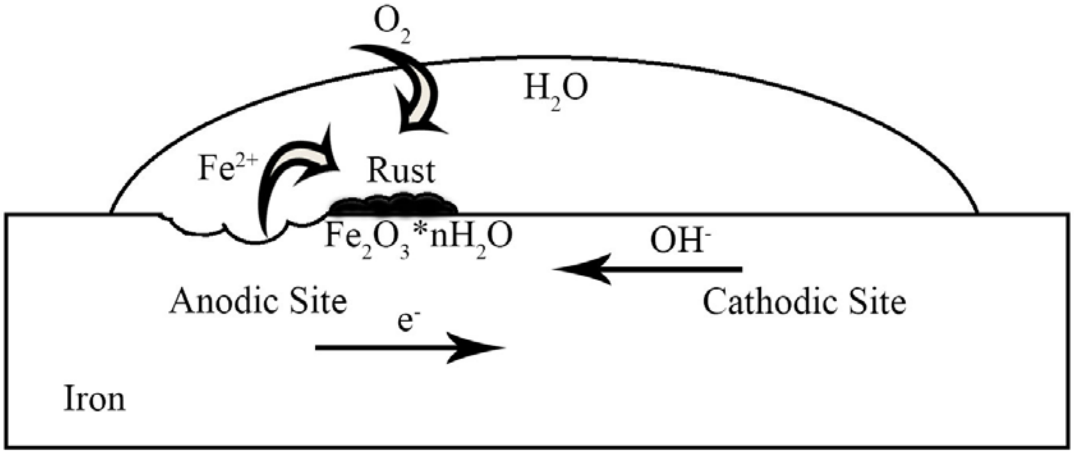

Figure 2.3: Surface corrosion of iron

$$2Fe(OH)_2 \xrightarrow{O_2, H_2O} 2Fe(OH)_3 \rightarrow Fe_2O_3 * nH_2O \tag{2.4}$$

The process occurs more rapidly with higher ionic conductivity(Guthrie, Battaat et al. 2002), which is why the presence of electrolytes, such as salt in water can increase the rate of the corrosion process. Within concrete, ferric rust at the surface of the reinforcing steel can result in cracking due to the large volumetric increase associated with the formation of the corrosion byproduct.

According to Mindess, Young, and Darwin (2002), reinforcing steel in concrete does not initially corrode due to the protection of concrete cover. The alkaline environment from the concrete results in the oxidation of $Fe(OH)_2$ to ferric hydroxide. Ferric hydroxide serves as a protective film that can limit the supply of oxygen and moisture to the metal thereby inhibiting corrosion. However, this occurs only at relative high pH, generally greater than 13. Once the pH level drops below 11.5, the oxide film is destroyed and corrosion can initiate. This reduction in pH level occurs naturally as concrete is exposed to atmospheric carbon dioxide (CO_2). The CO_2 can diffuse into porous concrete and react with alkaline substances in the pore solution. This carbonation process consumes calcium hydroxide according to the reaction:

$$Ca(OH)_2 + CO_2 \rightarrow CaCO_3 + H_2O \tag{2.5}$$

The pH of pore water in hardened Portland cement paste can be reduced from as high as 13.5 to about 8.3 when all $Ca(OH)_2$ is converted to $CaCO_3$ (Bioubakhsh 2011). The carbonated zone in normal concrete is within 1 inch and could be higher with increased severity of exposure conditions, such as the presence of cracks due to internal and external stress and carbonate shrinkage.

Even under low pH conditions, the corrosion process can be limited by controlling the availability of oxygen and moisture (Mindess, Young et al. 2002). For concrete with low permeability or in a condition when the pores are filled with water, the diffusion of oxygen is greatly reduced, thereby limiting corrosion. As an example (Mindess, Young et al. 2002), concrete containing silica fume have superior corrosion performance compared to concrete without silica fume at the same water to cement ratio. The initial reduction in pH associated with the use of silica fume is more than offset by the reduction in permeability.

The presence of chloride ions can add to the corrosion process by destroying the oxide film on steel and producing ferrous chloride corrosion products. Even at high alkalinity, significantly high concentrations of chloride can initiate the corrosion process. Once the chloride content exceeds a threshold level, chloride ions can break the passive layer to form an anode on the steel surface, starting the corrosion process. Factors that can influence the chloride threshold are the type of cement, water to cement ratio, curing and compaction, moisture content, type of steel and surface condition, and oxygen availability (OECD 2002). Chloride ions can also react directly with iron ions to produce corrosion byproducts. Chloride ions and iron ions combine to form iron-chloride complex (EQUATION 2.6), which then reacts with hydroxyl to form ferrous hydroxide and also releases the chloride ions that allow the reaction to continue (EQUATION 2.7) (Mindess, Young et al. 2002).

Iron-chloride complex: $$Fe^{2+} + Cl^- \rightarrow [FeCl]^+ \tag{2.6}$$

$$[FeCl]^+ + 2OH^- \rightarrow Fe(OH)_2 + Cl^- \tag{2.7}$$

2.3 Transport Mechanism of Chloride in Concrete

Build-up of chlorides on concrete surfaces allows for ingress of corrosive solution further into the concrete reaching the embedded steel. The mechanism of penetration depends on whether the surface is fully saturated or cycles between wetting and drying. Chloride ions are transported by hydrostatic pressure when the surface is saturated and by absorption when the surface is subjected to wet-dry cycling (Gergely, Bledsoe et al. 2006). The steady-state flow of liquid under hydrostatic pressure is directly proportional to the hydraulic gradient and can be described by Darcy's law (EQUATION 2.8), where the coefficient of permeability is influenced by the pore structure of concrete (Bioubakhsh 2011). Specifically:

$$v = Q/A = K(\Delta h/\mathrm{L}) \tag{2.8}$$

Where:
v = velocity of flow
Q = flow rate
A = cross-sectional area of the sample
K = coefficient of permeability
Δh = drop in hydraulic head
L = thickness of sample

The equation suggests that water is driven through the concrete when there is a difference in hydraulic head. However, the contribution of permeability is minimal for concrete that is not under constant water pressure (Bioubakhsh 2011). Another mechanism associated with the transport of chlorides through concrete is diffusion. Diffusion occurs when there is a concentration gradient. Models for prediction of chloride ingress are based on Fick's laws. Fick's first law describes diffusion under unidirectional and constant mass transfer, where the rate of transfer across a section area is proportional to the concentration gradient and the diffusion coefficient. Fick's second law describes diffusion when the concentration changes with time. The diffusion coefficient can be assumed a function of many variables such as maturity, temperature, humidity, water-cement ratio, cement type, aggregate size, curing regime, and chloride concentration (Bioubakhsh 2011). Liquid can also be transported into the concrete through absorption. Absorption occurs in unsaturated porous concrete by capillary suction or sorptivity. The transport mechanism is driven by surface tension and is a function of the liquid viscosity, density, surface tension, and the pore structure of the porous material (Pitroda 2013). The pore structure of concrete depends on a variety of factors including concrete mix-design, curing regime, and compaction. The sorptivity of concrete can be determined from the linear relationship between the square root of time and the depth of liquid penetration from the surface (EQUATION 2.9).

$$A = b + S\sqrt{t} \tag{2.9}$$

Where:
A = depth of liquid penetration
b = initial absorption
S = sorptivity
t = time

2.4 Modeling Chloride Transport

The use of anti-icing treatment for snow and ice is a major source of chloride on pavements and bridge components. Chloride contents can be directly deposited on exposed steel components or can diffuse through the pores in concrete and steadily build up at the depth of the reinforcement. The mechanism of penetration and transport depends on whether the surface is fully saturated or cycling between wetting and drying. Chloride ions are transported by hydrostatic pressure when the surface is saturated and by absorption when the surface is subjected to cycles. Models for prediction of chloride ingress are based on Fick's second law of diffusion. The one-dimensional model (Equation 2.10) is a particular solution to the relationship and is dependent on well-defined variables for composition of the concrete, fracture state, surface concentration, and time. Equation 2.10a models chloride concentration at depth given a constant surface concentration, C_0, and 2.10b models concentration at depth x given a linear, time-dependent increase in surface concentration.

$$C(x,t) = C_0\left\{1 - erf\left(\frac{x}{2\sqrt{D_c t}}\right)\right\} \tag{2.10a}$$

$$C(x,t) = kt\left\{\left(1 + \frac{x^2}{D_c t}\right) erf\left(\frac{x}{2\sqrt{D_c t}}\right) - \left(\frac{x}{\sqrt{\pi D_c t}}\right) e^{-x^2/4D_c t}\right\} \tag{2.10b}$$

Where
C=the concentration of a chemical species
C_0=the concentration of a chemical species at the surface
x=linear distance from the exposed surface
t=time
$D_{c=}$ diffusion coefficient
k=accumulation rate of species x at the surface

Cyclic wetting and drying is a pervasive issue for reinforced concrete structures exposed to chlorides, such as marine structures, particularly in the splash and tidal zones; parking garages, in areas exposed to deicer salts; and highway structures, such as bridges and other elevated roadways. Hong and Hooton (1999) examined the effects of cyclic wetting and drying on chloride ingress into concrete from sodium chloride-based solutions. Cyclic wetting and drying was associated with continuous movement of aqueous solutions through concrete pores. This cyclic action accelerates durability concerns because it subjects the concrete to the movement and accumulation of adverse chemicals, such as sulfates, alkalis, acids, and chlorides. Hong and Hooton measured chloride profiles within samples exposed to various durations and numbers of cycles using the potentiometric titration method (1999). Two samples contained slag and/or silica fume with a 0.4 w/cm (water to cementing materials ratio) and one with a 0.3 w/cm. The researchers found that longer drying times increased the rate of chloride ingress. A strong correlation between the depth of chloride penetration and the square root of the number of cycles was discovered (Hong and Hooton 1999).

Bioubakhsh describes the accelerated transport of chlorides through absorption (Bioubakhsh 2011). Sorption processes draw chloride laden water into the concrete surface rapidly by capillary action if the pores are empty. Chlorides can then undergo diffusion processes to continue ingress. However, if the concrete dries to a deeper depth and is subsequently rewetted, the chlorides can again be drawn further into the monolith.

2.5 Protection against corrosion

Based on the known chemical reaction process of corrosion, strategies to protect against corrosion usually minimize the availability of oxygen and moisture required to supply the cathodic reaction. This can be achieved through four general categorical approaches: reduction of the permeability of the concrete, installation of protective membranes on the concrete, application of protective coatings on the steel, and active suppression of the electrochemical process (1)

Corrosion protection measures are based on four keys considerations: environment, materials of construction, design detailing, and cost (2) Environmental considerations take into account the potential for corrosive chemicals and excessive moisture to remain in contact with the steel surface for an extended amount of time. Type of environment can range from the rural area, where there may be limited exposure to chemical or deicing salt to the marine environments, where there is constant exposure to airborne salt and moisture. Regions with high average daily traffic (ADT) and significant winter precipitation may experience more severe exposure due to more frequent use of deicing salt. Typical design options will be site-specific, where more corrosive environments will require a high durability protection system. Other options can include detailing in a way to avoid contact between corrosive agents and steel surfaces. However, such measures are generally not cost effective.

According to Albrecht and Hall (2003) research on atmospheric corrosion of structural steel indicates that the use of weathering steel shows benefits over carbon steel within various environments. A compilation of reported test results is shown in Figure 2.4. As shown in the figure, corrosion losses for weathering steel stabilize over time to provide protection against further corrosion in rural and industrial environments. In marine environments, the corrosive loss is significantly lower for weathering steel, but does continue to progress further over time rather than stabilize.

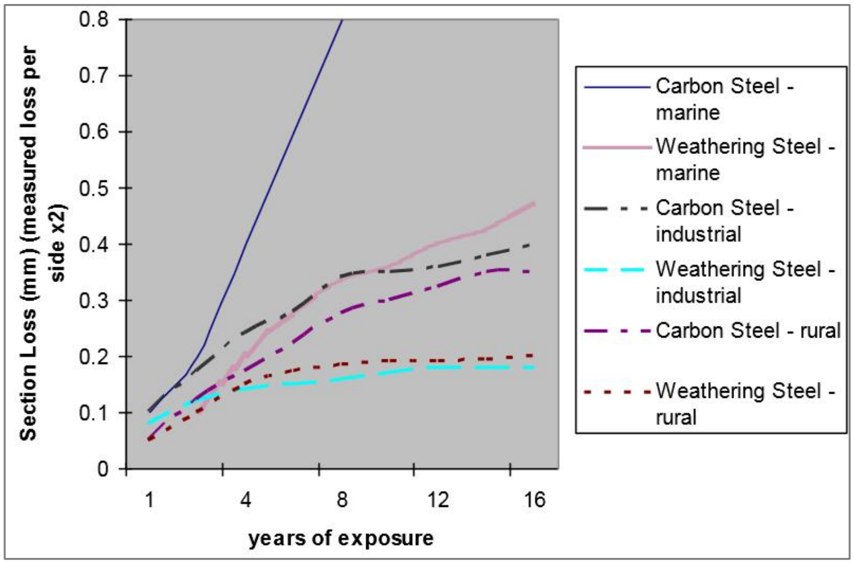

Figure 2.4: Graph of corrosive for carbon and weathering steel in various environments (reproduced from (2)

A special characteristic of weathering steel is the ability to form an adhering corrosion product layer that protects the interior steel from further corrosion. Compared to ordinary structural steel, the basic metallurgical difference of weathering steel is the addition of chromium, copper, and nickel alloying elements. However, research indicates that the ability for weathering steel to fully develop an anticorrosive layer depends on the geometry, environmental conditions, and steel composition (3) The process requires cycling between wet and dry conditions and requires rain water to flush the surface of contaminants followed by a fast drying time without ponding. Furthermore, according to Morcillo (2013), bare weathering steel is not recommended in continuous moist exposure or marine atmospheres where the protective layer does not form.

Another protective strategy against steel corrosion is design of systems that can prevent the chlorides from coming into contact with the steel. FHWA Technical Advisory T5140.22 (1989), “Uncoated Weathering Steel in Structures” provides several guidelines for proper application and maintenance of uncoated weathering steel. Design details include: diverting water from vulnerable components, painting superstructure steel girder over a length at least 1.5 times the depth of girder from bridge joints, and eliminating details that may possibly collect or trap chloride-laden water. Maintenance measures also described in the guideline include maintaining roadway drainage through removal of deposits and vegetation.

For coated structural steel, the current practice is to use a multicoat system. Surface preparation includes abrasive-blasting to remove millscale. This process not only removes initial contaminants that promote corrosion, but also enhance coating performance. Similar surface preparation is performed on bare weathering steel. The first coating is usually a zinc-rich primer follow by two additional coating layers over the primer. The zinc-rich primer provides protection to the steel substrate by acting as the sacrificial layer during corrosion. An intermediate epoxy coating provides protection from moisture, oxygen, and electrolytes. The top-most coating adds physical protection against deterioration from ultra-violet radiation and provides long term aesthetic. The three coating system with inorganic or organic zinc-rich primer, epoxy midcoat, and polyurethane topcoat can have an estimated service life of 30 years (4) Two-coat and one-coat systems are also considered in some applications as reducing the number of coats can greatly reduce the initial production cost. Current research has focused on verify the effectiveness of reduced coatings without sacrificing corrosion protection performance. Research through the FHWA by Yao, Kodumuri and Lee (2011) evaluated the possibility of a one-coat system as a performance comparison to the standard two and three coats systems. Performance was evaluated using accelerated laboratory testing and outdoor exposure conditions. Results from the research ranked the traditional three-coat system as having the best overall performance followed by one-coat high-ratio calcium sulfonate alkyd (HRCSA) and high-build waterborne acrylic (HBAC). Conclusions from the research indicated that HRCSA performed well in both accelerated laboratory testing and under outdoor exposure conditions(5)

An alternative to painted or epoxy coated protection of steel surfaces is metalized coating. The process typically involves melting zinc or aluminum alloy onto the steel surface. Sealer and finish coat can also be added in addition to metalizing for further protection. The process provides excellent corrosion protection even in marine environments (2) Hot-dip galvanization is a popular method of coating an entire steel component with zinc. Bridge guard rails are typically galvanized steel. The process involves dipping a component into molten zinc, which can be repeated for multiple layers. Corrosion protection performance will depend on the thickness of the zinc cover. A limitation of the process is the requirement to fully immerse the component, which restricts the size of the components that can be galvanized.

Preventive measures to protect embedded steel from corrosion in concrete include the use of high-quality impermeable concrete with low water to cement ratio and large concrete cover. Also, the recommended concrete cover for reinforcement is 2 ½ inches (6) Some of the methods to lower the permeability of concrete include: addition of pozzolans in the mix design, using high density concrete overlays, and using high-strength concrete to prevent cracking. Pozzolans commonly used in concrete mix are coal fly ash (pulverized fuel ash or PFA), ground granulated blast furnace slag, silica fume, and metakaolin (calcined clay). These pozzolans must first be converted into amorphous or glassy form and should be finer than 325 mesh (45 microns) to react readily in the curing process (7) During the curing process, pozzolans act as supplementary cementation materials and the process can continue over many years. Addition of pozzolans results in a denser, harder, and more durable concretes, with reduced permeability and as well as greater resistance to deterioration. Although these measures can not completely prevent corrosion, the rate of penetration of corrosive agents can be reduced.

Another effective method in the protection of bridge decks is to use protective membranes. The membrane can be placed directly onto the newly constructed or existing bridge deck then overlaid by an asphalt wearing surface to produce a barrier to penetration of moisture and deicing salts. According to the National Cooperative Highway Research Program (NCHRP) Synthesis 425 (2012), 60% of U.S. state agencies use waterproof membranes on bridge decks with greater usage on existing bridge decks than new bridges. The membrane product can be either pre-formed sheet system or liquid system. Both systems involve the application of a primer on the concrete surface followed by installation of the membrane and then a tack coat for increased bond to the asphalt overlay. A similar membrane system has been used on concrete decks in parking garages (8) The system consists of first using sealer or primer for adhesion of the membrane, then installing the waterproof membrane, and finally installing a wear coating. The waterproof membrane serves to seal existing cracks and prevent the further ingress of chloride ions and water. The wear coat should contain embedded aggregate to provide abrasion resistance and protect the membrane. A tie coat is added to bond the aggregate to the wear coat. However, using a membrane system has its own limitations. Application of membranes is not possible at joints or curbs where contaminated water can leak underneath. Another common problem is improper bonding with the concrete surface, which allows for chloride-laden water transport underneath the membrane. A limitation of waterproof membrane system on bridge decks is the service life of the wearing surface, as de-bonding can occur for grades greater than 4% (9) According to NCHRP Synthesis 425 (2012), expected service life of waterproof membranes range from 16 to 20 years for installation on new bridge decks and as low as 6 years on existing bridge decks.

A more widely use alternative in protection of bridge deck corrosion is using fusion-bonded epoxy coating on the surface of embedded steel. Adding an epoxy coat allows protection from penetration of water, air, or chemicals that promote corrosion of the rebar. The coating also serves as an electrical insulator to minimize the flow of corrosion current(10) The outer coating prevents the formation of anodes when the coating is adhered tightly to the steel, also preventing the steel from acting as a cathode. Recent study on the service life of uncoated steel rebar (black rebar) and epoxy coated rebar (ECR) in bridge deck estimates that the service life for black rebar is 35 years while the service life for ECR is 70 years (11) However, using epoxy coating has an adverse effect when the coating is not tightly bonded to the steel surface. Prolonged exposure of ECR to moist environments can result in debonding and softening of the coating (10) The result is accelerated corrosion due to crevice corrosion, where high concentrations of chloride ions buildup under the coating (12) The same phenomenon is true for exposed coated steel. Special considerations such as fabrication, transportation, erection methods, and service environment should be properly addressed in specifications to ensure the integrity of the coating.

Recent developments also take advantage of the electrochemical process of corrosion to prevent corrosion by using conducting polymers. The use of polypyrrole and polyaniline electrodeposited on steel component can act as anodic protection to reduce the rate of corrosion (13) The polymerization process used in layering passivizes the iron surface with a layer of iron tartrate to buffer the metal in corrosive environments.

2.6 Measurement and Detection of Chlorides

Indirect, nondestructive tests for determining chloride concentrations and effects of chloride exposure to reinforced concrete and steel components are limited due to the difficulty of measuring elemental composition of materials at depth without destructively accessing the interior region of the sample. Recently, researchers at the University of Kansas Center for Research explored application of resonant modulus testing, a standardized test method, for determination of the corrosive effects of four of the most widely used deicing chemicals. In their research, concrete specimens were exposed to weekly wetting and drying cycles in distilled water and in solutions of sodium chloride, calcium chloride, magnesium chloride, and calcium magnesium acetate with either a 6.04 molar ion concentration, equivalent in ion concentration to a 15% solution of NaCl, or a 1.06 molar ion concentration, equivalent in ion concentration to a 3% solution of NaCl, for periods of up to 95 weeks. The effects of exposure were evaluated based on changes in the dynamic modulus of elasticity and the physical appearance of the specimens at the conclusion of the tests. The study determined that at lower concentrations, sodium chloride and calcium chloride yield a relatively small change in the dynamic modulus of concrete. At high concentrations, sodium chloride has a greater but still relatively small adverse effect (Darwin, Browning et al. 2007).

Direct assessment of chloride content in concrete is enabled by a number of experimental methods, including argentometric titration, potentiometric measurements (ion selection electrodes), and atomic absorption. Recent techniques have been proposed to estimate chloride penetration resistance such as the determination of electrical conductance of concrete and the qualitative measurement of chloride penetration front by means of a colorimetric test. However, in both cases a quantitative evaluation of chloride concentration cannot be obtained, which prohibits use of such testing in predicting the corrosion rate in reinforcing steel (Proverbio and Carassiti 1997).

A more advanced analytical technique that can be used to quantitatively determine chloride concentrations in concrete structures is the X-Ray Fluorescence (XRF) method. This is an analytical method suitable for sampling across large structural surfaces since measurements can be carried out in an exceptionally short time compared to other techniques.

Another well-known technique and instrument used in several studies for measuring surface chloride concentrations is the SOBO-20 instrument produced by Boschung. The SOBO instrument applies the principle of measuring the electrical conductivity of a fluid and a predetermined calibration between the electrical conductivity measurement and salt concentration of the fluid. This instrument spreads a measuring fluid, which consists of 85% water and 15 % acetone, onto the road surface and then measures the electrical conductivity of the fluid. The SOBO-20 calculates the quantity of salt on the road surface per unit area (g/m^2) using the known parameters such as the volume of the measuring fluid and the electrical conductivity (Lysbakken and Lalagüe 2013).

In the Norwegian University of Science and Technology, experiments were carried out on brine, granular salt and recrystallized salt using the SOBO-20 to accurately determine the amount of salt present on the pavement. Also, these experiments were set up to quantify the factors such, as the acetone content, the type of salt and the surface conditions, that may affect the accuracy of the SOBO-20 in the measurements of salt on winter pavements since there is little documentation on the quality of this technique.

To quantify the factors mentioned above that may affect the accuracy of the SOBO-20 instrument; six different tests were performed of which four were on a smooth surface. A calibration test was performed to determine whether there were errors directly related to the instrument. The calibration test was performed with fully dissolved brine applied on a smooth surface. The brine was applied on a glass dish with a pipette in small droplets and repeated ten times for each salt quantity tested. After testing, the results showed that the SOBO-20 is able to measure dissolved salt on a smooth surface quite accurately

(Lysbakken and Lalagüe 2013). Also in the study, an investigation on the acetone content in the measuring fluid test was performed to find out if the absence of acetone would influence the measuring results. Measuring fluid that consisted of distilled water only was tested and compared to acetone-water mix. From this test, it was observed that using the correct amount of acetone in the measuring fluid is crucial to obtain a reasonable salt reading with the SOBO-20. It was evident also that using a lower amount of acetone than recommended in the instrument manual, produced higher indications of salt concentration. It was discovered that using only distilled water in the measuring fluid, the SOBO-20 measured salt quantities ranging from 45-66% greater than the applied quantity (Lysbakken and Lalagüe 2013).

Also in the Norwegian University study, a salt grain test was performed to analyze the level of underestimation of the readings obtained from the SOBO-20 on granular salts. For this study, salts in the form of crystals were applied on dishes and measured with the instrument. From the results, it was evident that the SOBO-20 underestimated the applied salt quantities. To conclude the study, recrystallized salt on smooth surface tests were performed to quantify the level of underestimation of salt quantities measured when testing on recrystallized salt. For this test, droplets of brine solution were applied with a pipette on a smooth surface and allowed to dry up over a 12 hour period and tested after. The results showed that the instrument underestimates the salt quantity when measuring surfaces applied with recrystallized salt. In conclusion, these experiments showed that the SOBO-20 accurately measures the quantity of salt applied in brine form on smooth surfaces but only detects between 5-6% of the granular salt on the surface (Lysbakken and Lalagüe 2013). The above study and principle of the SOBO-20 inspired the surface chloride absorption method using XRF that is described in this report.

2.7 Experimental techniques for determining the impact and pattern of chlorides on concrete components

Many researchers have been concerned with the damaging effects that deicers have on concrete components. In a study funded by the Iowa Department of Transportation, the effects of different deicers on concrete surface deterioration were investigated by conducting environmental simulations on concrete samples that have been applied with deicers such as NaCl, $CaCl_2$, $MgCl_2$, calcium magnesium acetate (CMA) of five different Ca/Mg ratios (Lee, Cody et al. 2000). In order to do this, reduced samples from small 3cm x 1.5cm x 1.5cm blocks were collected from seven Iowa highway concretes. Subsequent submersions of the samples in 100 mL of deicing solutions were evaluated and enclosed in polymethylpentene containers. These containers remained stored at 58°C for 132 hours.

After this stage, the samples were emptied from their containers, and then dried at 58°C for 24 hours. Following 24 hours, these samples air cooled at 25°C, and then set into the solutions for 132 hours at 25°C. The same procedure was done at 58°C. After 132 hours, the samples were again removed from the 58°C solutions and air cooled to 25°C. In a freezer at -4°C, samples were then kept for 24 hours and air warmed to 25°C after. Positioned in their solutions at 25°C, the blocks were then placed at 58°C for 132 hours again. These procedures were carried out until there were detections of visual deterioration on the sample surfaces. Finally, it was concluded that disintegration of the concrete was produced by magnesium chloride. In conclusion, calcium magnesium acetate ended up as the most damaging deicing solution. This solution caused damage to concretes containing dolomite coarse aggregates combined by increasing the reactions released by magnesium to form destructive brucite. On the other hand, sodium chloride caused the least decay under the drying and freezing time frame (Lee, Cody et al. 2000).

The Swedish National Road and Transport Research Institute conducted a field study using the SOBO-20 (described previously) to investigate the patterns of residual salt brine on a road surface and the mechanisms involved in the movement of the salt from the road to roadside. In this study, the road tested was divided into nine segments from one edge of the road to the other: road edge, in the right and left wheel path, in-between the wheel paths, at the road center likewise for other side. After testing, it was discovered in the first couple of days that the amount of salt on the roadway and on the pavement was low. Residual salt was observed to remain on the road surface 18 hours after the salting of the bridge had taken place. The assumption made for the slow decline of the residual salt on the road surface was that the road surface conditions were dry to moist. Salting was repeated 7 days after the first application and also 2 days after the second application. Days after, measurements indicated that residual salt concentrations were highest as they gathered between the wheel path and in the median (Blomqvist and Gustafsson 2004).

In the study above, a model was developed using the results from the two inner wheel tracks to represent the amount of residual salt on the road surface available to roadside exposure. Presented is the equation (2.11) developed

$$RS = S * e^{-k*PC_{eqacc}} \tag{2.11}$$

Where

RS =residual salt
S= salt used
PC_{eqacc}= accumulated private cars equivalents

The model above is used to determine the change in residual salt concentration under the action of vehicular transport. The model uses the initial salt application and the traffic count as factors influencing the rate of dispersion. The model suggested that the remaining amount of salt on the road surface after the days of application was 12.689 g/m² and the coefficient k was 0.2027.

Another relevant study that provides data on the decay of brine concentration with traffic was done by the Ohio Department of Transportation. In the research, a field study was developed to investigate the brine residue on the road surface using the SOBO-20 instrument. For this investigation five four-lane test sites were used and at each of these sites four test sections were marked up on a shoulder lane for measurement of the brine residue after application at each period of exposure to traffic. Brine was applied along the entire test site at an application rate of 40 gal/lane mile by the ODOT personnel. Brine samples were obtained and measured in the laboratory to verify the concentration. The brine residual was measured over time and the amount of traffic exposure was determined as well using portable until the brine decayed. The measurements of the brine residual were correlated with weather data and the traffic count (Mitchell, Hunt et al. 2003).

The salt on the surface of the pavement was expected to decay as a function of time and traffic but other factors such as the porosity of the pavement contributed to some distortion in the trends shown by the salt. It was observed also that the brine concentration decreased after about 7 hours of traffic of about 1500 vehicles. Of the five test sites, three sites exhibited strong data to develop residual equations as a function of time and vehicular traffic. The exponential decrease of brine in the field was incorporated into laboratory brine, ice and specimen bonding temperature findings and the effective ice prevention temperatures as a function of time and traffic at standard application rates were determined for two sites. The above research was relevant for the present report because the methodology of the controlled field testing described in Chapter 6 is similar to that used in the above research (Mitchell, Hunt et al. 2003). Based on the literature review on corrosion, the effects of the deicers, the pattern of residual salt and the various testing instruments, a greatly improved understanding of chloride ingress was gained to make decisions on methodologies to be used in this report presented

2.8 Test Methods for Evaluation of Corrosive Effects of Deicing Chemical

Several testing methods have previously been developed to evaluate the corrosive effects of coated and uncoated steel surfaces, including both standardized methods and methods developed for individual research projects. Standardized methods included those from the American Society for Testing and Materials (ASTM) and International Standards Organization (ISO). Both organizations provide testing protocols for evaluating atmospheric corrosion and corrosion during immersion in salt solutions. Standard test methods for evaluation of atmospheric corrosion is outlined in ASTM G50 “Standard Practice for Conducting Atmospheric Corrosion Tests on Metals” (14)and ISO 9226 “Corrosion of Metals and Alloys - Corrosivity of Atmospheres – Determination of Corrosion Rate of Standard Specimens for the Evaluation of Corrosivity”(15) These tests are used to evaluate corrosion resistance of metals when exposed to service weather at a particular testing site. Quantitative data are recorded as mass loss that is then converted to a corrosion rate. Accelerated test methods include those that expose test specimens to extreme corrosive environments, such as salt spray and immersion in salt solution. Standards for immersion tests include ISO 11130 “Corrosion of Metals and Alloys – Alternate Immersion Test in Salt Solution” (16)and ASTM G31 “Standard Guide for Laboratory Immersion Corrosion Testing of Metals”(17) Test procedures developed by the Strategic Highway Research Program (SHRP) cover evaluation of corrosive effects of deicers or other aqueous solutions through continuous immersion of test specimens in solution (18) The recommended testing period for the SHRP test is up to 8 weeks for data collection. Alternatives to these standards include the addition of cycling the test specimen between wet and dry to better represent field exposure. An example of a cyclic immersion test is the test procedure by the Pacific Northwest Snowfighters (PNS). The test procedure calls for application 30 mL of test solution per square inch of steel coupon surface (19) The sample coupon is immersed for 10 minutes followed by 50 minutes of air exposure over a testing period of 72 hours for each test. Corrosion rates are calculated based on percent mass loss over the testing period. The Society of Automotive Engineers (SAE) also adapted cyclic corrosion testing in their standardized test method. Metal test specimens are placed in an enclosed climate controlled chamber and subjected to a humid stage, salt application stage, and dry stage (20) Due to the complex nature of corrosion, detailed procedures are often specific to the application and results are typically used for comparative purposes.

Test procedures used in this study for evaluation of different deicing strategies on reinforced concrete are based on ASTM G109 “Standard Test Method for Determining Effects of Chemical Admixtures on Corrosion of Embedded Steel Reinforcement in Concrete Exposed to Chloride Environments”(21) The testing setup consists of concrete samples with two embedded layers of reinforcing bars, one top rebar and two bottom rebars, that is exposed to cyclic ponding and drying of sodium chloride solution on the top concrete surface (Figure 2.5). Typical concrete cover for the top rebar is 0.75 inch. Electrical current flow is monitored between the two layers of reinforcement for signs of corrosion of the top rebar. Researchers using the test method indicate that the time to failure is much longer than the six months noted in the standard (22) The time required for corrosion of the embedded steel ultimately depends on the rate of chloride ingress through the concrete cover and the amount of chloride required to initiate active corrosion at the reinforcement. Study on the critical chloride content show scattered results that depends on interconnected and time-dependent variables for the quality of steel-concrete interface, the pH of pore solution, and the electrochemical potential of the steel (23)

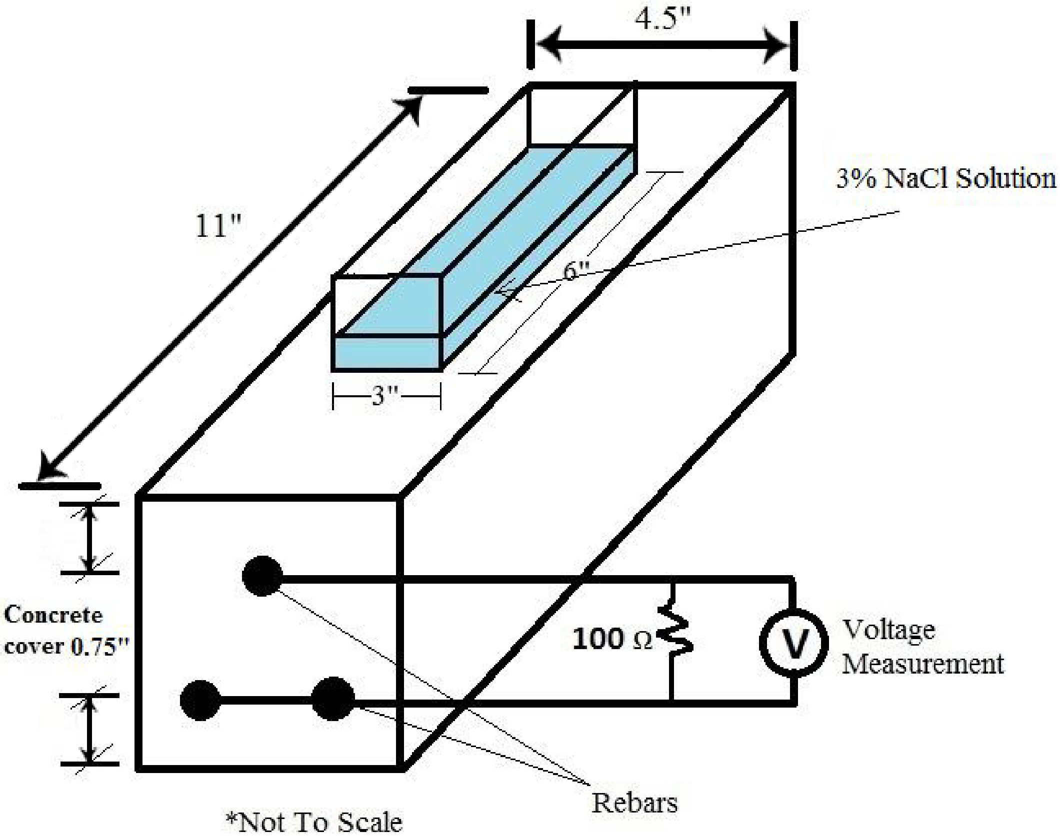

Figure 2.5: Specimen setup for ASTM G109 test method

Modifications to the standard test method include adjusting the number of rebars, changing the resistor value between rebar layers, modifying the ponding solution and concentration, or the cycling rate between wet and dry. In the literature, evaluation of the performance of various reinforcing steel and concrete-mix design have been performed using the standard ASTM G109 and a modified ASTM G109 test method. A modified procedure performed by Trejo, Halmen, and Reinschmidt (2009) stored samples at high temperature (100˚F) and high humidity environments instead of laboratory room temperature and humidity. The overall results show that 70 out of 216 (32%) standard samples achieved active corrosion and 159 samples out of 335 (47%) modified samples achieved active corrosion after a test period of 49 months. Also, about half of the activated samples were actively corroding after a testing period of 32 months using standard procedures while only 27 months were needed to achieve corrosion in half of those from modified procedures. The results indicate that high temperature and humidity increase the effective corrosion rate for the modified test method. An active condition indicates that the total corrosion coulombs (C) (calculated from the voltage measurement across the 100 Ω resistor and test time) had reached 150 C or above. According to ASTM G109, a value of 150 C is consistent with a macrocell current of 10 μA over six months, at which point there is sufficient enough corrosion for visual inspection.

Since corrosion of embedded steel largely depends on the rate of chloride ingress in concrete, it is useful to investigate the transport mechanism. Differences in chloride buildup are observed between exposure conditions of wet/dry cycling and continuous immersion. Concrete specimens exposed to the same salt concentration in wet/dry cycles tend to show an increase in surface concentration, while the surface concentration is held constant for immersed specimens. The net effect has been shown to result in similar chloride profile for both exposure conditions after six months of exposure (12) However, this same study showed that an increase in temperature from the original 20°C to 30°C or 40°C resulted in greater chloride content for specimens exposed to wet/dry cycles after the same test period. This is due to an increase in the initial sorptivity of the concrete surface when the initial moisture content is low and stabilizes as the number of cycle increases causing the moisture content to reach equilibrium (12) When the moisture content is low, the effective porosity is greater and the higher volume of empty pores encourages the absorption. The study indicates that the depth of free chloride penetration is initially smaller than the depth of salt solution penetration due to chloride binding. Due to reduction in absorption, the depth of salt solution eventually decreases while chloride penetration continues with each wetting phase through diffusion. The study also indicates that the depth of chloride penetration can be predicted from the equilibrium weight sorptivity, salt solution concentration, concrete mix, time, and number of cycles.

3 Effectiveness of Chloride-Based Roadway Treatments

The effectiveness of deicing treatments may be characterized as a function of their ice melting capacity and the temperature range in which they are active. All three of the anti-icing and deicing treatments considered in this work avail the same ice-melting agent, sodium chloride. Differences between the treatments include the addition of traction material in the salt-sand mix and the addition of liquid water in the brine solution. Thus, the concentration of the anti-icing agent varies between treatment types as does its physical state as either crystalized or in solution at the time of application.

In order to relate the effectiveness of the three treatments, the ice melting rate of each treatment was determined as well as the freezing point of various sodium chloride solutions. Methods provided by the Strategic Highway Research Program and ASTM were used to make these determinations. Analysis of the results is also provided in order to relate the effectiveness of treatments applied at a variety of concentrations.

3.1 Freezing point of Salt Solutions

The freezing points of solutions having various concentrations of deicing materials were determined by the method described in ASTM D1177, “Standard Test Method for Freezing Point of Aqueous Engine Coolants” (ASTM 2012). This method has been used to evaluate the freezing point of deicing chemicals by other state transportation departments. The experiment is accomplished by placing the solution to be tested inside of a vacuum dewar that has been fitted with a stirring rod and a temperature measuring device. The dewar is submerged in a cooling bath of fluid in a suitable temperature range for causing the deicing solution to freeze. Once the dewar is submerged in the cooling bath, the temperature of the solution is measured and recorded until the deicing solution begins to freeze. Figure 3.1 provides a schematic of the test method as described by ASTM. In this work, the procedure was set-up as shown in Figure 3.2. The stirring was accomplished by way of a mechanical device that lifted the stirring coil up and down in the solution at a regular rate of approximately 60 strokes per minute. The cooling bath was comprised of dry ice submerged in a solution of 91% isopropyl alcohol. Temperature was measured with a thermistor connected to a data acquisition system that sampled the thermistor resistance once per second. The temperature vs. resistance relationship was established by way of data from the thermistor manufacturer.

Brine solutions were prepared with road salt collected from NCDOT in concentrations of 0%, 2.91%, 5.75%, 10.31%, 18.7% and 23%. The purity of the salts tested was not verified; however rock salt for highway use has a minimum specified sodium chloride content of 95%. 100mL of the solution was used for each test and was preconditioned to a temperature of 10 ºC -15ºC above the expected freezing point before starting the measurements. Each solution was tested in triplicate.

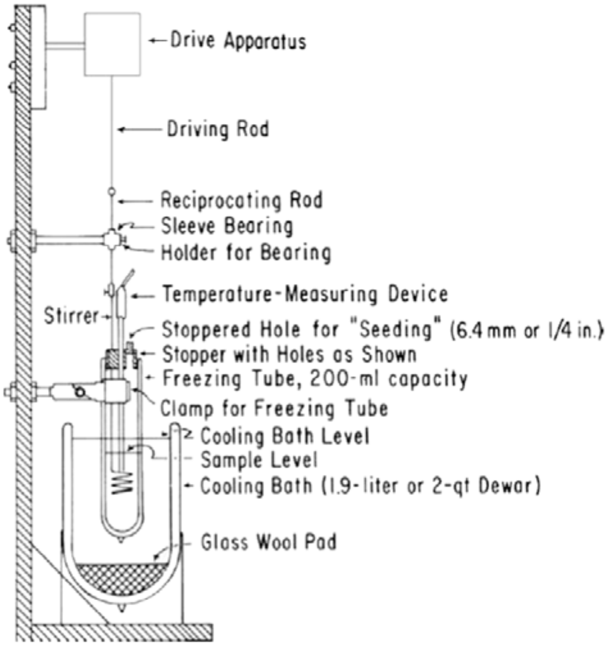

Figure 3.1: Freezing point test set-up schematic from ASTM D1177-2012 (ASTM 2012)

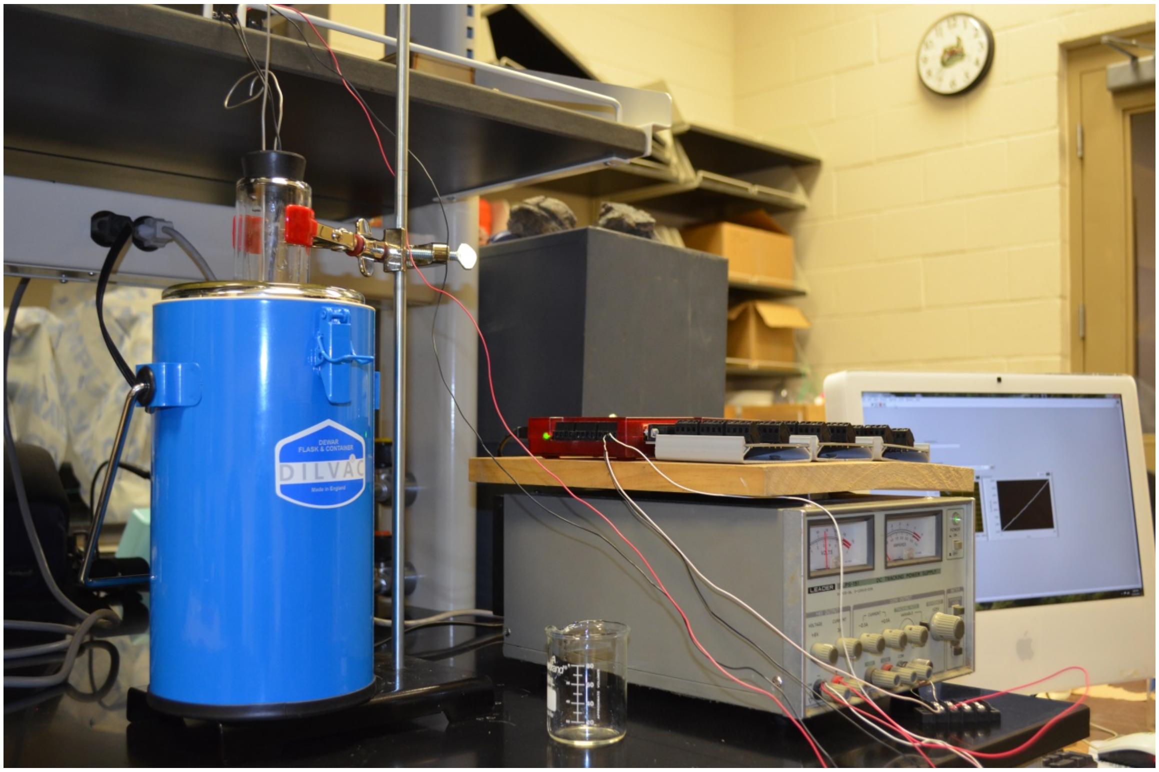

Figure 3.2: Apparatus for measuring freezing point of chloride solutions

Once data is collected, the freezing point is easily identified by a change in the slope of the time vs. temperature curve. At the freezing point, the temperature of the solution ceases to decrease due to the latent heat of fusion. This point may be observed in Figure

3.3 through Figure 3.8 as occurring immediately after a brief dip below the freezing point caused by supercooling. Figure 3.3 plots the results of the control test, in which the freezing point of deionized water was measured. As can be seen in the graph, as well as in Table 3.1, the freezing point of the deionized water with no addition of salt was measured very close to the known value for pure water, 0ºC. Values for the other solutions tested are also given in Table 3.1 as the average of three tests. The 23% brine solution had a freezing point of -21.986ºC. As is apparent in Figure 3.9, the relationship between concentration and freezing point in the range of 0-23% is essentially linear. However, the theoretical relationship between sodium chloride concentration and freezing point is also known to have the curvature shown in Figure 3.9.

Table 3.1: Measured freezing temperatures for NaCl solutions at various concentrations

Solution Concentration [w/w%]	Average of Three Tests[C]
0	0.001
2.91	-1.886
5.75	-3.744
10.31	-7.143
18.7	-15.630
23	-21.986

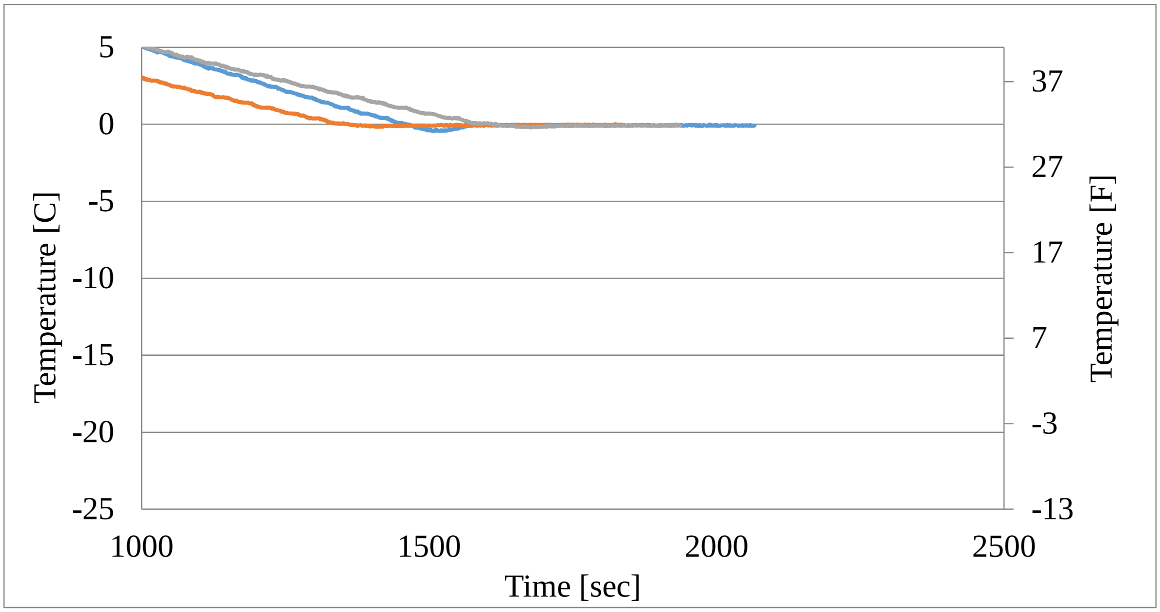

Figure 3.3: Freezing point of solution with 0% NaCl (control)

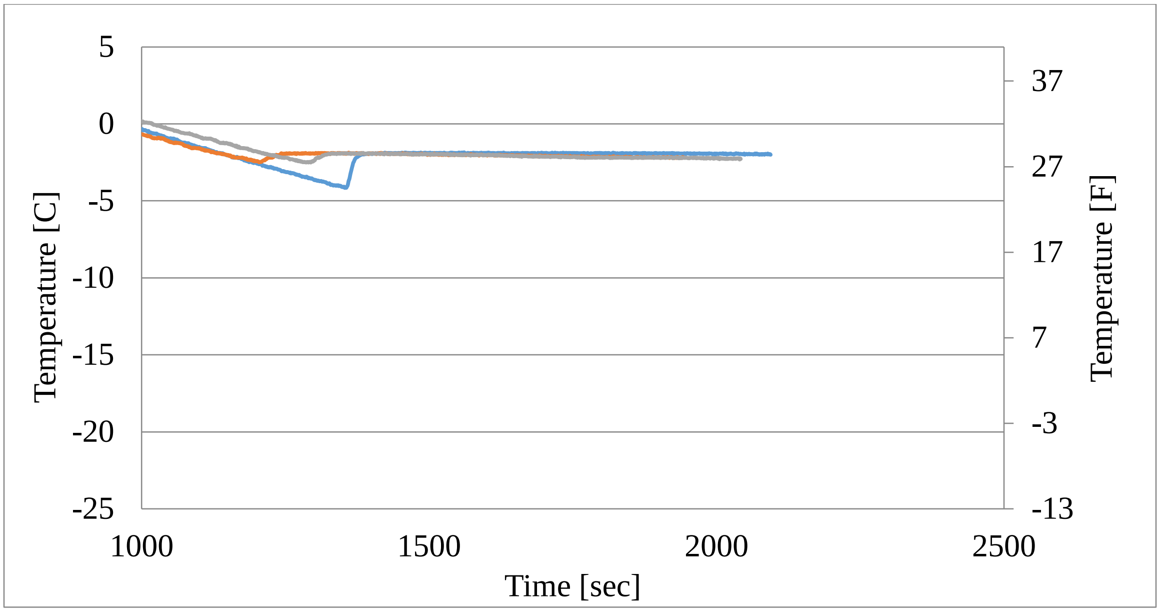

Figure 3.4: Freezing point of solution with 2.91% NaCl

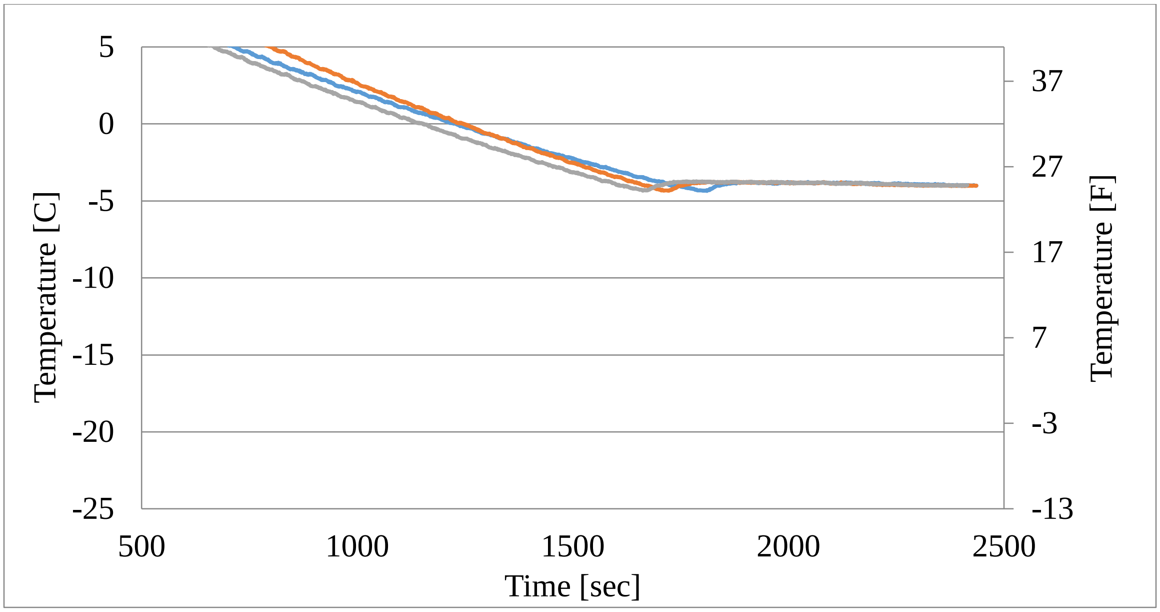

Figure 3.5: Freezing point of solution with 5.75% NaCl

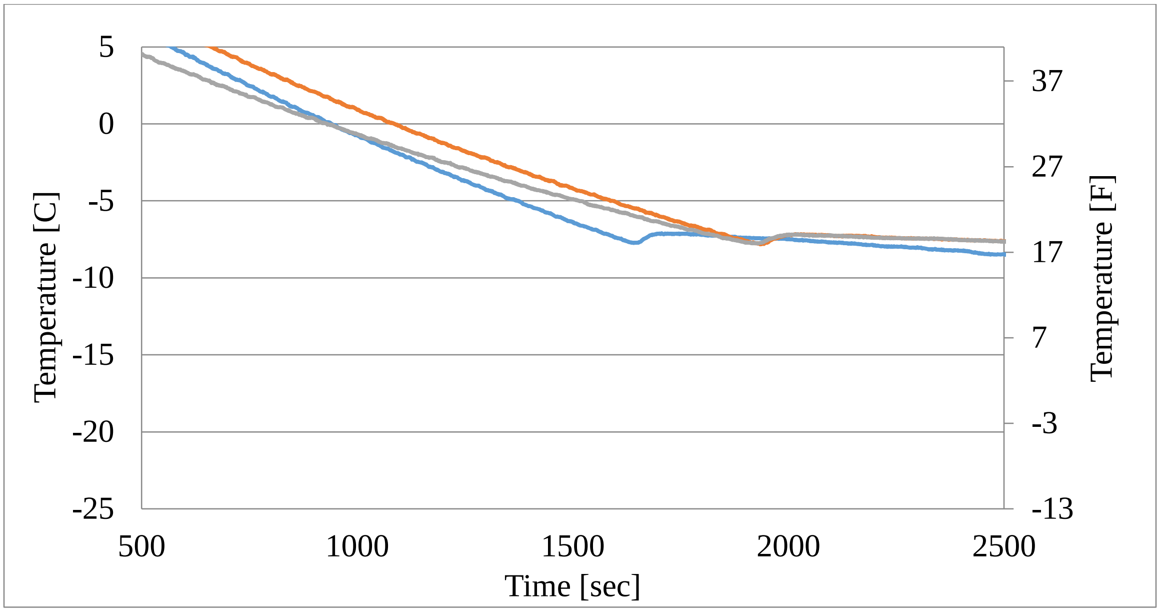

Figure 3.6: Freezing point of solution with 10.31% NaCl

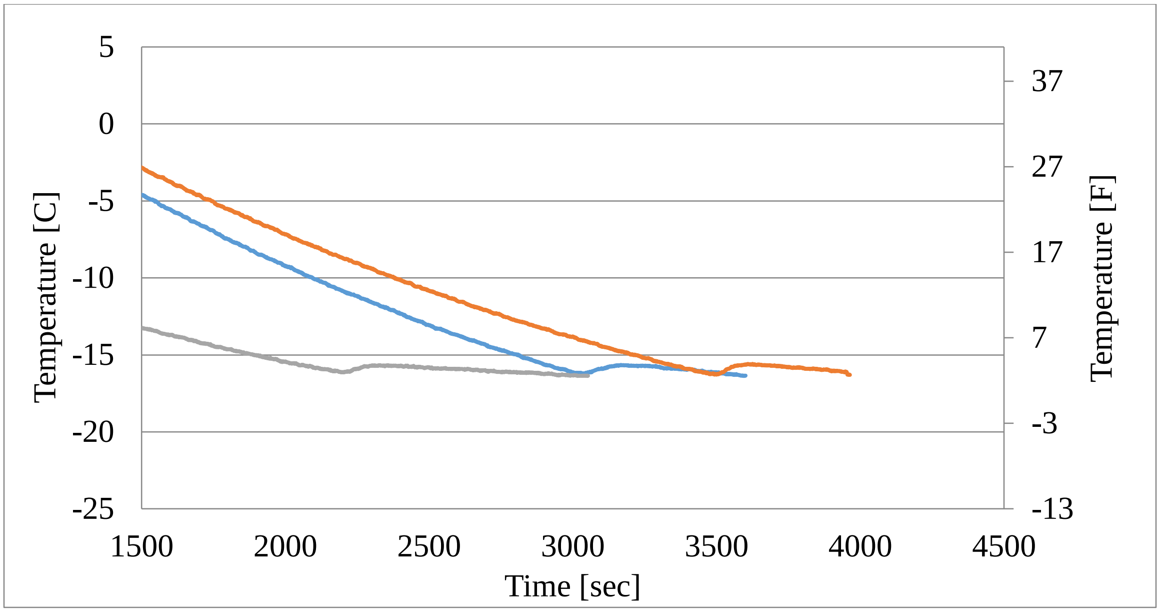

Figure 3.7: Freezing point of solution with 18.70% NaCl

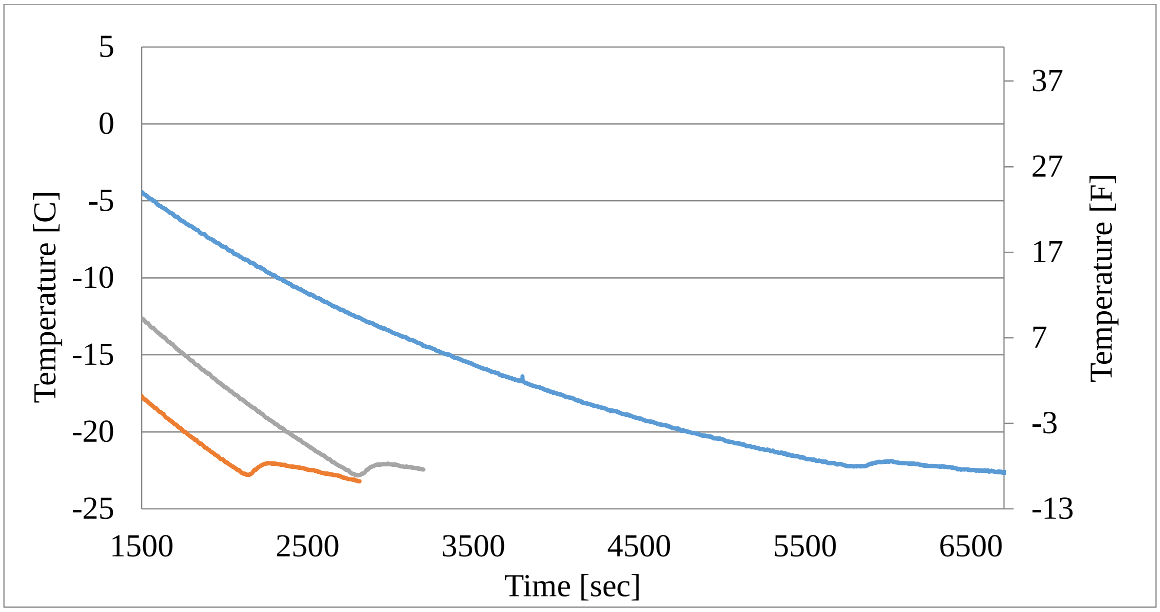

Figure 3.8: Freezing point of solution with 23.00% NaCl

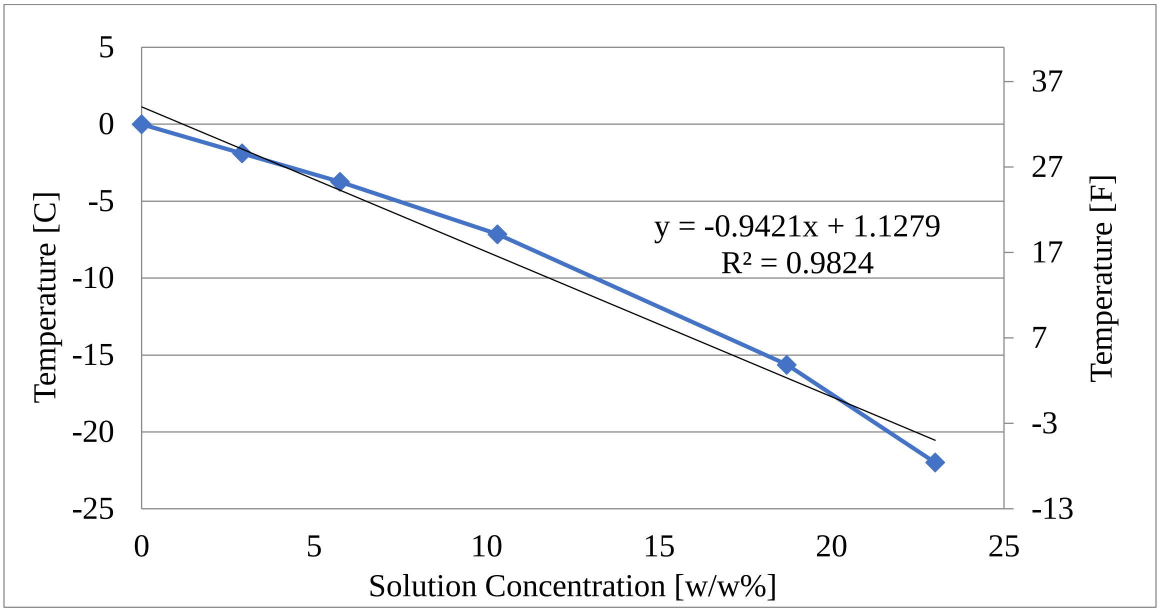

Figure 3.9: Relationship between solution concentration and freezing point

3.2 Ice Melting Capacity of Deicing Solutions

The second aspect of deicer effectiveness that was measured in this study is thawing capacity. For this test, two methods outlined by the Strategic Highway Research Program in the "Handbook of Test Methods for Evaluating Chemical Deicers" were employed (Chappelow, McElroy et al. 1992). For solid deicers, Method H-205.1 "Test Method for Ice Melting of Solid Deicing Chemicals" was used. For the brine solution, Method H205.2, "Test Method for Ice Melting of Liquid Deicing Chemicals" was used. In both test protocols, the procedure entails preparing pans of ice at a variety of temperatures, adding the deicing agent and measuring the quantity of ice melted after ten minute time intervals up to one hour. The experiment occurs within a temperature controlled chamber. The mass of ice melted is measured by removing liquid from the pan and measuring its quantity in a syringe. The melted solution is then replaced so the brine can continue melting more ice. The results are given as the quantity of ice melted normalized by the quantity of deicing agent applied to the ice surface.

For this work, the experiment was executed in a Cincinatti Sub Zero (CSZ) environmental chamber fitted with a custom door as shown in Figure 3.10. This equipment is capable of measuring and maintaining internal temperatures to 0.1ºC within the -3.9ºC to -15º range required for the test. The custom door allowed the test operator to manipulate the ice pans inside the chamber without opening the door or causing a change in internal temperature. The interior of the chamber is shown in Figure 3.11. Six pans of ice fit in the unit at one time.

Figure 3.10: Environmental Chamber used for freezing tests

Figure 3.11: Interior of environmental chamber and pans containing ice and deicing agent

The pans of ice are each 22.9 cm (9") in diameter. Each was filled with 0.32 cm (1/8") ice by adding 130 ml of water and then freezing it overnight at the target test temperature. The SHRP test method recommends the quantities of deicer that should be used for each test type. For the solid deicer tests, 4.17 g of deicer was applied and for the liquid deicer tests, 3.8 ml of solution was applied. The solid deicers included salt and salt-sand mixes prepared with materials supplied by NCDOT. The purity of the rock salt in the sample collected from NCDOT was not verified; however it is required to be at least 95% per trade specifications. The salt-sand mix was prepared by blending 2.085 g of rock salt with 2.085 g of silica sand. The brine was prepared as a 23% (w/w) solution using the same salt provided by NCDOT mixed with deionized water. Figure 3.12 shows the salt-sand mixture prior to adding it to the samples. Each of the deicers was preconditioned to 0ºC (32ºF) prior to applying them to the surface of the ice samples.

The test protocol was started by adding the deicing agent to the pan of ice. After ten minutes, the pan was tilted to a 45º angle to allow any melted ice to drain to the bottom of the pan. It was collected in a syringe and quantified by weighting to 0.0001g. The melted ice was then quickly returned to the pan and the pan was untilted to flat. Measurements were made after 10, 20, 30, 45 and 60 minute intervals.

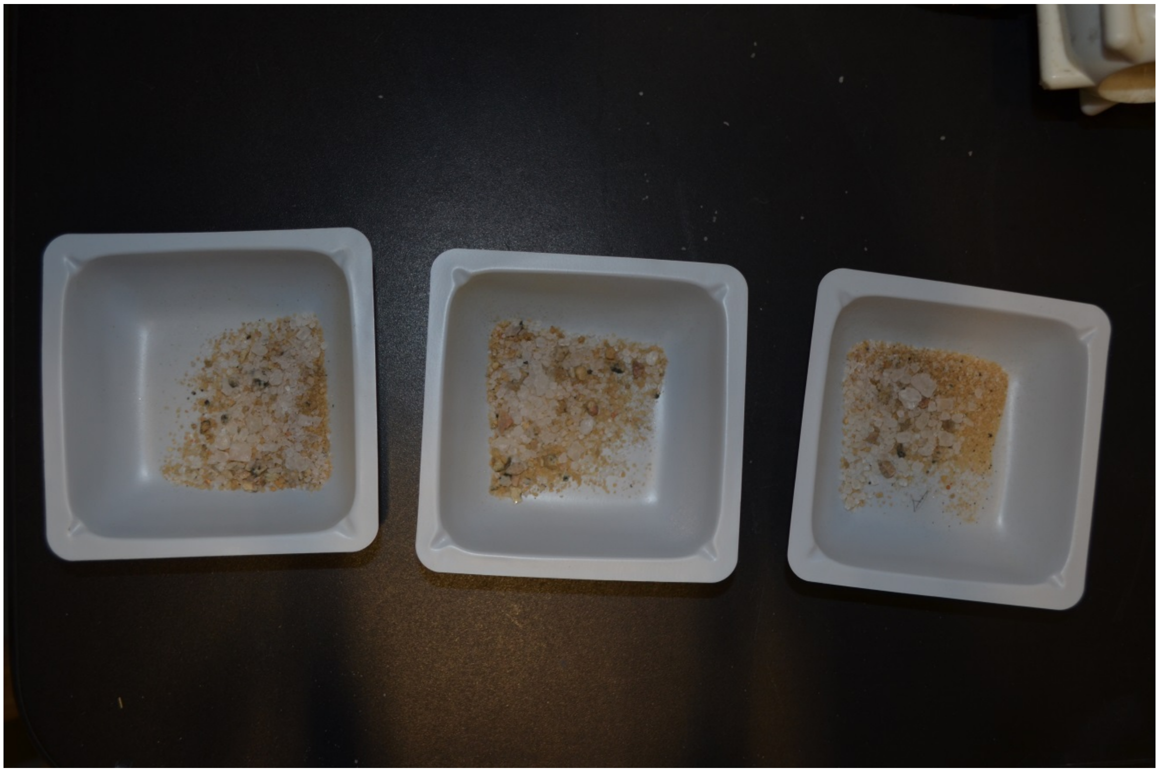
Figure 3.12: Portioned deicing materials (salt-sand mix shown)

The results of the ice melting tests are shown Table 3.2, Table 3.3, and Table 3.4. The values presented have been adjusted for the mass of dissolved deicer present in each so that they only represent the quantity of ice melted. Results are also plotted in Figure 3.13, Figure 3.14 and Figure 3.15. These Figures are presented with units of mass of ice melted per mass of salt applied. Thus, each of the applications is normalized for the total amount of salt that it contains. It is apparent that the two granular applications, salt and salt-sand, have equivalent performance when evaluated in this normalized fashion. Although, the un-normalized data presented in Table 3.2, Table 3.3, and Table 3.4 shows that the amount of ice melted by the salt only application was twice that of the salt-sand application since the salt-sand mix contains only half the deicing agent. Negative values associated with the brine measurements indicate that less solution was recovered than was initially added. This is expected since some small film of brine adheres to the ice.

When viewing the results normalized by salt content, the differences in the performance of the brine mixtures and the granular applications are also notable. Figure 3.13 shows that the brine treatment was unable to melt any ice when applied at -15ºC (5ºF) although the granular treatments did melt small quantities. In the case of the brine applied to -15ºC (5ºF) ice in this test, the brine simply remained ponded on top of the ice disk throughout the test. Although both materials should perform in a similar fashion at this low temperature, the solid applications outperformed the liquid application. It is possible that the rock salt contained impurities that generated small amounts of heat as they dissolved. Also, the salt was delivered at a temperature of 0ºC (32ºF), which means it could have warmed the area around each grain sufficiently to cause melting and initial dissolution.

Table 3.2: Ice melted by Brine (B1-B3), Salt (S1-S3) and Salt-Sand (SS1-SS3) after 10, 20, 30, 45 and 60 minutes at -15.0ºC (5.0ºF)

Time:	10 Minutes		20 Minutes		30 Minutes		45 Minutes		60 Minutes	
	Ice Melted [g]	Ice Melted per g salt added [g]	Ice Melted [g]	Ice Melted per g salt added [g]	Ice Melted [g]	Ice Melted per g salt added [g]	Ice Melted [g]	Ice Melted per g Salt added [g]	Ice Melted [g]	Ice Melted per g salt added [g]
B1	-0.35	-0.32	-0.96	-0.87	-0.80	-0.72	-0.92	-0.84	-0.89	-0.80
B2	-0.87	-0.81	-0.88	-0.83	-0.60	-0.56	-0.61	-0.58	-0.37	-0.35
B3	0.44	0.40	0.33	0.30	0.29	0.26	-0.90	-0.82	-0.38	-0.34
Avg.	-0.26	-0.24	-0.50	-0.47	-0.37	-0.34	-0.81	-0.74	-0.55	-0.50
S1	1.40	0.34	2.33	0.56	3.72	0.90	3.72	0.90	4.65	1.13
S2	0.93	0.26	1.86	0.52	1.86	0.52	1.86	0.52	3.72	1.04
S3	1.86	0.47	3.72	0.93	4.19	1.05	5.58	1.40	6.51	1.63
Avg.	1.40	0.35	2.64	0.67	3.26	0.82	3.72	0.94	4.96	1.27
SS1	0.00	0.00	3.00	1.44	4.21	2.01	4.10	1.96	5.38	2.57
SS2	-0.01	0.00	0.00	0.00	0.30	0.14	0.89	0.42	1.30	0.61
SS3	-0.05	-0.02	0.27	0.13	0.47	0.23	0.62	0.30	1.13	0.54
Avg.	-0.02	-0.01	1.09	0.52	1.66	0.79	1.87	0.89	2.60	1.24

Table 3.3: Ice melted by Brine (B1-B3), Salt (S1-S3) and Salt-Sand (SS1-SS3) after 10, 20, 30, 45 and 60 minutes at -9.4ºC (15.1ºF)

Time:	10 Minutes		20 Minutes		30 Minutes		45 Minutes		60 Minutes	
	Ice Melted [g]	Ice Melted per g salt added [g]	Ice Melted [g]	Ice Melted per g salt added [g]	Ice Melted [g]	Ice Melted per g salt added [g]	Ice Melted [g]	Ice Melted per g Salt added [g]	Ice Melted [g]	Ice Melted per g salt added [g]
B1	1.90	1.56	2.02	1.66	2.23	1.84	2.17	1.79	2.15	1.77
B2	2.06	1.77	2.81	2.42	2.66	2.28	2.73	2.34	2.77	2.38
B3	2.00	1.73	1.61	1.39	1.93	1.67	1.81	1.57	2.07	1.79
Avg.	1.99	1.69	2.15	1.82	2.27	1.93	2.24	1.90	2.33	1.98
S1	3.61	0.91	6.46	1.62	9.50	2.39	12.35	3.10	14.25	3.58
S2	6.18	1.58	10.45	2.67	12.35	3.15	15.96	4.07	16.15	4.12
S3	4.75	1.22	8.55	2.20	11.21	2.89	13.49	3.48	14.73	3.80
Avg.	4.85	1.24	8.49	2.16	11.02	2.81	13.93	3.55	15.04	3.83
SS1	3.67	1.75	6.41	3.06	8.05	3.84	9.75	4.65	10.46	4.99
SS2	3.80	1.82	6.07	2.91	7.17	3.43	9.04	4.33	10.22	4.90
SS3	5.12	2.45	7.52	3.61	8.22	3.94	8.86	4.25	9.17	4.40
Avg.	4.19	2.01	6.67	3.19	7.81	3.74	9.22	4.41	9.95	4.76

Table 3.4: Ice melted by Brine (B1-B3), Salt (S1-S3) and Salt-Sand (SS1-SS3) after 10, 20, 30, 45 and 60 minutes at -3.9ºC (25.0ºF)

Time:	10 Minutes		20 Minutes		30 Minutes		45 Minutes		60 Minutes	
	Ice Melted [g]	Ice Melted per g salt added [g]	Ice Melted [g]	Ice Melted per g salt added [g]	Ice Melted [g]	Ice Melted per g salt added [g]	Ice Melted [g]	Ice Melted per g Salt added [g]	Ice Melted [g]	Ice Melted per g salt added [g]
B1	7.59	6.66	4.70	4.12	16.09	14.12	15.96	14.00	15.72	13.78
B2	8.78	7.45	16.05	13.62	16.96	14.39	16.81	14.26	16.60	14.09
B3	8.01	6.44	15.78	12.68	16.83	13.52	17.00	13.66	16.61	13.35
Avg.	8.13	6.85	12.17	10.14	16.63	14.01	16.59	13.97	16.31	13.74
S1	16.30	3.94	26.68	6.44	32.01	7.73	40.74	9.84	42.68	10.31
S2	13.58	3.19	23.28	5.46	32.01	7.51	38.80	9.11	41.71	9.79
S3	11.25	2.74	23.28	5.68	31.04	7.57	37.83	9.23	44.62	10.88
Avg.	13.71	3.29	24.41	5.86	31.69	7.61	39.12	9.39	43.00	10.33
SS1	6.45	3.09	14.02	6.72	15.78	7.56	18.97	9.09	20.97	10.05
SS2	7.98	3.83	14.64	7.03	18.09	8.69	21.30	10.23	21.82	10.48
SS3	7.00	3.36	11.92	5.72	15.59	7.49	17.71	8.50	19.38	9.31
Avg.	7.14	3.43	13.53	6.49	16.49	7.91	19.33	9.28	20.72	9.95

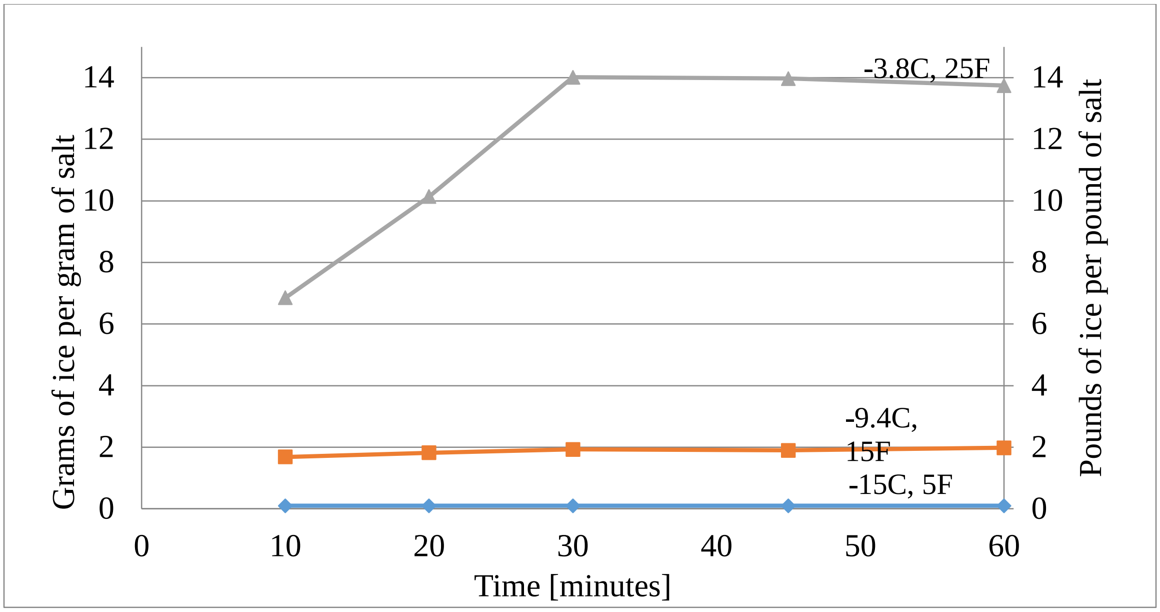

Figure 3.13: Ice melting rate of 23% brine solution at -3.8C, -9.4C and -15C

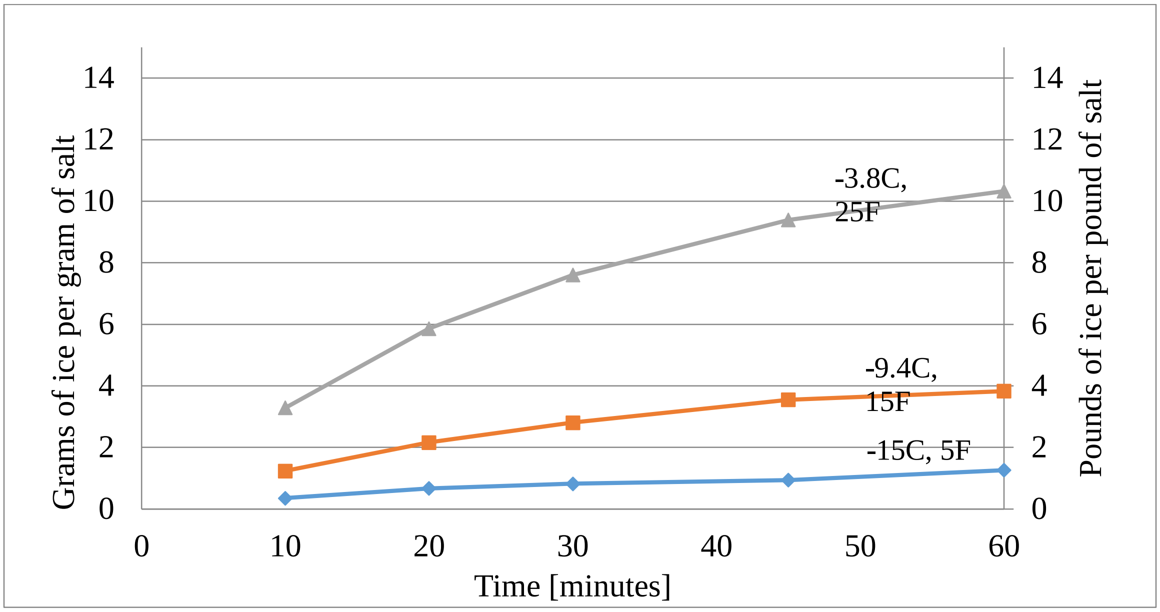

Figure 3.14: Ice melting rate of granular salt at -3.8C, -9.4C and -15C

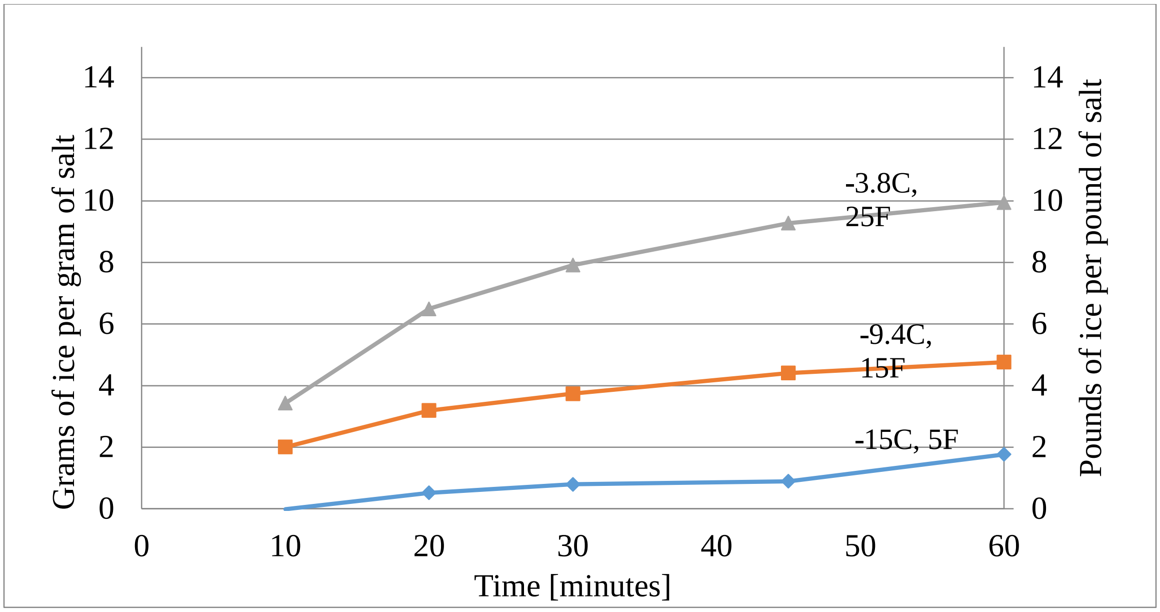

Figure 3.15: Ice melting rate of salt-sand mix at -3.8C, -9.4C and -15C

In order to compare the relative ice melting rates of the three treatments, Figure 3.16, Figure 3.17 and Figure 3.18 present the treatments together at each temperature range tested. In these plots, it is also apparent that the salt and salt-sand treatments have essentially equivalent performance since the quantity of salt applied is normalized. Figure 3.18 shows the improved performance of the brine at the higher temperature, -3.8ºC (25ºF). In this case, the brine very rapidly melted 14 times as much ice as the mass of salt applied. However, it then becomes too diluted to melt any more.

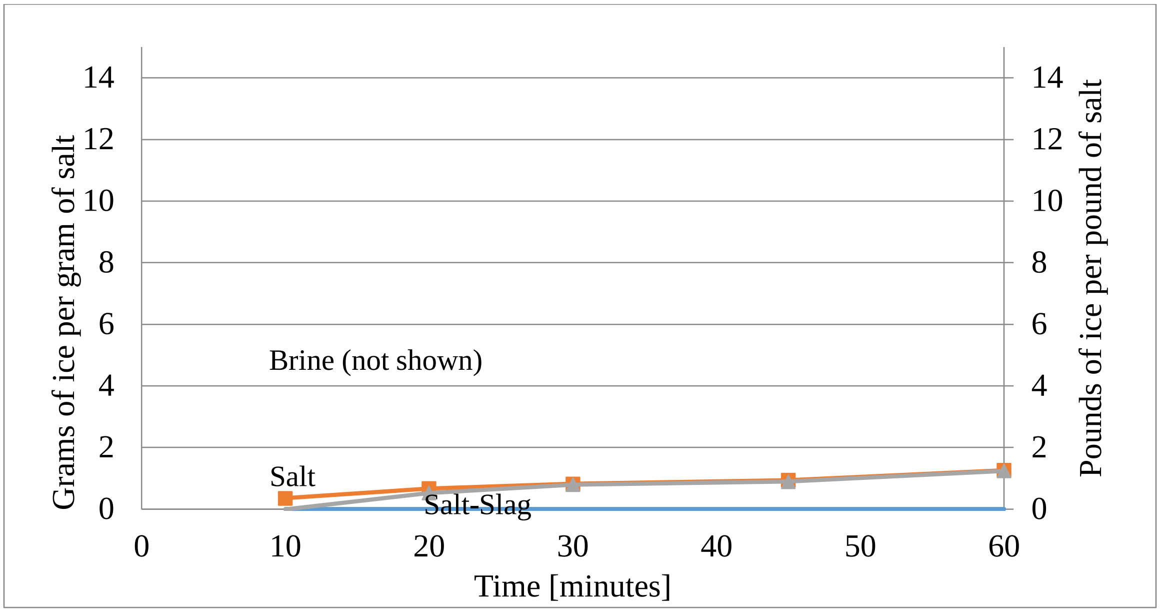

Figure 3.16: Relative ice melting rate of three deicers at -15ºC (5ºF)

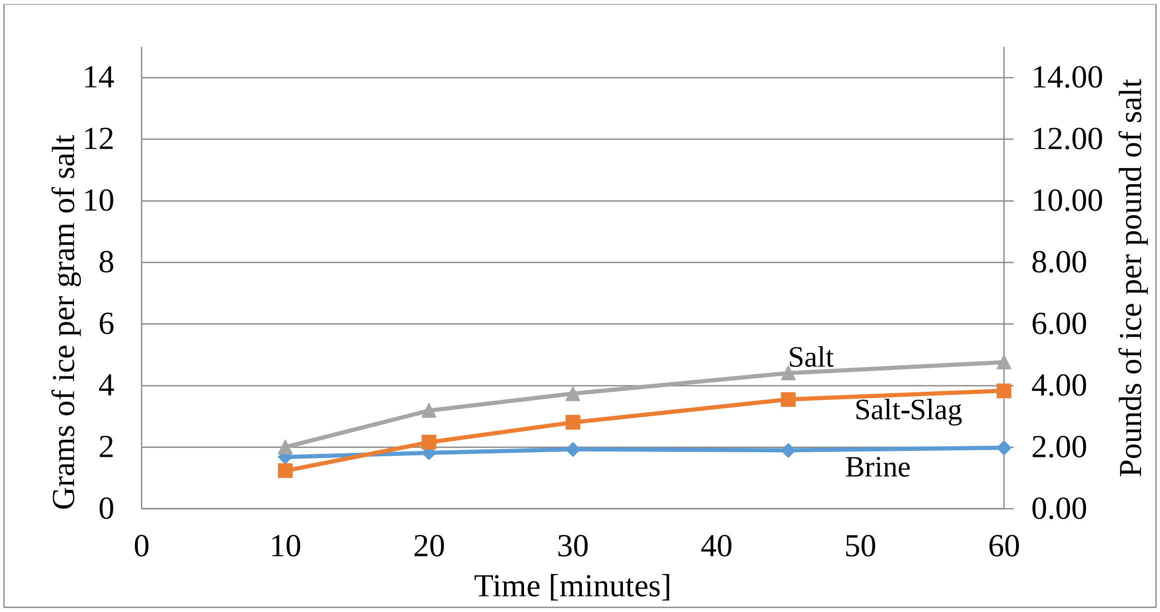

Figure 3.17: Relative ice melting rate of three deicers at -9.4ºC (15ºF)

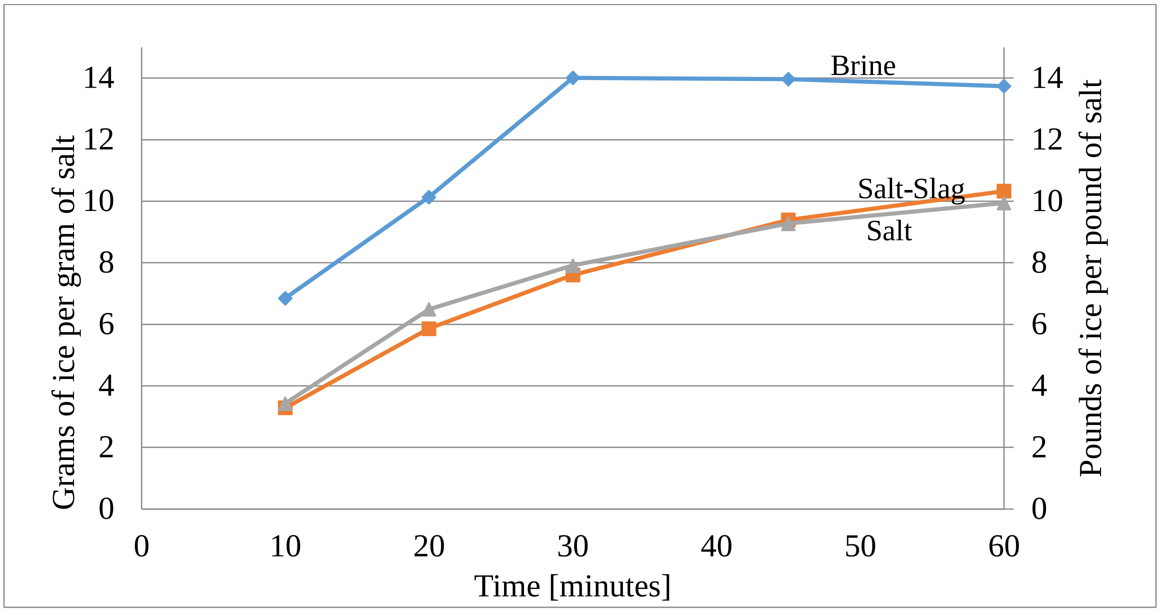

Figure 3.18: Relative ice melting rate of three deicers at -3.8ºC (25ºF)

The previous Figures have been presented in a normalized fashion in order to highlight the key differences between the performances of crystalline salt applications and dissolved salt applications. Presented as values normalized by units of deicer applied, these do not easily compare the ice melting power of the treatment in the concentration that it is typically applied by NCDOT. Using application rates of 150 lb/lane mile for salt and salt-sand mixes and 35 gallons/lane mile for brine applications, the quantity of salt applied to the unit area of the ice pans use in the experiment was computed. The mass of ice melted at the three temperature ranges presented above for each of the actual application rates are shown in Figure 3.19, Figure 3.20 and Figure 3.21. It is apparent that all three deicers melt very little ice at temperatures below -9.4ºC

(15ºF). Brine became quite effective for ice melting in the -3.8ºC (25ºF) test, however, the granular salt melted more ice due to the greater quantity of salt associated with its application method.

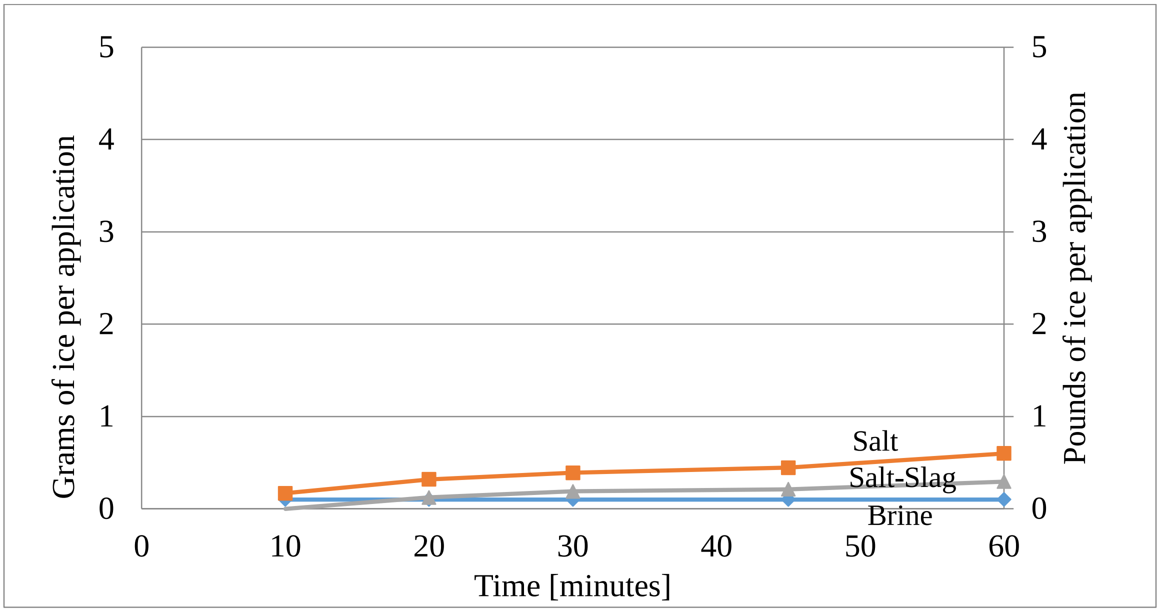

Figure 3.19: Ice melting at application rates used by NCDOT for -15ºC (5ºF)

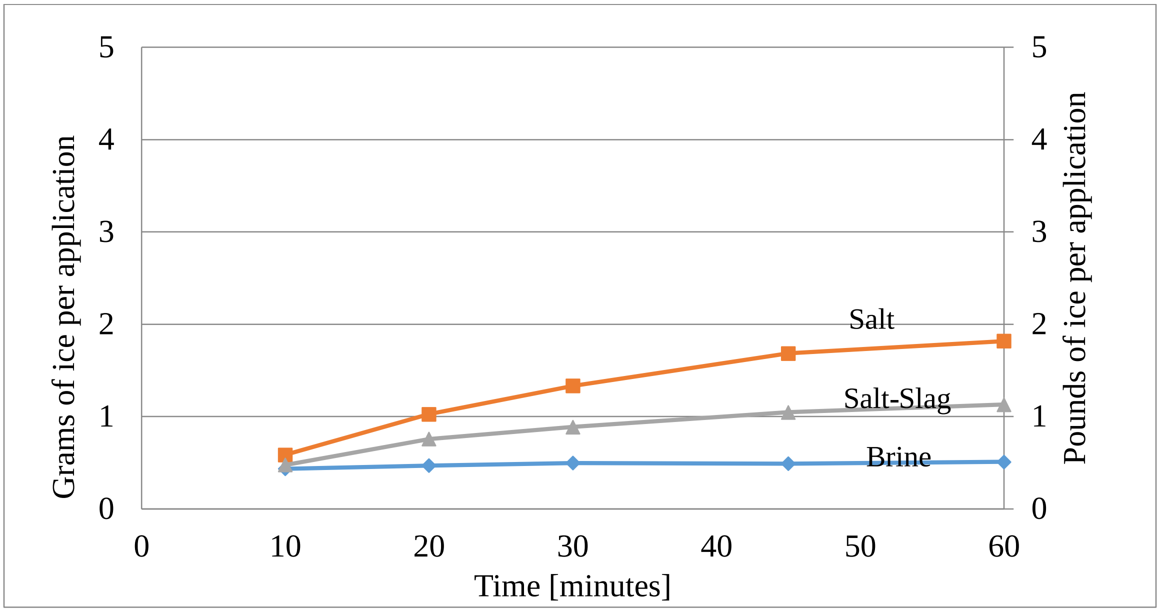

Figure 3.20: Ice melting capacity at typical application rates for -9.4ºC (15ºF)

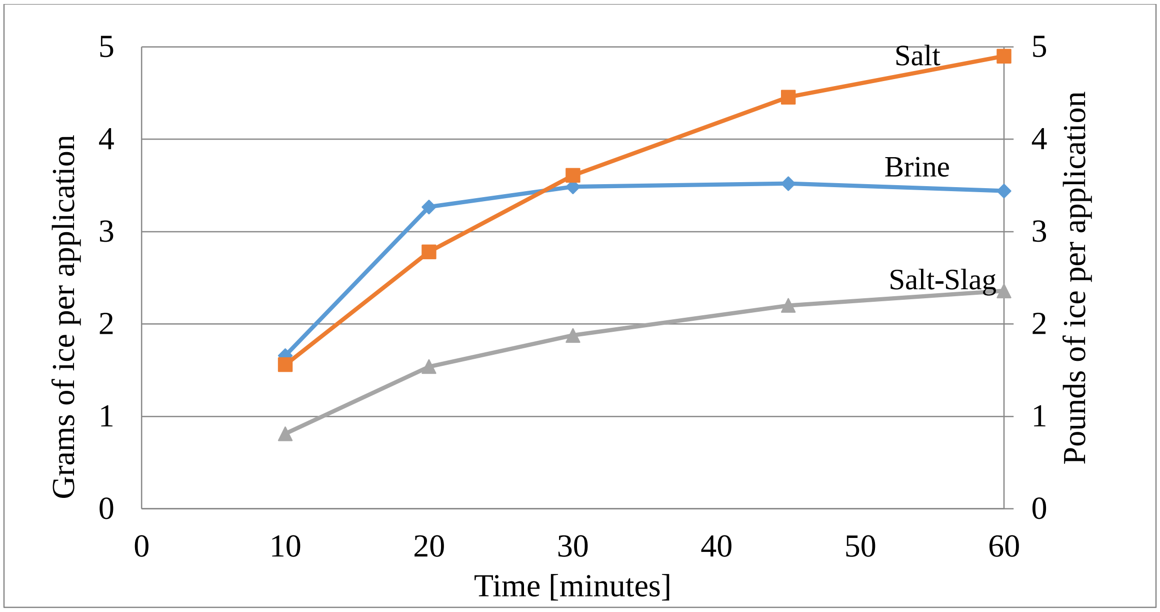

Figure 3.21: Ice melting capacity at typical application rates for -3.8ºC (25ºF)

3.3 Conclusions

Key conclusions from the experiments presented in this section mirror the anecdotal observations of deicers used in the field.

- The freezing point of salt solutions is lowered as the concentration of the salt increase. Pure water freezes at 0°C. When the solution is saturated with sodium chloride, the freezing point is reduced to -21.986 °C. The relationship of concentration and freezing point for concentrations between 0% and 23% is essentially linear for practical purposes.
- The ice melting capacity of deicing applications is directly related to the quantity of salt that is applied per unit area of roadway. Brine solutions underperformed granular applications at low temperatures below -9.4°C, but outperformed at higher temperatures. This effect observed in the laboratory may be an artifact of the test methods used since there is not a theoretical basis for the behavior.
- At the application rates often used for ice clearance in NC, the granular salt application shows the greatest ice melting capacity.

4 Corrosive Effects on Reinforced Concrete Components

The corrosive effects of deicing and anti-icing treatments on reinforced concrete are strongly related to the onset of corrosion in the reinforcing steel being accelerated by the actions of chlorides. Although deicing treatments are known to cause deleterious effects on the concrete itself, such as scaling, these impacts were outside of the scope of this project. The investigation presented here was undertaken as a combination of laboratory-based experiments as well as field-based observations made to distinguish whether there are significant differences between the corrosive impacts of the three deicing materials. Within the laboratory, concrete specimens were exposed to freeze-thaw-flush cycling with regular application of deicing treatments. After 490 freezing cycles, the specimens were removed and the accumulated chloride was measured along a series of points within the first inch of concrete depth. In the field, chloride concentrations were likewise measured at the surface and at shallow depths prior to a salting season and again after the salting season. Differences were used to estimate the yearly build-up of chlorides within the concrete as a result of a known number of road salt applications.

4.1 Laboratory Investigation of Chloride Ingress

Applications of sodium chloride deicing and anti-icing strategies under controlled freeze-thaw cycles were proposed to generate data on the transport of chloride ions related to each treatment type on samples that mimic concrete bridge decks. The study was conducted on a typical bridge deck concrete mix with embedded reinforcing steel. The deicing treatments for the study included brine, granular, and granular-sand mix. This section presents the methodology and experimental results obtained from simulation of typical winter exposure including: cycles of freeze-thaw temperatures, wetting and drying, and snow followed by deicing applications. Analysis of the data is presented to evaluate the variation in diffusion of chloride ions for each deicing and anti-icing application strategy.

4.1.1 *Standardized Method for Assessing Chloride Ingress and Corrosion in Reinforced Concrete Specimens*

The standard method for studying the effects of chemical admixtures on embedded steel reinforcement is outlined in ASTM G109, Determining Effects of Chemical Admixtures on Corrosion of Embedded Steel Reinforcement in Concrete Exposed to Chloride Environments (ASTM 2013). The test is used to evaluate the corrosivity of embedded metals in concrete exposed to different corrosive environments. The test is set up for a chosen concrete mixture proportion and steel cover that allows chlorides to ingress from the top of the sample surface and to proceed to the steel rebar. The source for the chlorides is a 3% solution ponded in a dam on top of the test specimen. Each test specimen includes one top rebar as an anode for corrosion current and two bottom-rebars as the cathode. Evaluation of steel corrosion is performed by measuring the voltage across the rebars and calculating the current across a connected 100 Ω resistor between the top and bottom rebars. The current is monitored over the testing period or until a sufficient amount of corrosion is occurring for visual evaluation.

The test method used in this study utilized the specimen setups and preparation described above. However, specimens were exposed to chloride through simulation of typical winter deicing treatments. Instead of ponding testing solution inside the dam, each testing surface was exposed to cycles of above freezing and below freezing temperatures, snow application, deicing treatments, and water flushing. Each cycle was designed to simulate typical highway bridge exposure during a snow event. In addition to monitoring the voltage across the attached resistor, Rapid Chloride Test (RCT) of the concrete surface was performed to analyze chloride content.

4.1.2 ***Preparation of Test Specimens***

Preparation of test specimens was similar to procedures outlined in ASTM G109. Specimens size were 11 x 6 x 4.5 inches with one reinforcement bar placed centered at 1 in. from the top and two bars placed 1 in. from the bottom and ¾ in. from the side. The steel reinforcements used were deformed 0.5 in. diameter rebars. Each bar was wire brushed to bare metal to remove contaminants, rust and mill scale. Bars were trimmed to 14 in. Each bar was drilled and tapped on one end and attached with a stainless steel screw and nut for the electrical connection. Electroplaters tape was used to cover the end of each bar leaving a middle portion of 8 in. in bare steel. In addition, 3.5 in. of neoprene tubing was used to cover the ends of each bar over the taped portion. The process exposed about 8 in. of steel to be tested and eliminate effects from the bar's ends. The protruding tubing at each end was sealed with silicone. Wood molds were prepared for each specimen with holes positioned to support the rebars in place during casting. Figure 4.1 shows preparation of the bar and mold.

A special specimen was prepared to measure the internal temperature fluctuations within the concrete specimens. A mold that did not contain reinforcing bars was also prepared to be cast with temperature sensors placed along the height of the specimen, as shown in Figure 4.2. Temperature sensors were placed in two columns, one at the center and another halfway between the center and outer face. Each column contained 5 sensors at one inch increment with the first sensor placed 0.5 in. from the bottom of the wood mold. Temperature sensors used were Vishay precision thermistors. Table 4.1 shows the resistance values for the thermistor used at different temperatures. There were a total of 13 test specimens: three for controls, three for each of the three deicing application type, and one for use as the temperature sensor.

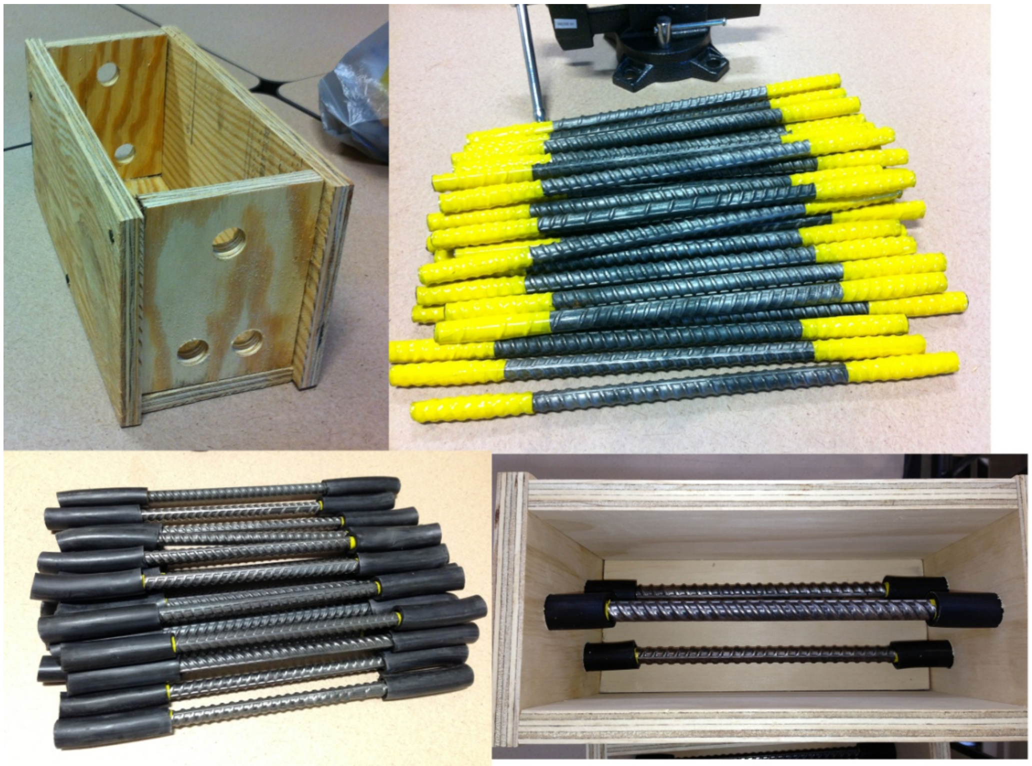

Figure 4.1: Preparation of reinforced bars and wood molding

Table 4.1: Resistance values of thermistors

Temp (°C)	Rt Ω
-15	15,950
-10	12,110
-5	9,275
0	7,162
5	5,574
10	4,372
15	3,454
20	2,747

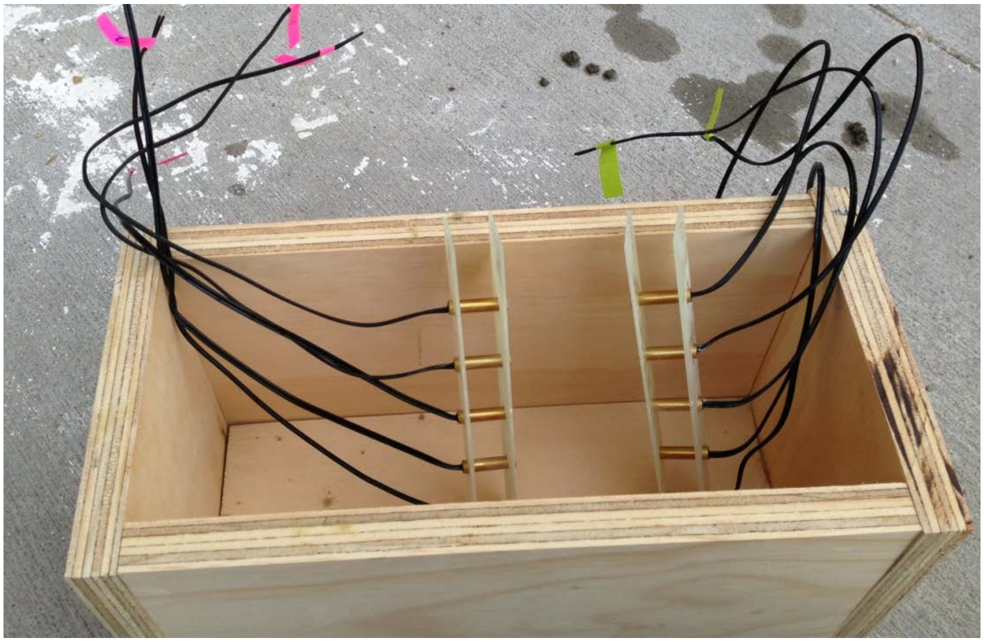

Figure 4.2: Molding for temperature sensor

The concrete mix used is presented in Table 4.2 and was replicated from a concrete deck mix approved by NCDOT for piedmont area bridges. The air-entraining admixture (MB-AE 90) from BASF was used to obtain 6% air content. The total volume of the batch prepared was 3.7 cubic feet. In addition to casting the thirteen specimens required for testing, 4”x8” cylinders to used for compressive strength testing were also prepared. An electric concrete mixer was used to mix the concrete. The final slump and air content measured were 0.5 inches and 6 %, respectively. To help consolidate the concrete, a vibration table was also used when filling the wood mold, Figure 4.3.

Table 4.2: Concrete mixture proportions used for cyclic testing specimens

Material	Quantity [lb/yd^3]
Coarse Aggregate – #78m	1,736
Fine Aggregate – Silica sand	1,152
Cement- Type ½	677
Water	340
Admixture – BASF MB-AE 90	

Figure 4.3: Pouring of concrete specimens

The specimens were allowed to cure for 28 days submerged in lime saturated water followed by two weeks of drying aging at 50% relative humidity and 22.8ºC (73ºF) ambient conditions. A 100 Ohm resistor was electrically connected to each test specimen between the top re-bar and the two bottoms re-bar. Plexiglass was used to create a dam on top of each of the 12 specimens. The dams were 7.62cm (3”) wide and 15.24 cm (6”) long with a height of 7.62cm (3”). Epoxy was used to seal the dam to the top of the specimen. Sika Top Seal 107 was used to seal the surface outside of the dam. Figure 4.4 shows the completed specimens loaded in the environmental chamber.

A compressive strength test was performed on the 10.16x20.32 cm (4 x 8”) cylinders to ensure a high enough compressive strength for a deck-mix. Two cylinders were tested after the curing period and were found to have achieved 43 MPa and 48 MPa (6,278 and 6,975 psi) compressive strength.

Figure 4.4: Finished specimens with attached wires and resistors

4.1.3 ***Experimental Test Program***

Prepared specimens were labeled for three controls, three samples for brine application, three samples for granular salt application, and three samples for salt-sand mix. The control samples included two blocks that were exposed to the freeze thaw cycle conditions but had only snow applied without deicing materials. The other control sample was maintained at room temperature with 400 mL of 3% salt solution for two week ponding and drying cycles, as described in ASTM G109.

The test program attempted to simulate field exposure on concrete bridge decks during a typical winter season in North Carolina. Weather features considered when preparing the program included: temperature cycling, above and below freezing temperature (freeze-thaw action), precipitations (rain and snow with wet-dry action), and deicing treatments (brine, granular salt, and salt-sand mix). To create an exposure regimen representative of North Carolina winters, weather information and winter deicing practices were considered. Weather information was obtained from 1991 to 2011 for the city of Asheville, NC through Weather Underground, a weather data service (24) The study examined winter seasons over the months of November through March over the 20 year period. The average amount of snow precipitation for one snow event was found to be 0.31 inches (Figure 4.5). Average temperatures were found to be -0.13°C (31.76°F) for the daily minimum and 11.31°C (52.36°F) for the daily maximum over the entire selected winter season. Out of the 3,019 days in the study, 1,557 days have a minimum temperature that is below freezing and a high that is above freezing temperature. Temperatures on days that indicated a snow event have an average minimum of -4.44°C (24°F) and a maximum of 3.33°C (38°F). Further studies of weather information were performed for the first 10 winter seasons (1991-2001) from the 20 years of weather data. The average number of snow or ice and rain events per season is shown in Table 4.3.

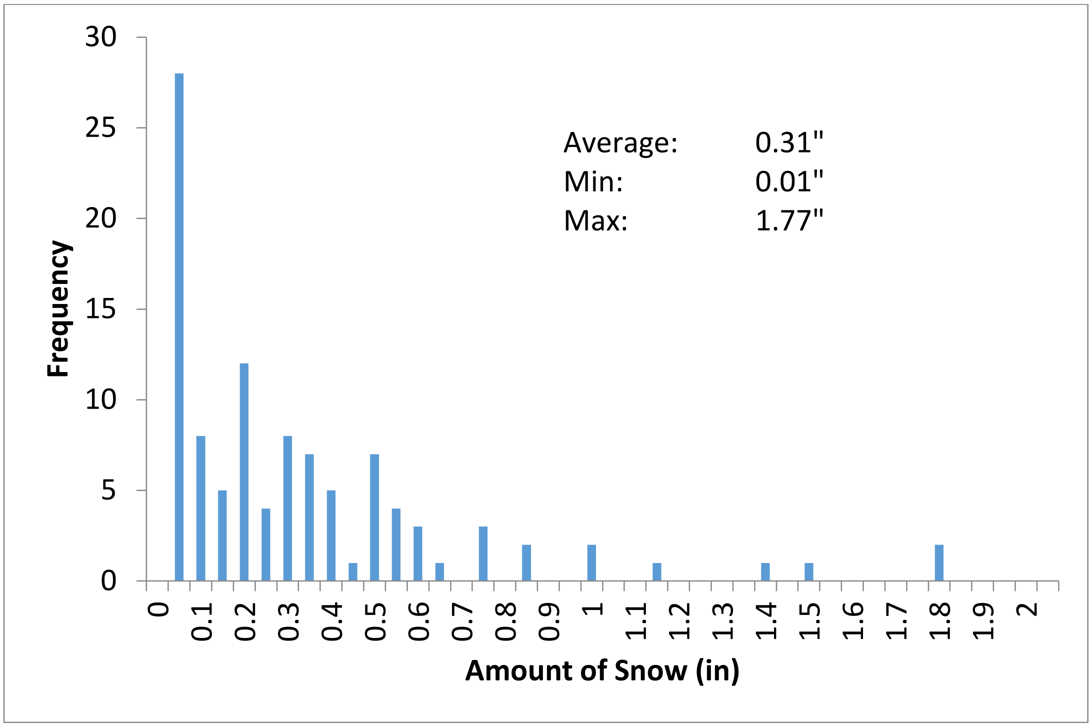

Figure 4.5: Amount of snow precipitation per event for 1991-2011 in Asheville, NC

Table 4.3: Details of typical winter conditions for Asheville, NC (1991-2001)

Winter Season #	1	2	3	4	5	6	7	8	9	10	
											AVG
Average Snow (in)	0.07	0.25	0.43	0.26	0.45	0.19	0.29	0.21	0.28	0.26	0.27
Average days between snow	32.75	23.25	9.89	4.69	4.55	15.83	11.44	13.14	24.80	13.44	15.38
Total snow events	5	5	10	14	30	7	10	8	6	10	10.50
Total snow (in)	0.37	1.25	4.33	3.67	13.36	1.31	2.92	1.64	1.66	2.55	3.31
Average Rain (in)	0.46	0.44	0.50	0.41	0.36	0.41	0.43	0.31	0.34	0.38	0.40
Average days between rain	4.17	2.94	3.87	2.92	2.57	2.88	2.92	3.04	4.14	4.06	3.35
Total rain events	37	52	39	51	59	53	50	50	37	36	46.40
Total rain (in)	16.9	22.91	19.37	20.76	21.4	21.54	21.59	15.72	12.71	13.78	18.67

Deicing material applications included 23% brine solution applied at a rate of 35 gallons per lane-mile, granular salt at a rate of 150 pounds per lane-mile, and 50%/50% salt-sand mix applied at 150 pound per lane-mile. For the exposed surface area of 3”x6” inside the dam, the application rate used were 0.78 mL of 23% brine, 0.402 gram of granular salt, and 0.201 gram of salt plus 0.201 grams of sand for salt-sand mix. These values were scaled up by three times from the actual rates for practical measurement and distribution on the test surface as well as a way to accelerate corrosive effects.

The cycle was set up to repeat during a 24 hour period, which included flushing with water (as by rain), deicing applications, and snow precipitation. Figure 4.6 shows the full one 24 hours cycle for the test program. The temperature was set to cycle between -6°C and 3°C (21.2°F - 37.4°F) in a sinusoidal wave pattern. The temperatures selected were lower than the average daily low for days that indicated a snow event to account for temperature lag on the concrete surface and ensuring adequate freeze-thaw actions. Each daily cycle consisted of seven freeze-thaw actions. The test program ran for 70 days. According to Asheville weather data, for a typical 20 years there are 1,557 freeze-thaw cycles; with a total of 490 simulated freeze-thaw cycles the approximate amount of years simulated by this experiment is 6.29. The total number of simulated snow events is 70, which can be approximated as 6.67 years based on the historical analysis of the average number of snow fall annually. The whole test program can be summarized as having an average simulated time of 6.5 winter seasons with three times the normal deicing application rate.

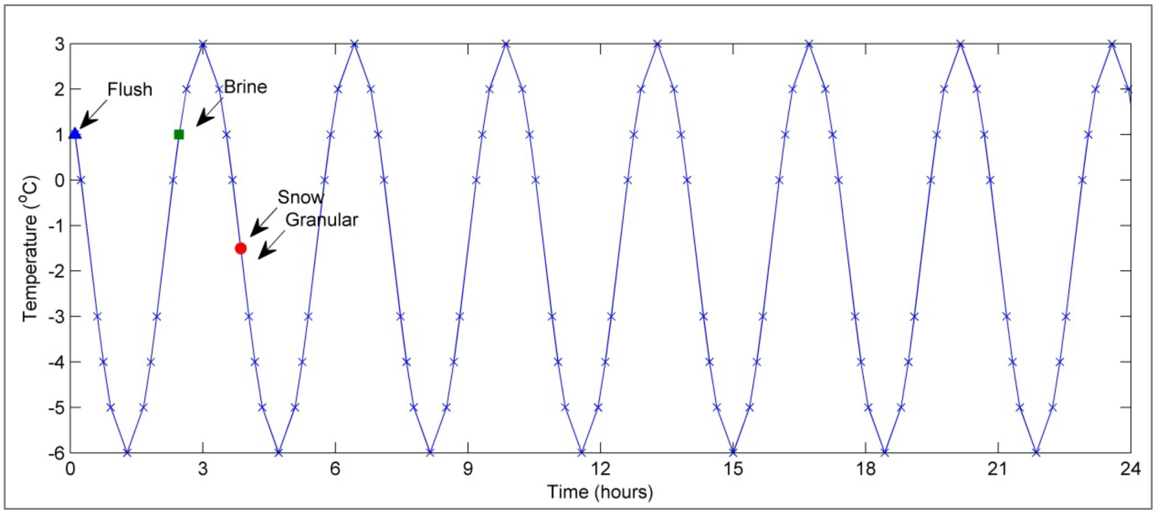

Figure 4.6: Environmental chamber setup for one cycle

The start of the cycle consisted of flushing (as by rain) while the temperature was set to 1°C (33.8°F). Flushing was performed by flooding the test surface with water, syringing the solution out of the Plexiglas dam, and then removing excess water with paper towels. Brine was applied 2.5 hours after flushing, when the chamber temperature reached 1°C (33.8°F). The concrete surface was dry at the time the brine was applied, as would be typical during field practices. Brine was applied by spraying the measured quantity of solution on the concrete surface using a syringe. This application technique provided for a generally uniform application of the brine across the dammed surface of the specimens. Snow was applied 1.5 hours after brine application when the temperature again declined below freezing. The chamber temperature at the time of snow application was -1.5°C

(29.3°F) with concrete surface temperature at 0.6°C (33.08°F). Snow was applied using 100 mL cup from finely crushed ice. Specimens receiving granular or salt-sand mix applications received measured quantities of the deicing chemicals applied manually on top of the snow. The cycle continued to alternate between high and low temperatures until another flush.

During the experiment, data acquisition was achieved by using Campbell Scientific data logger to monitor and record voltage differentials between the rebars and thermistor circuits at one minute intervals (Figure 4.7). In addition, current chamber temperature and humidity were recorded using the chamber's built-in sensors.

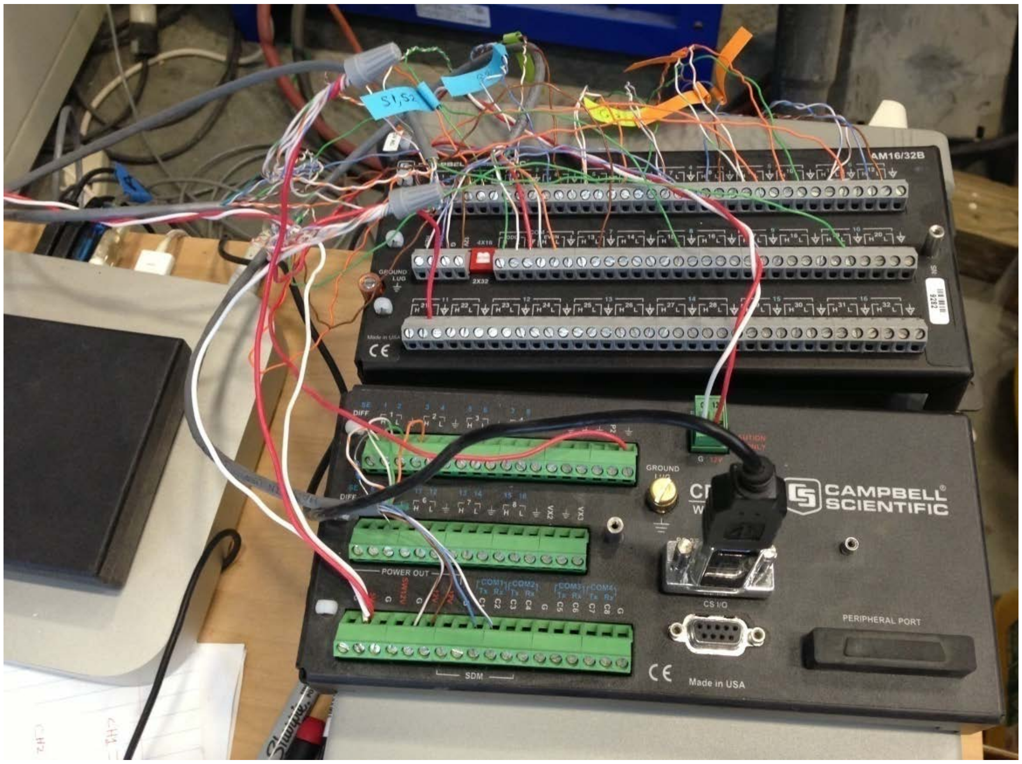

Figure 4.7: Data logger used to record voltage readings

Thermistor circuits were set up with a7.5 kΩ resistor connected in series with the thermistor and 5 V running through the circuit. Voltage measurements were measured across the 7.5 kΩ resistor by the data logger (Figure 4.8). The thermistor resistances were calculated according to Equation 4.1:

$$Rt = \frac{(V)Rr}{Vr} - \mathrm{Rr} \tag{4.1}$$

Where:
V = 5 volts
Rt = resistance of thermistor
Rr = resistance of parallel resistor (7.5 kilo-Ohm)
Vr = voltage reading across *Rr*

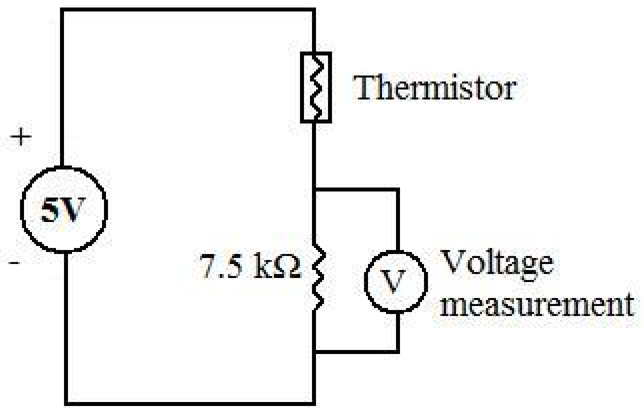

Figure 4.8: Schematic of thermistor circuit

Thermistor resistance values were compared to the manufacturer temperature to resistance curve to determine temperature.

Figure 4.9 shows the typical recorded temperature with overlay of chamber ambient temperatures and temperatures of concrete block at 0.5" depth. Figure 4.10 shows a closer view of temperature readings when brine and snow with deicing treatments was applied.

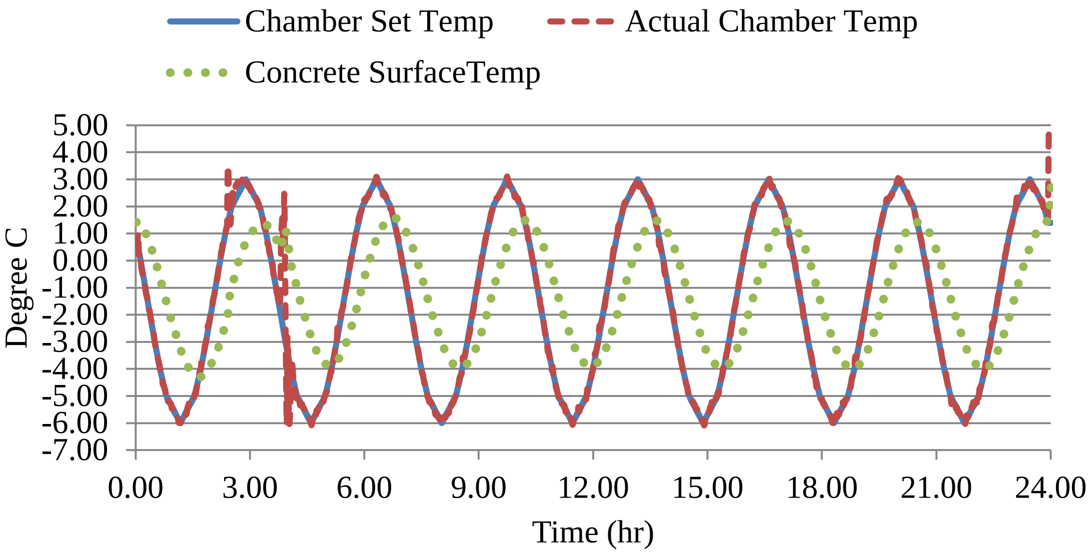

Figure 4.9: Overview of temperature readings of one cycle

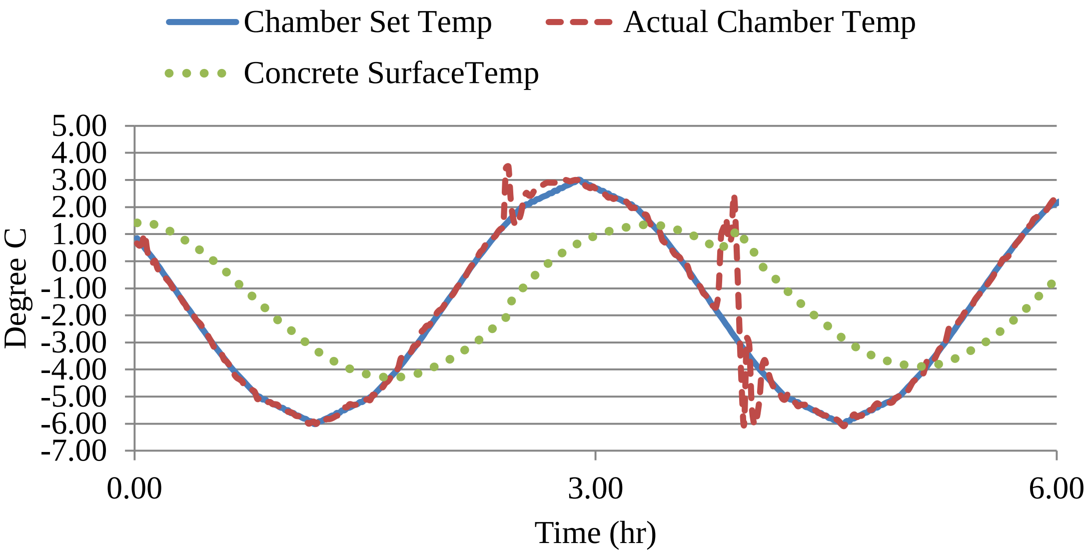

Figure 4.10: Temperature readings at brine, snow, and deicing application

The figures indicates that chamber temperatures were well maintained to the set temperatures at specific times. A deviation from the actual and set temperature occurs when the chamber door was opened to allow for snow and deicing treatments. As shown in Figure 4.10, the first deviation of the measured temperature from the set-point occurs two hours and 30 minutes into the cycle, when brine was applied. The second deviation occurs at four hours into the cycle, when snow and granular treatments were applied. Measurements of concrete temperatures at 0.5” depth indicate a lag in temperature change compared to the ambient temperatures. The extreme high and low temperatures were 1.6°C and -4°C as compared to the set temperature at 3°C and -6°C for the chamber environment. The temperatures plot also indicated a lag time of 26 minutes from peak ambient to concrete temperatures.

Cyclic exposures of freeze-thaw, snow, and deicing treatments were ended after 14 weeks. Concrete powder samples were collected from each sample for chloride content measurement. Powder samples were collected by drilling the samples using an electric drill press. Each sampling point was drilled at five increments of 0.2” for a total depth of 1”. A total of three sampling points were drilled for each test specimen to reduce uncertainties associated with sampling as well as the potential for uneven application of deicing materials across the surface of each test specimen. To profile the chloride concentration with depth, the Rapid Chloride Test (RCT) was performed on the collected powder. Standard procedures were used for the RCT test with equipment and materials sourced from Germann Instruments. Per manufacturer recommendations, each powder sample was measured to 1.5 gram and placed in an extraction vial. The vials were left to extract chloride ions overnight before measuring the chloride content of the solution with the ion-selective electrode. Measurements were compared to calibrated curves prepared from solutions of known chloride concentration.

4.1.4 ***Results from Controlled Laboratory Testing***

Chloride concentrations at each depth for the three sampling points were averaged together for each sample. The averaged results for each testing sample are shown in Table 4.4.

Table 4.4: RCT results at 0.2” depth increments

Depth (in.)	Chloride Percent (Cl%)				
	Snow Ctrl	3% Ponding	Brine	Granular	Sand-Mix
0.20	0.064	0.394	0.329	0.341	0.293
0.40	0.050	0.272	0.230	0.229	0.204
0.60	0.040	0.160	0.100	0.115	0.089
0.80	0.040	0.065	0.044	0.052	0.048
1.00	0.039	0.050	0.041	0.042	0.046

Plots of the chloride concentration at increasing depths within the sample are shown in Figure 4.11. The greatest chloride concentration was found in the specimen that was ponded with 3% solution. This specimen had much greater exposure to the chloride solution than the specimens that only experienced intermittent dosing. The granular salt treatment and brine treatment had very similar concentrations determined at each depth and the salt-sand mix was slightly lower. The control specimen represents the background chloride content of the concrete mixture.

Table 4.5 presents the mass of salt that was contained in each of the deicing applications applied in one cycle. The quantity of salt contained in one treatment of brine and one treatment of salt-sand mix are very similar. The salt contained in one treatment of pure rock salt is nearly twice that of the other treatments. The 100 mL of simulated snow used was equivalent to 55 mL of water once melted. Using the mass of salt for each treatment type and considering the amount of snow that was applied, the concentration of salt in the melted snow was calculated to compare the solution concentration associated with each treatment type. The resulting treatment concentrations are shown in Table 4.6.

Table 4.5: Calculated mass of salt added to specimens in one application for each treatment type [g]

Snow Control	0
Sand-Mix	0.201
Brine	0.205
Granular	0.402
3% Ponding	12.22

Table 4.6: Calculated salt concentration in solution for each treatment type w/w%]

Snow Ctrl	0
Sand-Mix	0.364

Brine	0.371
Granular	0.726
3% Ponding	2.960

Figure 4.12 relates the concentration of the solution created by the deicing material to the quantity of chloride discovered at each depth sampled. It is apparent that the concentration of the chloride at each depth is related to both the concentration of the source solution as well as other factors. These other factors likely include the duration of the exposure cycle as well as the application type. For instance, the 3% solution has at least three times the chloride content of any of the deicing strategy solutions, however, the chloride content found in the concrete is not three times higher. For a purely diffusionary transport process, as described by Equation 2.10, the concentration of chloride found at a given depth should be directly proportional to the concentration at the surface. If this were the mechanism that describes the results found in Figure 4.12, all points from 0.050% (the baseline value) and the point representing 3% solution should lie along the same straight line. This relationship is illustrated by the dot-dash line in Figure 4.12. Instead, the points lie above the line, although they represent solutions that were only intermittently in contact with the surface. This would indicate that the wetting and drying or freezing and thawing cycles impact the rate of ingress. Further, they impact ingress in different ways for the granular and liquid deicing applications. The salt-sand treatment and the brine treatment have nearly the same quantity of chlorides per application, however the brine consistently results in higher concentrations within the concrete mass. This relationship is highlighted by the position of points relative to dashed curve plotted along the 0.4” depth results. This indicates greater ingress may occur when brines are applied to dry pavement as opposed to granular treatments being applied to wet pavements. Sorption processes, by which capillary action draws liquids into porous material, would explain the additional ingress associated with the brine applications.

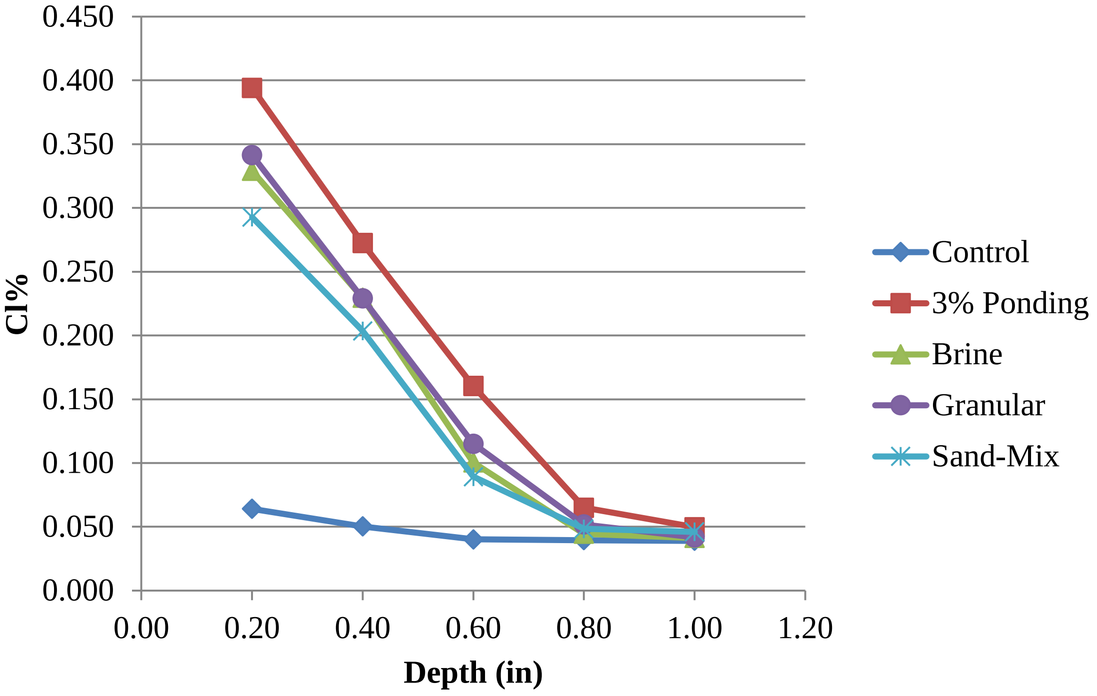

Figure 4.11: Chloride concentrations at depths for each treatment type

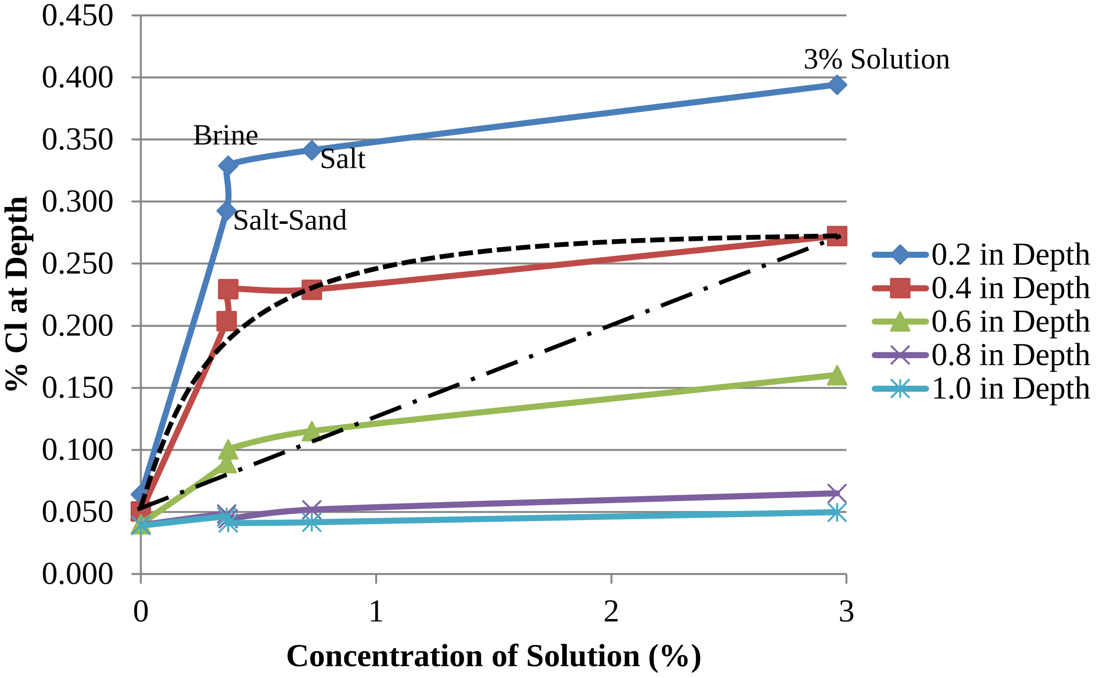

Figure 4.12: Plot of surface solution concentration and RCT chloride percent

To generalize the amount of chloride build-up that occurs with varying application rates for the three treatment types, a plot of built-up chloride concentration per application at the 0.2” depth is plotted versus the application rate for brine, granular, and salt-sand mix (Figure 4.13). The application rate for brine is given in gallons per lane-mile and granular salt is applied in pounds per lane-mile. This relationship is based on the experiment results that were obtained using the procedures described in this chapter and assumes a linear relationship between application rate and build-up at the 0.2” depth. However, with these assumptions considered, the results indicate that granular and brine treatments have very similar impacts to chloride build-up in the concrete. This trend is also was also found in field results that will be presented in Chapter 6.

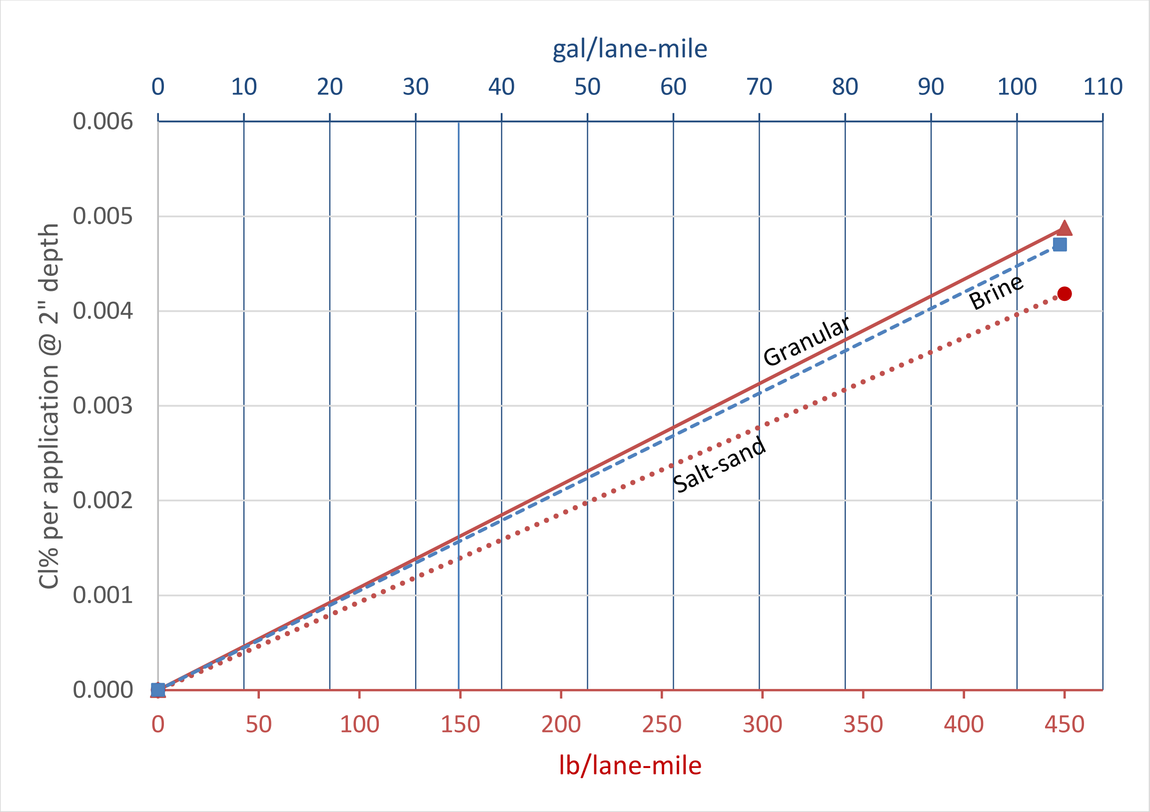

Figure 4.13: Plot of Cl% per application at 0.2” depth vs application rate

4.2 Summary of Cyclic Testing

Results indicate that there is a difference between chloride ingress observed for anti-icing brine treatments and granular deicing treatments on reinforced concrete specimens. A similar chloride profile was observed for brine and granular specimens although each application of granular salt contained about twice the amount of salt as used in the brine application. The difference can be explained due to differences in the time characteristics of the surface concentrations. Brined specimens received solutions of initially high salt concentration applied directly to the dry surface while granular specimens received granular salt treatment after snow was deposited. The greater amount of chloride ingress observed in the brined specimens is attributed to high rates of initial absorption of the higher sodium chloride concentrations at the dry surface of the concrete. In contrast, the surface of specimens treated with granular applications was initially exposed to melted snow prior to the applications of the treatment. The presence of the winter precipitation both works to saturate the pores at the surface of the concrete to reduce absorption rates and also dilutes the concentration of the granular salts applied to the surface. These findings are consistent with a field study conducted by Prah-Ennin (2013), which found higher initial chloride concentrations for deck subjected to brine application compared to granular applications. Average surface chloride measurements were also found to remain higher for the brine treatment until flushing of the surface by rain. The results also indicated that chloride ingress for granular deicing treatments are not proportional to the amount of salt applied. This was observed in the current study, where the granular salt applications, which contained twice the amount of salt compared to salt-sand mix, exhibited an increase of 1.16 times the chloride content at the 0.2” depth relative to the salt-sand applications.

4.3 Seasonal Field Measurement of Chloride Ingress

The objective of this component of the research was to characterize corrosive effects associated with annual winter maintenance practice using a field sampling of bridges. Through obtaining data at several bridges in both the Asheville and Greensboro regions, investigation of the influence of the different treatments, precipitation, and traffic count on the relative chloride build-up occurring over a typical winter season was observed. The objective of developing an understanding of the influences of chloride build-up in structural components, and correlations with functional properties was to devise a prediction model to inform recommendations on allocation of rehabilitation resources and prioritization of post-winter maintenance efforts. The difference between the objective of this section and the previous sections of this chapter is the presence of the real winter event during which the measurements are obtained.

4.3.1 ***PART I- Pre-Season Sampling of Residual Chloride Concentrations***

In this part of the study, data was obtained for the pre-snow season for only the Greensboro bridges and, due to inclement weather, bridge sampling was not possible for the bridges in Asheville. Additionally, sampling of the bridges after the snow season was not possible because the weather in North Carolina was exceptionally mild that year and did not require NCDOT maintenance crews to apply significant quantities of deicing materials in either the Triad or Mountain areas studied. The following section presents selection criteria, interesting results from the 2011 pre-season sampling, and challenges that were encountered. Because the team was not able to complete the sampling routine, this section is presented as proof-of-concept of the methods used to measure spatial distribution of chlorides on bridge surfaces. The results were also used to revise the sampling protocol in the 2012-2013 pre and post-season sampling study so this presentation of the first year results provides rationale for the eventual sampling routine that was followed in the second project year.

4.3.1.1 Bridge Selection

In early September 2011, NCDOT Guilford (Division 7) and Buncombe (Division 13) suggested 10 and 11 bridges for the study, respectively. The bridges were visited and documented by the research team so that the following criteria could be applied to select the final set of bridges included in the study.

4.3.1.2 Bridge Selection Criteria

The condition and accessibility of the deck, pier caps, steel girders, and guardrails were the primary features investigated and documented in each site visit. The selection of the bridges was based on the following criteria:

- Structure Type and Wear Surface: Since chloride transport in reinforced concrete is of primary interest, only bridges with concrete wearing surfaces were considered. Likewise, steel girders (weathering steel or painted) were preferred to examine corrosive effects on steel members below the deck.
- Accessibility to Pier Caps: Sampling of chloride concentrations on the pier caps and ends of steel girders requires physical assess to each member to obtain readings and collect samples. The selection of bridge decks with heavy, high-speed traffic or pier cap heights over 15ft was prohibited due to safety and accessibility concerns.
- Bridge Age and Condition of Members: Since the objective of the research is to measure surface chloride concentrations both above and below the deck, chloride transport to members below the deck needed to be plausible for candidate bridges. Therefore, the age of the structure and condition of the joints was used to guide selection of bridges with joint distress, cracking, and other pathways for chloride transport to the components below deck.

4.3.1.3 Greensboro Bridges Selected

From the 10 bridges suggested by Division 7 personnel, only two of the bridges met all section criteria; two additional bridges were selected based on prior usage of the bridges in a chloride-related NCDOT sponsored research project. The bridges selected are detailed in Table 4.7 and photographs are provided in Figure 4.12 and Figure 4.13.

Table 4.7: Selected bridges in the Greensboro region

Bridge	Bridge Number	Height to Pier Cap	Concrete Deck	Concrete Wear Surface	Steel Girders	Other Notes
NC62 over I-85	400524	10 ft.	Yes	Yes	Weathering steel	
NC62 over US421	400090	11 ft.	Yes	Yes	Painted and corrosion	Aluminum and Galvanized Guardrails

Washington Street Bridge	400221	<15 ft.	Yes	No*	Painted and corrosion	
East Lee Street Bridge	400003	5 ft.	Yes	No*	Painted and corrosion	Largely accessible without a ladder

*These two bridges were selected because diffusion coefficients were established from prior research (Tempest 2004). During previous sampling at this bridge, the deck had a concrete wear surface, but had since been overlaid with asphalt. This limited the sampling sites to only the curb, parapets, girders, and pier caps for these two bridges.

NC 62 over I-85

NC 62 over US 421

Figure 4.12: Photographs of pier cap and steel girder condition and accessibility for two selected bridges in the Greensboro area

Washington Street Bridge

East Lee Street

Figure 4.13: Photographs of pier cap and steel girder condition and accessibility for the other two selected bridges in the Greensboro area

4.3.1.4 Asheville Bridges Selected

From the 11 bridges suggested by Division 13, all the bridges were visited and four of the bridges were selected based on the proposed criteria. The bridges selected are described in Table 4.8 and photographed in Figure 4.14 and Figure 4.15.

Table 4.8: Selected bridges in the Asheville region

Bridge	Bridge Number	Height to Pier Cap	Concrete Deck	Concrete Wear Surface	Steel Girders	Other Notes
I-40 over NC 9	100492	12 ft.	Yes	Yes	Painted, but wearing off	Signs of joint distress and leakage, galvanized guardrails and concrete parapets
I-40 over SR2856 (Dennis St.)	100484	11 ft.	Yes	Yes	Painted, rusting at beam ends	Signs of joint distress and leakage, galvanized guardrails and concrete parapets
NC 280 over I-26 Exit 40	440240	13 ft.	Yes	Yes	Weathering steel with epoxy coated ends	Galvanized guardrails concrete parapets, drains near abutment
Monte Vista Road Bridge	100295	20 ft.*	Yes	Yes	Recently painted	Galvanized guardrails, signs of previously high joint leakage

*Height to pier cap exceeds initial selection criteria. However, the pier cap is still accessible by the research team and can be sampled safely.

I-40 over NC 9

I-40 over SR 2856 (Dennis St.)

Figure 4.14: Photographs of pier cap and steel girder condition and accessibility for selected bridges in the Asheville area

NC 280 over I-26 (Exit 40)

Monte Vista Rd. Bridge

Figure 4.15: Photographs of pier cap and steel girder condition and accessibility for selected bridges in the Asheville area

4.3.1.5 Procedure for Bridge Sampling

Concrete Deck

- The X-Ray Fluorescence handheld analyzer was used to take surface chloride readings at three locations on the length of one span: at the near joint, the midspan, and the end joint (See Figure 4.16).

- At each location, a series of three data collection points were sampled corresponding to the approximate locations of the midspan of the lane, the wheel path, and the curb.
- Each data collection point consisted of obtaining nine measurements to form a statistical basis for analyzing the surface concentration data. An acrylic spacing jig was developed to protect the window of the XRF analyzer, maintain a consistent stand-off distance for the instrument, and enforce a uniform sampling grid.

In addition to the XRF readings, powder samples were obtained at each of the data collection points after the surface concentrations were measured. The procedure for collecting powder samples consisted of:

- Drilling the deck surface to an approximate ¼” to ½” depth at three locations within the region of the data collection point.
- Collecting the powder generated during drilling in a pre-labeled sampling container.
- Cleaning the drill bit and collection tools with denatured alcohol to remove any residual chloride concentration.
- Photographs of the general condition of the concrete deck as well as the locations of measurements and powder samples were also collected.

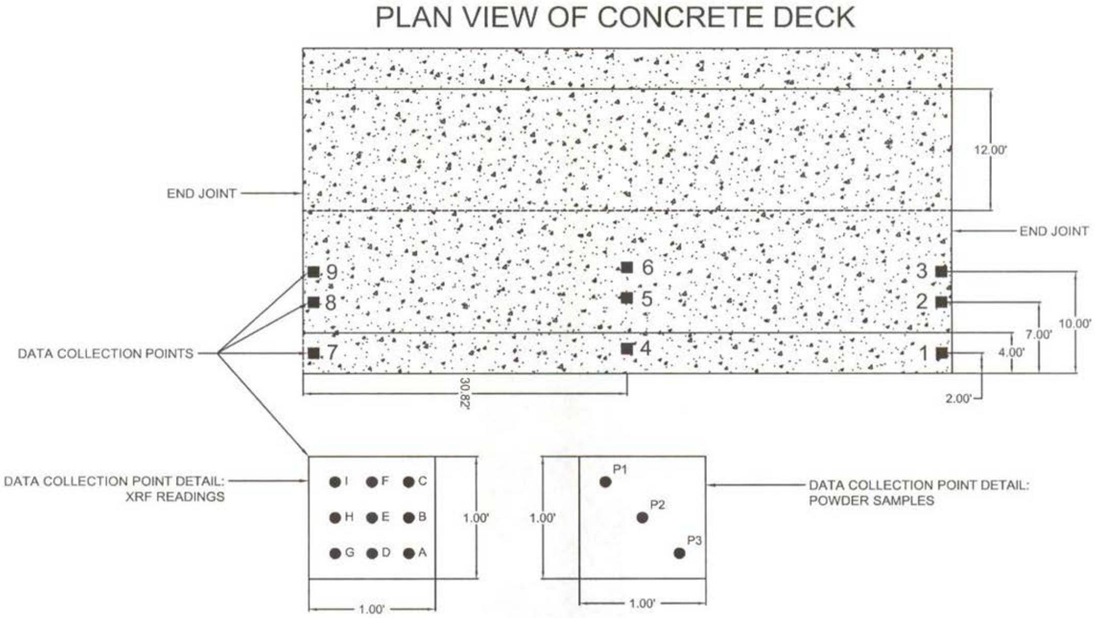

Figure 4.16: Plan view of generic concrete deck showing surface concentrations sampled by XRF and locations of powder samples obtained for RCT analysis

Guardrails and Concrete Parapets

- Data was collected using the XRF analyzer across the guardrails and concrete parapets. Three data collection points of nine samples, analogous to the sampling used on the deck, were used on the parapets.

Below Deck Components

- Readings were taken with the X-ray Fluorescence (XRF) analyzer on the pier cap and the visibly most distressed joints.
- Concrete powder samples were obtained from the top surface of the pier cap
- Using the X-Ray Fluorescence (XRF), data was collected from the steel girders at select regions of interest.

Sampling Procedure for Concrete Powder

Concrete powder was collected from the deck, the parapets, and the pier caps. Three holes were drilled for powder collection at each sampling area at a depth of about ½". Sample collection typically followed the procedure outlined below:

- No effort was made to clean the concrete surface with a wire brush since the intent of the study is to collect the surface materials.
- The drill bit and collection tools were wiped with denatured alcohol after every sample to remove residual chlorides
- The sampling hole was drilled with 1½"-diameter masonry bit in a rotary hammer
- The concrete powder was collected using a dustpan and small sampling spoon that fit inside the hole. The powder was stored in pre-labeled small zip lock bags for transport back to the laboratory.

4.3.1.6 Results

Greensboro Data Acquisition

On the 1st of December 2011, the team visited the NC 62 over I-85 Bridge to measure the initial chloride concentrations on the surface of the deck, the pier caps and the girders. The XRF analyzer measured very low concentrations of chloride at points on the deck, with the majority of readings below the detection threshold of the device. This would indicate that all residual surface chlorides are naturally washed from the deck surface by the fall season. Detectable concentrations were only measured on the pier caps and the guardrails. The chloride concentrations measured on the girders were taken from the flanges and the web in a straight line of sampling points 3 inches apart. Since there were low levels of detectable chlorides on the girders, readings were taken for every other point. Color mapping of data has been used to provide a means of examining the spatial distribution of chloride concentration. A typical color map developed from RCT measurements across the deck is presented in Figure 4.17. The highest concentration was measured to be 0.35% by mass, or 0.134 lb/yd^3, and was found to occur in the travel lane of the deck.

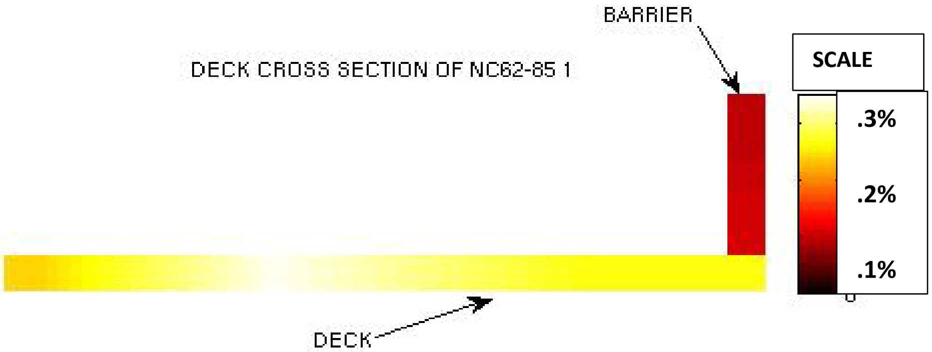

Figure 4.17: Spatial distribution of chloride concentration at ½" depth in the NC 62 over I-85 Bridge as determined by RCT from the powder samples

On the 2nd of December 2011, the team visited the NC 62 over 421 and the East Lee St. bridges. On both of these bridges, the deck surfaces once again had insignificant chloride concentrations below the detection threshold of the XRF analyzer. The highest chloride concentration, determined by RCT, was 0.02% or 0.00763 lb/yd^3 and was observed along the center of the lane as depicted in the color map in Figure 4.18. Although the chloride concentration is lower than measured in the NC 62 over 421, both spatial distributions indicate that the highest chloride concentration at ½" depth on the deck occurs in the travel lane specifically within the midlane.

Figure 4.18: Spatial distribution of chloride concentration at ½" depth in the East Lee St. Bridge as determined by RCT from the powder samples

The pier caps of these bridges registered significantly higher surface chloride concentrations, likely due to the greater age and poorer condition of expansion joints. With a greater ease of accessibility at the East Lee St. Bridge, a larger grid of samples were obtained across the exterior surface of the exterior girder. Figure 4.19 presents an overlay of a color map of the surface concentrations measured by the XRF analyzer on a picture of the uniform sampling grid. The spatial distribution reveals larger concentrations along the beam end as well as directly below the edge of the concrete block. These concentrations decrease with distance down the girder surface as expected of a gravity driven flow. The plausibility of this distribution lends credibility to the XRF analysis but suggests that sharp gradients in chloride concentration may be found on steel components, which may require a prohibitively large spatial density of sampling to properly characterize these surfaces.

Figure 4.19: Overlay of chloride concentrations on photo of sampled steel girder

Overall, it was observed that the bridges with greater joint deterioration had higher concentrations of surface chlorides below the deck, on pier caps, and girder ends. However, insufficient data was obtained in the first year of the project to definitively conclude this correlation. Over the course of the winter of 2011-2012, there were no significant winter events requiring application of deicing and anti-icing solutions. Consequently, the bridges in this study were not revisited for post-season measurement.

Asheville Data Acquisition

Due to inclement weather, sampling of the Asheville bridges prior to the first application of anti-icing and deicing treatment was not possible. As with the Greensboro bridges, this research task for the Asheville bridges was rescheduled in the winter of 2012-2013. Given knowledge obtained in the pre-season sampling of the Greensboro bridges, revisions to the sampling strategy were proposed to improve the usefulness and statistical significance of the measurements sought. Reasons for the adjustment of the protocol include the fact that, the field data obtained produced evidence that dry surface XRF measurements on concrete components are very low and often below the detection threshold of the device. Also it was also observed that the chloride concentrations on steel components varied significantly over even a small local region so point sampling of residual chloride concentration with XRF on steel components is not likely to produce meaningful and consistent data. Some of the sampling spots were eliminated as well due to time constraints.

4.3.2 ***<u>PART II - Pre-Season Sampling of Residual Chloride Concentrations</u>***

Since the pre-season sampling in 2011 was not completed with follow up post-season sampling due to lack of significant treatment over the winter season, sampling of these bridges had to be repeated in pre-season for 2013. Two of the bridges initially selected were found to have asphalt overlays, so alternative structures were sought for the second year effort. Bridges that were known to receive substantial amount of salt applications were specifically requested. The pre-season field measurements for the Asheville bridges were obtained in two days, the 8th and 9th of October 2012 and the post-season measurements were obtained on the 4th and 5th of March 2013. The Greensboro bridges were sampled on the 28th to 30th of November 2013 for the pre-season and resampled from the 6th to 8th of March 2013 for the post-season. Below are tables listing the new bridges that were sampled in Asheville and Greensboro.

Table 4.9: New selected bridges in the Asheville Area

Bridge	Bridge Number	Height To Pier Cap	Concrete Deck	Concrete Wear Surface	Steel Girders	Other Notes
SR 1684 over US-19	100324	15 ft.	Yes	Yes	Painted but wearing off	Expansion joints leaking; several deck patches
SR 2531 over I-40	100495	16 ft.	Yes	Yes	Weathering steel	Hairline to 1/16 in. wide vertical cracks through parapets
SR 2207 over US-19	100407	14 ft.	Yes	Yes	Painted but wearing off	Localized paint system failure at beam ends

Figure 4.20: Photograph of deck surface for Asheville bridge (SR 1684 over US-19)

SR 2207 over US-19

SR 2531 over US-19

Figure 4.21: Photographs of deck, pier cap and steel girder conditions for two selected bridges in the Asheville.

Table 4.10: New bridges selected in the Greensboro Area

Bridge	Bridge Number	Height to pier cap	Concrete Deck	Steel Girders	Other Notes

SR 3045 over I-40/85	400374	17 ft.	Yes	Weathering steel with painted ends	Expansion joint has surface rust near curb
US 220 over NC 62	400004	16 ft.	Yes	Painted steel	Beam ends have areas of paint peeling and surface rust
SR 3000 over I-40/85	400372	17 ft.	Yes	Weathering steel with epoxy coated ends	Pier cap has horizontal cracking
NC 62 over US 421	400090	10 ft.	Yes	Weathering steel	Areas of joint missing
NC 62 over I-85	400524	11 ft.	Yes	Painted and corrosion	Aluminum and Galvanized Guardrails
SR 1480 over I-85 B	400276	17 ft.	Yes	Weathering steel with painted ends.	Expansion joints at abutment are drying out, cracking and separating

Vickery Rd over I-85 Bus

Mt Hope Rd over I-40

McConnell Rd over I-40

Figure 4.22: Photographs of the Greensboro bridges receiving granular salt

NC 62 over I-85

US 220 over NC 62

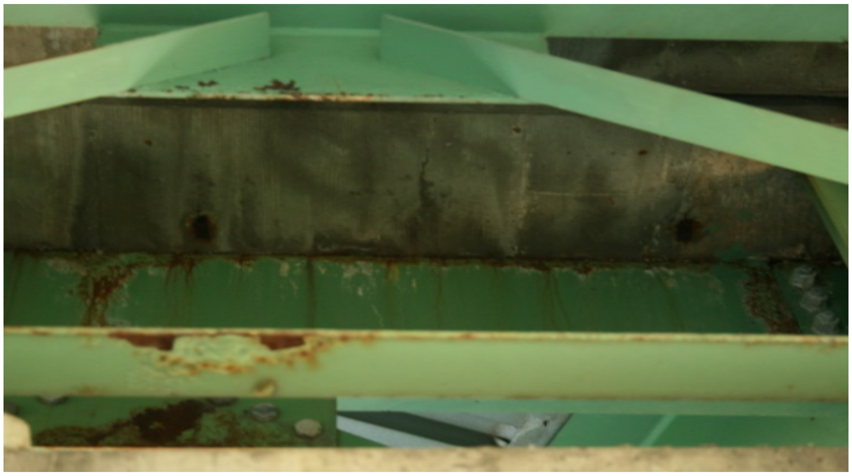

NC 62 over 421

Figure 4.23: Photographs of the Greensboro bridges receiving both brine and granular salt

4.3.2.1 <u>Revised Bridge Sampling Procedure</u>

A new bridge sampling procedure was established and used in the 2012-2013 seasonal sampling of the residual chloride concentrations. The procedure was adjusted to address challenges encountered in prior field testing and to optimize the data collection based on factors such as time and number of samples obtained.

Concrete Deck

- Three measurements were taken at each collection point to form a statistical basis for analyzing the surface concentration data. To measure the surface concentrations (at 0” depth) with the XRF handheld analyzer, temporary dams were created with hot-melt glue at three locations around each data collection point. 10mL of deionized water was then poured into each ring (See Figure 4.26) to bring any recrystallized salts near the surface into solution. The glue ring served as a reservoir that held the deionized water in place while the salts dissolved into the solution. These rings mimicked the principles of the SOBO-20 instrument previously described that deposits a liquid solution to measure the surface concentration of chlorides, but also allowed a longer time for the crystallized salts to enter into solution. This method was developed due to the fact that the readings obtained from the 2011 field sampling yielded results that were below the detection threshold of the XRF handheld analyzer due to the state of the salts. This technique was validated in the lab at UNCC in a technique presented in Appendix A. An acrylic spacing jig was used to protect the window of the XRF analyzer, maintain a consistent stand-off distance from the instrument, and enforce a uniform sampling grid.
- The X-Ray Fluorescence handheld analyzer was used to take surface chloride readings along the length of one span at three locations: at the near joint, the midspan, and the far joint.
- Data collection points were sampled at the approximate location of the mid-span of the lane, the wheel path, and the curb.

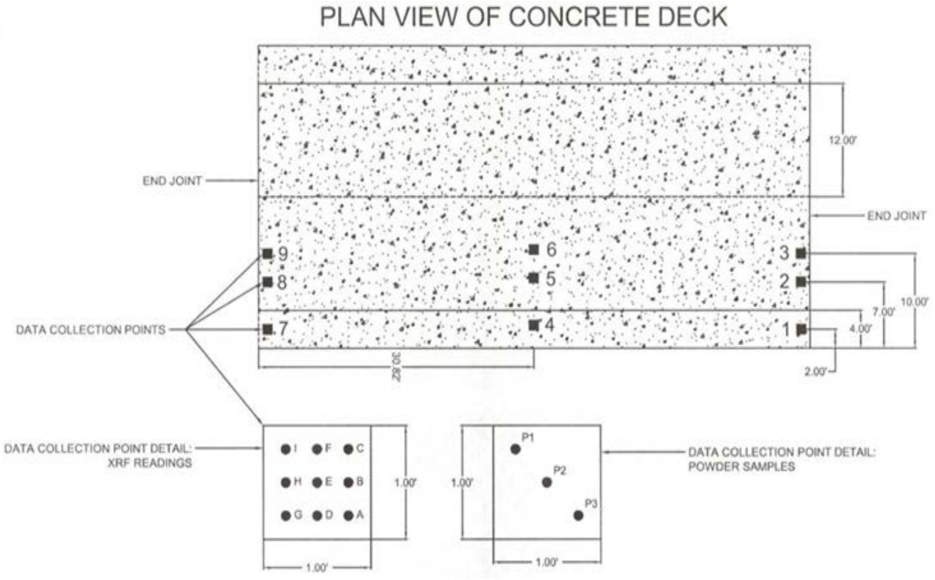

Figure 4.24: Plan view of generic concrete deck showing surface locations sampled by XRF and locations of powder samples obtained for RCT analysis

Figure 4.25: XRF set on the acrylic spacing jig

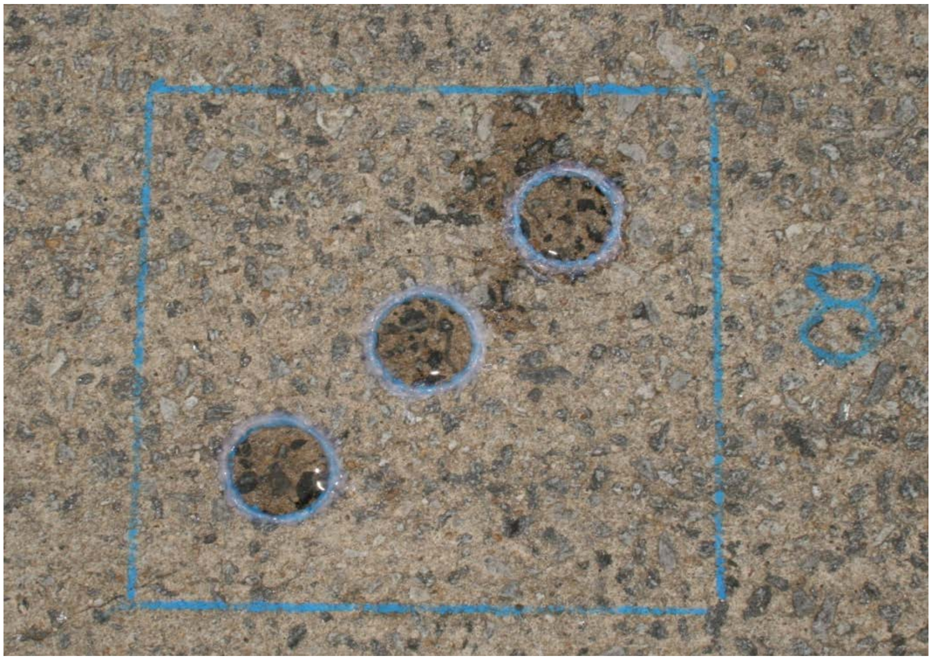

Figure 4.26: Glue rings on a location

In addition to the XRF readings, powder samples were obtained at each of the data collection points after the surface concentrations are measured. The procedure for collecting powder samples consisted of:

- Drilling the deck surface to an approximate ½" depth at three locations within the region of the data collection point (See Figure 4.27).
- Photographing the general condition of the concrete deck as well as the locations of measurements and powder samples were taken.

- Collecting all powder samples for chloride content analysis using the XRF

Below Deck Components

- On the pier caps, two areas of 1ft² on the two different pier caps was marked using the 1’ x1’ acrylic grid previously developed and used on the bridge deck tests. One data collection point of three readings was sampled for each section of the bridge with the XRF analyzer using the surface chloride absorption technique, presented in Appendix A of this report, on the pier cap along the most visibly distressed joint line. Powder samples were also obtained according to the same protocol used on the deck.

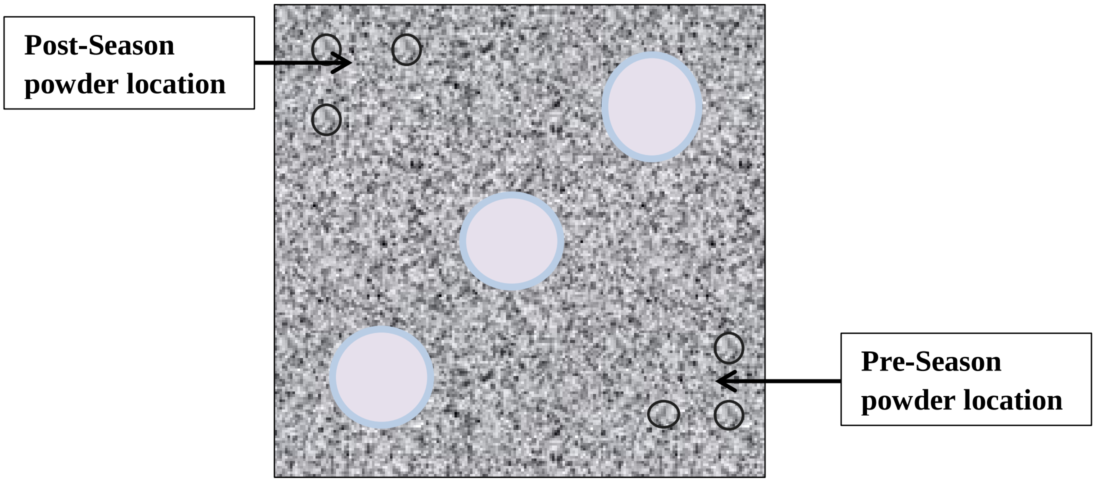

Figure 4.27: XRF test points on both the cap and the deck

- For the girder surfaces, during the pre-season measurements for 2011, it was observed that the measurements were well below the detection threshold of the XRF handheld analyzer for majority of the bridges with only one exception (E. Lee Street bridge). Also chloride levels registered varied largely on each point measured. To address this measurement difficulty, the research team installed sacrificial steel coupons for corrosive loss measurement rather than using the XRF surface analysis. The details of this component of the field sampling is presented in the following chapter, which deals specifically with corrosive effects on exposed structural steel surfaces.

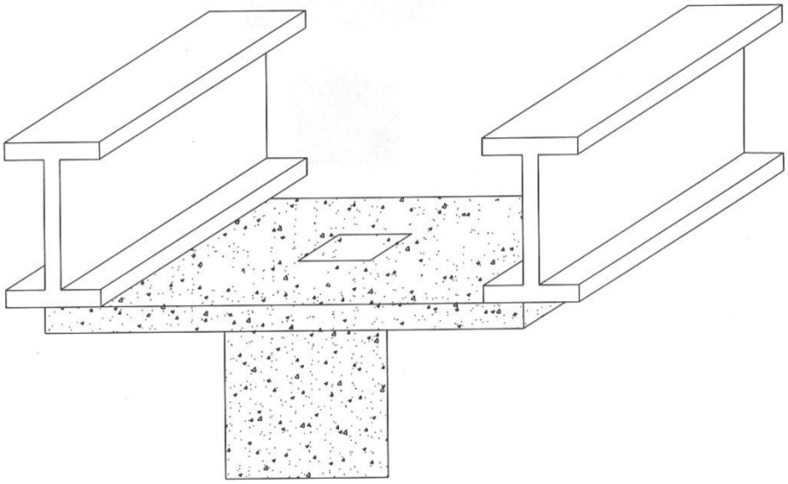

Figure 4.28: Sketch of the sampling area on the pier cap

4.3.2.2 ***Results and Interpretation of the Surface Concentrations***

Since the intent of this study is to provide information regarding the level of exposure of various bridge components to deicing salt as well as the temporal variation in surface concentration following dispersion by traffic and dilution from precipitation, pre-season and post-season surface chloride concentrations were measured. For the pre-season measurements, the chloride concentrations on the deck surface were very low but using the surface chloride absorption technique gave generally consistent results. Substantial increases in the concentration of chloride on various locations were observed between the pre-and post-season as well. There were some moderate levels of chloride concentration that were measured in the ½" depth powder samples for both the pre-and post-season of the field study. Also, significant changes in the 1" to 5" profiles with depth were developed from the pre-season powder samples obtained. The table below shows average surface concentrations at 0" depth, using the surface chloride absorption technique, obtained pre-season and post-season for all the bridges tested.

During the 5 month period between the pre-season and the post-season, a series of weather events took place. In the Table 4.12 and Table 4.13, the dates of the snow events during the 5 month interval for both Asheville and Greensboro respectively are summarized. From these weather records, it was deduced that the bridges studied in Asheville received about 8 applications during the period of measurements. Also, in Greensboro, from the bridge salt application log summarized in Appendix B, the bridges received 4 applications. Comparing the weather from the two locations, it can be observed that in both Asheville and Greensboro, February was the month receiving the highest number of snowfalls, although the most significant snowfall event for Greensboro occurred in January.

During the post-season measurements in Asheville, the deck surface showed visual signs of a substantial amount of salt on the deck surface therefore, it was expected that the Asheville bridges would produce higher average changes in the chloride concentration between the pre-season and the post-season. In Greensboro, the bridge deck surfaces did not show evidence of any residual salt, as observed in the surface chloride concentrations (Table 4.11) the changes that occurred were very small.

The powder samples collected at 0.5” depth were measured using the XRF analyzer in the laboratory. All measurements reported represent the average of 5 readings that were sampled for 60 seconds. The results were recorded and arranged by the location on the bridge for each individual bridge. Chloride concentrations on the sidewalk, parapet, wheel path, mid-lane, and pier cap locations were averaged together to develop generalized component observations for each application type. The post season chloride concentrations for the Asheville bridges showed substantial increases in chloride in the sidewalk and wheel paths. For the Greensboro bridges, the increases in chloride concentration for the various locations on the bridge were as high as a 7.07 lb/yd³. The build-up of chloride concentrations in the sampled components of at each bridge are shown in Figure 4.29, Figure 4.30, and Figure 4.31 and summarized in Table 4.14.

Table 4.11: Average surface chloride concentrations of bridges sampled

Bridge Name	Bridge #	Treatment Type	Bridge Age	Pre-Average Surface Conc.@ 0” depth (lb/yd³)	Post-Average Surface Conc. @ 0” depth (lb/yd³)
NC 62 over I-85	400524	Brine + Granular Salt	32	0.421	1.154
NC 62 over 421	400090	Brine + Granular Salt	40	0.588	0.702
US 220 over NC 62	400004	Brine + Granular Salt	33	0.278	0.551
McConnell over I-40	400372	Granular Salt	19	0.874	0.725
Mt Hope over I-40	400374	Granular Salt	19	0.449	1.106
Vickery over I-85 Bus	400276	Granular Salt	10	0.600	0.658
SR 1684 over US-19	100324	Granular Salt Sand Mix	43	0.671	6.776
SR 2207 over US-19	100495	Granular Salt Sand Mix	38	0.528	3.496
SR 2531 over I-40	100407	Granular Salt Sand Mix	34	0.442	6.170

Table 4.12: Summary of Greensboro snow events during study period

Date	High Temperature °F	Low Temperature °F	Precipitation (Inches)
1/17/2013	49	32	2.45
1/25/2013	25	21	0.11
2/2/2013	40	19	0.05
2/16/2013	42	28	0.12
2/22/2013	43	32	0.31

Table 4.13: Summary of Asheville snow events during study period

Date	High Temperature °F	Low Temperature °F	Precipitation (Inches)
12/29/2012	45	29	0.15
2/1/2013	43	21	Trace
2/2/2013	43	20	Trace
2/3/2013	48	29	0.01
2/16/2013	35	23	Trace
2/19/2013	55	34	0.1
2/26/2013	39	32	1.54
3/1/2013	39	31	Trace
3/2/2013	42	27	0.01
3/3/2013	33	23	Trace

Table 4.14: Average change of chloride concentration by component type and bridge studied [lb/yd^3]

Bridge Name	Treatment Type	Bridge Age	Side walk	Wheel path	Mid lane	Cap
NC 62 over I-85	Brine + Granular Salt	32	0.91	2.06	2.39	0.00
NC 62 over 421	Brine + Granular Salt	40	1.91	1.48	1.51	0.00
US 220 over NC 62	Brine + Granular Salt	33	0.00	1.62	0.10	0.59
McConnell over I-40	Granular Salt	19	1.49	2.00	1.35	0.11
Mt Hope over I-40	Granular Salt	19	2.39	3.54	3.18	0.43
Vickery over I-85 Bus	Granular Salt	10	2.98	3.44	7.07	0.09
SR 1684 over US-19	Granular Salt Sand Mix	43	1.92	1.81	1.07	2.86
SR 2207 over US-19	Granular Salt Sand Mix	38	1.95	3.81	3.14	1.05
SR 2531 over I-40	Granular Salt Sand Mix	34	21.00	7.63	6.16	3.07

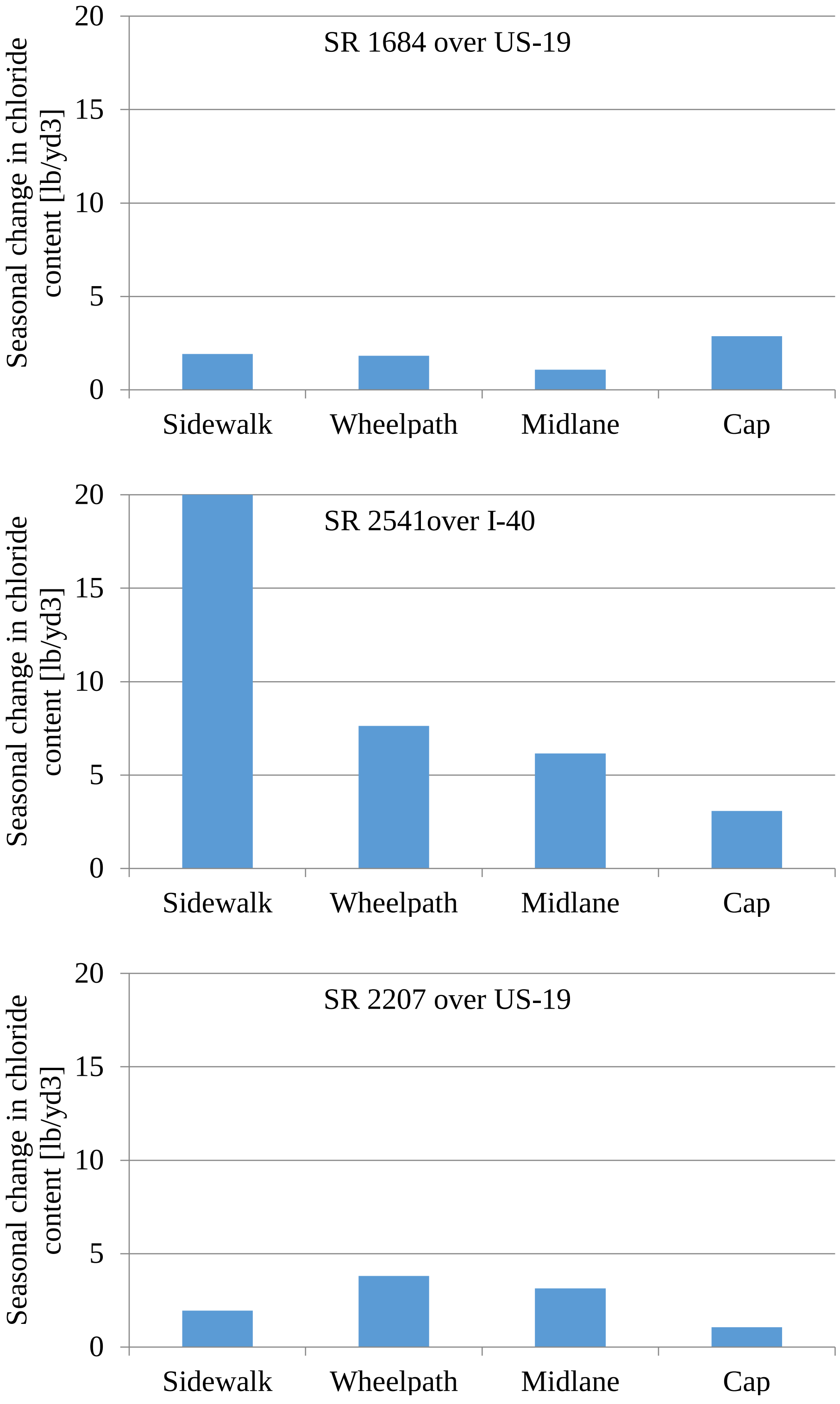

Figure 4.29: Chloride concentration at the 0.5” depth of the Asheville Bridges receiving salt sand mix treatment)

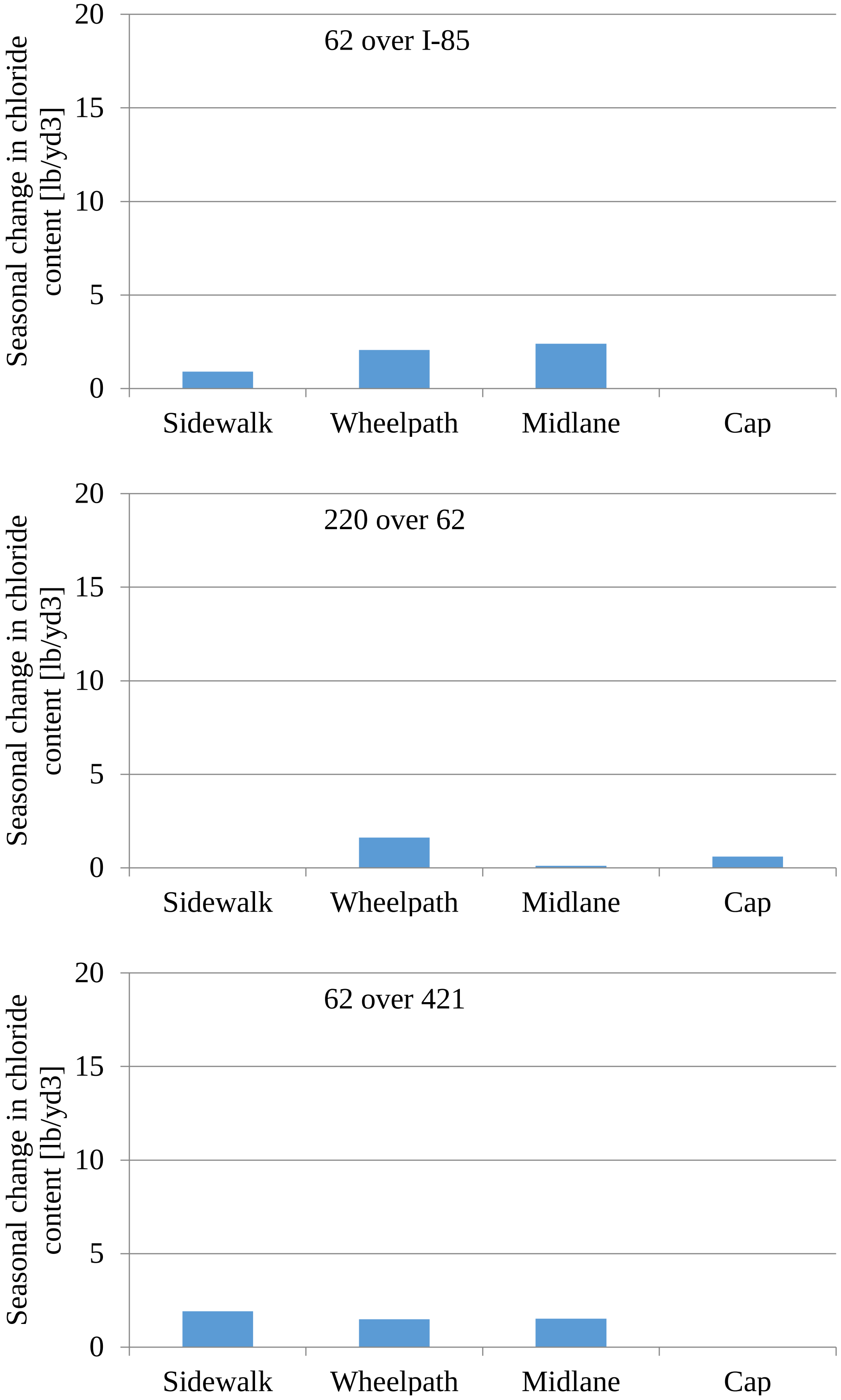

Figure 4.30: Chloride concentration at 0.5” for the Greensboro bridges receiving both Brine anti-icing and granular salt deicing treatment

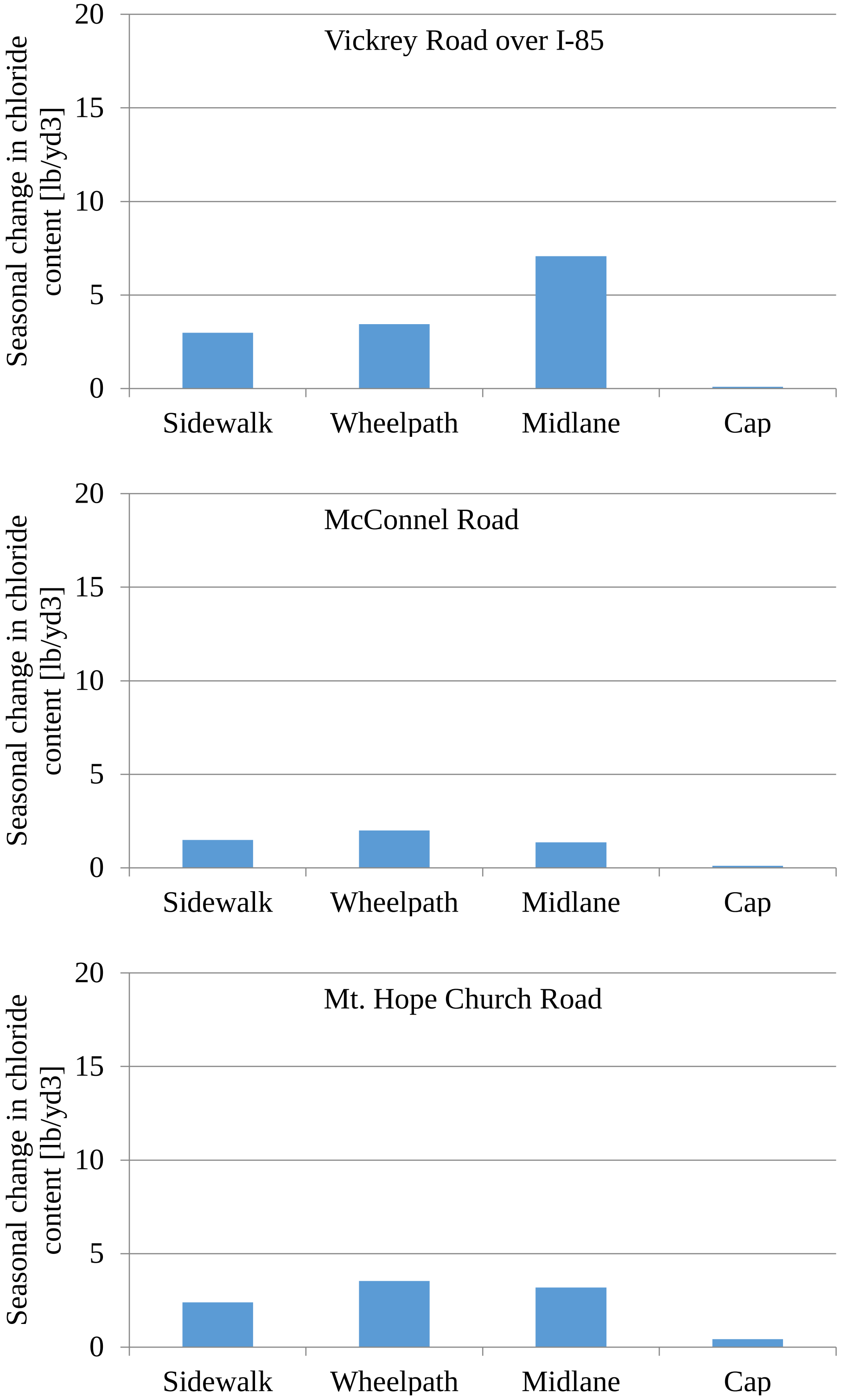

Figure 4.31: Chloride concentration at 0.5” for the Greensboro bridges receiving only granular salt deicing treatment

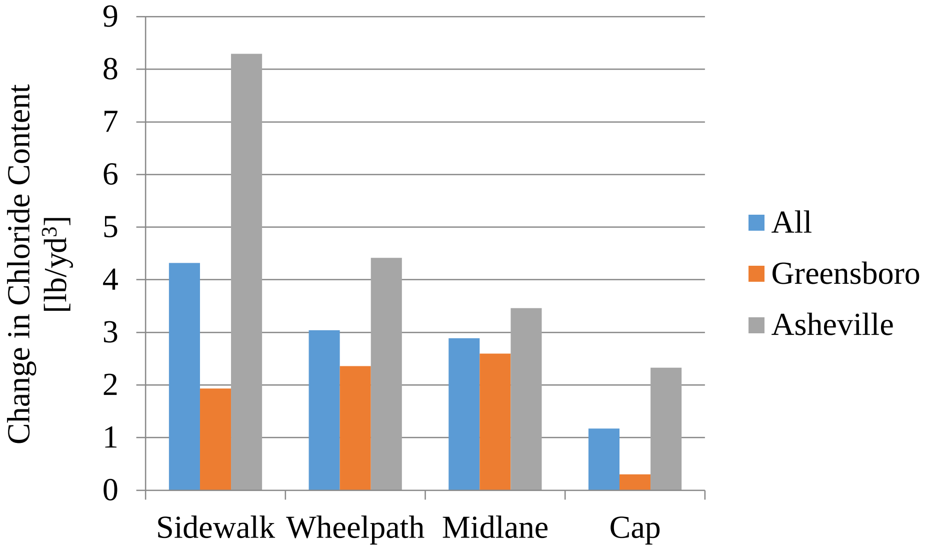

Figure 4.32: Average build-up at ½" depth by region and component [lb/yd^3]

4.3.2.3 Results and Interpretation of the Factors Influencing the Chloride Concentrations

The results in seasonal chloride variation are consistent with those discovered by other researchers (Luping, Nilsson et al. 2011). The fluctuation in chloride concentrations from between before the salting season to after the salting season can be significant in field conditions. Increases of up to 6.1 lb/yd^3 were found using the method of dissolving chlorides at the surface and measuring with XRF. Increases of up to 7.6 lb/yd^3 were found by measuring the chloride content of powder samples collected from the ½" depth. The results show the most significant build-up of chloride concentrations in the above-deck horizontal surfaces. In general, Asheville bridges exhibited significantly greater chloride concentration increases between the Fall and Spring than Greensboro. Even when normalized by the number of applications of deicing materials, the build-up is not proportional with that found in Greensboro. As can be seen in Figure 4.33 there is no easily discernable pattern of greatest corrosive potential associated with any of the treatments.

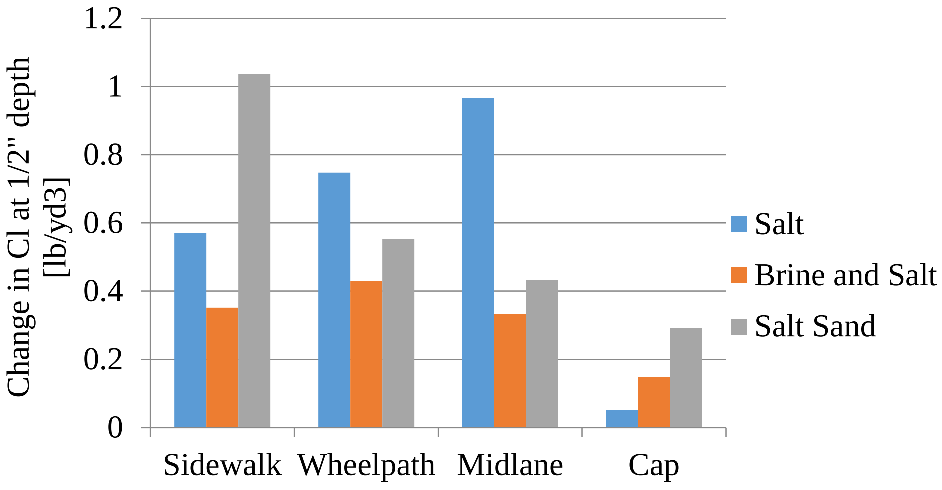

Figure 4.33: Build up per application at ½” by treatment type

The ingress of chloride is impacted by a number of characteristics related to the environment, the quantity of salt applied, bridge parameters and the concrete itself. Environmental characteristics include relative humidity, traffic, precipitation, and temperature. Bridge design characteristics include the slope and crown of the bridge deck, the condition of the joints and the drainage system. The concrete characteristics are related to permeability, crack patterns and chloride binding capacity. The parameters measured in this study include number of salt applications and type of salt application. As the objective of the study is to determine significant differences in the corrosive impact to bridges by the various deicing and anti-icing materials, several multi-parameter plots are presented in the figures below. Bridge characteristics included age, joint rating, and ADT. Although the dataset is limited, Figure 4.34 shows poor correlation between chloride build-up at the pier cap and joint rating. This implies that there are transport mechanisms for salts to move from the deck to the cap, other than via drainage through the joint. Splashing and wind convection are two documented mechanisms for this transport. However, because most of the pier caps studied in this work were associated with bridges having had joint rating of 2, there is not sufficient data to rule out correlation. Figure 4.35 shows poor correlation between bridge age and build-up of chloride concentration. It is known that the diffusion coefficient changes with time, and that concrete has a capacity to bind chlorides. Although these characteristics could explain reduced susceptibility of older concrete to chloride ingress, the data shown in Figure 4.35 do not reveal a strong correlation at all. While there is a slightly better correlation between the build-up of chloride concentration and bridge ADT, as shown in Figure 4.36, there are still strong statistical outliers that indicate interaction with other significant factors. However, since there is evidence of an underlying correlation between both bridge age and ADT, a multi-parameter surface plot was develop to investigate the influence of both parameters simultaneously. Figure 4.37 presents the experimental data correlated with two parameters together with a best-fit power function. In this case, there is significantly improved correlation of the parameters within the statistical model with the measured chloride ingress. The correlation indicates that young bridges with low ADT experience the greatest increase in chloride concentration at the 0.5” depth during the salting season. Old bridges with high ADT showed the lowest increase in chloride concentration. As Figure 4.38 reveals, the chloride concentration measured in the pre-season showed the same relationship. This finding could be biased by the very small sample size of nine bridges considered in this work.

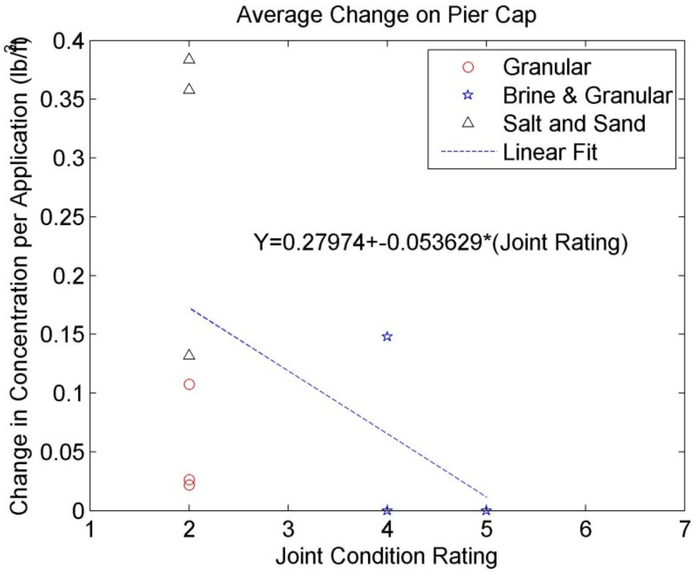

Figure 4.34: Average change in chloride concentration at pier cap for various joint ratings

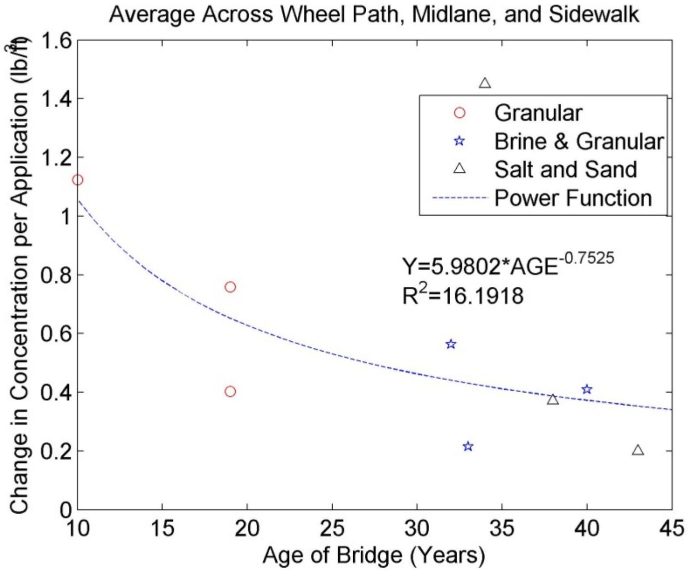

Figure 4.35: Average change in chloride concentration across bridge deck for various bridge ages

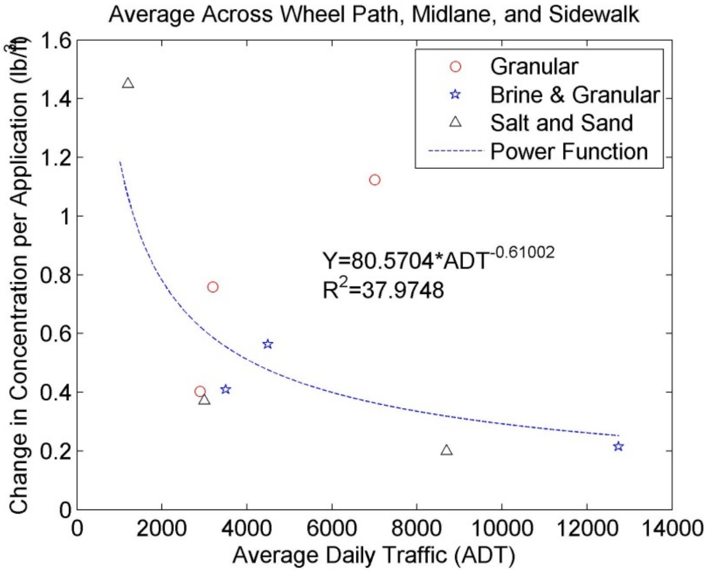

Figure 4.36: Average change in chloride concentration across bridge deck for various bridge ADT

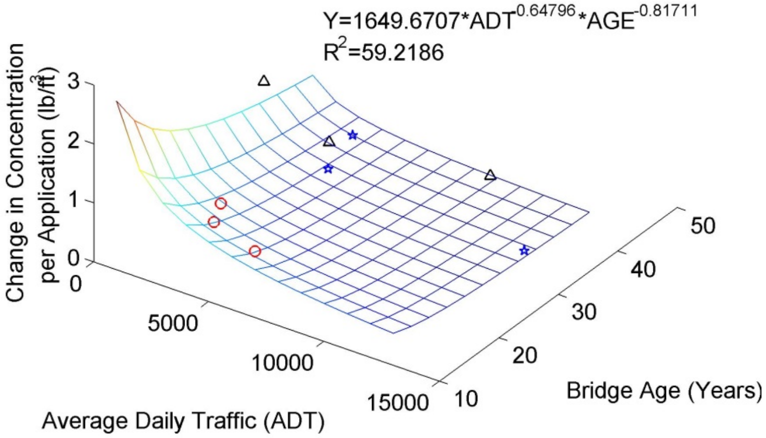

Figure 4.37: Average change in chloride concentration across bridge deck correlated with two parameters: ADT and bridge age

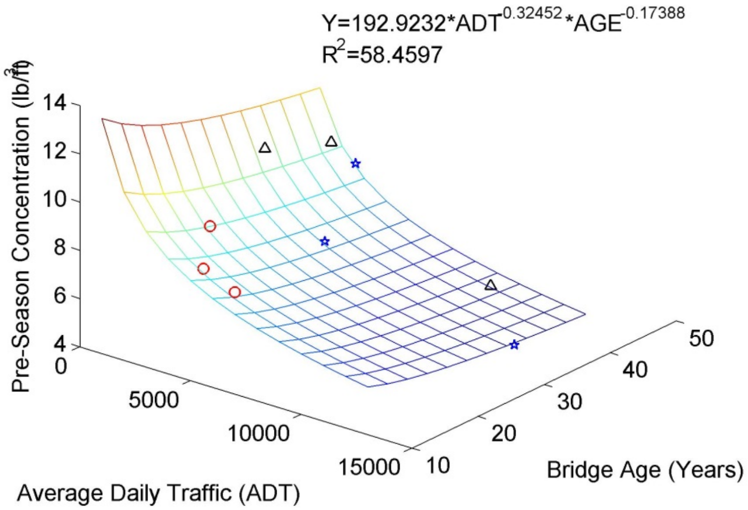

Figure 4.38: Pre-season concentration of chloride correlated with age and ADT

4.3.3 ***Conclusions and Potential Source of Bias, Errors and Uncertainties***

The data collected from field measurements as well as controlled laboratory testing revealed few differences in the corrosive potential associated with each of the three deicing methods. The concentration of chloride that was transported to shallow depths within the concretes studied was more influenced by the number of applications, the characteristics of the concrete and the environmental characteristics than by the application type. Small differences were found with the brine application and are attributed to sorption processes that occur when solution is introduced to the surface of dry concrete. However, this difference was found to be less than 10% at depths greater than ½”. These results suggest that the corrosive impacts of chloride based deicers are significantly more dependent on external factors, particularly application frequency, bridge age, and ADT, more than application type.

5 Corrosive Effects on Steel Components

In addition to concerns related to reinforced concrete components, the use of sodium chloride as a deicing strategy for road safety is a major cause for chloride initiated corrosion on exposed structural steel members of highway bridges. The exposed steel components subject to corrosion include both above deck members, such as guardrails, and the primary superstructure below the deck, including stringers, floor beams, diaphragms, and bearing surfaces. Deicing and anti-icing treatments applied to the deck surface eventually migrate to different exposed surfaces either in solid form or as dissolved in liquid concentrations by the action of vehicle traffic and environmental factors, such as wind and gravity. Anticipating exposure to specific elements is likewise particularly challenging because it is dependent on so many external factors. Furthermore, the corrosive potential is affected by the concentration of the solution that component is exposed to, which can vary from 23% for direct exposure from brine treatment and saturated liquid concentrations to diluted concentrations developed through dispersion and mixing with precipitation.

The research team devised a series of laboratory and field tests to examine the impact of different deicing treatments and the transport mechanisms and concentrations associated with typical applications. This chapter presents the following sections:

- **5.1 Laboratory Investigation on Bare and Treated Steel Specimens**: Laboratory testing of corrosion rates of bare and treated steel alloys was performed for representative exposure concentrations. This testing was performed using both an SHRP standardized test method originally proposed for the project scope as well as a modified test method developed by the research team to more realistically mimic field exposure of steel components. The test result provide insight on the influence of solution concentration on corrosion rate, performance of various alloys in corrosive environments, and performance of mitigation techniques on inhibiting corrosion of steel components.
- **5.2 Laboratory Investigation of Undercutting of Surface Treatments**: Laboratory testing was performed on painted, epoxied, and galvanized steel coupons with scored surfaces to investigate the long-term performance of mitigation treatments. Standardized methods were used to characterize undercutting of the surface treatments by the sodium chloride-based solutions and the results provide insight on the performance of these surface treatments.
- **5.3 Field Investigation with Controlled Application**: In parallel with the controlled application study performed at the Billy Graham pair of sister bridges described in the prior chapter, surface concentrations of steel superstructure components were measured in the field to investigate differences in chloride transport and accumulation on components below the deck for granular, salt-sand, and brine application strategies.
- **5.4 Field Measurement of Corrosion at Regional Bridge Sites:** In parallel with seasonal concrete measurements in Asheville and Greensboro, the research team installed sacrificial steel coupons to superstructure components for a one year duration. Results of corrosion over a typical winter season are presented in a statistical model to explore effects related to treatment strategy and location.

5.1 Laboratory Investigation on Bare and Treated Steel Specimens

A laboratory study was conducted to evaluate the corrosive effects of sodium chloride-based solutions on coated and bare steel alloy specimens at different levels of salt concentration. The study was conducted for typical coating methods and steel alloys used in North Carolina bridges. This subsection presents the methodology and experimental results obtained from two different test methods: the Strategic Highway Research Program (SHRP) test method for evaluation of corrosive effects of deicing chemical on metals (SHRP H-205.7) and a modified cyclic corrosion test developed by the research team to more realistically replicate the field exposure conditions. Analysis of the results provides comparison of the corrosion rates associated with different bare steel alloys and the performance of paint, epoxy, and galvanization surface treatments across a range of sodium chloride concentrations.

5.1.1 ***<u>SHRP H-205.7 Test Method</u>***

The SHRP H-205.7 test method for evaluating the effect of deicing chemicals on metals involves submerging metal coupons of different composition into prescribed concentrations of deicing solutions for different exposure times to measure the corrosion rates. The SHRP H-205.7 test method is outlined in SHRP-H-207.5 with reference to ASTM Standards: ASTM G31-72 Standard Practice for Laboratory Immersion Corrosion Testing of Metals, ASTM G1, “Standard Practice for Preparing, Cleaning, and Evaluating Corrosion Test Specimens”, and ASTM C876, “Standard Test Method for Half-Cell Potentials of Uncoated Reinforcing Steel in Concrete” (ASTM 1972, Chappelow, McElroy et al. 1992, ASTM 2009, ASTM 2011). An important feature of this test method to note is that the specimens are continuously submerged in solution for the duration of the testing. This is unlikely to be representative of the actual exposure conditions in the field and, furthermore, the research team discovered that continuous submersion is not appropriate for solutions of high chloride concentrations. The results from this testing are presented to document the findings of the research team with the SHRP methodology originally approved for the scope of the research project. However, the research team cautions that the results from a modified cyclic exposure test detailed in the next subsection of the report are more realistic and should be used as the basis for any conclusions drawn from this research effort.

The steel alloys investigated in this study were selected from frequently used alloys in NC bridges. The grades included were A36 carbon structural steel, A572 high-strength low-alloy columbium-vanadium structural steel, and A588 high strength low-alloy structural steel with atmospheric corrosion resistance. The SHRP H-205.7 test method is applicable to bare metal coupons only and was used in this study as a preliminary test for corrosive effects on bare metal specimens at 0, 3%, and 23% concentrations. The study was conducted over the full eight week period prescribed by the test method and the results were used to evaluate the corrosion rate for each alloy at two extreme concentrations.

In preparing samples for the test method, the recommendation in the ASTM G31-72 standard was followed by using large surface-to-mass ratio and small ratio of edge area with minimum thickness to minimize the area of exposed end grain. Also, careful dimensional measurements were made with a micrometer to permit accurate calculation of exposed area. A band saw was used to cut each 3/16 inch thick specimen into 1 inch by 2 inch dimensions. To identify each steel grade, a hole of ¼ inches diameter was drilled into each specimen using a metal drill press at unique locations. Each coupon was also stamped with a unique serial number using a hammer-stamp tool. Figure 5.1 shows the dimensions and layouts for each steel grade.

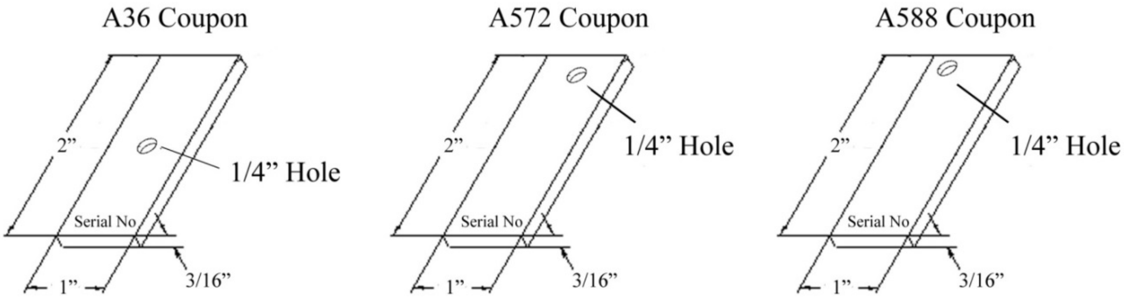

Figure 5.1: Test coupon layouts for each steel grade

The primary equipment for the SHRP test includes an air pump, flow meter, pH meter, saturated calomel electrode, and voltmeter. The air pump and flow meter develop an aeration system to deliver and regulate air flow to all the sodium chloride solutions in the test cells. The pH meter and voltmeter along with the calomel electrode are used to monitor the acidity of the solutions and the corrosion potential. Figure 5.2 shows the primary equipment used for the test setup.

Cleaning of corroded test specimens was performed according to ASTM G1 to ensure an ideal cleaning procedure that would only remove corrosion byproducts and not the base metal. An ultrasonic cleaner was used according to SHRP recommendations. The acid solution used for ultrasonic cleaning contained 50 grams of stannous chloride and 20 grams of antimony trioxide in 1,000 mL concentrated hydrochloric acid. Other cleaning materials included a metal wire brush, acetone, and ethanol. Cleaned specimens were weighted using an analytical balance with 0.1 mg resolution.

Other setup materials included:

1) Fishing line: for hanging metal specimen in each test cell
2) Insulated electrical wire: for connecting the test electrode to the voltmeter
3) Brass screws and nuts: for attaching electrical wire to the test electrode
4) Silicon sealer: for sealing the electrical wire to the test electrode
5) Test cell container: 2.5 quart plastic container to hold the deicing solution
6) Test cell lid: for covering of test solution and hanging of the metal specimens
7) Air Tubing: for directing air to each test cell
8) Sodium chloride and deionized water: for preparing test solutions
9) Magnetic stirrer: for dissolving salt into solution

Figure 5.2: SHRP test equipment: cleaner, air pump, flow meter, electrode, and meters

5.1.1.1 Details of Test Procedure

In the SHRP H-205.7 test procedure, the test cells that hold the exposure solution and specimens are prepared using 2.5 quart plastic containers. In executing the test, each container was first cleaned using ethanol and air dried prior to filling of test solutions to remove any residual ions and contaminants. Sodium chloride test solutions were prepared using deionized water to ensure that municipal water-treatment ions, such as chloride, are absent from the test and control solutions. Select solution concentrations were developed as a percent weight of sodium chloride dissolved in deionized water. During preparation of all solutions, a magnetic stirrer was used to fully dissolve the salt into solution and initial pH of each test solution was recorded. Each test cell contained a total of nine specimens of a single steel alloy: eight test specimens and one "electrode" specimen. Specimens were cleaned, rinsed twice with acetone, air dried, and the initial weight was recorded to the nearest 0.1 mg. A nylon string was then tied to each test specimen at the ¼" identification hole to permit each specimen to be suspended within the test cell. The "electrode" specimens are identical to the test specimens, but were prepared by attaching an insulated electrical wire to a single metal specimen using screw and nut. The electrical connection at the screw was sealed using silicon to prevent development of a cathodic surface at this connection. Test cell lids were punched with nine hanging locations around the circumference for hanging of the specimens and a center hole to attach the air tubing. Figure 5.3 shows the setup for the immersion test.

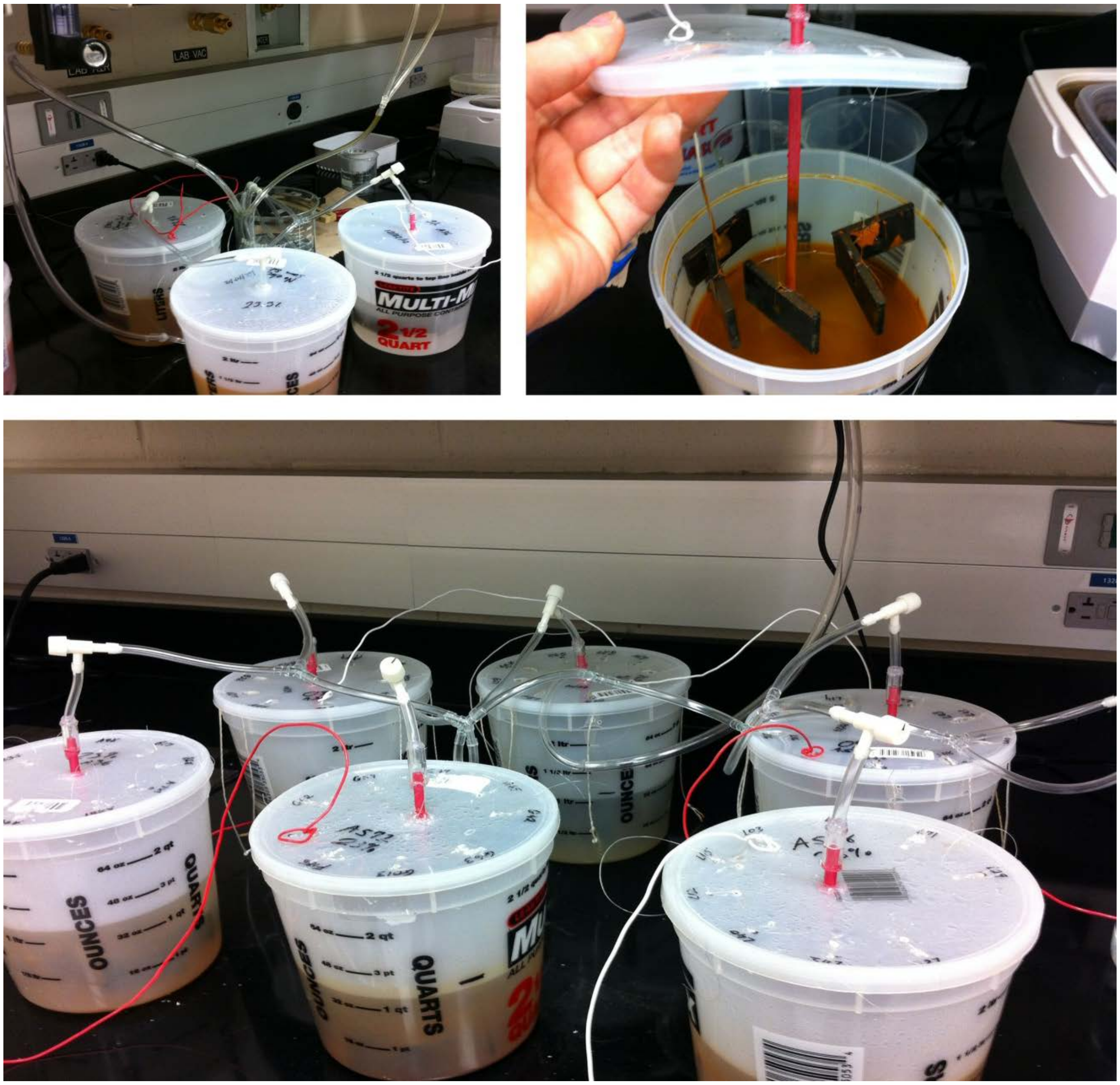

Figure 5.3: SHRP H-205.7 test setup with specimens submerged in solution

Preparation of the test included filling the test cell with prepared solution and placing the lid in position with specimens hanging in solution. An air tube was attached through the lid at the center to aerate the solutions. A flow meter was used to produce air bubbles at a constant rate maintained at around 100 cc air/min. Solutions were filled so that test specimens were fully submerged and any evaporation of the solution throughout the course of the eight week test duration was compensated for with deionized water. Each test was conducted with a single test cell for each unique steel alloy at a particular sodium chloride concentration. Specimen exposure times were durations of one, two, three, four, six, and eight weeks, as recommended by the SHRP standard. In accordance with the test standard, one specimen was removed from each test cell at the one, two, three, and four week exposure times and two specimens were removed at the six and eight week exposure times. After each exposure period, test specimens were removed for cleaning and then reweighed to measure the corrosive loss over the exposure duration. The pH and corrosion potential for each test cell were also measured at each exposure time when samples were removed for measurement. The corrosion potential was measured by placing the calomel electrode inside the solution and connecting the wire to the negative terminal of a voltmeter along with the wire from the electrode specimen to the positive terminal.

After each specimen was exposed for the required time, it was removed for cleaning and reweighing. The removed specimen was first placed in water follow by wire brushing of the surface. Acetone was used to wipe any remaining rust particles. The specimen was then placed into acid solution to be clean using an ultrasonic cleaner. After removal from the acid solution, the specimen was rinsed and wiped dry with acetone. Figure 5.4 shows images of the specimens before and after the cleaning process for corroded specimens.   A similar cleaning procedure was used on un-exposed, un-corroded coupons to determine the expected weight lost due to the cleaning process only. Table 5.1 shows the weight loss from the cleaning procedure for un-corroded coupons.

Figure 5.4: Before and after cleaning of corroded specimens

Table 5.1: Weight loss of test specimen due to cleaning only

Steel Type	Original weight (g)	After cleaning (g)	Weight lost (g)
A36	48.4433	48.4323	0.011
A572	46.6577	46.5963	0.0614
A588	42.4916	42.3465	0.1451

Corrosion rates were determined based on corrected weight lost, specimen area, time, and specimen density. Specimen densities used were 7.83, 7.86, and 7.87 (g/cm^3) for the A36, A572, and A588 alloys, respectively. The determination of corrosion rate is through the following equation:

$$CR = \frac{K * W}{A * T * D} \tag{5.1}$$

Where: CR (mpy) = corrosion rate (mils per year)
K = constant = 3.45x10^3 (unit conversion factor)
W = corrected weight lost (mg)
A = specimen area (cm^2)
T = time (hr)
D = specimen density (g/cm^3)

5.1.1.2 ***Results from SHRP H-205.7 Test***

The results obtained for A36 steel with exposure to solutions of 0%, 3%, and 23% sodium chloride concentrations are presented in Figure 5.5 with numeric data provided in Table 5.2. While the results exhibit expected corrosive losses for specimens exposed to 3% sodium chloride solutions, the results obtained for the specimens exposed to 23% brine solutions appear unexpected and warrant further discussion. One would expect that the higher concentration of sodium chloride dissolved in the solution and the corresponding lower pH of the solution would accelerate the corrosion of the test specimens and lead to larger weight losses than measured in the 3% solution. However, the corrosion of iron in the steel specimens requires oxygen and the solubility of oxygen in solutions with high salt concentrations is significantly low. Consequently, the use of the SHRP H-205.7 test method is not appropriate for high concentrations of sodium chloride solutions since the levels of dissolved oxygen are too low to supply the corrosion reactions. The results are confirmed by those obtained for A572, which are shown in Figure 5.6 and Table 5.3, and those for A588 steel presented in Figure 5.7 and Table 5.4. Results obtained for all steel alloys exhibited virtually no difference in weight losses recorded in de-ionized control solutions and in fully saturated 23% brine solutions. This implies that the dissolved oxygen available within saturated 23% sodium chloride solutions is so low that corrosion is effectively inhibited by the nature of the test method. Due to this phenomenon within higher concentration solutions as well as the non-representative exposure of the steel specimens under continuous submersion, the research team developed a modified test program to subject the coupons to cyclic exposure to sodium chloride solutions followed by air exposure and drying. The description of this modified test and results obtained for the different steel alloys and surface treatments is presented in the following subsection of the report.

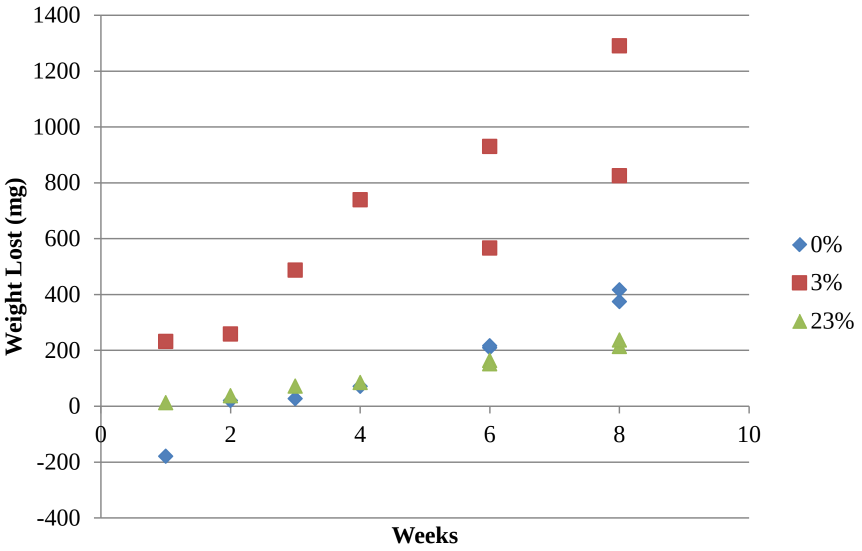

Figure 5.5: Results for A36 Steel using SHRP test method

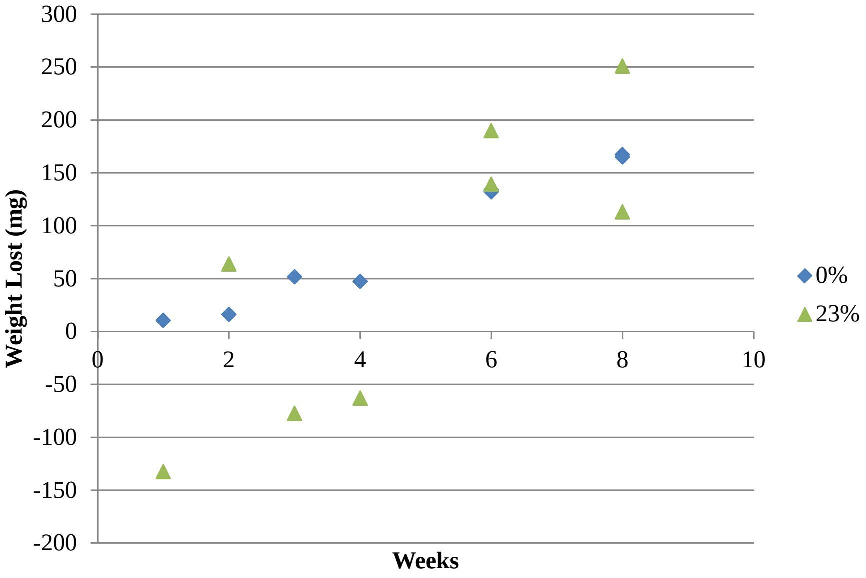

Figure 5.6: Results for A572 Steel using SHRP test method

Table 5.2: Results for A36 steel at 0%, 3%, 23% NaCl using SHRP H-205.7

A36 Steel					
Weeks	**Weight Lost (mg)**	**Corrected wt. Lost (mg)**	**Corrosion Rate (mpy)**	**pH**	**Potential (-mV)**
0% Deionized Water					
1	-169.5	-180.5	-36.688	6.7	320.5
2	30.3	19.3	1.961	6.45	261.5
3	37.3	26.3	1.782	6.8	330
4	81.1	70.1	3.562	7.76	341.6
6	219.4	208.4	7.060	8.17	423
6	226.3	215.3	7.294	8.17	423
8	384.5	373.5	9.490	7.93	602
8	427	416	10.569	7.93	602
3% NaCl Solution					
1	242.8	231.8	47.116	7.4	725
2	269.1	258.1	26.231	6.41	740
3	498.1	487.1	33.003	6.24	753
4	749.8	738.8	37.542	6.04	741
6	941.3	930.3	31.515	5.93	760
6	577.3	566.3	19.184	5.93	760
8	1301.3	1290.3	32.783	6.96	742
8	835.9	824.9	20.959	6.96	742
23% NaCl Same Solution with Electrode					
1	14.1	3.1	0.630	4.85	719
2	37.2	26.2	2.663	5.15	720
3	45.4	34.4	2.331	5.47	737
4	71.5	60.5	3.074	5.9	748
6	183.3	172.3	5.837	6.22	725
6	175.1	164.1	5.559	6.22	725
8	261.9	250.9	6.375	7.15	714
8	252.6	241.6	6.138	7.15	714

Table 5.3: Results for A572 steel at 0% and 23% NaCl using SHRP H-205.7

A572 Steel					
Week	**Weight Lost (mg)**	**Corrected wt. Lost (mg)**	**Corrosion Rate (mpy)**	**pH**	**Potential (-mV)**
0% Deionized Water					
1	71.7	10.3	2.086	6.25	225.2
2	77.5	16.1	1.630	6.74	319.6
3	113.1	51.7	3.489	7.05	265.3
4	108.6	47.2	2.389	7.43	300.1
6	193.3	131.9	4.451	8.14	231
6	195.3	133.9	4.519	8.14	231
8	228.5	167.1	4.229	7.88	268
8	226.3	164.9	4.174	7.88	268
23% NaCl Solution					
1	-71.2	-132.6	-26.849	5.1	701
2	125.1	63.7	6.449	5.19	734
3	-15.9	-77.3	-5.217	5.49	747
4	-1.6	-63	-3.189	5.83	735
6	200.6	139.2	4.698	6.21	698
6	251.1	189.7	6.402	6.21	698
8	312.2	250.8	6.348	6.98	712
8	174.3	112.9	2.858	6.98	712

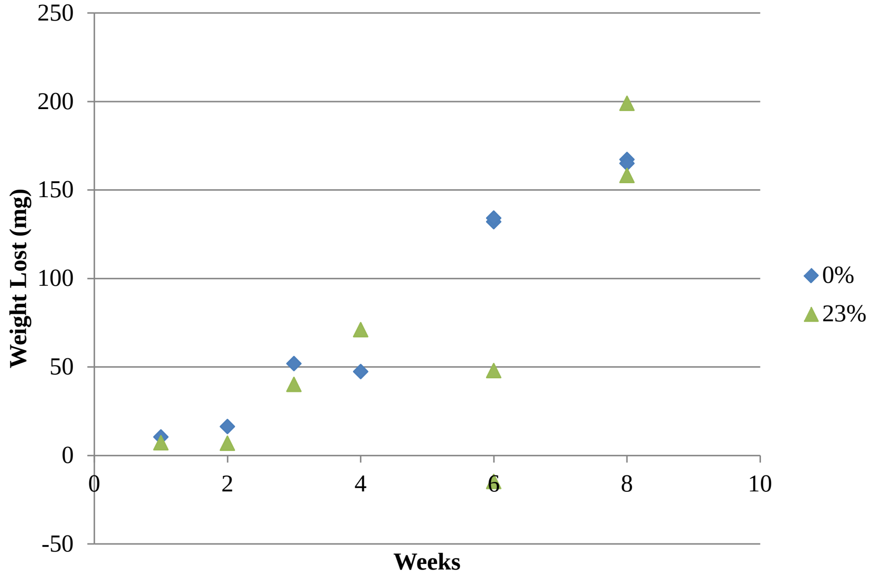

Figure 5.7: Results for A588 Steel using SHRP test method

Table 5.4: Results for A588 steel at 0% and 23% NaCl using SHRP H-205.7

A588 Steel					
Week	**Weight Lost (mg)**	**Corrected wt. Lost (mg)**	**Corrosion Rate (mpy)**	**pH**	**Potential (-mV)**
0% Deionized Water					
1	141.3	-3.8	-0.768	6.8	267.1
2	162.3	17.2	1.739	6.37	285.6
3	186.3	41.2	2.777	7.28	237.3
4	212.7	67.6	3.418	7.13	230.1
6	251.1	106	3.573	8.14	231
6	257.1	112	3.775	8.14	231
8	253.1	108	2.730	7.9	221
8	240.7	95.6	2.417	7.9	221
23% NaCl Solution					
1	152.1	7	1.416	5.65	700
2	151.8	6.7	0.677	4.95	714
3	185	39.9	2.690	5.44	724
4	216	70.9	3.584	5.74	710
6	192.8	47.7	1.608	6.34	711
6	130.2	-14.9	-0.502	6.34	711
8	303.1	158	3.994	7.18	705
8	343.9	198.8	5.025	7.18	705

5.1.2 ***Modified Laboratory Test Method: Cyclic Corrosion Test***

As previously detailed, application of the standard SHRP H-205.7 test method revealed limitations in testing for corrosive effects on bare metal surface at high sodium chloride concentrations. Specifically, the high concentration solutions have insufficiently low solubility of oxygen to supply the corrosion reaction and, since the specimens are continuously submerged in this solution, the corrosion is inhibited. To introduce sufficient oxygen to develop corrosion in specimens subject to higher concentration solutions and to better simulate natural atmospheric exposure, a modified testing procedure was developed and forms the basis from which the majority of experimental conclusions related to steel corrosion are based for this study. The modified test procedure involved regularly cycling the test specimen between submersion in the test solution and natural atmospheric drying at a fixed duty cycle. The timing for each cycle was selected for sufficient exposure of specimen's surface to testing solution and a drying time that resulted in complete drying of the specimen under regular atmospheric conditions. The process aims to produce more accurate replication of the natural corrosion process, since constant submersion is not typical for steel components in highway bridges. This test method was patterned after Q-Lab Technical Bulletin on cyclic corrosion testing (Q-Lab Corporation 2009). However, with the exception of this change in the submersion of the specimens in the sodium chloride solution and an additional cleaning procedure used for removal of the corrosion byproducts, the research team maintained the remaining applicable recommendations and procedures of the SHRP H205.7 test.

5.1.2.1 Test Procedures

Preparations of test specimens and data collection procedures were adopted from the SHRP method, including the prescribed test duration of eight weeks. Likewise, removal of exposed specimens was performed at one, two, three, four, six, and eight weeks with a duplicate specimen at six and eight weeks. The following study was conducted for 0%, 3%, 5%, and 23% sodium chloride solution concentrations across all three steel alloys (A36, A572, and A588). Coated specimens were also included in the test matrix to investigate the performance of these coatings in inhibiting corrosion. Coating types included were: galvanized A36, painted A572, epoxy coated A572, and epoxy coated A588. All steel coupon specimens requiring coating were sent to NCDOT, where the coating was applied to ensure consistency with field applications.

The modified test setup developed for the cyclic exposure routine was similar to the SHRP procedure except that steel specimens were hung using fishing line from a lever arm above the test cell or container. The lever arm was periodically cycled to transition the specimens from submersion to atmospheric exposure at a fixed period. Equipment and material used for the cyclic corrosion test included: wooden stands, AC powered linear solenoid actuators, a wall-plug timer to control the dunking cycle, 5 gallon pails with sand to serve as counter-weight, and 2.5 quart plastic buckets to contain the test solutions. A schematic of the developed apparatus is shown in Figure 5.8. Each lever arm was attached with testing specimens at one end and the other with counter-weights. The arm was connected to a wood stand with a metal hinge to allow for a seesaw motion. The dunking of the specimens was controlled by two linear solenoids with 1" retraction stroke for each lever arm. A wall timer provided power to the solenoids at a fixed dunking interval of two minutes every two hours. When power was switched on, each solenoid retracted, pulling the counter-weight end up and lowering the specimen end into placed containers with testing solution. After two minutes, power was cut off releasing the solenoid and consequently also bringing the specimens out of solution due to the slightly heavier counter-weighted end of the lever. To accommodate all specimens in a single test matrix, the test set up used two lever arms each supporting 112 specimens. Figure 5.9 shows the test set up used for the cyclic corrosion test.

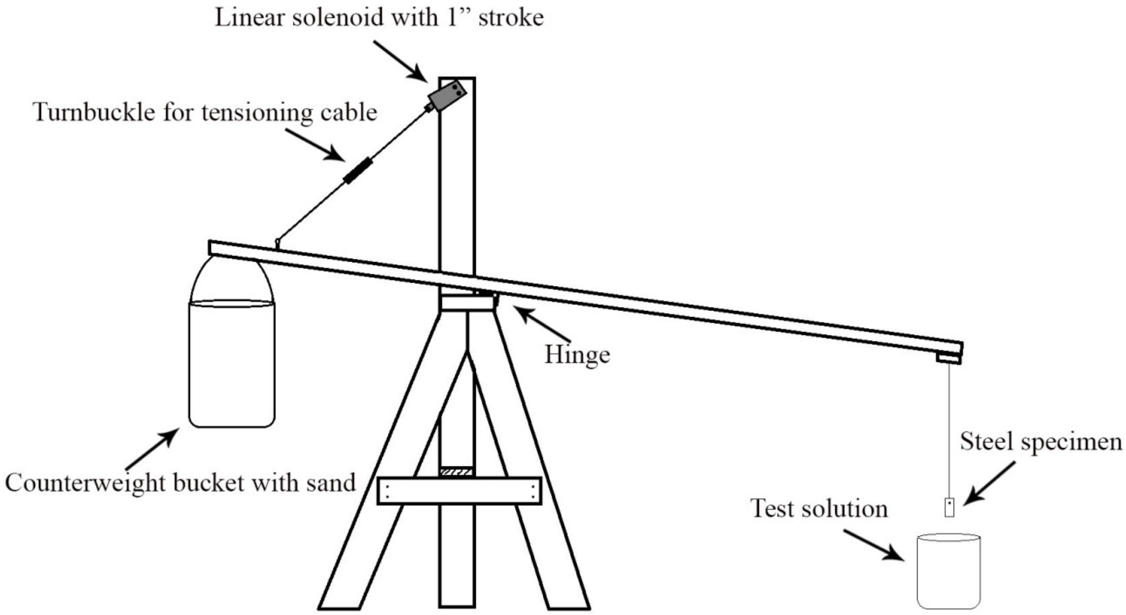

Figure 5.8: Schematic of dunking apparatus

Figure 5.9: Fixtures used for dunking motion in cyclic corrosion test

As in the prior standardized test, each test cell contained eight test specimens of a single alloy at a fixed solution concentration. The complete test matrix encompassed 28 test cells, which accommodates all combinations associated with four different solution concentrations, three different bare steel alloys, and the four coated alloys. Similar to prior tests, evaporation of the test solution was adjusted to the original level with deionized water. Typical specimens retrieved following the exposure cycles were either heavily corroded if bare steel, coated with white rust if galvanized, or absent of distress if coated with paint or epoxy (Figure 5.10). Initially, the cleaning process for corroded specimens consisted of mechanically cleaning with metal wire brush follow by the same ultrasonic acid bath. However, following this cleaning process specimens were found to still retain significant corrosive byproducts, as seen in Figure 5.11. Consequently, the cleaning procedure was revised to follow the wire brushing and ultrasonic bath with a round of sand blasting. Acetone was used to remove rust product between each cleaning process. The surface condition of the specimens after the sand blasting, shown in Figure 5.12, was sufficiently cleaned of corrosive byproducts and therefore sand blasting was desirable if it was found to not remove a significant amount of the base metal. To quantify the loss of base metal due to the cleaning process alone, cleaning of unexposed, un-corroded specimens was performed for each steel alloy and weight losses were recorded following each cleaning treatment. The results, shown in Table 5.6, confirm that the sand blasting safely removes corrosive byproducts from the steel specimens with only nominal loss of base metal that is less than the losses produced by cleaning in the ultrasonic acid bath. Consequently, all weight losses reported in this study are from measurements taken after wire brushing, ultrasonic acid bath, and sand blasting and have been normalized to account for the expected base metal loss for each corresponding steel alloy as reported in this table.

Table 5.5: Weight losses from cleaning of un-corroded specimens

Steel Type	Acid cleaning (g)	Sand blasting (g)	Total (g)
A36	0.0110	0.0120	0.0230
A572	0.0614	0.0087	0.0701
A588	0.1451	0.0111	0.1562

0% Control Solution

3% Sodium Chloride Solution

5% Sodium Chloride Solution

23% Sodium Chloride Solution

Figure 5.10: Visual condition of steel coupons after 4 week exposure in cyclic test procedure (From left to right: A36, A572, A588, Galvanized A36, Epoxy Coated A588, Epoxy Coated A572, Painted A572)

0% Control Solution

3% Sodium Chloride Solution

5% Sodium Chloride Solution

23% Sodium Chloride Solution

Figure 5.11: Visual condition of steel coupons from 4 week exposure after wire brushing and ultrasonic acid bath (From left to right: A36, A572, A588, Galvanized A36, Epoxy Coated A588, Epoxy Coated A572, Painted A572)

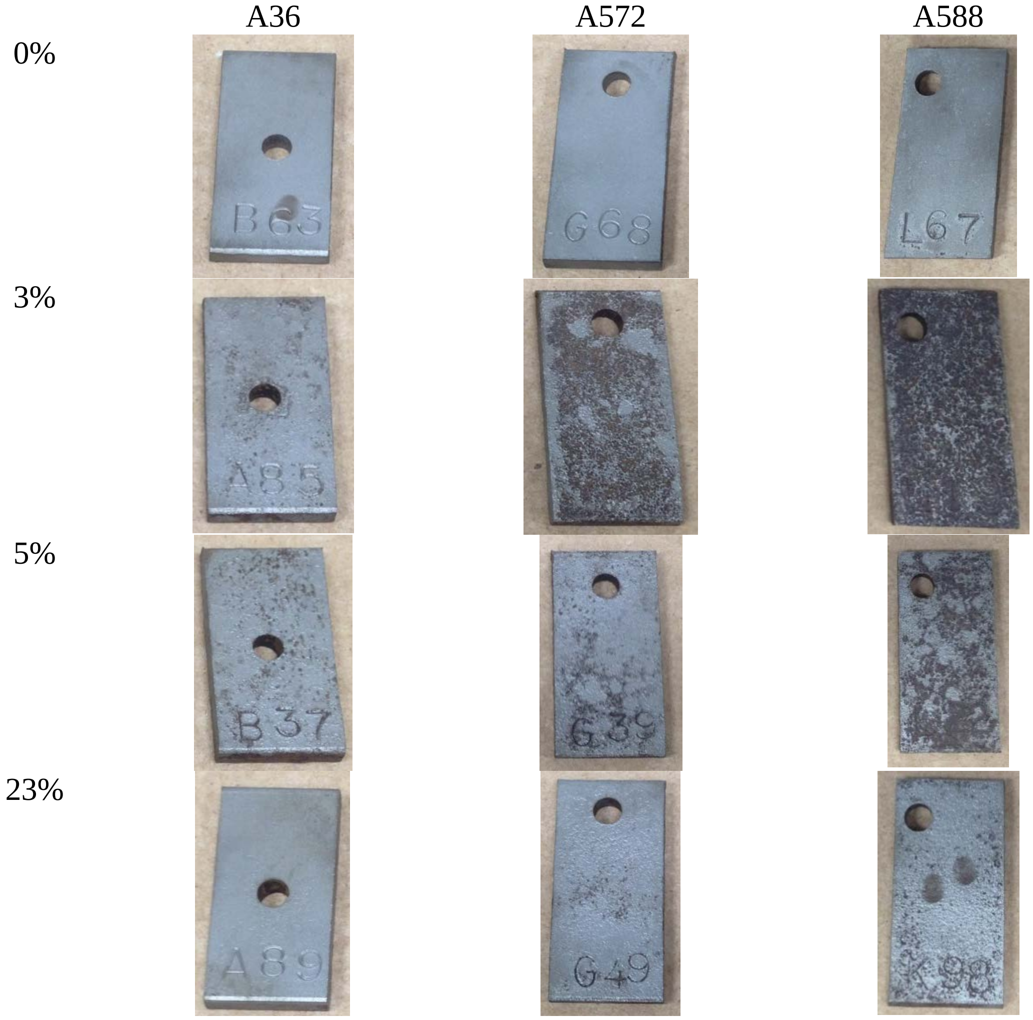

Figure 5.12: Visual condition of uncoated steel coupons from 4 week exposure after wire brushing, ultrasonic acid bath, and sand blasting

5.1.2.2 ***Results from Cyclic Exposure Tests***

The weight loss recorded for each uncoated steel alloy was plotted against time for each solution concentration and is presented in Figure 5.13. These plots exhibit the expected increase in corrosive losses with time for solutions containing sodium chloride. In general, the A588 and A572 steel alloys exhibited comparable corrosive losses, while the A36 steel generally exhibited slightly less corrosive loss. Furthermore, while the 3% and 5% concentrations yielded similar weight losses, the specimens subject to 23% concentrations were found to exhibit less corrosion. When the corrosive losses are plotted against the solution concentration for each steel alloy (Figure 5.14), this phenomenon is more readily identified. This disparity in rate of corrosion continues over time, as the difference between losses observed in the 23% solution specimens and lower concentration solutions increases over time.

To quantify the losses in terms of corrosion rates, Equation 5-1 previously presented was applied to the measurement data. The average corrosion rate over the course of the eight week test program was computed and is presented in Table 5.6. The table presents the surface corrosion rate in mils per year and confirms that the rate of corrosion for A36 is the lowest, while that of A588 is generally the highest. However, the estimate for the A588 steel at 3% concentration is likely biased by the data point obtained at two weeks of exposure which can be visually identified as an outlier. If the corrosion rate obtained from the point is discarded, the average corrosion rate obtained for the A588 steel alloy at 3% concentration is reduced to 77.6 mpy. Consequently, the A588 and A572 steel alloys exhibited nearly identical corrosion rates over the course of the test program. In contrast, A36 steel exhibited approximately 10-22% lower rates of corrosion compared to the average of the A572 and A588 alloys for the sodium chloride concentrations tested.

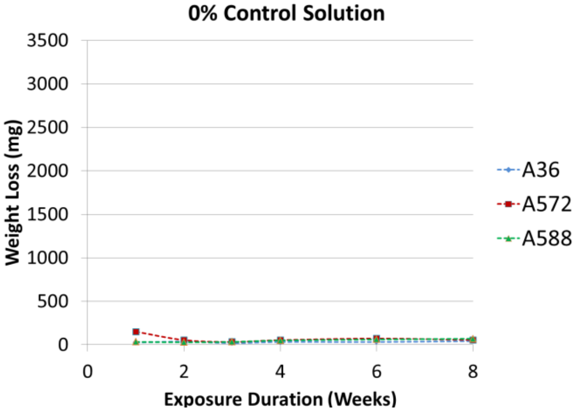

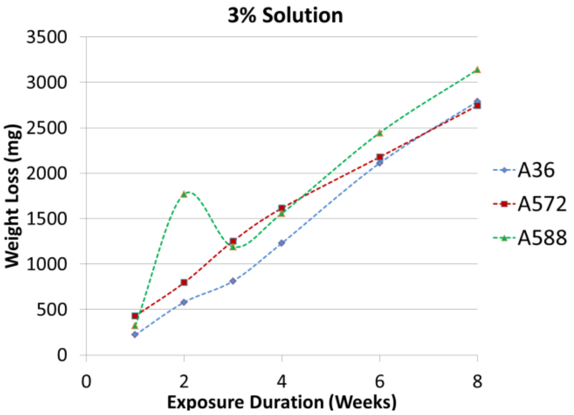

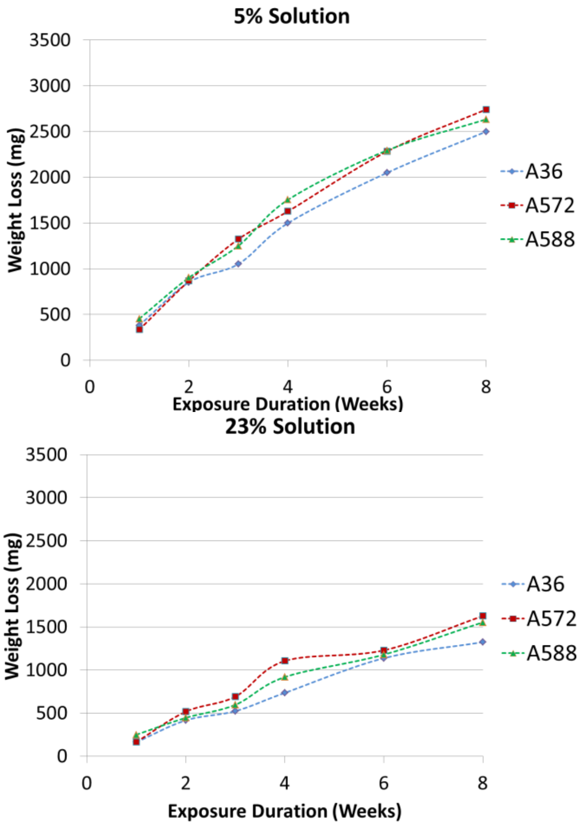

Figure 5.13: Comparison of corrosive losses measured on bare steel alloys for different concentrations of solution

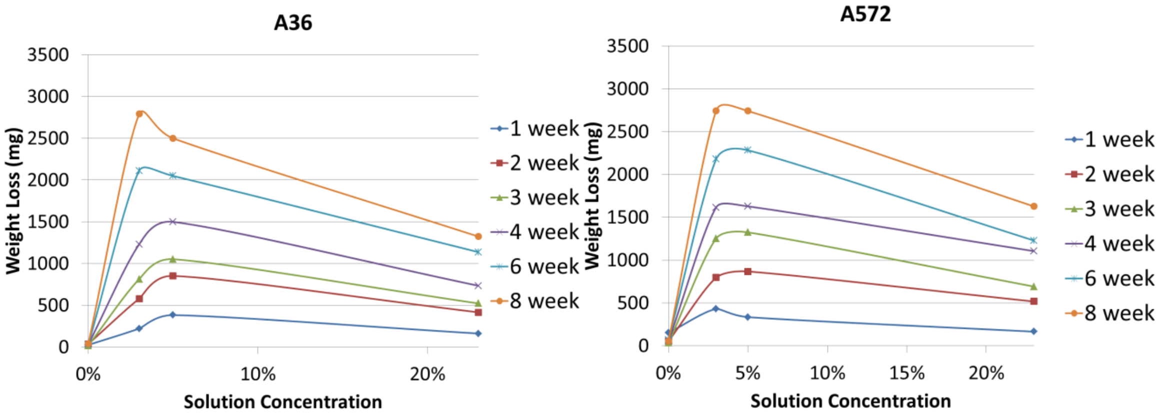

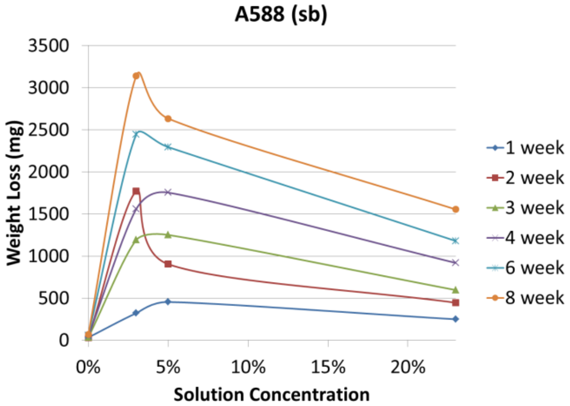

Figure 5.14: Comparison of corrosive losses measured as a function of solution concentration

Table 5.6: Corrosion Rates for different alloys with exposure concentrations [mpy]

	A36	A572	A588
De-Ionized Water	2.4	7.5	3.1
3% Solution	60.7	79.9	94.7
5% Solution	74.2	79.3	83.8
23% Solution	36.7	45.3	36.7

Weight losses measured on the painted A572, epoxy coated A572, and epoxy coated A588 were insignificantly low (generally only 10's of mg) and within the uncertainty bounds of the test and cleaning methods. These three coating methods did not exhibit any visual signs of distress over the eight week duration of the test program and so no conclusions can be drawn on the relative performance of each surface treatment method. However, the following section of the report will document an additional test performed on scratched specimens that provides significant insight on the undercutting of surface treatments. In contrast, the galvanized A36 steel did exhibit weight losses up to 1600 mg after the 8 week cyclic exposure. This weight loss is attributed to loss of the protective zinc coating as all specimens were observed to only exhibit “white rust” typical of such galvanizations and not ferric rust. Exposure of the zinc protective layer to sodium chloride in solution produces a reaction that breaks down the zinc to zinc chloride. The cyclic testing performed in the laboratory reveals that this loss of the protective layer occurs steadily over the first few weeks of exposure, but after four weeks there are few additional losses. Exposure of the galvanized A36 steel to all sodium chloride concentrations produced this behavior with the same observed increased rate of corrosion in the 3% and 5% solutions compared to the 23% solution. In general, the loss of the protective galvanized layer continued until about 70% of the original weight of the layer was consumed (Figure 5.16). Afterwards, very little loss occurred throughout the remainder of the eight week test program. Interestingly, the corrosion of the galvanized protective layer exhibited the same trend with solution concentration as the uncoated steel specimens, where the specimens subject to 23% solution exhibited less corrosion than those subject to 3% or 5% solution. However, over time this difference was less significant as the corrosion rates decreased after approximately 70% of the weight of the galvanized layer was consumed.

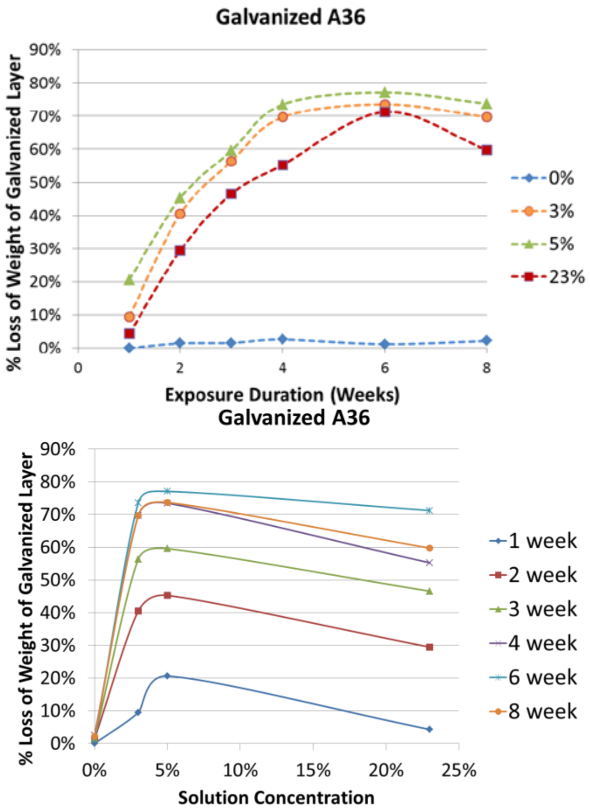

Figure 5.15: Loss of sacrificial galvanization layer during exposure to sodium chloride solutions in cyclic test: a) as a function of time; b) as a function of solution concentration

5.2 Laboratory Investigation of Undercutting of Treatments

5.2.1 ***Modified Cyclic Test for Evaluation of Coated Specimens***

In the cyclic exposure testing, painted, epoxy coated, and galvanized steel specimens were found to provide essentially complete protection to the underlying steel coupons of the eight week test duration. However, such testing only evaluates the effectiveness of complete protective treatments and does not account for accelerated deterioration that might occur after the surface coating is comprised by wear. For an evaluation of coated specimens and their effectiveness after exposure to corrosive environment, a secondary cyclic test program was conducted based on two ASTM standards: D7087, “An Imaging Technique to Measure Rust Creepage at Scribe on Coated Test Panels Subjected to Corrosive Environments,” and D1654, :Evaluation of Painted or Coated Specimens Subjected to Corrosive Environments.” The study was performed on painted A572 steel, epoxy coated A572 and A588 steel, and galvanized A36 steel over eight weeks of exposure to 3% sodium chloride solution and 0% (deionized water) as the control solution. This test method provides a means of comparing the development of corrosion on the substrate across different coatings and steel alloys. The results are based on rust creepage area measurements around the scribe line after eight weeks of exposure. Each coating system was also rated for corrosion performance through representative mean creepage calculated by imaging software.

5.2.2 ***Test Procedure for Scribed Coated Specimens***

Coated specimens were prepared for this secondary cyclic test by mechanical scribing using a motorized circular blade. A Dremel tool with 1 mm circular blade was used to scribe each specimen along its length. Each scribe line was cut by positioning the blade at 90 degree angle penetrating the coating and scratching the bare metal surface. Scribe lines were approximately 3 cm in length with endpoint away from the specimen edge or hole. Figure 5.10 shows scribed specimens for each coating type.

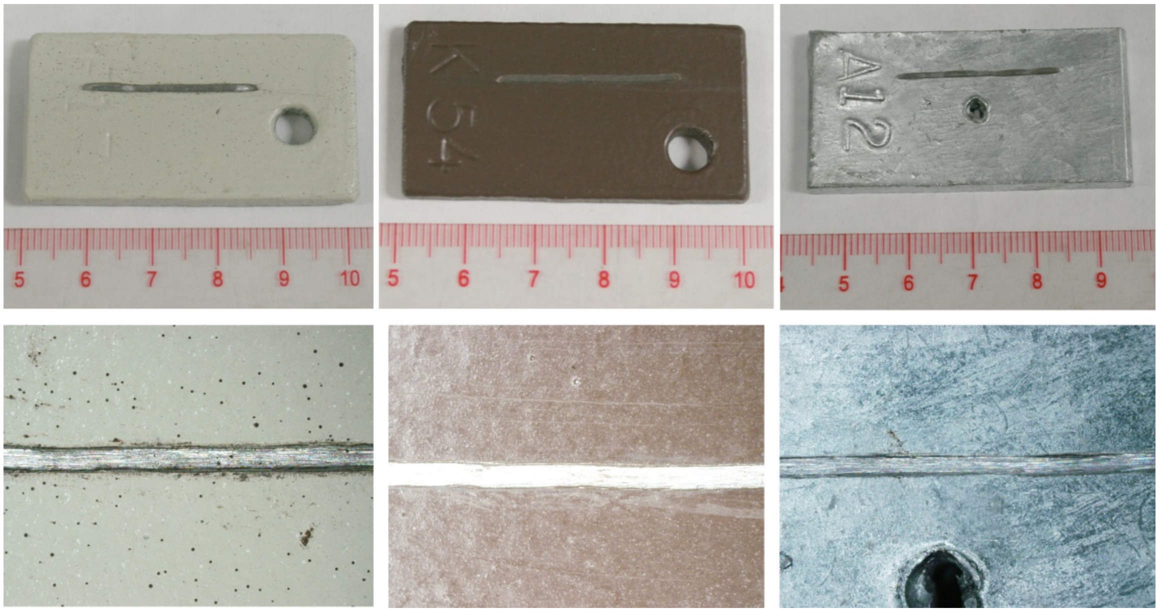

Figure 5.16: Scribed painted, epoxied, and galvanized specimens, from left to right

In the test program, specimens were exposed to 0% and 3% concentrations of sodium chloride in deionized water through cycling of wetting and drying. Consistent with prior testing, specimens were repeatedly submerged in test solution for two minutes follow by atmospheric drying for two hours. The same dunking apparatus from the previous cyclic corrosion test was used for the test set-up. Each test cell contained three specimens of a coating system. A total of eight test cells were set-up with 24 specimens to accommodate the four different coated specimen types at both the 0% and 3% salt concentrations. Figure 5.11 shows the test setup with specimens hung from a lever arm that can lower and raise specimens in and out of the test container. The specimens were allowed to cycle in and out of the solution for a period of eight weeks. Evaporation of test solutions were refilled with deionized water to the original solution level. Photographs on the progress of each specimen were taken at the end of each week.

Figure 5.17: Scribe test setup for cyclic wetting and drying corrosive exposure

At the end of the eight weeks testing period, specimen coating was removed to examine the corrosion of the substrate. Painted and epoxied coatings were removed by soaking the specimens in acetone and mechanically brushing the coating off using a metal wire brush until the coating was removed around the scribe area. The specimen surface was rinsed and wiped clean using paper towels soaked in acetone. Galvanized specimens were cleaned by dissolving the galvanized layer in acid solution and cleaned with acetone. The acid solution used contained 50 gram stannous chloride, 20 gram antimony trioxide in 1,000 mL concentrated hydrochloric acid. Cleaned specimens were then examined and photographed using a digital microscope. The scribed area observed within the view of the microscope corresponds to 17.5 mm along the length of the scribed line. Imaging analyses were done using Olympus Stream Essentials software package.

Rating of failure at the scribe line for each coating system was determined based on areas of the substrate that were discolored due to corrosion. The software package used had the capability to capture and examine an area of 17.5 mm by 13 mm, which was the area used to examine the test specimen. Before capturing images of corroded specimens, the software was calibrated using a known length at a particular zoom of the microscope. Images of corroded specimens were captured at the calibrated zoom from a mounted camera on the microscope. The captured image was imported to the software for analysis. Rust creepage areas were determined for each specimen by tracing the discolored corroded area around the scribe line and using the software to calculate the total area. The area calculated included the original area of the scribe line. Figure 5.12 shows the microscope and a screen shot of the tracing method used.

Figure 5.18: Corroded area determination using microscope captured image

The mean creepage was calculated based on ASTM D7087 from the obtained discolored areas and the considered scribe length, equation (5.2). A rating number was determined for each coating system using the provided table in ASTM D1654. A replicate of the table is shown in Table 5.7

.

The mean creepage was calculated as:

$$C = \frac{A}{2L} \tag{5.2}$$

Where: C = mean creepage in mm

A = area of discolored by tracing in mm^2

L = length of scribe line from which corroded area was integrated in mm (17.5 mm for this study)

Table 5.7: Rating table used based on ASTM D1654

Rating of Failure at Scribe Using Mean Creepage	
Millimeters	Rating Number
Zero	10
Over 0-0.5	9
Over 0.5-1.0	8
Over 1.0-2.0	7
Over 2.0-3.0	6
Over 3.0-5.0	5
Over 5.0-7.0	4
Over 7.0-10.0	3
Over 10.0-13.0	2
Over 13.0-16.0	1
Over 16.0 to more	0

5.2.3 ***Results from Cyclic Exposure of Scribed Coated Specimens***

Weekly images of the specimen after exposed to the test solution are presented in Figure 5.13 and Figure 5.14 for the 0% and 3% sodium chloride concentrations, respectively. Images selected for the figure correspond to the most affect specimen out of the set of three replicates used in the testing. Similar corrosion progression was observed for the remaining two replicates. As can be seen in the photographs, no coating damage was observed for the 0% or deionized water test solution in any of the four coating systems over the eight weeks testing period of this study. Slight rust discoloration was observed early in the test program within the scribe line for epoxy coated A588; however, no progression of corrosion was observed with increased exposure time in deionized water. Coated specimens cyclically exposed to 3% sodium chloride test solution showed notable corrosion in and around the scribed line for all four coating systems. Coating undercutting and blistering was observed for both epoxied and painted specimens. The The galvanized specimens can been seen to be coated with both the white rust previously observed in the non-scribed specimens characteristic of the corrosion of the sacrificial zinc protective layer. However, this white rust is clearly mixed with the red rust characteristic of ferric corrosion indicating that subsurface steel was also subject to corrosive losses.

Evaluation of blisters was based on the ASTM D714 standard for evaluating degree of blistering of paints. The blister sizes were assigned a numerical value on a scale from 10 to 0, where 10 indicates no blistering and 8 represents the smallest size that can be seen by unaided eye. Given the subjectivity associated with assigning these blister ratings, a four step scale was used for blister sizes using the values of 8, 6, 4, and 2 as the blister size increases in size. Frequency was rated also on a four step scale as few, medium, medium-dense, and dense. Table 5.8 below summarizes the blister size and frequency rating for epoxied and painted specimens exposed to 3% NaCl. Blistering was seen only along the scribe line and no blistering was observed at other coating surfaces. For reference, specimens with a blister rating 2 have a blistering size at 2.5 mm or above in diameter. Observation of blisters in coating indicated that epoxy coating on A588 steel provides the least effective solution out of the three coating systems after wear and exposure of the underlying steel. This is closely followed by epoxy coating on A572, which suggests that epoxy coating in general provides the least ideal surface treatment to inhibit corrosion if the surface treatment is compromised by mechanical wear. With regard to blistering, the best performance was obtained by painting of the A572 alloy.

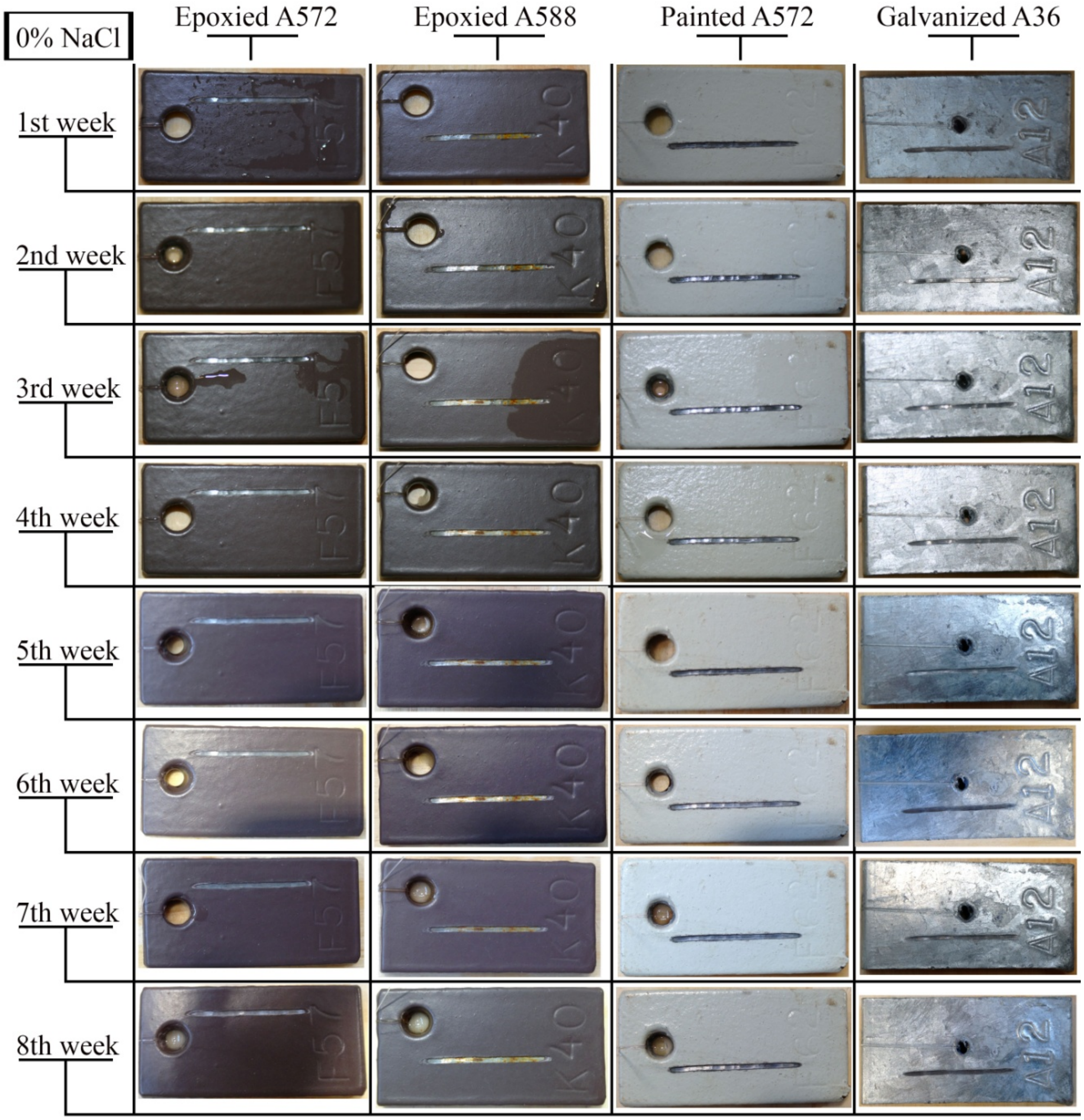

Figure 5.19: Coated steel specimens exposed to deionized water shown at weekly intervals

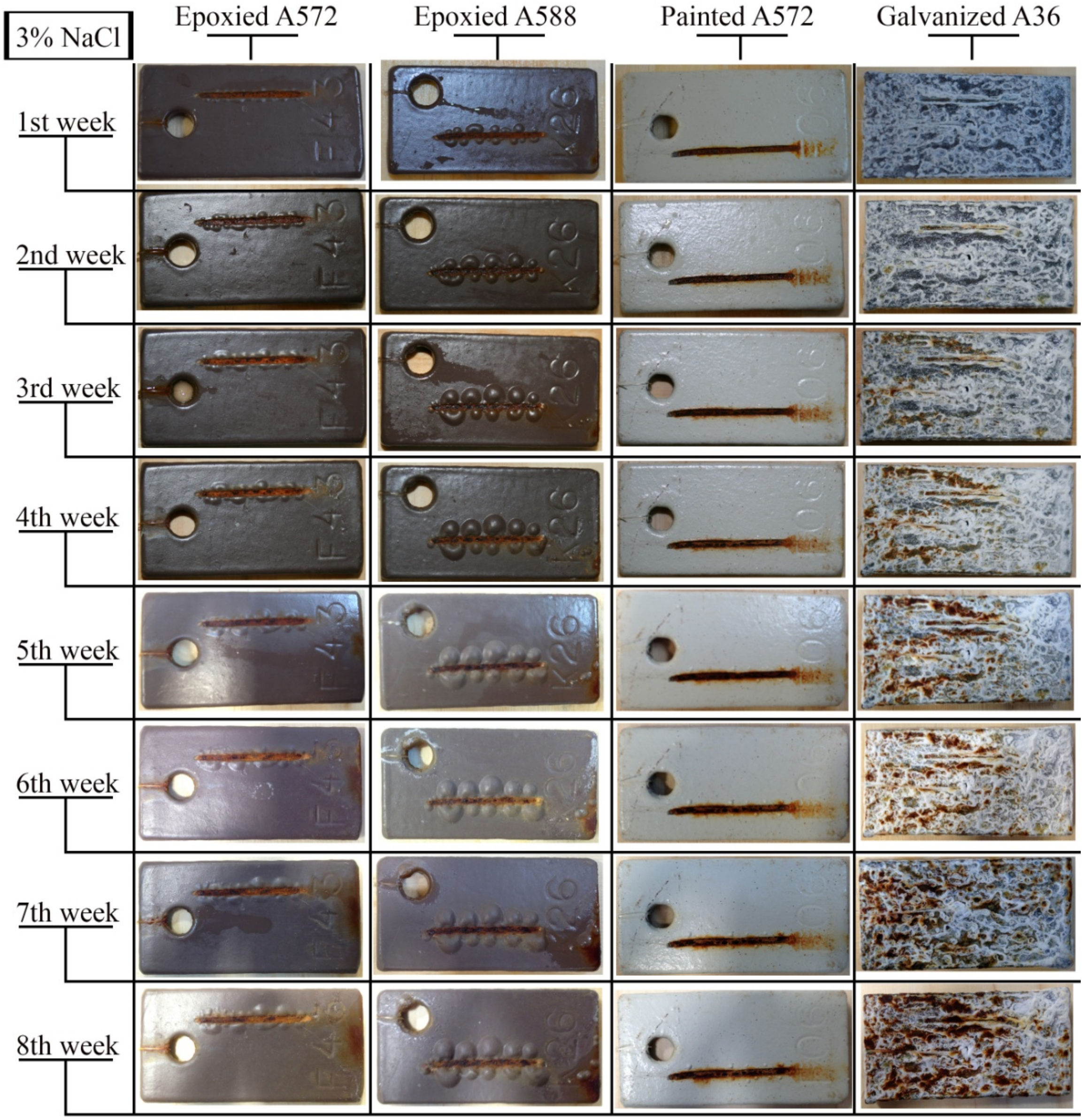

Figure 5.20: Coated steel specimens exposed to 3% NaCl solution shown at weekly intervals

Table 5.8: Size and frequency rating for blistering of epoxied and painted specimens

3% NaCl	A572 P		A572 E		A588 E	
	Size	Frequency	Size	Frequency	Size	Frequency
Week 1	10	n/a	8	Medium Dense	6	Medium Dense
Week 2	10	n/a	6	Dense	4	Medium Dense
Week 3	10	n/a	6	Dense	2	Dense
Week 4	8	Few	6	Dense	2	Dense
Week 5	8	Medium	6	Dense	2	Dense
Week 6	8	Medium	6	Dense	2	Dense
Week 7	8	Medium	6	Dense	2	Dense
Week 8	8	Medium Dense	6	Dense	2	Dense

Unlike the epoxy coated and painted specimens that show corrosion only occurring around the scribed line, galvanized A36 coupons exhibit a wider area of corrosion across the galvanized surface. Since the galvanized coating or the zinc layer is a metal layer it will naturally corrode. Imaging results of galvanized specimens show a clear progression of corrosion on the galvanized layer with time. The image also indicates that more corrosion occurred toward the upper end of the specimen where more brownish discoloration characteristic of the ferric corrosion can be seen. Unlike the upper end, the bottom end experienced more exposure to the test solution with longer wetting period due to gravity driven flow of solution from the upper end to the lower end during atmospheric drying. Likewise, the build-up of white rust byproducts can also be seen more toward the bottom end of the specimen. The build-up of insoluble products in that form is likely a combination of crystalized salt and zinc patina or corroded zinc by-products. The build-up of byproducts could create an impervious layer that potentially slows the corrosion of the zinc, which could explain why the bottom end is less corroded. Figure 5.15 shows microscope images at the scribe line of three galvanized specimens at the end of eight weeks exposure. With the galvanized layer removed, little corrosion is seen on the scribe line; instead most of the corrosion occurred on the zinc layer with remnants of corrosion products throughout the specimen surface. Due to the protected galvanized layer little to no corrosion is seen on the base metal surface outside of the scribe line.

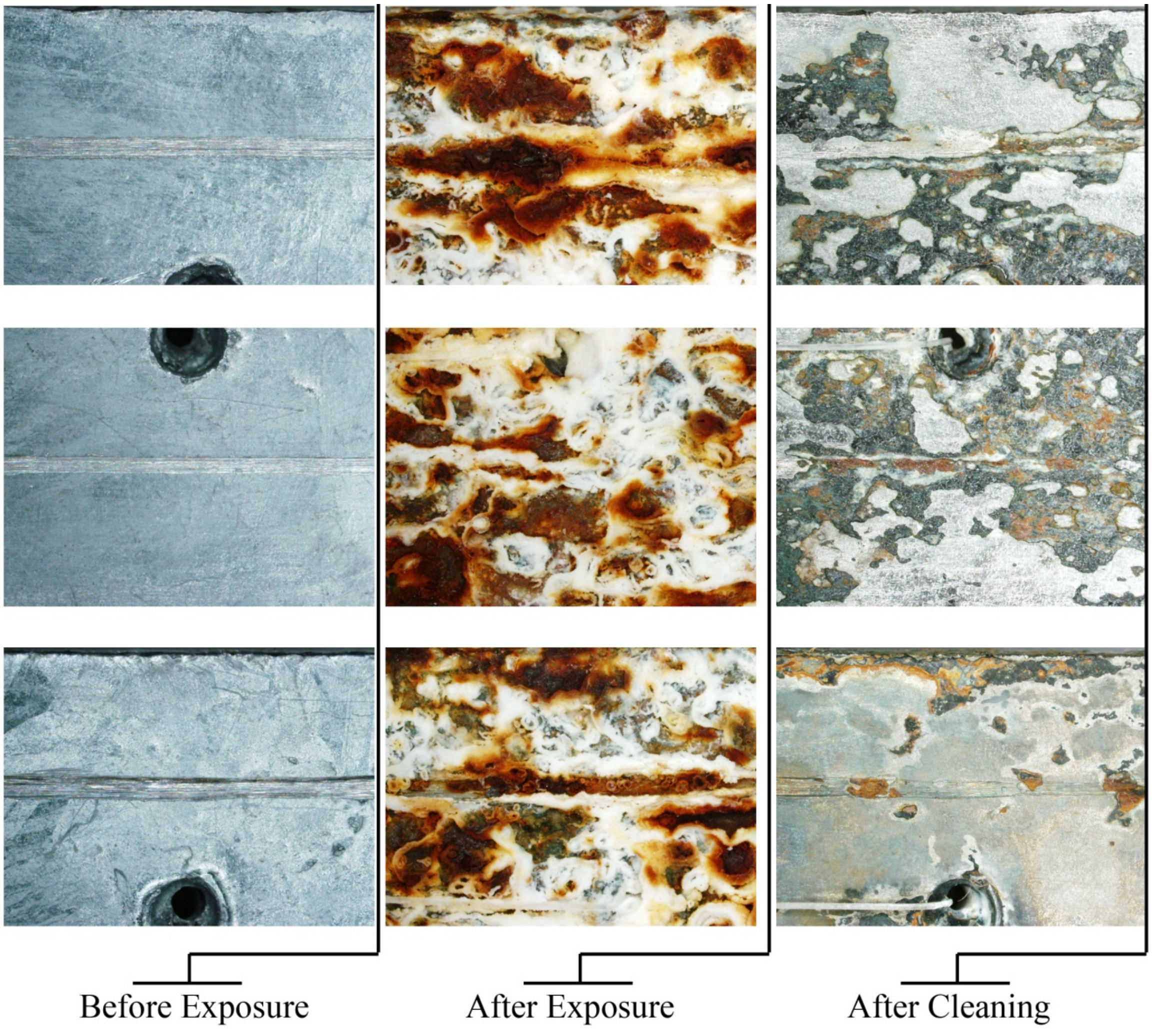

Figure 5.21: Microscope images of galvanized specimens

Calculations of mean creepage for scribed epoxy coated and paint specimens were calculated based on the rust areas under the coating and the scribe length of 17.5 mm using equation (5.2) above. Captured images of rust areas after removal of epoxy and paint coatings are shown in Figure 5.23 through Figure 5.25. Results of rust area, mean creepage, and rating of failure at the scribe are shown in Table 5.9 for three specimens of each coating system.

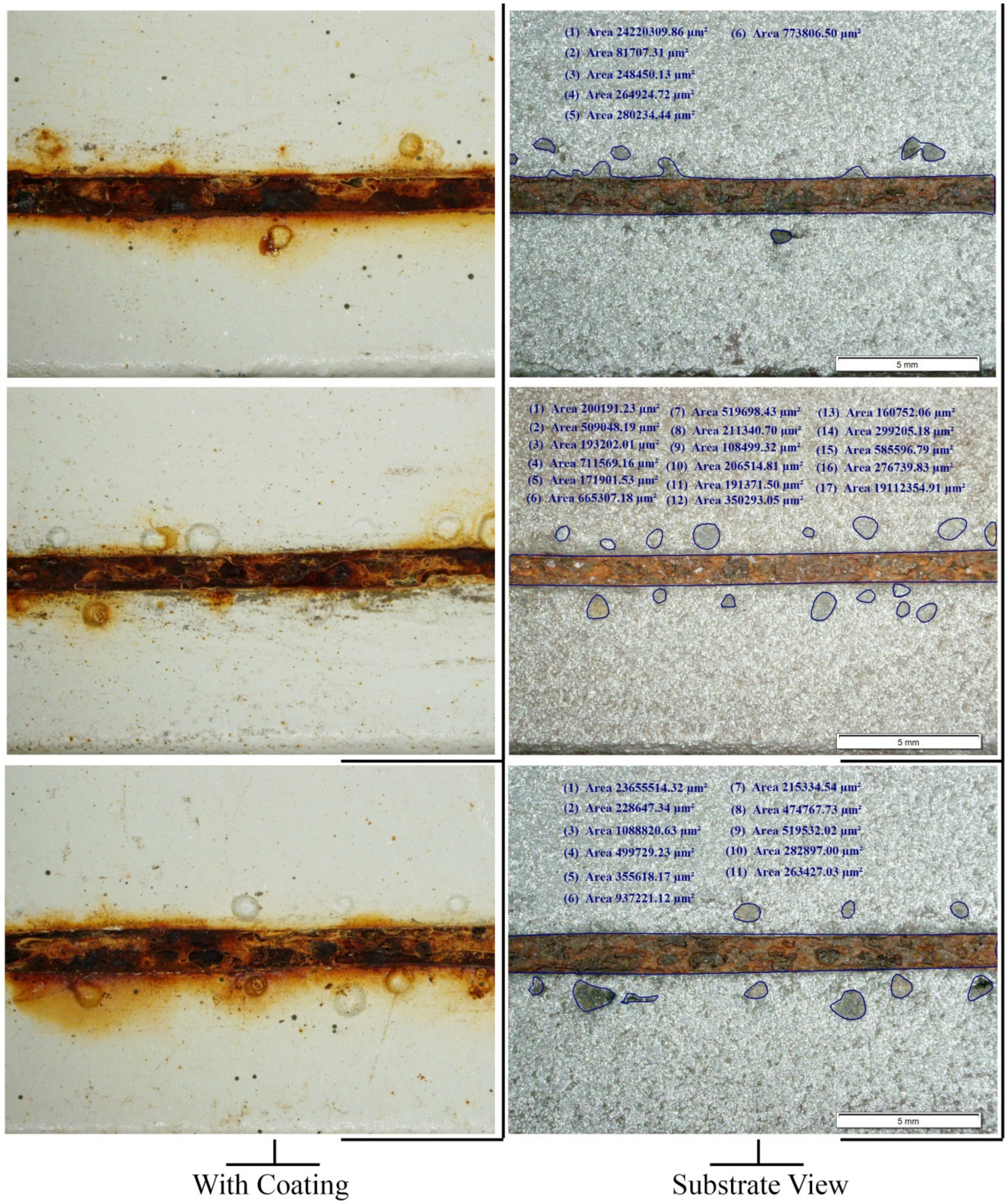

Figure 5.22: Microscope images of painted A572 specimens

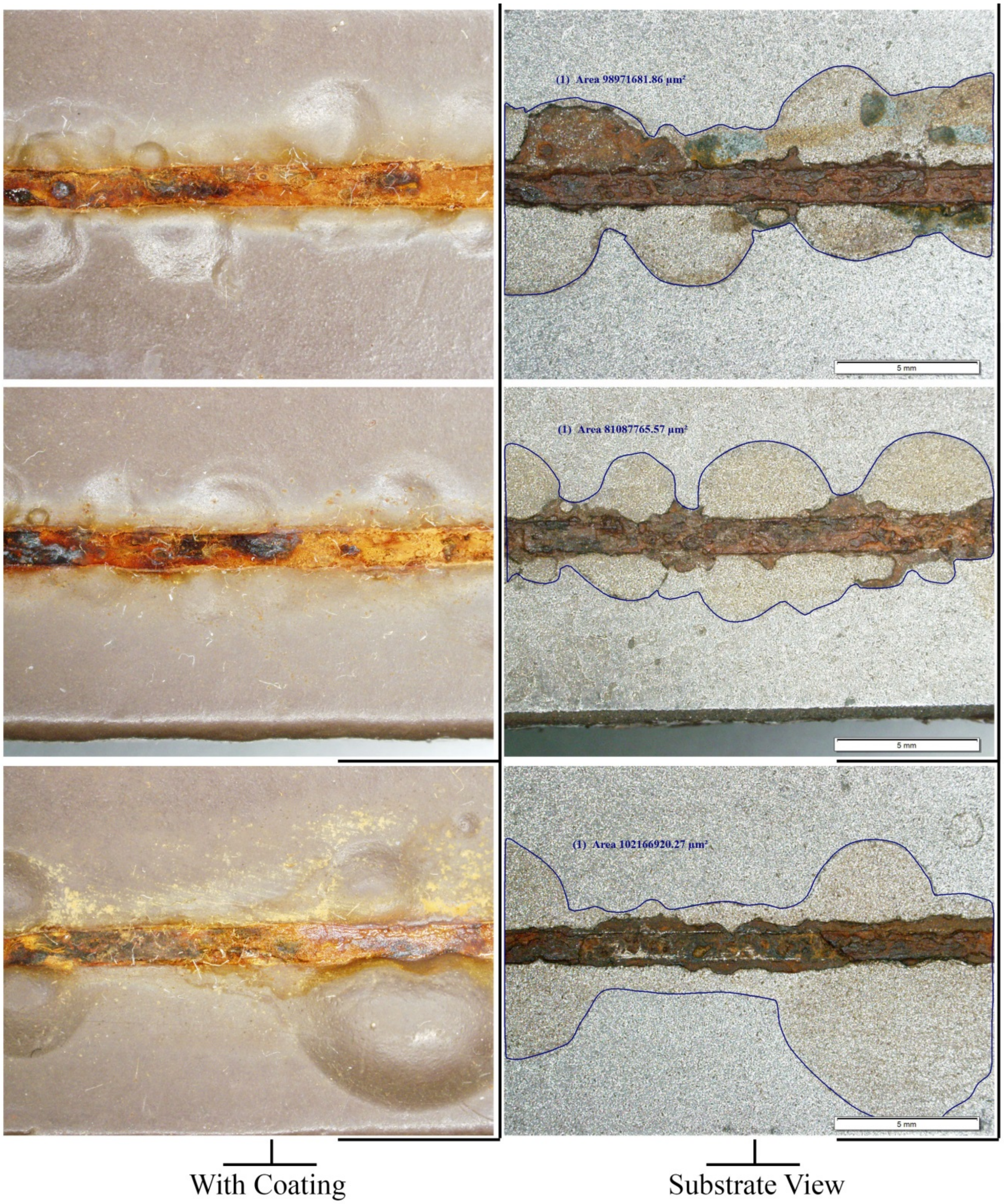

Figure 5.23: Microscope images of epoxy coated A572 specimens

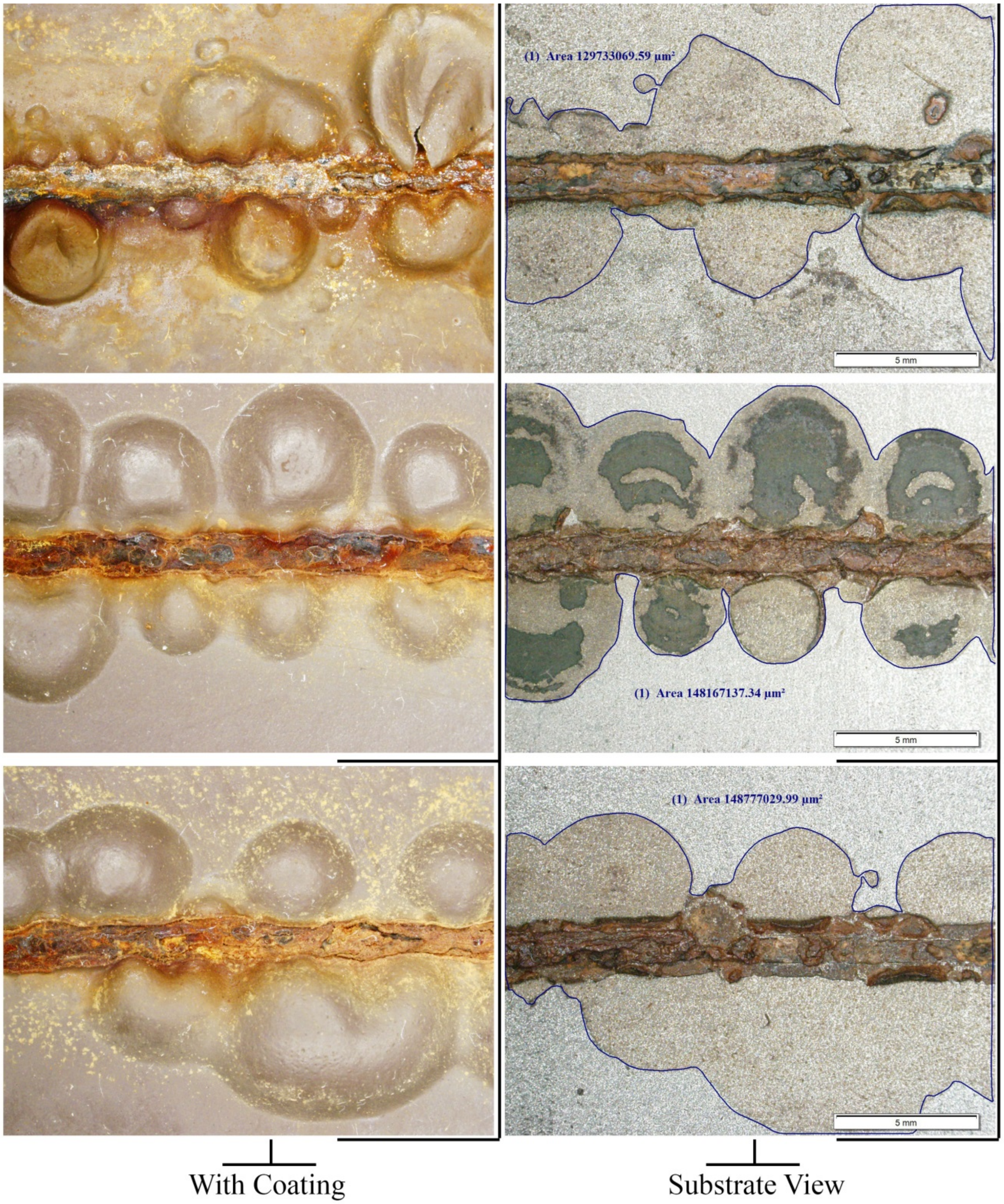

Figure 5.24: Microscope images of epoxy coated A588 specimens

Rating numbers were determined based on criteria given in Table 5.7. The rating ranges from 0 to 10, 10 being the highest rating with zero rust creepage under the coating. Rating numbers were consistent for all three specimens with painted A572 having the highest coating performance with a value of 8 follow by epoxied A572 at 6 then epoxied A588 at 5.

Table 5.9: Result of scribe test for painted and epoxied specimens

Specimen Number	Rust Area (mm^2)	Mean Creepage (mm)	Rating
Epoxied A572			
F11	81.09	2.31	6
F13	102.17	2.92	6
F43	98.97	2.83	6
Painted A572			
F74	24.47	0.70	8
F12	28.52	0.81	8
F06	25.87	0.74	8
Epoxied A588			
K54	129.73	3.70	5
K39	148.78	4.25	5
K26	148.17	4.23	5

Given the performance of the painted specimens relative to the epoxy coated specimens in terms of both blistering and mean creepage, the results of the laboratory test program suggest that painting should be preferred to epoxy coating for protection of exposed steel components in highway bridges. However, it should be noted that the study considered only the performance of the coating systems after identical mechanical scribing and does not consider the resistance of either coating system to mechanical wear nor does it consider environmentally driven deterioration of either coating system, which may be different. The results do clearly shown that once the steel under the coating is exposed there is significant undercutting of the epoxy coating which leads to accelerated corrosion, whereas the bond between the paint and the steel is more resistant to this undercutting.

5.3 Field Measurement of Corrosion at Regional Bridge Sites

To generate quantitative data for evaluating the impact of sodium chloride deicing and anti-icing application strategies on steel components below the deck, a field test program was conducted over a sample of nine bridges in North Carolina. The study was conducted over one winter season for selected bridges in the Greensboro and Asheville regions. This chapter presents the methodology and experimental results obtained from installation of sacrificial steel coupons on girder components to simulate typical field exposure conditions at specific locations across the bridges in the study. The field installation of samples replicates natural factors that cannot be readily simulated under laboratory conditions and produces spatial data on the exposure of superstructure elements most susceptible to corrosive damage under each of the sodium chloride treatment strategies. Statistical analysis of corrosive losses is presented to evaluate predominant factors associated with corrosive loss in superstructure elements exposed to deicing and anti-icing solutions in normal service conditions.

5.3.1 ***<u>Details of Experimental Test Program</u>***

Steel specimens used were 3/16 inch thick, uncoated A36 steel with dimensions of 23.5 inches long by 2 inches wide (Figure 5.25). Preparation of the specimens included sand blasting to achieve a uniform gray metal surface followed by cleaning with acetone to remove corrosive ions and contaminants. Prior to cleaning, each specimen was stamped with an identification number for reference. The samples were weighed to the nearest 0.01 gram prior to installation in the field.

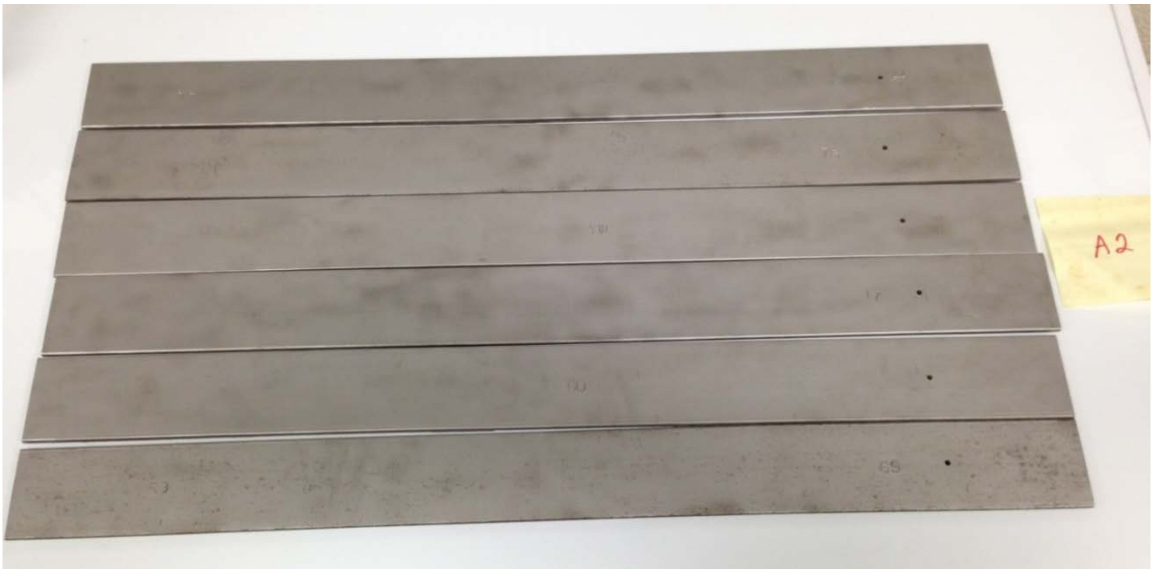

Figure 5.25: Steel specimens prepared prior to installation on bridge girders

Field installation sites were selected at both exterior and interior girders, which in this report are designated as C1 and C2, respectively, (Figure 5.26). At each exterior and interior girder location, sample specimens were mounted on both the web and bottom flange of the girders, designated as exterior for exposure toward the outside and interior for exposure on the inside (under the bridge deck), (Figure 5.27).

Figure 5.26: Testing sites for atmospheric exposure of metal coupons

Figure 5.27: Coupons placement and location for atmospheric exposure

Circular ceramic magnets were used to attach the specimens to the bridge girders. Prior to attachment, each steel sample was wiped with de-natured alcohol to remove any residual chloride introduced during handling. The sacrificial coupons were installed at the end of November and collected at the beginning of March to capture one winter season. The deicing applications applied to each bridge were obtained from NCDOT through reports that designated the treatment type and number of treatments applied. A summary of these report logs is presented in Table 5-10. The sampling corresponds to the same nine bridges investigated in the field study for seasonal chloride concentration measurements in the deck, piers, and parapets. This sampled set of bridges included three bridges receiving four applications of granular deicing treatment in Greensboro, three bridges receiving two applications of anti-icing brine and two applications of granular deicing treatment in Greensboro, and three bridges receiving eight applications of salt-sand mix deicing treatment in Asheville.

Table 5.10: Deicing application data for all bridges

Bridge Locations		Brine	Granular	Salt-Sand	Total
Greensboro	NC 62 over I-85	4	4		4
	Vickery Rd over I-85 Business		4		4
	Mt Hope Church Rd over I-40		4		4
	US 220 NB over NC 62	4	4		4
	McConnell Rd over I-40		4		4
	NC 62 over 421	4	4		4
Asheville	SR 1684 over US 19,23,70			8	8
	SR 2207 over US 19,23			8	8
	SR 2531 over I-40			8	8

5.3.2 ***Corrosive Losses Measured by Location***

The sacrificial steel coupons were collected in March at the same time that powder samples were retrieved from the deck, parapets, and piers for chloride content analysis. The exposed steel test specimens were cleaned and reweighed according to ASTM G1 standard practice for preparing, cleaning, and evaluating corrosion test specimens (ASTM 2011). The cleaning process included wetting and mechanical removal of corrosion byproducts using a wire brush follow by cleaning in an ultrasonic acid bath and then sand blasting. The acid solution used consisted of stannous chloride, antimony trioxide, and concentrated hydrochloric acid. The mass loss of each specimen was determined and recorded by comparing the original weight to the cleaned corroded weight. To determine the expected weight loss of base metal due to the cleaning process alone, an unexposed, un-corroded specimen was cleaned using the same cleaning procedures. The cleaning loss was then used as an adjustment factor in determining the actual weight lost due to corrosion only. Control weight loss during acid cleaning and sand blast are 0.40 gram and 0.22 gram, respectively. Weight losses recorded for the 71 sacrificial coupons that were retrieved from the field are shown by location in Table 5.11 in grams.

The average recorded weight losses by location on the superstructure are shown in Table 5.12 and Figure 5.28 for each test location with respect to the treatment applications in Greensboro and Asheville bridges. The calculated percentages are based on the weight loss with respect to the original coupon weight. It is important to note that Asheville bridges received twice the number of applications which likely explains an overall higher average loss at all locations except for web of interior girders.

Table 5.11: Weight losses for field samples after adjusting for expected cleaning loss

Location	Greensboro Bridges						Asheville Bridges		
	G1	G2	G3	G4	G5	G6	A1	A2	A3
Exterior Girder (C1)									
Web-exterior	1.5g	0.42g	0.48g	5.60g	1.00g	1.38g	3.18g	7.30g	11.4g
Web-exterior				5.24g		1.34g	2.22g	8.18g	7.40g
Web-exterior									5.34g
Web-exterior									11.2g
Web-interior		0.28g	0.54g			0.02g	4.54g	4.84g	9.66g
Web-interior						2.94g	4.92g	4.02g	
Web-interior									6.84g
Web-interior									8.68g
Flange-exterior	4.1g	2.84g	2.88g		2.68g				
Flange-interior	1.9g	2.42g	4.04g	1.12g	2.84g		5.86g	5.02g	
Interior-Girder (C2)									
Web-interior	0.42g	0.04g	4.0g	0.36g	0.92g	0.84g	1.52g	5.78g	0.50g
Web-interior	0.54g		0.68g	2.54g	8.32g	0.5g	1.12g	3.3g	2.00g
Web-interior							1.28g	4.66g	
Web-interior							2.14g	3.28g	
Flange-interior	2.42g	1.34g	0.32g	1.10g	2.42g	1.82g		12.7g	
Flange-interior	1.46g		0.64g	7.74g	2.84g	3.72g			

Table 5.12: Average weight loss and percentage of original weight for all bridges

Location	Exterior Girder, Exterior Web	Exterior Girder, Interior Web	Exterior Girder, Exterior Flange	Exterior Girder, Interior Flange	Interior Girder, Interior Web	Interior Girder, Interior Flange
Greensboro Granular Salt (4 Applications)	0.63g (0.053%)	0.41g (0.034%)	2.80g (0.236%)	3.10g (0.261%)	2.78g (0.234%)	1.51g (0.127%)
Greensboro Granular & Brine (4 Applications)	3.01g (0.253%)	1.48g (0.125%)	4.10g (0.345%)	1.51g (0.127%)	0.87g (0.073%)	3.04g (0.256%)
Asheville (8 Applications)	7.04g (0.593%)	6.21g (0.523%)	n/a	5.44g (0.459%)	2.56g (0.216%)	12.68g (1.07%)

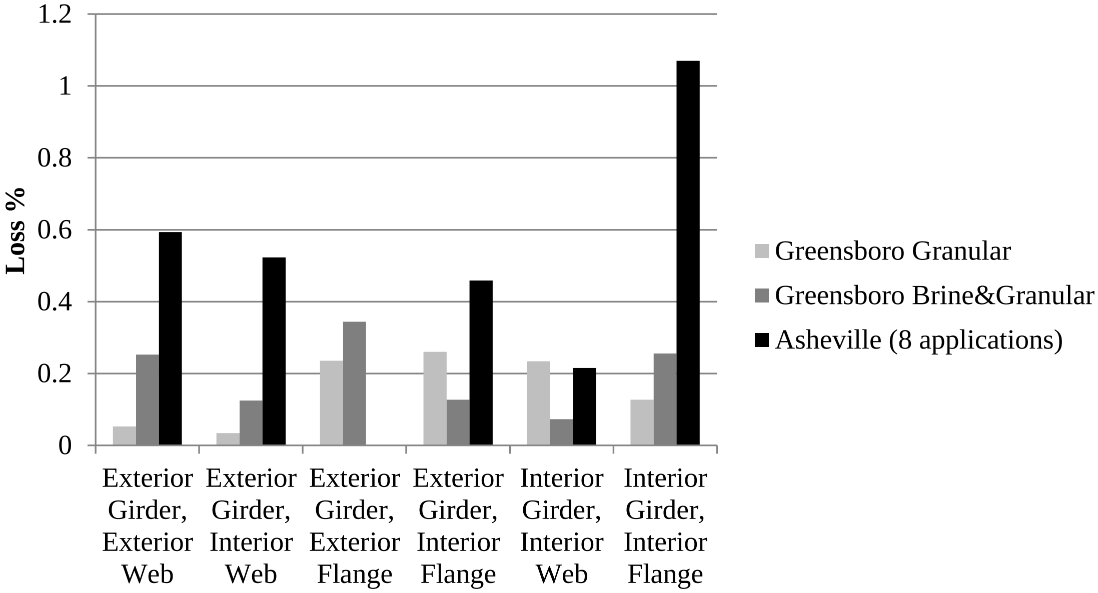

Figure 5.28: Average percent losses for girder locations and treatment types

The test results show that for the three different deicing treatments, the average corrosive loss across all testing locations is 0.158% for four granular salt applications, 0.197% for four brine with granular salt applications, and 0.572% for eight salt-sand deicing applications, respectively. The corresponding results normalized per application are 0.0395% for granular deicing, 0.0493% for brine anti-icing followed by granular deicing, and 0.0715% for salt-sand deicing mix. When comparing the average corrosive losses for all flange locations versus all web locations, the flanges are found to experience about 1.5 times more corrosion compared to web components. Additionally, the highest overall corrosive weight loss was found at the interior flange of an interior girder. This measurement was taken on a bridge with an expansion joint in poor condition, so it is expected that the interior girder would experience higher chloride concentration from gravity directed flow from the lane on the deck receiving deicing treatment. Bridges receiving granular only treatment in Greensboro exhibited the greatest corrosive losses at interior flanges of the exterior girders with an average of 0.0653% per application. Likewise, bridges in Greensboro receiving both granular treatment and brine anti-icing exhibited the greatest corrosive losses at the exterior flanges of the exterior girders with an average of 0.0863% per application. Lastly, the highest corrosive loss recorded for Asheville bridges was observed at the interior flange of interior girders, with 0.134% per application. In the case of Asheville bridges, no sample was retrieved for exterior flange at exterior girder. However, from field observations the appearance of corrosion on the exterior and interior flange surface of exterior girders is similar. This consistent record of higher corrosive losses at the flange locations reinforces the finding that corrosion is more of a concern across the bottom flange of girders rather than on the web. This is a rational finding since the bottom flange of a girder is a horizontal surface that can easily collect corrosive run off from the bridge deck. However, even though the result shows that the flange yields the highest corrosive loss, the results were based on a limited sample size for the flange location.

For Greensboro bridges, which were reported as receiving either four applications of granular salt or four applications of granular salt with brine, there is an overall higher corrosive loss on bridges receiving granular salt with brine pre-treatment. Computing the average total losses at all the test locations, the overall loss is 24.8% higher or 1.25 times greater for bridges receiving both granular and brine treatment compared to granular treatment alone. Supporting this trend, higher corrosive loss from the combination of brine and granular can be seen at four out of six test locations. The exceptions are interior flanges at exterior girder and interior web at interior girder where granular treatment only exhibits higher loss.

5.3.3 ***Statistical Analysis of Probable Significant Factors***

Further study of the experimental data with the functional properties of the bridges and locations of the specimens were performed using the MiniTab statistical regression and modeling software package. The software was used to examine factors that may significantly affect the corrosive losses of steel bridge components in addition to the significance of the deicing or anti-icing treatment strategy employed. Factors that were considered included bridge age, under clearance height, traffic count, railing type (open or solid), deck joint condition rating, and traffic direction (whether the test location was facing oncoming traffic below the bridge). This functional information was obtained from NCDOT bridge inspection reports along with observations recorded during field work. The corrosive mass losses were normalized to losses per application for the analysis by dividing by four for Greensboro samples and eight for Asheville samples.

Figure 5.29 presents the independent effects or main effects for each of the factors on the mean corrosive mass loss in grams, with the overall mean represented by the horizontal line. The collection of plots show the average corrosive loss associated with each factor independently, which can be used to evaluate whether there is a likely significant effect on the average amount of corrosive mass loss linked to that factor. For instance, the main effects plot for railing type indicates that regardless of whether the railing on the bridge was open or solid there was no significant effect on the amount of corrosion since there is no statistically significant difference in the average corrosive loss measured in either case. Similarly, whether the sample is facing oncoming traffic or not did not produced a significant effect on average mass loss, since this plot also exhibits a flat slope. In both cases, the small variation can be readily attributed to error and uncertainty in the sampling, interaction effects from other factors, and the limited sampling size. In contrast, the main effects plot for the sampling location is useful in identifying which locations experience the most corrosive loss. The highest mean corrosive loss is associated with the exterior flange follow by exterior web, interior flange, then interior web surfaces.

The plot for application types reveals that salt-sand mix treatments in Asheville produced the highest average corrosive losses follow by bridges receiving brine with granular treatment then granular treatment alone. Plots of other factors including bridge age, traffic count, and clearance indicate that there are significant effects associated with each factor. The traffic count in particular indicates that with low traffic count there is an overall higher corrosive loss; however, a clear trend cannot be implied over the entire range for traffic count. Similarly for the others factors, only a particular condition within the range seemed to promote higher corrosive mass loss.

The main effects plots can provide useful indications of general trends associated with each condition within each factor; however, it lacks consideration of the interaction amongst factors on the corrosive loss observed. Also, bias from the data set could arise from grouping of conditions that may isolate only a particular bridge or set of bridges. A good example of this effect can be seen in the plot for deck and joint condition that implies that there is a slightly higher average mass loss on bridges with “good” rating compared to “fair” and “poor”. While statistically this may be the case, since the main effects plot takes into consideration all the average effects from all other factors, such a conclusion can be misleading. In other words, the data may show that there is a higher overall loss for “good” deck rating, but this may not be true for each individual factor. Interaction effects between other factors that may be more significant can skew the overall average and mask the actual relationship between joint conditions and expected corrosion losses.

The interaction effects model was developed to take into consideration the effect of multiple factors and how those factors act together to influence the corrosive mass loss. The matrix of resulting interaction effect plots is presented in Figure 5.30. An interaction plot is also useful in separating out the more influential variables in instances where several significant effects interact producing a main effects plot that can be misleading, especially when the differences in individual effects is large. There are no interaction effects between two factors when the plot shows relatively horizontal lines from one condition to another within a factor plotted against another factor. The horizontal lines indicate that the main effect is neither increasing nor decreasing for each condition. Due to limited collected data, certain interaction plots are incomplete for particular conditions where the data is too sparse and thereby determination of a comprehensive analysis of interaction was not possible.

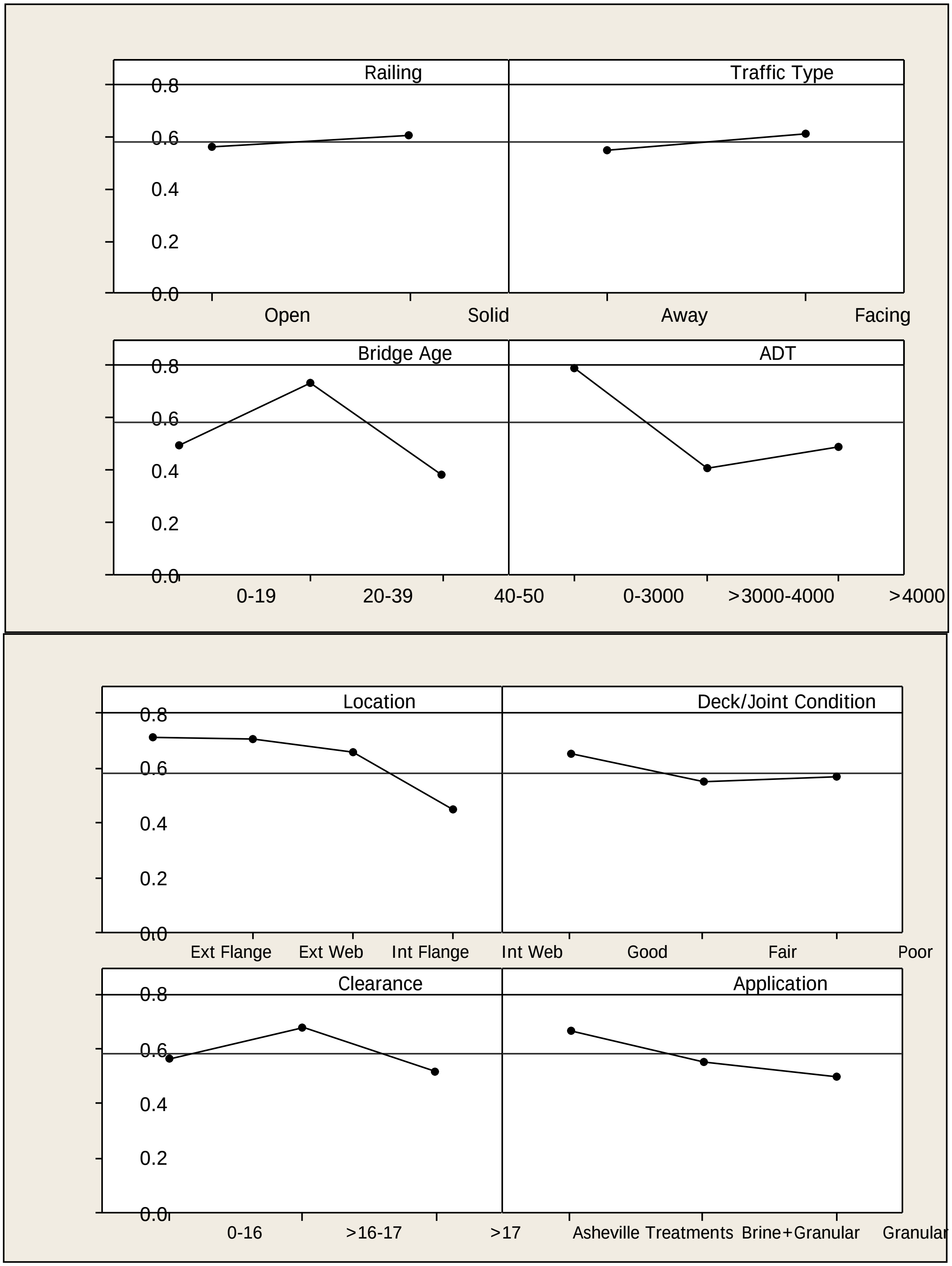

Figure 5.29: Main effects plots for explanatory factors on mean corrosive loss in grams

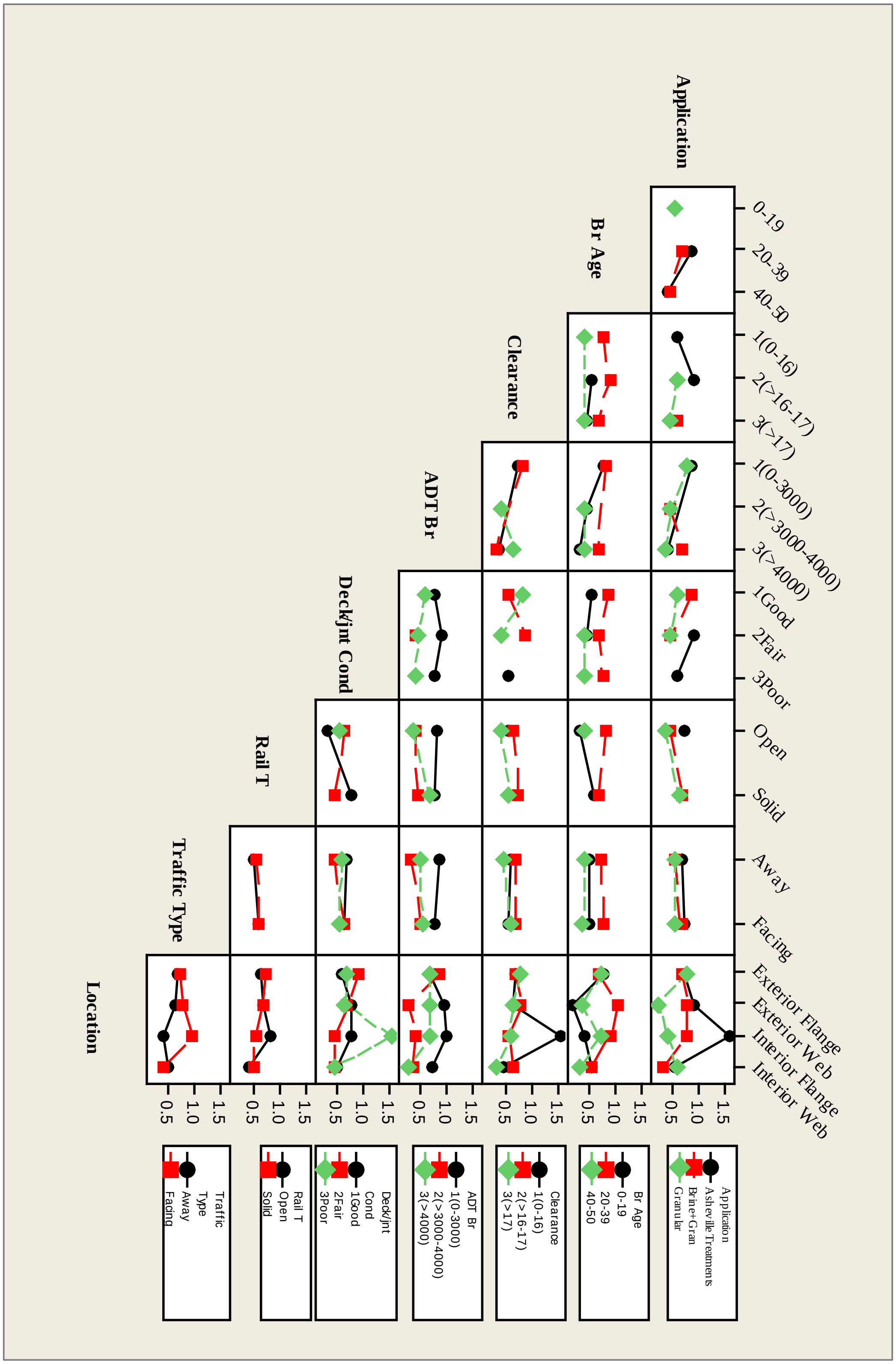

Figure 5.30: Interaction effects of explanatory factors on mean corrosive loss in grams

The following list of factors identifies significant effects and interactions observed by the research team when interpreting the main effects and interaction effect plots from the statistical model:

Plausible effects supported by expected responses:

- Traffic type by location interaction: there is little to no interaction effect for traffic type with the other factors except location. Traffic type by location shows that the components facing traffic have greater corrosive loss when the location is at an interior flange. This might be expected as vehicular traffic moving under the bridge may aid in the transport of chloride laden moisture to the superstructure components facing the traffic direction.
- Deck/joint condition rating by location interaction: although the main effects plot indicates a higher corrosive loss with joints in good condition, the interaction effects plot clearly shows that one of the most significant factors is joint condition and that bridges with poor joint condition exhibited markedly higher corrosive losses on the interior flange of girders, which is where the chloride build-up would be expected to occur if transported through the expansion joint. Note, however that the only bridges featuring poor condition ratings for the expansion joint were in Asheville, so this influence of condition rating can only be concluded for granular/salt-sand deicing mixes and should not be generalized yet to brine anti-icing applications without further experimental evidence.
- Application type: Salt-sand mix treatments in Asheville showed the highest corrosive loss, however the main effect is greatly skewed by a very large average corrosive loss measured at the interior flange in the Asheville set of bridges. As noted, the bridges in Asheville also have more compromised expansion joints than those in Greensboro. Therefore, the larger measured rates of corrosion are not unexpected since the expansion joint is the primary route by which chlorides can transport to steel components below the deck. In the absence of this outlier, the salt-sand treatments in Asheville are comparable to bridges receiving application of brine pre-treatment and granular deicing. The lowest corrosive losses were measured on components of Greensboro bridges receiving only granular deicing applications.
- Average Daily Traffic: the main effects model indicates that lower traffic count is associated with greater corrosive loss for all deck conditions. This is expected as traffic can transport chlorides from the surface of the bridge. Residual concentrations and long-term corrosion may be higher for low ADT bridges. At high ADT, the effect is less for brine with granular application. The interaction effects model shows that when the joint condition is good, there is little difference in corrosive losses observed below the deck. However, for bridges with fair or poorly rated joints, the low ADT bridges are associated with significantly higher corrosive losses. Again, it is important to note that the set of bridges sampled only produced bridges with poor joint condition in Asheville, which received salt-sand mix. Therefore, too many conclusions should not be drawn from this statistical model without further study.

Unexpected effects:

- Age by rail type interaction: greater corrosive losses are observed in mid-range age bridges (20-39 years) for open rail type versus closed rail.
- Age by location interaction: mid-range age bridges (20-39 years) consistently exhibited the highest corrosive losses, with a particularly high difference in corrosive losses at web of exterior girders.

The interaction effects plot can help to identify the interaction of factors or predictors; however, when interpreting the interaction effect one must also consider the statistical significance of each predictor variable. A stepwise regression analysis is appropriate to identify a useful subset of predictors and to model the relationship between the response and predictors. In Minitab, a forward stepwise regression procedure starts with an empty model and progressively adds the most significant variable for each step until all variables not in the model have p-values that are greater than the specified alpha value. For each predictor, the statistical test computes a p-value that indicates the probability that the coefficient for the predictor is zero. A low p-value, typically less than 0.0,5 indicates that the associated explanatory variable is statistically significant to the model at the 95% confident level or better. The selected alpha value is 0.2, which will allow explanatory variables with p-value less than or equal to 0.2 to enter the model. It is important to note that a p-value can change when additional variables are added during the stepwise process. The method aims to create a general linear model that considers all feasible explanatory variables but then selects only those variables that have the most significant predictive power.

The regression analysis included 21 candidate predictors and mass loss in grams for each coupon as the response. The three deicing treatment types included salt-sand for Asheville bridges and applications of brine and granular for Greensboro bridges. All three variables were entered as continuous variables with the number of treatments applied for each type as indicated in Table 5.13. Other predictors were input as categorical variables with assignment of either 1 or 0. For rail type, 1 indicates a solid rail and 0 indicates an open rail. Likewise, for traffic type 1 indicates the mounted coupons were facing traffic. Remaining categorical predictors were coded with 1 if the condition is true under that category and 0 if it is false. Table 5.13 shows a summary of all predictor variables used for the regression analysis.

The initial regression pass considered all predictor variables, which ended after six steps with six remaining variables. As noted during step 4 the p-value for rail type increased from 0 to 0.724 when the term for clearance above 17 feet was added to the model. At the last step, the p-value for rail type was reduced to 0.5, also the highest for all remaining variables followed by 0.022 for good joint condition. With such a high p-value, rail type can be concluded as not statistically significant for the model. Rail type also showed a variance inflation factor (VIF) of 3.98, the highest from the remaining variables. The VIF value measures the level of variable redundancy, ranging from 1 to 10, with 1 as not correlated and 10 for highly correlated to other predictors. Rail type indicated a moderate level of redundancy and statistical insignificance to the model and therefore can be removed without jeopardizing explanatory power of the model. The second regression was run with rail type removed from the set of predictors.

Table 5.13: Predictor variables used in stepwise regression analysis

Candidate Term	**Category (continuous)**			
Application Type (3 terms)	Salt-sand	Brine	Granular	
	Category (0, 1 condition)			
Location (4 terms)	Exterior Flange	Exterior Web	Interior Flange	Interior Web
Age(yrs) (3 terms)	0-19	20-39	40-50	
Clearance (ft) (3 terms)	0-16	>16-17	>17	
ADT(Average daily traffic) (3 terms)	0-3000	>3000-4000	>4000	
Joint Condition (3 terms)	Good	Fair	Poor	
Rail Type (1 term)	Solid	Open		
Traffic Type (1 term)	Facing	Away		

The MiniTab output for the second regression analysis is shown in APPENDIX 4.2. The analysis ended in five steps, with salt-sand, granular, age (20-39), ADT above 4,000 and interior web as remaining predictors. P-values for all five predictors show statistically significance at 93.9% confidence level with the highest p-value of 0.061 for ADT above 4,000. VIF's for all predictors range from 1.59 to 2.29 indicating low redundancy in explanatory variables. The result for both forward selection methods did not include brine application as a remaining predictor, due to the selected alpha value at 20%. However, brine application is an important predictor to include in the final regression model along with granular and salt-sand. Including brine application in the model will enable general comparison of the corrosive impact between the three different application types. Consequently, the MiniTab output with brine manually included in the analysis is shown below:

Predictors included: Salt-sand, Brine, Granular, Age (20-39), ADT(>4k), Interior Web

```
Method
Categorical predictor coding  (1, 0)

Analysis of Variance

Source          DF   Adj SS   AdjMS  F-Value  P-Value
Regression       6  1112.01  185.336    37.32    0.000
  Salt-sand      1   245.80  245.797    49.49    0.000
  Brine          1     6.89    6.889     1.39    0.243
  Granular       1   140.81  140.809    28.35    0.000
Age(20-39)     1    43.06   43.064     8.67    0.004
ADT(>4k)       1    24.63   24.628     4.96    0.029
  Interior Web   1    45.61   45.607     9.18    0.004
Error           65   322.83    4.967
  Lack-of-Fit   43   225.54    5.245     1.19    0.340
  Pure Error    22    97.29    4.422
Total           71  1434.85

Model Summary

      S    R-sq  R-sq(adj)  R-sq(pred)
2.22859  77.50%     75.42%      73.68%

Coefficients

Term            Coef  SECoef  T-Value  P-Value   VIF
Salt-sand     0.6752  0.0960     7.03    0.000  3.32
Brine          0.453   0.385     1.18    0.243  2.63
Granular       0.729   0.137     5.32    0.000  1.60
Age(20-39)
  1            1.982   0.673     2.94    0.004  3.01
ADT(>4k)
  1           -1.266   0.569    -2.23    0.029  1.89
Interior Web
  1           -1.680   0.554    -3.03    0.004  1.98

Regression Equation

Mass Loss (g) = 0.6752 Salt-sand + 0.453 Brine + 0.729 Granular
+ 1.982 Age(20-39)_1 - 1.266 ADT(>4k)_1 - 1.680 Interior Web_1

Fits and Diagnostics for Unusual Observations

         Mass
Obs  Loss (g)    Fit   ResidStdResid
 28     7.740  3.080   4.660       2.17  R
 31     8.320  1.235   7.085       3.31  R
 62    12.680  7.384   5.296       2.47  R
 70     0.500  5.704  -5.204      -2.41  R

R  Large residual
```

The result shows that by including brine, its p-value is 0.243 which put it just above the default alpha value at 0.2. The final regression model is:

$$Mass\ Loss\ (g) = \ 0.6752\ Salt\text{-}sand + 0.453\ Brine + \ 0.729\ Granular$$

$$+ 1.982\, Age(20-39) - 1.266\, ADT(>4k) - 1.680\, Interior\ Web \qquad (4.1)$$

Where:
Salt-sand, brine, and Granular = application number
Age (20-39), ADT(>4k), and Interior Web = 1 if the condition is true

The final regression model shows positive relationship for salt-sand, brine, granular, and bridge's age between 20 to 30 years and negative relationship for ADT above 4,000 and interior web to mass loss. These relationships are as expected and reinforce the main effects plots for these predictors. According to the model coefficients, granular has the largest impact followed by salt-sand then brine. The final model has an R-squared value of 77.5% and an adjusted R-squared value of 75.42%. These are indications of what percentage of variation in the response is explained by the predictor variables. The adjusted R-squared values only increase with each regression step when the new term improves the model more than would be expected by chance.

The main assumptions for the multiple regression models are: the errors are normally distributed, the variance of the error is equal for all observations, and there is a linear relationship between response and explanatory variables. The model over and under predictions or residuals was plotted to check for normal distribution or bias in the model. Figure 4.9 includes the histogram of residuals plot and residuals versus fits plot to check for normal distribution and variance of error for all observation, which should show random distribution of residuals on each side of 0. The plot indicates that the assumptions for the most part are valid. Linear relationships were established through converting of explanatory variables into binary categories using 0 and 1. It is important to note that the regression model presented was based on the collected data for this study. Potential error could be due to factors that were not considered that could also influence the corrosive loss in the actual field environment. Furthermore, the data set could contain points that have high variability or nonlinearity that are not fitted well in the model. Due to limited data in the data set, there is no statistical basis for eliminating those points and furthermore doing so would create a gap for certain conditions within a factor.

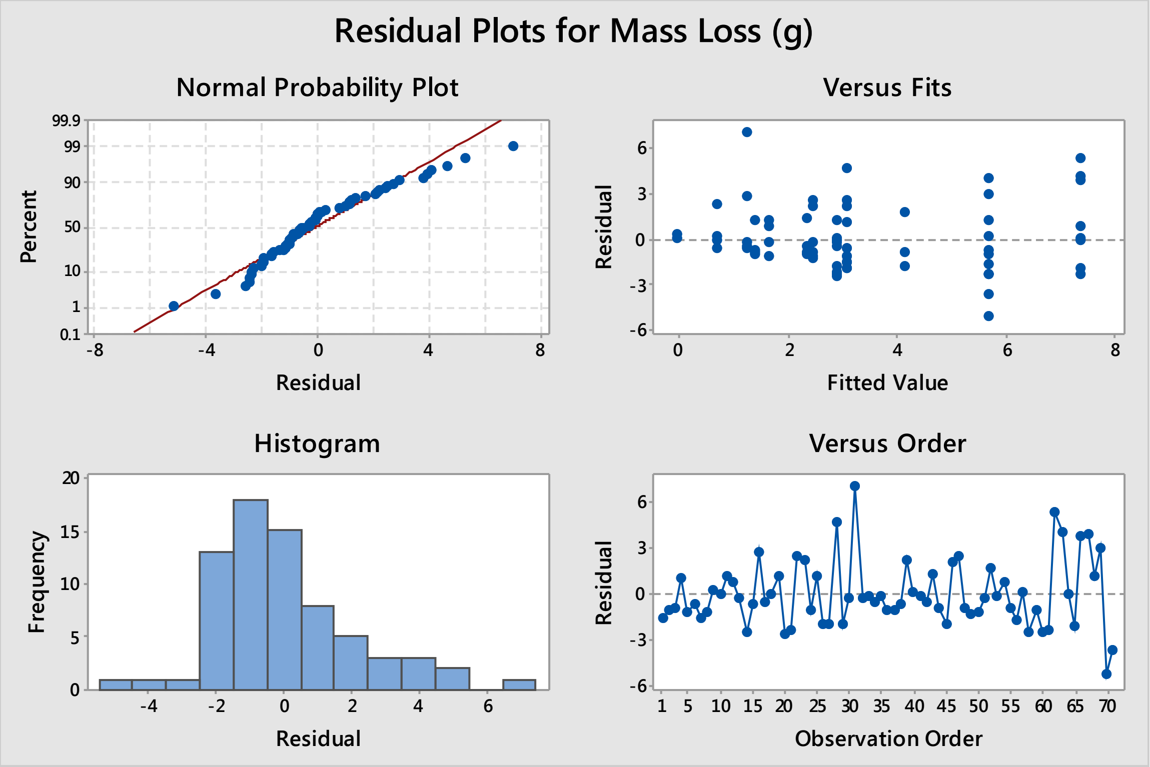

Figure 5.31: Plots for checking model assumptions

5.4 Summary of Field Measurements of Steel Corrosion

A field test program was conducted to generate quantitative data for evaluating the impact of sodium chloride deicing and anti-icing applications on the transport of chloride and the associated corrosive losses on bridge girders. Sacrificial steel coupons were installed at different girder locations under normal service conditions and were retrieved after one winter season to determine the corrosive mass loss. Statistical analysis of the collected mass loss per application indicates that granular treatment is 1.08 times worse than salt-sand mix and 1.6 times worse than brine. This is largely due to the tendency of granular salt to be transported to below deck components. Accumulation of granular salt at the joint and increase in chloride measurements at the girders from granular application was observed also observed during the field study presented in Chapter 6. Results also indicate that the bottom flange on girders experience about 1.5 times higher in corrosive mass loss compared to web components.

Further statistical analysis of the experimental data with the functional characteristics of the bridges and locations of the specimens was performed using MiniTab statistical regression and modeling software package. Based on the main effect plots within a particular factor, there is an indication of higher average corrosive loss for bridges that are between 20-39 years old, bridges with low traffic count, and at the exterior flanges of girders. Significant effects and interaction of factors were identified for plausible effects including:

1) Lower traffic count is associated with greater corrosive losses, but at high traffic count the effect is less pronounced for granular with brine application.
2) Interior flanges facing traffic exhibit greater corrosive loss compared to other locations on interior flanges not facing traffic.
3) Bridges with poor joint condition exhibited higher corrosive loss on the interior flange of girders.
4) Asheville bridges exhibited large average corrosive loss at the interior flange, which has been attributed to poor condition of expansion joints.

A reduced order model that contained significant variables was constructed to explain the variation in observed corrosive mass loss. The reduced final regression model included six terms: salt-sand, brine, granular, bridge age between 20 to 30 years, ADT above 4,000, and interior web, which were determined to be statistically significant at or above the 75.7% confidence level. The final model has an adjusted R-squared value of 75.42%. The presented model was based only on data collected for this study. With additional observations or inclusion of other important explanatory factors a more complete model can be established.

6 Time and Spatial Characteristics of Deicing and Anti-icing Sodium Chloride Concentrations

6.1 Chloride Concentrations across the Deck

Controlled application of anti-icing and deicing solutions was proposed to permit measurement of the temporal and spatial distribution of surface concentrations associated with each treatment method. Different spatial concentrations and time characteristics are expected for granular salt, salt sand mix and salt brine due to different dispersion and transport mechanisms. This component of the research will help quantify the potential corrosive effect of each treatment method under field conditions as well as identify specific bridge components that are most susceptible to corrosive effects under each deicing method. During this component of the study, two adjacent bridges of the same design are used to provide similar lanes for independent application of each treatment method while minimizing site-specific and environmental factors.

6.1.1 ***Bridge Selection for Study***

In early January 2012, the research team requested a list of bridges in the Charlotte area meeting selection criteria based on design components and accessibility. Consistent with long-term seasonal field sampling performed in this project, the main components of interest are the deck, pier caps, the steel girders, and the guardrails. The selection of the bridges was based on the following criteria:

- Structure Type: Since the chloride transport in reinforced concrete is of interest, only bridges with concrete wear surface (decks) were considered for this study. Likewise, steel girders (weathering steel or painted) were preferred to examine corrosive effects below the deck. Lastly, the structure needed to have multiple spans to permit the research team to measure chloride concentration on pier caps.
- Access: the structural elements of interest had to be safely reachable by the research team. This restriction excluded selection of bridge decks with high-speed, heavy traffic or pier caps heights over 15ft.
- Bridge Age and Condition of Joints: the bridge had to show enough distress that chloride transport to components below deck was plausible. Therefore, the age of structure and the condition of expansion joints was used to guide selection.
- Travel Distance to Bridge: Since the team was going to be working at the bridge over the course of several days, the travelling distance from the University to the bridge would ideally be short.
- Sister Bridge: a single bridge could not be used since three treatment methods would be applied and the potential of “tracking” chloride-based solutions from one area to another was expected to be strong. Consequently, preference was given to sister bridges that would enable the three treatment solutions to be applied at unique conditions while maintaining consistent structural design features.

6.1.2 ***Description of Selected Bridge***

The sister bridges selected for this study were US 521 (Billy Graham Parkway) over US 74 (Wilkinson Blvd.) at Bridge 590459 (NB US 521) and Bridge 590460 (SB US 521). These bridges were built in 1981 and are located in State Highway Department District 10. The bridges have a concrete wear surface and the structure type is a reinforced concrete cast-in-place deck on steel girders. The girders are weathering steel with signs of accelerated rusting on the beam ends. In addition, there are signs of leakage through the expansion joints to components below the deck. Most of the joints are in compromised conditions; in addition to general wear, some sections were completely missing and permitted one to visually look through the joints. Additionally, the bridges have concrete parapets and galvanized guardrails. The total structure length is 193ft over three spans with the maximum span length being 117ft. According to the field inspection report, the bridge deck has thin cracks in all spans up to 1/16 inches wide. Longitudinal cracks in the span ends up to 1/16 inches are also noted in the bridge report. For these bridges, the weathering steel showed signs of further rusting on the beam ends at the piers, however there were no signs of any significant section loss. Figure 6.1 provides the cover page of the most recent bridge inspection report.

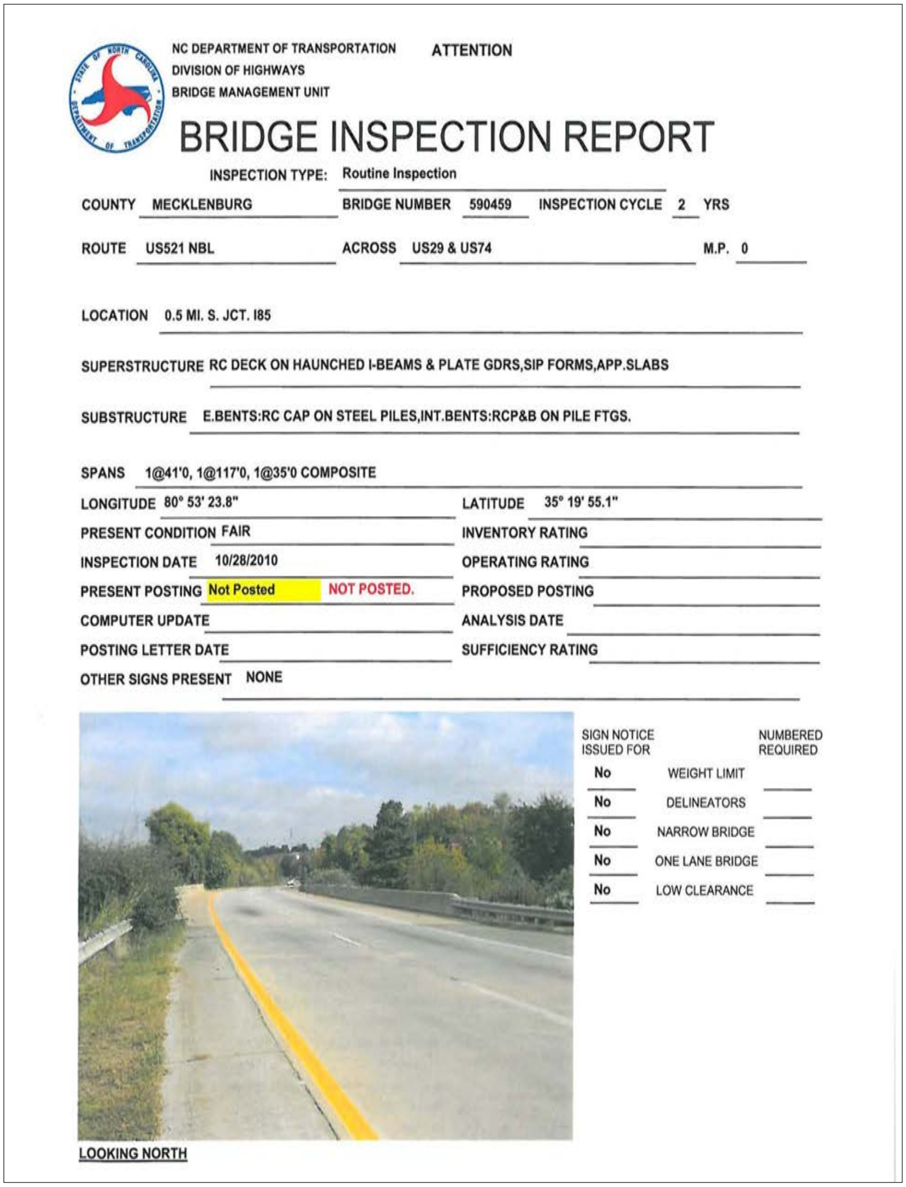

NC DEPARTMENT OF TRANSPORTATION
DIVISION OF HIGHWAYS
BRIDGE MANAGEMENT UNIT

ATTENTION

BRIDGE INSPECTION REPORT

INSPECTION TYPE: Routine Inspection

COUNTY MECKLENBURG
BRIDGE NUMBER 590459
INSPECTION CYCLE 2 YRS

ROUTE US521 NBL
ACROSS US29 & US74
M.P. 0

LOCATION 0.5 MI. S. JCT. I85

SUPERSTRUCTURE RC DECK ON HAUNCHED I-BEAMS & PLATE GDRS,SIP FORMS,APP.SLABS

SUBSTRUCTURE E.BENTS:RC CAP ON STEEL PILES,INT.BENTS:RCP&B ON PILE FTGS.

SPANS 1@41'0, 1@117'0, 1@35'0 COMPOSITE

LONGITUDE 80° 53' 23.8"
LATITUDE 35° 19' 55.1"
PRESENT CONDITION FAIR
INVENTORY RATING
INSPECTION DATE 10/28/2010
OPERATING RATING
PRESENT POSTING Not Posted NOT POSTED.
PROPOSED POSTING
COMPUTER UPDATE
ANALYSIS DATE
POSTING LETTER DATE
SUFFICIENCY RATING
OTHER SIGNS PRESENT NONE

SIGN NOTICE ISSUED FOR		NUMBERED REQUIRED
No	WEIGHT LIMIT	
No	DELINEATORS	
No	NARROW BRIDGE	
No	ONE LANE BRIDGE	
No	LOW CLEARANCE	

LOOKING NORTH

Figure 6.1: Structure details for the bridge used in the controlled application study from a recent bridge inspection report

6.1.3 ***Testing Procedure***

For the Billy Graham bridges, the following test protocol and schedule was developed for the field testing:

- Initial marking of sampling locations and collection of baseline surface chloride concentration readings was performed the week before the actual testing initiated. The deck was marked with a blue paint marker using an acrylic sampling grid with circles spaced at 3 inch intervals in a single line offset about one foot from the expansion joint over the pier. See Figure 6.2 for a representative layout of marked sample locations.
- The exterior lane of each bridge was used for all testing. The northern bridge received granular salt and salt-sand treatment at opposite ends of the span. The southern bridge received only brine application. In the cases of the granular salt and salt-sand mix, the bridge surface was pretreated with water to mimic the presence of winter precipitation that would likely be present when applying such deicing solutions (Figure 6.3). This measure was taken since it is expected that a measurable difference in surface transport and initial salt dissolution would occur between a dry and wet surface.
- The X-ray fluorescence (XRF) handheld analyzer was used to take surface chloride readings along the single line offset about one foot from the expansion joint over the pier (Figure 6.4). This sampling line produces a cross-section of the bridge spanning from the parapet to the median and including at least 80 measurement points. Consistent with prior field and laboratory testing, the XRF was configured for soil mode with a 30 second sampling duration.
- Once sampling on the deck was completed, XRF analysis data was collected along the guardrails and concrete parapets (6 points along the height for both) (Figure 6.5).
- The sampling routine was completed immediately after application of the treatment solutions, then at 1 day, 3 days, 4 days, and then once a week thereafter.
- Photographs of the general conditions of the concrete deck and the measurement locations were obtained to document the test procedure.

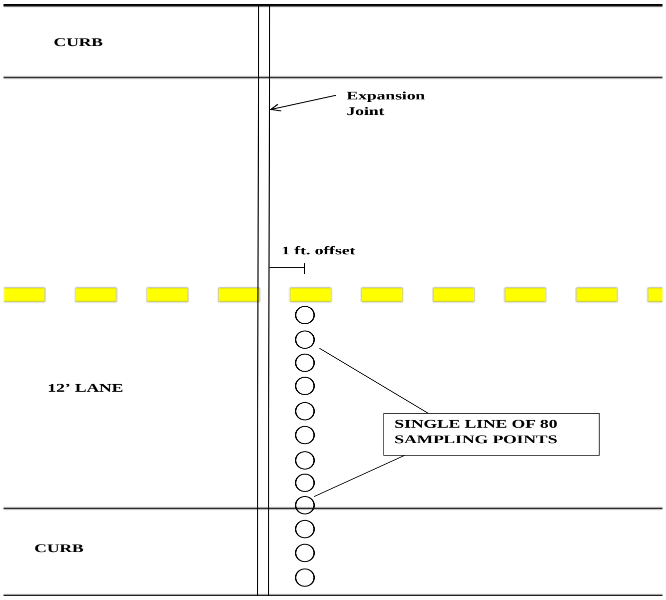

Figure 6.2: Markings on the bridge surface along the joints

Figure 6.3: Granular salt application on the bridge

Figure 6.4: XRF sampling on the deck

Figure 6.5: Sampling locations on the parapet

6.1.4 ***Daily Test Record and Results***

Provided below in Figure 6.6 is an aerial photograph of the plan view of the bridges and the sections where each treatment was applied. The northern span received granular salt and salt-sand treatment at opposite ends of the span. The southern span received only brine application. In the cases of the granular salt and salt-sand mix, the bridge surface was pretreated with water to mimic the presence of winter precipitation that would likely be present when applying such deicing solutions. The different treatment applications are shown in Figure 6.7, Figure 6.8, and Figure 6.9 following on the next page.

Figure 6.6: Plan view of the two bridges and the application sections

Figure 6.7: Granular salt and sand mix application

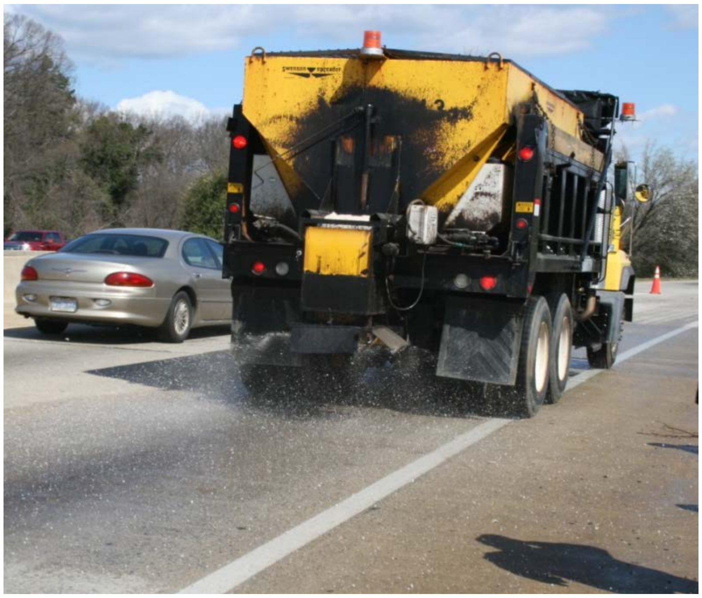

Figure 6.8: Granular salt application

Figure 6.9: Brine application

Day 1 (03/05/2012)

Immediately after the granular salt sand mix was applied, the team measured the surface chloride concentrations using the XRF. This process was repeated once more to examine any immediate influence associated with drying. Then, granular salt was applied to the deck over the opposite pier and readings were carried out with the XRF. Consistent with the prior section, a repeated series of measurements was obtained after initial drying of the surface. The research team then moved to the other span where brine was applied and measurements were taken immediately thereafter. The caps and girders were not measured on this day due to time constraints although the team anticipated that there would have not been any transfer of chloride within that time period. Due to miscommunication with the truck operator, additional granular salt was applied near the mid-span of the bridge. Since traffic might track this salt into the salt sand mix region, the research team cleaned the surface of the deck near the mid-span to minimize this potential effect. However, the data from the salt sand region did show a marked increase in subsequent testing, which is likely a result of this additional granular application.

Results for the initial surface chloride concentrations associated with each treatment method immediately after application and then again after drying are presented in Figure 6.10. These readings were obtained before there was any traffic and associated transport of surface chlorides by mechanical means. The data reveals that no significant changes occur during the initial drying and that the surface concentrations are highest for the brine solution, followed by the granular salt, and then the salt sand mix. The application flow rate used during application of the salt sand mix visually appeared to be slower than during the granular salt application, which may explain the stark difference in the initial concentrations between these seemingly very similar deicing solutions. Interestingly, uniformly high surface chloride concentrations were measured for the brine solution in the curb and the nozzle directed streaking associated with brine application is clearly visible in the variation of chloride concentrations measured in the travel lane. Readings as high as 35% apparent chloride were observed with the XRF on this day (T=0). Although maximum surface concentrations measured in the region of application of granular salt were not as high as the brine, the distribution was more uniformly strong and initially more concentrated in the travel lane.

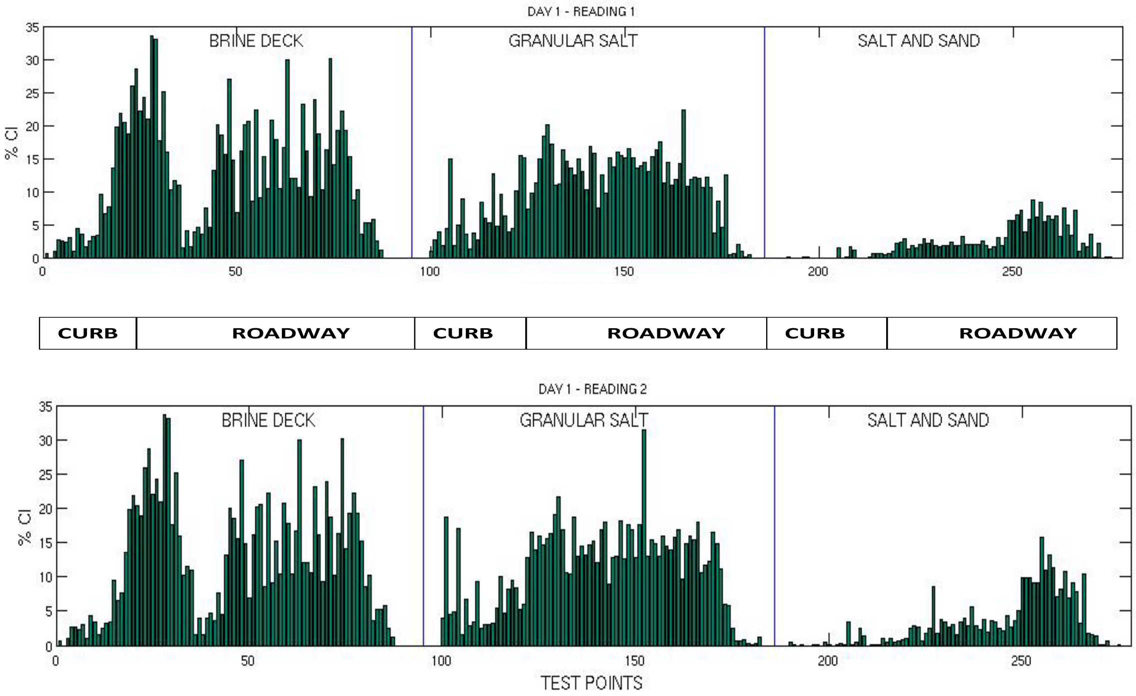

Figure 6.10: Chloride levels on deck after application without any traffic interference

Day 2 (03/06/2012)

Upon returning to the bridge after 24 hours of routine traffic flow, the most plain visual observation was that there was a significant accumulation of granular salt in the expansion joints, as seen in Figure 6.11. The measured surface chloride concentrations for each treatment region after 24 hours are presented in Figure 6.12, where the rise in concentration for the salt sand mix can be seen to increase compared to the prior day. This is expected to be largely due to miscommunication with the truck operator in the prior day, which resulted in depositing of additional granular salt in the region just ahead of the sampling grid used for the salt-sand mix. Although the researchers attempted to sweep this granular material from the roadway, it is likely that traffic caused a transport of this granular salt into the granular salt sand mix section over the course of the day. Additional observations in the data following one day of traffic flow were:

- The granular salt section registers a slight decrease to be associated with traffic induced-transport.
- Brine surface concentrations in the curb were nearly unchanged while those in the travel lane were reduced yet the high concentrations streaks were still observable both visually and in the measured data.

The photograph in Figure 6.13 illustrates the residual streaking effect produced by the directionality of the brine application jets.

Figure 6.11: Accumulation of granular salt in the joints after a day of traffic flow

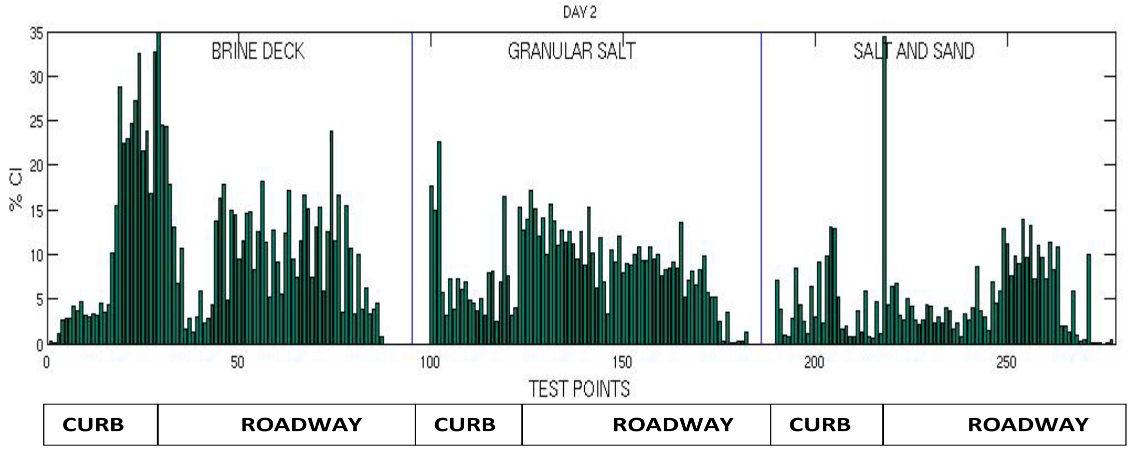

Figure 6.12: Surface chloride concentrations after 24 hours of traffic flow (without any precipitation events)

Figure 6.13: Residual brine streaks on the deck surface 24 hours after application.

Day 3 (03/07/2012)

The team was not able to take readings on this day because there was a strict restriction on the use of the roadway due to a surprise visit by President Obama to Charlotte.

Day 4 (03/08/2012)

The chloride concentration measured after three days from application exhibit a significant decrease from prior days (Figure 6.14). These reductions are attributed to traffic-induced transport of chlorides since no precipitation events had yet occurred. Notable observations in the data set are:

1. Although surface concentrations did decrease in the curb where brine was applied, the concentrations remain significantly high;
2. In general, the curbs have greater residual surface concentration of chlorides than the travel lanes; and
3. Concentrations showed the greatest decrease in the wheel path, while concentrations in the travel lane remain high between the wheel paths.

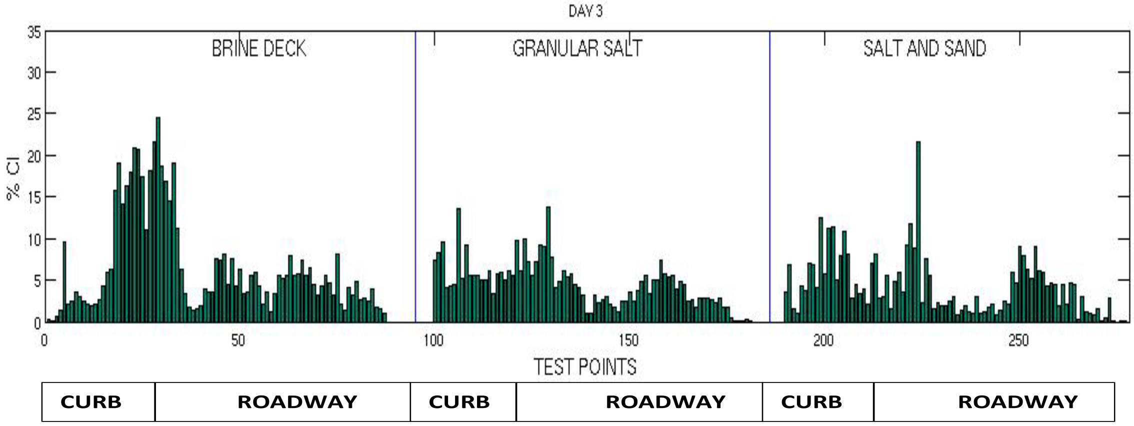

Figure 6.14: Surface chloride concentrations after 72 hours (3 days) of routine traffic (without any precipitation events).

Day 5 (03/09/2012)

On the morning of the fifth day of testing, 0.16 inch precipitation in the form of rain occurred around 2:00am. Upon sampling the surface concentrations across each of the controlled application regions, the research team confirmed that bulk of the surface chlorides were washed from the surface of the deck by the rain (Figure 6.15). Since the vertical scale is maintained with the prior figures, this data illustrates the drastic change in the chloride concentrations occurring after precipitation. The maximum surface chloride concentrations had dropped from measurements as high as 35% to 0.009% apparent chloride. This suggests that precipitation is the predominant factor affecting residual chloride concentrations after application for all treatment approaches. Due to the condition of the joints and the visible presence of granular salt in the joint material, an increase in the concentration on components below deck was anticipated after this precipitation event and confirmed in results.

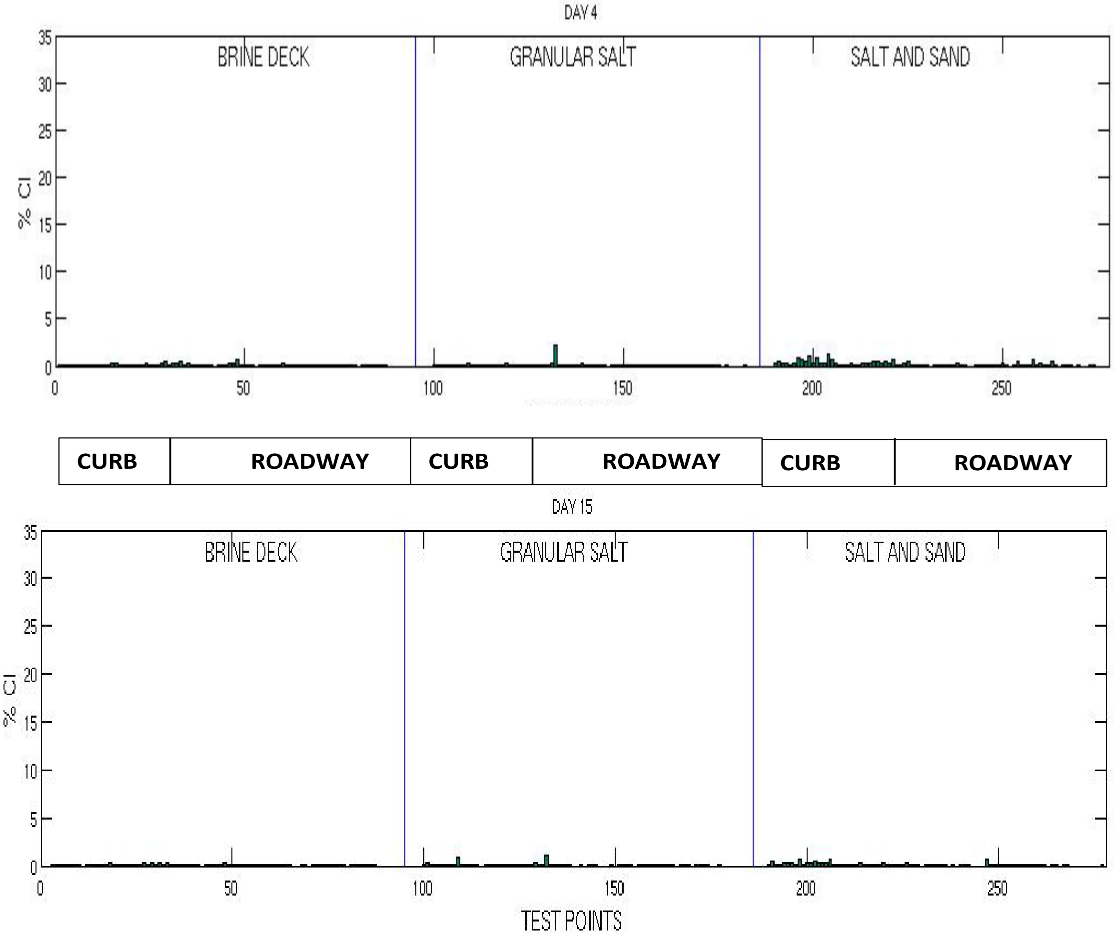

Figure 6.15: Surface chloride concentrations on the deck after first precipitation event

Table 4.6 shows the average chloride concentrations on the locations measured on the bridge deck over the 5 day period of testing. It can be observed in Figure 6.16 and Figure 6.17 that the brine had the highest average concentration during initial application both in the lane and the curb. As time progressed, the average chloride concentration decreased steadily at a largely linear rate. On day 5 (March 9, 2012), the averages of all the treatment methods decreased drastically due to rain and continued to decrease at a steady rate thereafter. The averages remained at trace levels on the deck throughout the remainder of the testing period after this first precipitation event.

According to the trend of the brine solution over time, the residual brine concentration in the absence of a precipitation event reduces steadily at a slow rate due to diffusion or other factors such as traffic-driven transport of the solution or recrystallized solids. It is seen in these figures that, the granular salt and the salt sand mix concentrations reduce in the lane as time progresses, but increase in the curb. This is can be explained by transport of the granular salts driven by traffic action within the lane. The field observations support that the granular salts are transported from the road to both the curb and the expansion joints, thus explaining the increase in the concentration in the curb for both the granular salt and salt sand mix section. Due to the traffic some granules also accumulated on the expansion joints and, depending on the joint condition on that section, the granules were transported to the pier cap and girders. It is important to note however that the mild slope of the deck could assist in this transport to the curb monitored resulting in slightly higher increases in chloride concentration than what may be typical for a deck will less slope or sloping in the opposite direction. Therefore, in the absence of any precipitation, one could extrapolate that the chloride concentration would have steadily accumulated on the curb area over time, while the deck concentrations would decrease to trace levels. These observations conclude that traffic plays the predominant role in the dispersion of granular salts, and consequently the chloride exposure of concrete decks, in the absence of rain.

Table 6.1: Average chloride concentration on Billy Graham deck over test duration

	Brine [Cl%]		Granular Salt [Cl %]		Granular Salt Sand Mix [Cl%]	
Day	Lane Avg.	Curb Avg.	Lane Avg.	Curb Avg.	Lane Avg.	Curb Avg.
1	14.083	11.128	11.256	8.970	3.414	0.845
			11.950	10.077	5.065	1.206
2	10.348	11.864	7.308	9.855	5.305	4.881
3	4.426	9.098	2.867	6.382	2.840	6.025
4	0.096	0.151	0.065	0.168	0.122	0.359
5	0.064	0.102	0.038	0.131	0.062	0.202

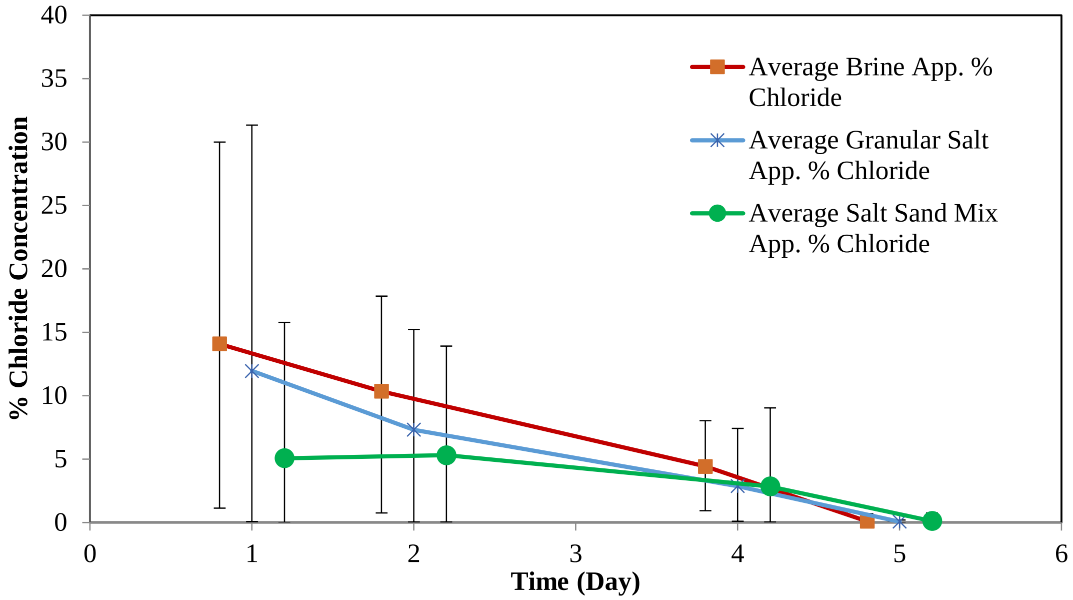

Figure 6.16: Average chloride concentration in the traffic lane for the different applications over 5 days

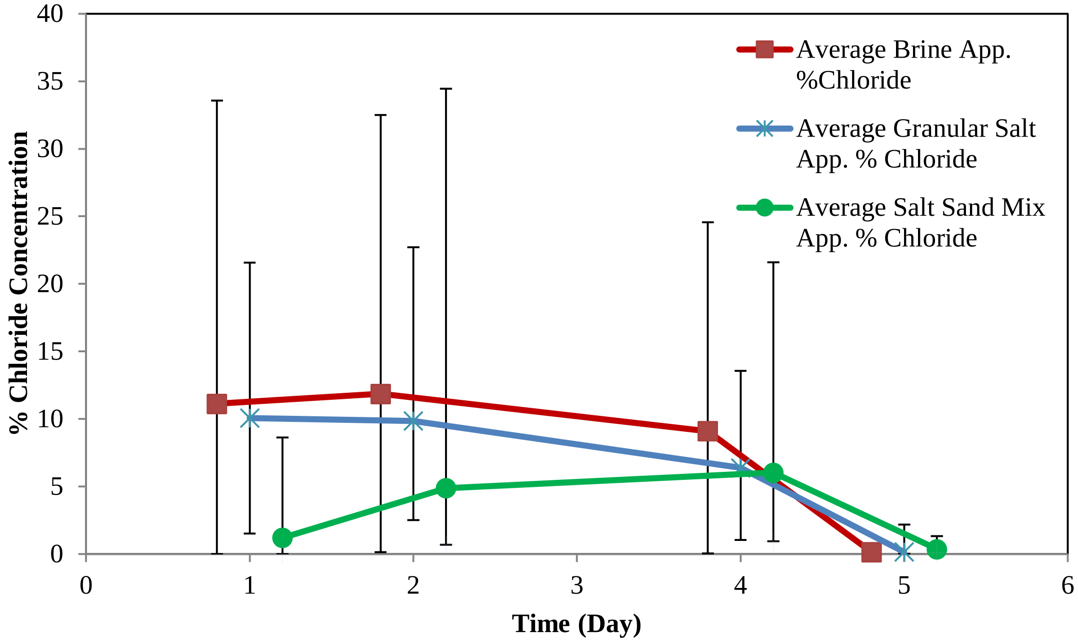

Figure 6.17: Average chloride concentration on the curb for the different applications over 5 days

6.1.5 ***Modeling Surface Chloride Concentration***

In modeling the trend of each application type, the average percentage results from the first three days were chosen to represent the amount of residual salt on the road surface available over the days. The reason for using three days is that there was a rain event on the fourth day that lowered the results close to zero. In order to find out the rate at which the salt was leaving the road and since the pattern seemed to be correlated to the traffic, the averages of the surface concentrations for each treatment was graphed against the days after the application both linearly (See Figure 6.18) and exponentially (See Figure 6.19). In both graphs, it can be seen that the brine and granular salt applications follow the same pattern and are different by a factor of 1.18 % over the days of testing. The exponential fit for the granular salt application falls on all the average three points exactly on the graph. Presented in Table 6.2 and Table 6.3 are the equations and R² values for the linear fit and the exponential fit respectively. Also, the average traffic was obtained from the bridge reports and related to the average chloride concentrations days after the application (See Figure 6.20). In doing this, the average daily traffic was multiplied by the number of days after the application. The average daily traffic for the bridge section applied with brine was 19,000 and the bridge for both granular salt and salt sand mix had an average daily traffic of 16,000.

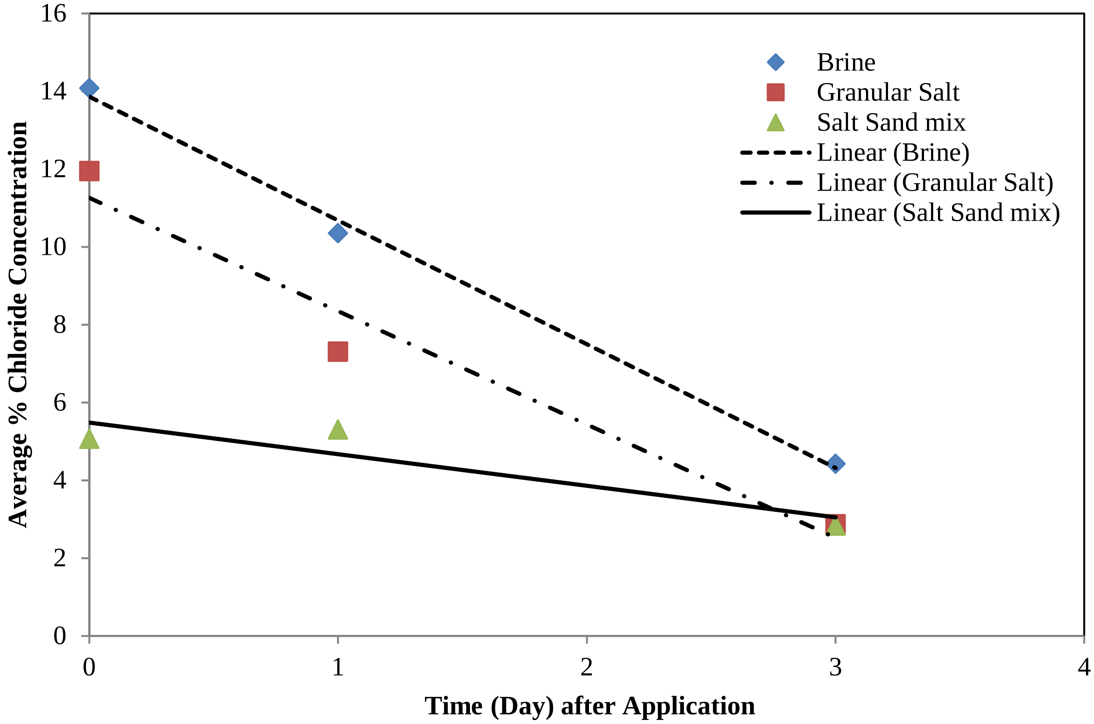

Figure 6.18: Linear fit of average % chloride days after application on deck

Table 6.2: Linear equations and R^2 of the three different applications on deck

Location	Application Type	Initial Chloride Concentration [Cl%]	Relationship	R²
Deck	Brine	14.08	y=-3.1821x+13.862	0.9964
	Granular Salt	11.95	y=-2.9124x+11.258	0.9594
	Salt Sand mix	5.07	y=-0.8117x+5.4855	0.8323

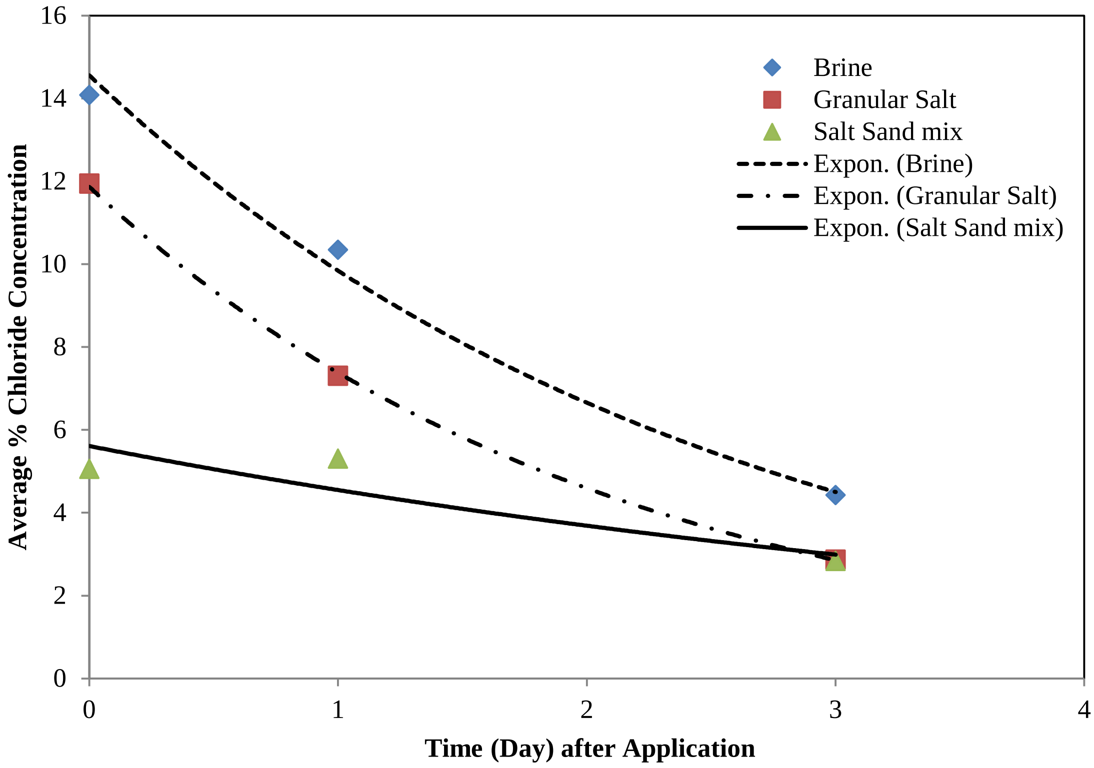

Figure 6.19: Exponential fit of average % chloride days after application

Table 6.3: Estimate of residual chloride concentration after time using exponential equations and R^2 of the three different applications of deck

Location	Application Type	Initial Chloride Concentration [Cl%]	Relationship	R^2
Deck	Brine	14.08	$y=14.56e^{-0.391x}$	0.9946
	Granular Salt	11.95	$y=11.869e^{-0.475x}$	0.9998
	Salt Sand mix	5.07	$y=5.6115e^{-0.21x}$	0.8483

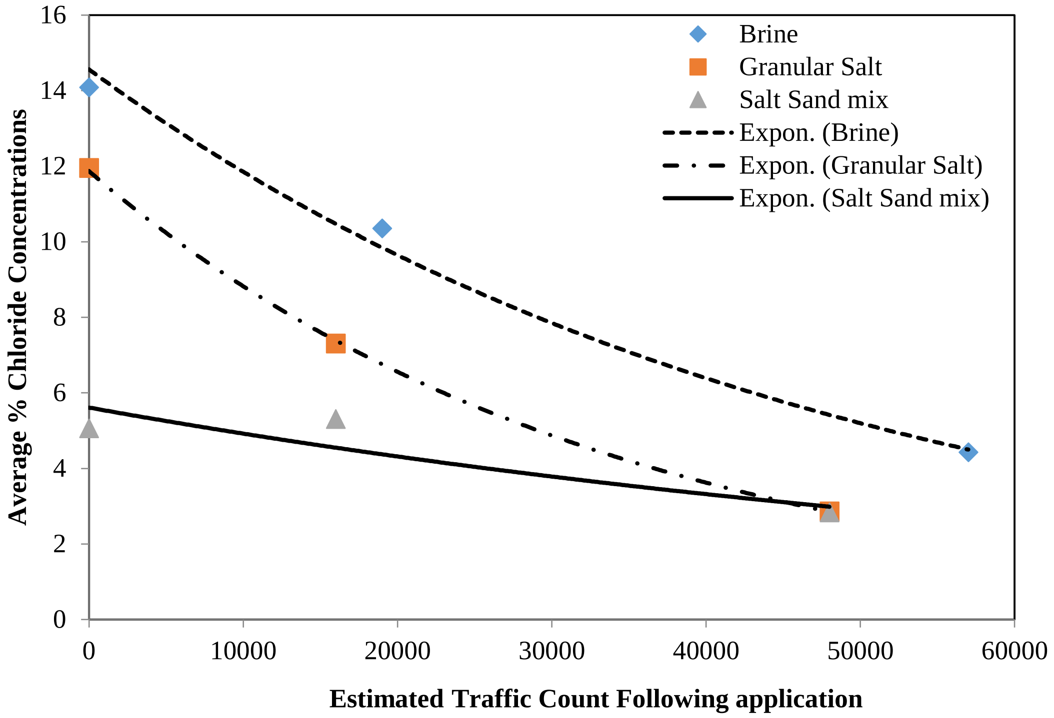

Figure 6.20: Exponential fit of average % chloride against the traffic on the bridges days after applications

Table 6.4: Estimate of residual chloride concentration after traffic using exponential equations and R^2 of the three different applications of deck

Location	Application Type	Initial Chloride Concentration [Cl%]	Relationship	R^2
Deck	Brine	14.08	$y=14.560e^{-2E-05x}$	0.9946
	Granular Salt	11.95	$y=11.869e^{-3E-05x}$	0.9998
	Salt Sand mix	5.07	$y=5.612e^{-1E-05x}$	0.8483

In this case, since traffic count occurred independently of the experiment, the term, Time, is simply a function of traffic. In the model developed by a research team at the Swedish National Road and Transport Research Institute, referenced in the literature review, the model is used to determine the change in residual salt brine concentration under the action of vehicular transport. The model approximates the residual salt on the surface days after the application and provides a coefficient of about 0.2027. In Table 4.9 are equations that determine the change in residual salt for the different deicing treatments used in North Carolina. The general equation for estimating the residual salt is:

$$LS = IS * e^{-k*ET}$$

Where

LS = Leftover Salt
IS = Initial Salt
ET = Estimated Traffic count following application

The coefficients for the different treatments are $k = 2*10^{-5}$, $3*10^{-5}$, $-1*10^{-5}$ for brine, granular salt and salt sand mix respectively. Coefficients for IS are 14.560, 11.869 and 5.612 for brine, granular salt and salt-sand mix, respectively.

6.1.6 ***Conclusions Developed From Controlled Field Testing***

Overall, it was observed that the granular salt and salt sand mix exhibited strong spatial-temporal characteristics associated with transport due to traffic flow and precipitation both above and below deck. In both granular forms, there was notable accumulation of salt in the expansion joints that later was transported to the pier caps and girder ends through gravitational flows driven by precipitation. Application of anti-icing brine solution produced markedly high surface concentrations of chlorides on the deck and, in particular, on the curb. However, transport of surface chlorides to components below the deck was not observed in the measurement set for the region of the bridge treated with the brine solution. This may be a feature of the application of brine and immunity from granular accumulation in the expansion joints or may simply be an artifact of better joint condition in this portion of the bridge tested.

In general, traffic produces plausible transport of surface chlorides with highest reduction of chloride concentrations in the wheel paths, lower reduction of chloride concentrations in the travel lane between the wheel paths, and significantly less reduction of chloride concentrations in the curb where vehicular travel would be less frequent. Precipitation was (by orders of magnitudes) a significantly larger factor in the transport of chlorides producing a nearly complete washing of the surface chlorides from the surface of the deck for all treatment solutions and transport of chlorides to components below the deck for regions with compromised joints. In this period, there were no snow events that could have affected the trends observed.

6.2 Field Investigation of Components below the Deck

This section describes field measurements of the transport of chlorides from deicing and anti-icing strategies to steel components below the deck during the controlled field study. Specifically, the regions sampled below the deck under each application area included:

- **Reinforced Concrete Pier Caps:** areas of 3ft² were demarcated and tested with the XRF using the 3x3 acrylic grid previously developed. This array of nine points was sampled for each section of the bridge corresponding to a unique treatment method. See Figure 6.21 and Figure 6.22 for a photograph and detailed drawing of the sampling grid on a representative pier cap respectively
- **Steel Girders:** XRF readings were also obtained from the girder ends along the web. Approximately 15 readings were obtained from each girder (Figure 6.23 and Figure 6.24).

Figure 6.21: Sampling grid used on the pier cap surface

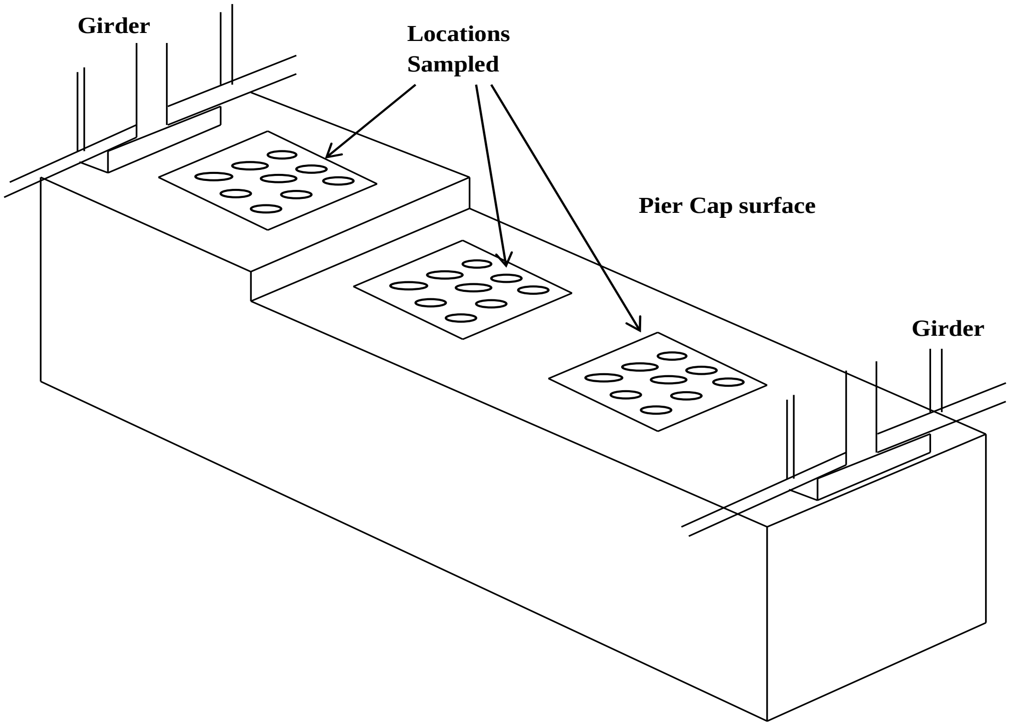

Figure 6.22: Detailed drawing of the locations sampled on the pier cap surface

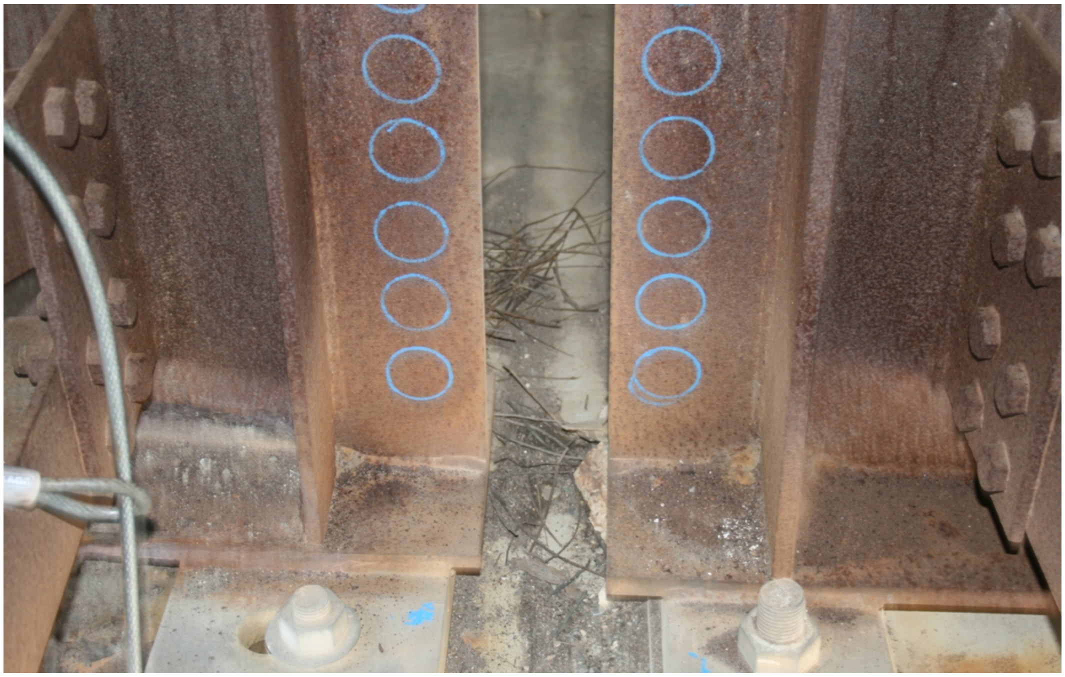

Figure 6.23: XRF handheld analyzer sampling on the pier and girders

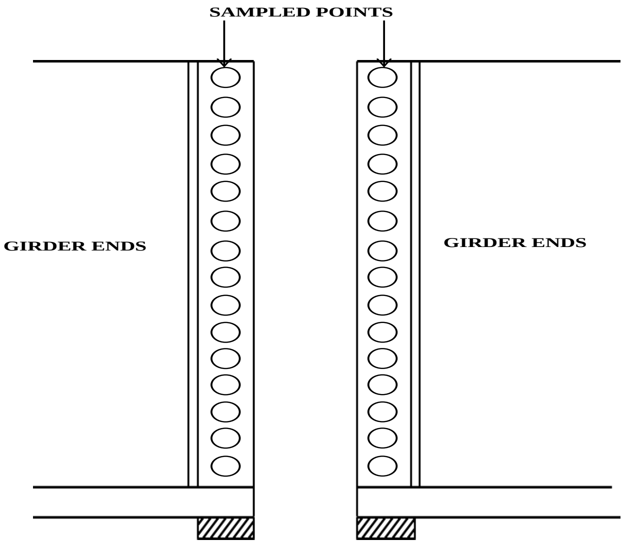

Figure 6.24: Detailed drawing of the 15 sampled points on the girder ends

6.2.1 *Measured Chloride Surface Concentrations on Below-Deck Components*

Since precipitation was found to exhibit such a pronounced effect on the surface chloride concentrations measured on the deck, a list of the precipitation events reported by the National Weather Service precipitation was prepared to summarize precipitation occurring during the test program (Table 6.5). The team visited the bridge once every week after the initial week of daily testing and this table also summarizes when readings were taken through the month.

Table 6.5: Recorded precipitation events over the course of the study and indication of dates of sampling

Date of Sampling	Days After Application	Precipitation (Inches)	Measurements Taken?
3/5/2012	0	0	YES
3/6/2012	1	0	YES
3/7/2012	2	0	
3/8/2012	3	0	YES
3/9/2012	4	0.16	YES
3/15/2012	10	0	YES
3/20/2012	15	0.02	
3/22/2012	17	0	YES
3/23/2012	18	0.01	
3/24/2012	19	0.12	
3/25/2012	20	0.01	
3/29/2012	24	0	YES

It was anticipated that there would be a slight increase in the chloride concentrations on all of the pier caps after surface concentrations were washed from the deck, but there is no indication of this phenomena in the results within the brine region. This may be an inherent feature of the transport of the brine solution, but it seems more likely that the generally better condition of the joint in this region inhibited the flow of chloride-laden precipitation to components below the deck. Over the monitoring time period, there was no observable increase in the concentration of chloride on the pier cap surface, however, a slight increase in chloride levels on the girders did occur.

The figures provided in this section, such as Figure 6.25, display an unfolded view of the components below the deck. The left hand side of the figure presents the girder ends on one side of the cap presented with the top side on the left and bottom on the right. In the middle of each subfigure are the three measured areas on the surface of the pier cap. Then, on the right-hand side are the girder ends on the opposite side of the cap presented with the bottom side on the left and top side on the right. In other words, any transport toward the center of the figure is an indication of transport down the girders and onto the pier cap. From Figure 6.25, it is observed that in the region of brine application the chlorides transported through the joints were so low in quality that no significant increase was measured anywhere below the deck except for very minor increases on the one girder.

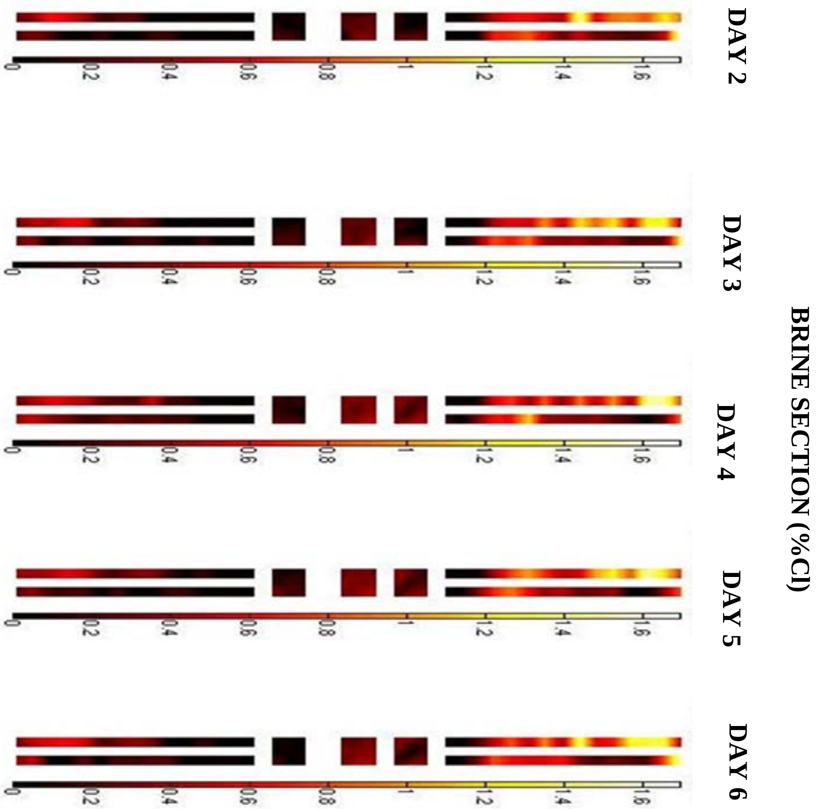

Figure 6.25: Surface concentration on girder ends and pier cap beneath the brine application (unfolded, projected view of the girder ends and the cap surface)

In this section below the application of granular deicing salt, the chloride concentrations increased drastically over the weeks after the initial rain event. It is important to note that the expansion joint in this region sampled was severely compromised and would have permitted the transport of chlorides to the components under the deck. Compounding this condition is the previously mentioned visual evidence of significant accumulation of granular salts in the joint prior to the precipitation event as driven by traffic transport (Figure 6.11). On the morning of March 9th, which was the first day after a precipitation event, the pier cap surface had a pool of water and the chloride concentrations were immediately measured to be significantly high within this region (Figure 6.26). During this time, there were also surface concentrations measured as high as 1.5% on the girder ends and pier caps as indicated by the XRF. After the first rain event, additional precipitation events produced some noticeable additional transport of surface chloride concentrations down the girder ends and over time the surface concentrations on the pier cap gradually reduced, indicating dilution and further transport of the initial concentrations.

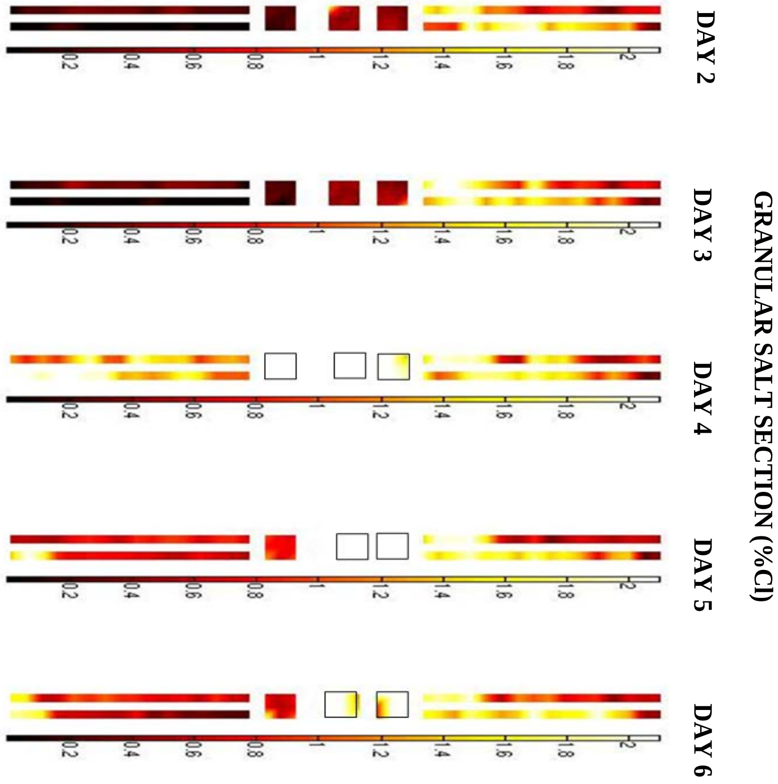

Figure 6.26: Surface concentration on girder ends and pier cap beneath the granular salt application (unfolded, projected view of the girder ends and the cap surface)

Comparing the condition of the joint in this section of the bridge to one in the prior section of granular salt, it was concluded that the joint was in overall good condition and significant transport of chlorides to components below the deck for this section was not expected. However, as with the granular salt region, a significant accumulation of salt was noticeable in the expansion joint in the initial days of testing prior to the first precipitation event. Measurements of surface chloride concentrations revealed that the chloride levels slightly increased over the week and after the rain event the changes became more observable on the cap surface (Figure 6.27). In contrast to the granular salt section where water was ponding on the pier cap, there were no noticeable signs of leakage of precipitation to the underside on either the girders or the pier cap. However, as with the granular salt section, concentrations spiked immediately after the first precipitation event, indicating transport of surface chlorides from the deck/joint to the components under the deck by precipitation. Thereafter, the surface concentrations gradually reduce with a more noticeable change occurring on the pier cap rather than on the girder ends.

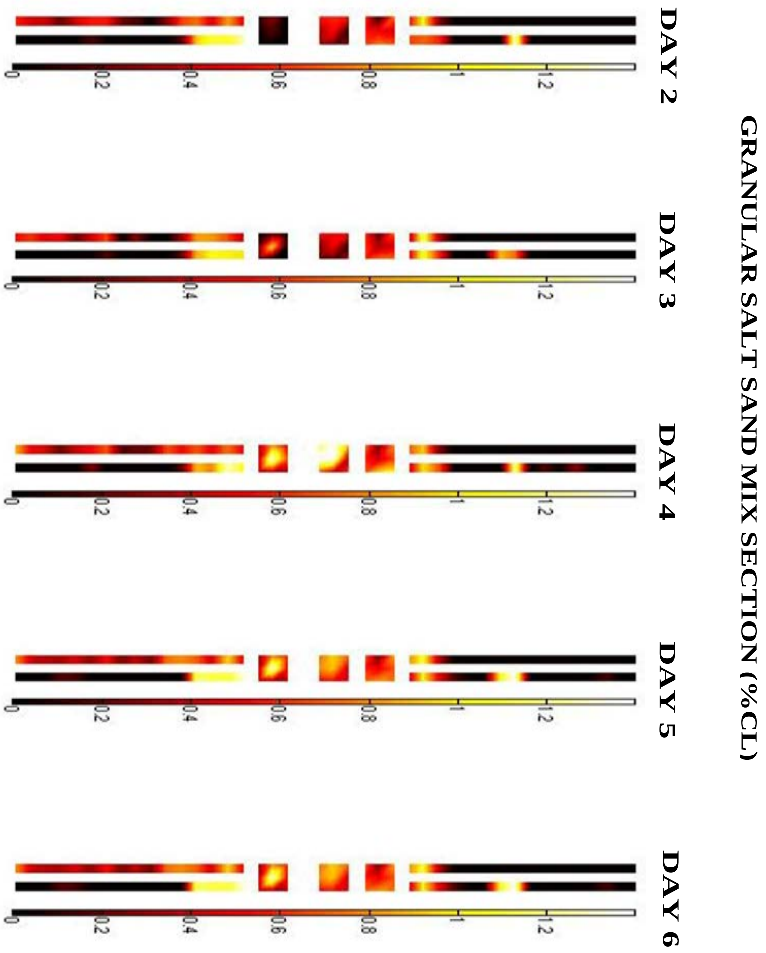

Figure 6.27: Surface concentration on girder ends and pier cap beneath the salt sand mix application (unfolded, projected view of the girder ends and the cap surface)

Table 6.6 shows the average chloride concentrations on the locations measured below deck over the 33 day duration of testing. This data is presented graphically in Figure 6.28 and Figure 6.29 with bars indicating the maximum and minimum concentrations observed for each treatment method. These graphs illustrate the strong increase in concentrations on the girder and pier cap for the granular salt, although this could be attributed to the joint conditions than the application method. The trend of the increase in chloride concentration on the girders and the pier cap almost follow the same pattern. Assuming that joint conditions of the different sections were the same, the figures on the next page would have showed all the application types following similar trends. For the brine solution and the salt sand mix section, the chloride concentration on the girders decreased initially after the rain event but then gradually increased slightly.

Table 6.6: Average chloride concentration on Billy Graham below deck components over testing period

	Brine (Cl conc. %)		Granular Salt (Cl conc. %)		Granular Salt Sand	

					mix (Cl conc. %)	
Day	Girder Avg.	Pier Cap Avg.	Girder Avg.	Pier Cap Avg.	Girder Avg.	Pier Cap Avg.
2	0.522	0.213	0.658	0.439	0.262	0.337
3	0.504	0.222	0.920	0.439	0.613	0.443
4	0.356	0.251	1.393	4.786	0.279	0.820
5	0.353	0.231	1.015	5.601	0.356	0.613
6	0.377	0.194	1.022	3.200	0.362	0.614
7	0.383	0.175	0.813	2.839	0.500	0.611
8	0.467	0.177	0.750	1.401	0.448	0.610

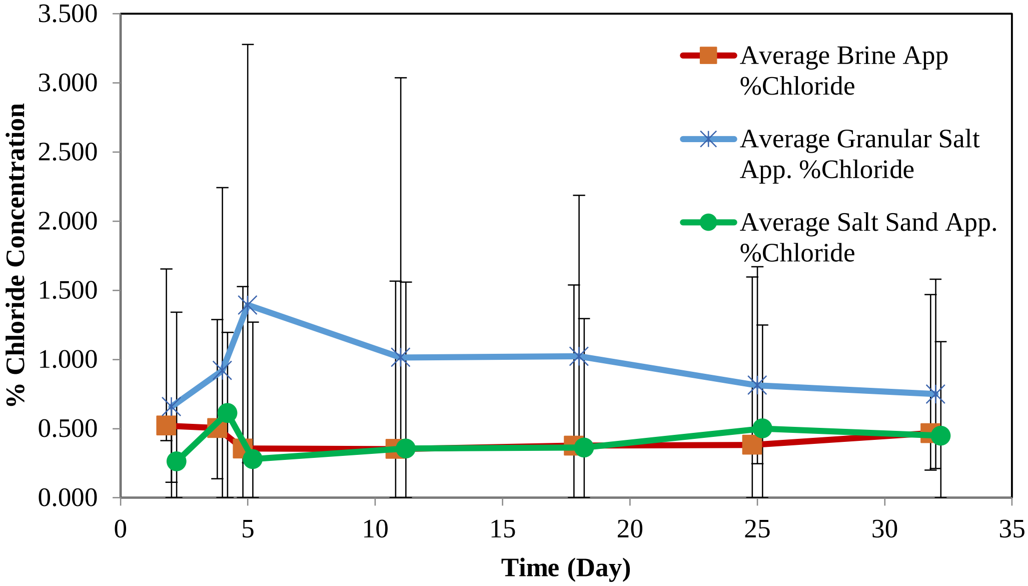

Figure 6.28: Average chloride concentration on the girders by application type over 7 days

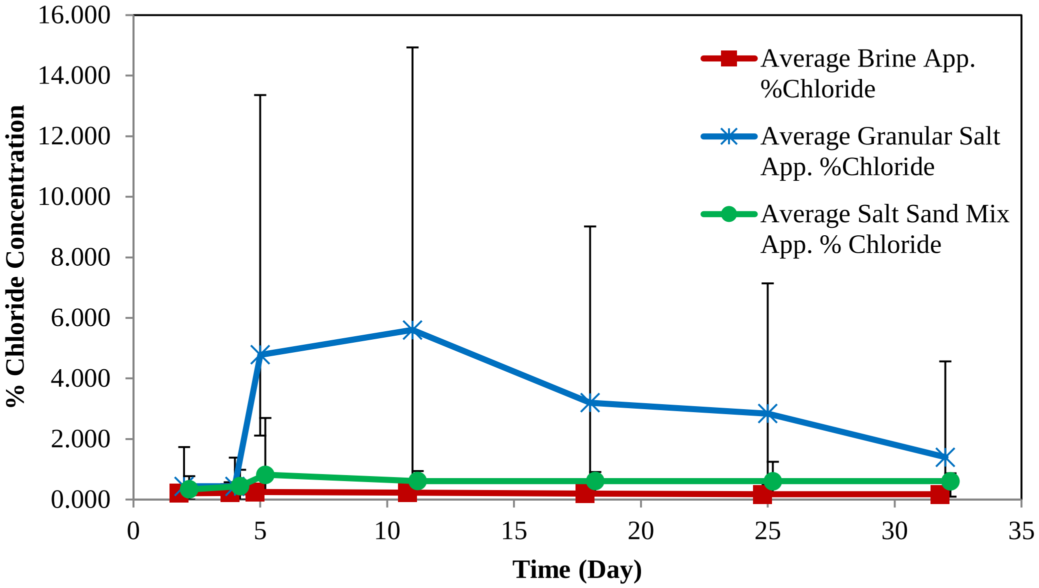

Figure 6.29: Average chloride concentration on the pier cap by application type over 7 days

7 Summary

The work described in this report was undertaken in order to discern the relative corrosive potential to bridge components associated with each of the three deicing or anti-icing strategies used in North Carolina. The three strategies investigated were granular salt application, application of salt-sand mixes and application of salt brine. Bridge components investigated included above-deck concrete elements, above deck weathering steel, below deck steel and concrete pier caps. A variety of laboratory methods and field methods were used in an effort to measure and compare the corrosive potential of each ice clearance method.

The ice melting agent common to each of these treatments is sodium chloride (NaCl). Consequently, differences in corrosive potential between the methods are not associated with the corrosion initiation mechanism of chloride. However, they are associated with the concentration of the solution on the surface, the duration of time it remains in contact with the surface, and the frequency of application. The severity of the corrosive potential is also strongly associated with the condition of bridge components at the time they are exposed. In addition to parameters that are directly linked to the treatment type, local environmental factors have far greater influence on the corrosive potential.

The key findings of each area of research described in this report are presented in the following sections.

7.1 Effectiveness of Chloride Based Roadway Treatments

The effectiveness of deicing and anti-icing treatments was characterized by measuring the ice melting capacity of salt, salt-sand and brine treatments and establishing the freezing point of salt solutions made with road salt provided by NCDOT. The freezing points of solutions having various concentrations of deicing materials were determined by the method described in ASTM D1177, “Standard Test Method for Freezing Point of Aqueous Engine Coolants” (ASTM 2012). The results determined that:

- The freezing point of salt solutions is lowered as the concentration of the salt increase. Pure water freezes at 0°C. When the solution is saturated with sodium chloride, the freezing point is reduced to -21.986 °C. The relationship of concentration and freezing point for concentrations between 0% and 23% is for practical purposes linear.

Two methods outlined by the Strategic Highway Research Program in the “Handbook of Test Methods for Evaluating Chemical Deicers” were employed to measure the ice melting capacity of the deiciers (Chappelow, McElroy et al. 1992). For solid deicers, Method H-205.1 “Test Method for Ice Melting of Solid Deicing Chemicals” was used. For the brine solution, Method H205.2, “Test Method for Ice Melting of Liquid Deicing Chemicals” was used. Key findings included:

- The ice melting capacity of deicing applications is directly related to the quantity of salt that is applied per unit area of roadway. When normalized by the quantity of salt contained in each application, the solid deicers performed identically. This implies that salt-sand mix could be applied at a rate that would melt ice as quickly as pure salt. It also implies that no ice melting benefit was realized by adding the sand. The sand functions purely as a traction material.

- Brine solutions underperformed granular applications at low temperatures below -9.4°C, but outperformed them at higher temperatures. This effect observed in the laboratory may be an artifact of the test methods used since there is not a theoretical basis for the behavior observed. However, it is also the case that salt grains can form pits in the ice and create areas of locally high deicer concentration. These pits can quickly drive ice melting. Brine solutions become diluted quickly.
- At the application rates often used for ice clearance in NC, the granular salt application shows the greatest ice melting capacity.

7.2 Corrosive Effects on Reinforced Concrete Bridge Components

The corrosive effects of deicers were quantified in the lab and in the field. Lab methods included an accelerated cyclic test in which concrete slabs were exposed to deice-freeze-thaw-flush cycles to simulate winter roadway maintenance actions. Slabs were treated with either salt, salt-sand mix or brine solutions. After 490 cycles, the chloride content at depths in the concrete up to 1” were measured. The following key observations were recorded:

- The concentration of chloride found at depths below the surface was not proportional to the quantity of chloride available in the solution at the surface. This indicates that processes other than diffusion were instrumental in the transport of chlorides into the concrete.
- The brine solution shows evidence of sorption transport. Brine solutions were applied to dry concrete, which would allow for movement of salt laden solution by capillary action. When melting snow is later present on the deck, further sorption can drive chlorides in capillary pores near the surface deeper into the concrete monolith. This process may indicate that brine has slightly greater corrosive potential on concrete surfaces than granular treatments applied to already wet decks.
- The presence of sand in the salt-sand mix did not seem to influence any of the transport processes. For dry-applied materials, the factor that most accurately estimated the concentration of chloride at depth was the concentration at the surface.
- The cyclic freezing, thawing and drying created a transport regimen that was more aggressive than static exposure. The samples having intermittent exposure to salts, water and freezing conditions achieved higher concentrations of chlorides at depth relative to the surface concentration than the control specimens that were continually ponded with 3% solution.

The corrosive effect on reinforced concrete was also measured with a field study. In this phase, concrete samples were taken from shallow depths in the Fall, before the winter maintenance season, and in the Spring, after the winter maintenance season. Measurement of chlorides at the surface was also made with a portable XRF device. These samples were collected from three bridges in Greensboro that received only granular salt, three bridges in Greensboro that received granular salt and brine and three bridges in Asheville that received salt-sand mixtures. The following list summarizes the observations from this phase of the study:

- Horizontal, above deck surfaces showed the greatest increase in chloride concentrations from Fall to Spring. Changes of up to 6.1 lb/yd^3 at the surface were found using the method of dissolving chlorides into solution and measuring with XRF. Increases of up to 7.6 lb/yd^3 were found by measuring the chloride content of powder samples collected from the ½" depth. However, interpreting this data is particularly challenging due to the limited number of bridges sampled and the fact that these quantities are known to not be stable throughout the year. They are typically high in the Spring and low in the Fall.
- No correlation was found between the magnitude of chloride concentration increase and application type. Statistical analysis of the measured changes in chloride concentration with other external factors, such as bridge age and ADT, revealed that the influence of the treatment type may be statistically less significant than other functional and environmental factors.
- In the statistical analysis of the measured dataset, no single parameter correlation was discovered to be significant. However, a multi-parameter correlation between age and ADT with generally strong correlation was found. This correlation was shown to exist both for the change in chloride concentration at the ½" depth over the winter season as well as for the absolute concentrations of chloride concentration measured in the pre-season and post-season. However, the sample size of nine bridges was too small to reasonably establish the reliability of this correlation.
- The normalized increase (concentration increase per documented treatment) in chloride concentration was greatest in Asheville. This indicates that climate, traffic or other environmental conditions in Asheville have a greater effect on the corrosive potential of road salts to reinforced concrete than the treatment method alone.

These findings have significance to NC policy and practice because the impact of deicer application may be heightened in regions of the state having longer drying periods between applications or frequent freezing and thawing cycles. Due to sorption, this may indicate that brine is likely to accumulate in concrete volumes more quickly.

7.3 Corrosive Effects on Steel Components

The corrosive impact to steel components was studied with a lab method and a field method. In the lab method, steel coupons were exposed to chloride solutions of various concentrations and the corrosion rate was documented for each alloy and solution concentration. Secondly, three protective coatings, galvanization, paint and epoxy, were evaluated for their ability to prevent undercutting corrosion during exposure to salt solutions. Lastly, bare metal coupons were installed on bridges prior to the salting season and collected for evaluation after one winter of exposure.

Results of the lab methods showed the following:

- Using the SHRP method of continuously submerging the steel coupons in chloride solutions provided valid results for only low concentration solutions due to the low dissolved oxygen content in high concentration solutions. The test was repeated with a modified method of intermittent exposure to the solution followed by a drying phase in ambient conditions.
- Results collected from the modified SHRP showed that in general, the A588 and A572 steel alloys exhibited comparable corrosive losses. The A36 steel generally

exhibited slightly less corrosive loss. Furthermore, while the 3% and 5% concentrations yielded similar weight losses, the specimens subject to 23% concentrations were found to exhibit less corrosion. Corrosion rates ranged from a low of 36.7 mils per year for A36 steel exposed to 23% solution to a high of 94.7 mils per year for A588 steel exposed to 3% solutions. The A588 material is expected to form an outer layer of corroded material when exposed to the atmosphere in order to protect inner, un-corroded steel. The test duration was not sufficient to determine if decreasing corrosion rates would be associated with this alloy after time.

- Coupons coated with paint or epoxy showed negligible loss. Galvanized coupons underwent loss of the sacrificial galvanization coating. Corrosion did not reach the depth of the substrate material.
- Coatings damaged by a scratch were exposed to the chloride solution. Undercutting and progress of corrosion was found to be most significant in epoxy coated specimens. Undercutting was less pronounced in painted specimens and not present in galvanized specimens.

Uncoated steel coupons were mounted at critical below-deck positions on nine bridges in NC. Corrosive losses were measured after one season of exposure to either salt, salt and brine, or salt-sand mix. The findings of this experiment were:

- For the three different deicing treatments, the average corrosive loss across all testing locations is 0.158% for four granular salt applications, 0.197% for four brine with granular salt applications, and 0.572% for eight salt-sand deicing applications, respectively. The corresponding results normalized per application are 0.0395% for granular deicing, 0.0493% for brine anti-icing followed by granular deicing, and 0.0715% for salt-sand deicing mix.
- When comparing the average corrosive losses for all flange locations versus all web locations, the flanges are found to experience about 1.5 times more corrosion compared to web components.
- Computing the average total losses at all the test locations, the overall loss is 24.8% higher or 1.25 times greater for bridges receiving both granular and brine treatment compared to granular treatment alone. Higher corrosive loss from the combination of brine and granular can be seen at four out of six test locations.

7.4 Time and Spatial Characteristics of Deicer and Anti-icer Concentrations on Bridge Surfaces

The three deicing and anti-icing solutions were applied to a dry bridge deck and their concentration was measured on above and below deck components after the action of traffic and weather during a period of 25 days, until their magnitudes were too low to detect. The following observations were made:

- The average initial surface concentrations associated with the various treatment methods were 14.08% for brine, 11.95% for granular salt, and 5.07% for salt-sand mix.
- The rate of surface concentration reduction with time was greatest for brine and granular salt treatments. The rate of reduction for the salt-sand treatment was lower, however the initial concentration was also substantially lower.

- The area treated with brine did not show increases in the concentration of chlorides on the shoulder beyond the initial measured concentration. This indicates that the brine remained in the lane. Both granular treatments caused slight elevations in the concentration found on the shoulder after the first day. This is due to traffic action moving the granular treatments from the roadway.
- The granular salt treatment spread to the girders after the first precipitation event. The brine treatments did not cause an increase in chlorides on the girder surfaces.
- The residual surface concentration over time and before precipitation can be modeled with an exponential function. Such models have also been proposed by other research groups.

7.5 Recommendations

7.5.1 ***Recommendations for Maintenance Policy***

The array of experiments described in this report do not indicate a significantly different degree of corrosive potential associated with the three predominant deicing treatments used in North Carolina. Instead, the potential of bridge components to be damaged by winter maintenance activities is more closely linked to the existing condition of bridges, the number of annual applications of any type, and characteristics of the service environment. There is insufficient evidence from this study to warrant allocating greater corrosion mitigation resources to bridges receiving any particular winter weather treatment. Rather, the allocation should be made based on the frequency of road salt applications and the susceptibility of the bridge design to corrosive damage.

Field observations and experimental results indicate that the following scenarios should be used to prioritize corrosion mitigation strategies:

Bridge condition characteristics:

- Poor joint condition, especially missing joint material
- Chipped or scratched paint on steel components
- Chipped or scratched epoxy coating on steel components
- Low ADT bridges, where vehicle-driven transport of chlorides from the surface may be low

Application characteristics

- Bridges where brine has been applied to dry pavement
- Cases in which deicing or anti-icing materials were applied without the subsequent arrival of significant precipitation

Environmental Characteristics

- Application of deicers following a long period without precipitation, or warm weather

Although the magnitude of impact of each deicer on corrosion is difficult to quantify without considering other environmental characteristics, the deicers were found to impact bridge elements in different ways. Thus, bridge inspections for regions that make greater use of certain deicers could be focused to detect the onset of damage related to winter maintenance.

Granular Treatments:
- Joints
- Pier caps
- Lower web and flange of girders

Brine
- Deck surfaces
- Above deck weathering steel

7.5.2 ***Recommendations for Future Research***

In the previous section, it was recommended that maintenance resources be allocated on the basis of salt application frequency rather than deicer type. However, it is likely that the severity of corrosion potential is variable based on application type as well as bridge service environment. In order to better understand these complex interrelationships, the following opportunities for further research are suggested.

7.5.2.1 ***Regionally Based Corrosion Assessment***

On a local scale, similarities in climate, traffic and deicer use can be linked to the general magnitude of corrosion damage. By tracking deicer application frequency, general weather patterns, and traffic counts and overlaying these with a survey of corrosion-related damage or maintenance activity, bridge management engineers can establish priority zones for application of corrosion mitigation resources. Corrosion coupons mounted on bridges for periods longer than those available during this study have also been used by other state transportation departments to establish local corrosion rates. Mounting such coupons would economically provide data regarding the aggressiveness of corrosion environments around North Carolina. The period that these coupons should remain in place should include several winters.

It was difficult in this study to establish the exact quantities of deicing materials that were applied to each bridge. One method of tracking could include GPS units that are triggered when the salt spreader is operating. Combined with spreader calibration data, this tracking system could very accurately track applications. Such data could be used to establish application frequency based maintenance resource allocations. It could also be used as an input to corrosivity mapping along with bridge inspection reports, weather data and corrosion coupon losses.

In conjunction with the proposed field testing, the bridge inspection and condition rating database could be statistically analyzed to evaluate relative impacts of deicing and anti-icing strategies. Such an effort would require knowledge on the winter treatment methods applied to primary, interstate, and local routes in each region analyzed for the study and assumes that that application of brine has been performed for a statistically significant duration to-date to generate any potential differences in bridge deterioration rates. The proposed work should perform multi-parameter regression of a significantly large number of bridges across the state using survival analysis techniques, such as Cox Proportional Hazards regression analysis, to overcome the statistical limitations encountered in the field testing performed for the current study.

7.5.2.2 Long Term Laboratory Testing

The current study revealed that laboratory testing under controlled conditions is likely to yield the most definitive physical evidence of the relative impact of deicing and anti-icing strategies, since external environmental and functional variables can be strictly controlled. Laboratory exposure of reinforced concrete specimens within the environmental chamber suggested unique differences between the exposure from granular and brine treatments that are most likely due to surface layer sorption. This sorption process is complex and time dependent. The accelerated exposure routine adopted in the current study to simulate several winters of treatment over a four month window could be repeated without any scaling of time durations to characterize the sorption process differences without any questions with respect to time scaling effects. In addition, laboratory test methods should be investigated to directly measure the rate of near surface sorption for brine and granular treatments, since this transport process appears to present a potentially significant difference between the impacts of treatment strategies. Furthermore, laboratory tests should be formulated to investigate differences in the surface adhesion of residual chlorides and residual concentrations following precipitation events and run-off. The reasoning behind such tests is that the rewetting of concrete surfaces pre-treated by brine solutions may initiate significant sorption of the chlorides into the concrete surface, whereas wetting of concrete surfaces with granular salts could likely lead predominantly to surface run-off of the chlorides.

References

Albrecht, P, and T. Hall. (2003). "Atmospheric Corrosion Resistance of Stuctural Steels." *Journal of Materials in Civil Engineering.*

American Concrete Institute. (2011). *Building Code Requirements for Structural Concrete (ACI 318-11) and Commentary.*

American Iron and Steel Institute. (1995). *Performance of Weathering Steel in Highway Bridges.*

Angst, U., and Ø Vennesland. (2009). *Critical chloride content in reinforced concrete-State of the art.* London: Taylor & Francis Group.

ASTM (1972). ASTM G31-72 Standard Practice for Laboratory Immersion Corrosion Testing of Metals. West Conshohocken, PA, ASTM International.

ASTM. (2003). *G1-03, Standard Practice for Preparing, Cleaning, and Evaluationg Corrosion Test Specimens.* West Conshohocken, PA: ASTM International. doi:10.1520/G001-03.

ASTM. (2004). *G31-72(2004), Standard Practice for Laboratory Immersion Corrosion Testing of Metals.* West Conshohocken, PA: ASTM International. www.astm.org.

ASTM. (2005). *D7087-05, Standard Test Method for An Imaging Technique to Measure Rust Creepage at Scribe on Coated Test Panels Subjected to Corrosive Environments.* West Conshohocken, PA: ASTM International. www.astm.org.

ASTM. (2007). *G109-07, Determining Effects of Chemical Admixtures on Corrosion of Embedded Steel Reinforcement in Concrete Exposed to Chloride Enviroments.* West Conshohocken, PA: ASTM International.

ASTM. (2008). *D1654-08, Standard Test Method for Evaluation of Painted or Coated Specimens Subjected to Corrosive Environments.* West Conshohocken, PA: ASTM International. www.astm.org.

ASTM. (2009). *C876-09, Standard Test Method forCorrosion Potentials of Uncoated Reinforcing Steel in Concrete.* WEST Conshohocken, PA: ASTM International.

ASTM. (2009). *D714-02(2009), Standard Test Method for Evaluating Degree of Blistering of Paints.* West Conshohocken, PA: ASTM International. www.astm.org.

ASTM (2009). ASTM C876-09 Standard Test Method for Half-Cell Potentials of Uncoated Reinforcing Steel in Concrete. West Conshohocken, PA, ASTM International.

ASTM. (2010). *G50-10, Standard Practice for Conducting Atmospheric Corrosion Tests on Metals.* West Conshohocken, PA: ASTM International. www.astm.org.

ASTM (2011). ASTM G1 - 03(2011) Standard Practice for Preparing, Cleaning, and Evaluating Corrosion Test Specimens. West Conshohocken, PA, ASTM International.

ASTM. (2014). *Steel Standards.* Accessed 2014. http://www.astm.org/Standards/steel-standards.html.

Bioubakhsh, S. (2011). The penetration of chloride in concrete subject to wetting and drying: measurement and modelling. PhD, University College London.

Blomqvist, G. and M. Gustafsson (2004). Patterns of residual salt on road surface: case study. Transportation Research E-Circular: Sixth International Symposium on Snow Removal and Ice Control Technology. Washington DC, Transportation Research Board of the National Academies

Boatman, Brandon. 2010. *Epoxy Coated Rebar Bridge Decks: Expected Service Life.*

Chappelow, C. C., A. D. McElroy, R. R. Blackburn, D. Darwin, F. de Noyelles and C. Locke (1992). Handbook of test methods for evaluating chemical deicers.

Darwin, D., J. Browning, L. Gong and S. R. Hughes (2007). Effects of deicers on concrete deterioration. Lawrence, KS, The University of Kansas Center for Research, Inc.

El-Shazly, A.H., and A.A. Wazzan. (2012). "Using Polypyrrole Coating for Improving the Corrosion Resistance of Steel Buried in Corrosive Mediums." *International Journal of Electrochemical Science.*

Federal Highway Administration Technical Advisory. (1989). *Uncoated Weathering Steel in Structures, T5140.22.*

Gergely, J., J. Bledsoe, B. Tempest and I. Szabo (2006). Concrete Diffusion Coefficients and Existing Chloride Exposure in North Carolina.

Gergely, J., Tempest, B., Bledsoe, J., Szabo, I. (2004). "Concrete Diffusion Coefficients and Existing Chloride Exposure in North Carolina." Mid-Term Progress Report NCDOT Research Project No. HWY-2004-12.

Gergely, Janos, Joshua Bledsoe, Brett Tempest, and Iosif Szabo. (2006). "Concrete Diffusion Coefficients and Existing Chloride Exposure in North Carolina." Research Project, Department of Civil Engineering, University of North Carolina at Charlotte.

Guthrie, J., B. Battaat and C. Grethlein (2002). "Accelerated Corrosion Testing." The AMPTIAC Quarterlt **6**(3).

Guthrie, Jeffrey, Brigittle Battaat, and Chris Grethlein. (2002). "Accelerated Corrosion Testing." *The AMPTIAC Quarterlt* 6 (3).

Hong, K. and R. D. Hooton (1999). "Effects of cyclic chloride exposure on penetration of concrete cover." Cement and Concrete Research **29**(9): 1379-1386.

Imperatore, S., and Z. Rinaldi. (2009). "Mechanical behavior of corroded rebars and influence on the structural response of R/C elements." Thesis.

Innov-X Systems, I. (2010). User Manual, Delta Family Handheld XRF Analyzers.

ISO. (2010). *11130, Corrosion of metals and alloys - Alternate immersion test in salt solution.* www.iso.org.

ISO. (2012). *9226, Corrosion of Metals and Aloys - Corrosivity of Atmospheres - Determination of Corrosion Rate of Standard Specimens for the Evaluation of Corrosivity.* www.iso.org.

Ketchan, S. A., L. D. Minsk, R. R. Blackburn and E. J. Fleege (1996). "Manual of Practice for an effective Anti-Icing Program: A guide for Highway Winter Maintenance Personnel." U.S. Department of Transportation Federal Highway Administration, FHWA-RS-95-202: 70.

Kline, E.S. (2008). "Steel Bridge: Corrosion Protection for 100 Years." *Journal of Protective Coatings and Linings* 22-31.

Koch, G.H, Brongers M.P., N.G. Thompson, Y.P. Virmani, and J.H. Payer. (2002). *Corrosion Costs and Preventive Strategies in the United States.* Washington, D.C.: FHWA.

Kogler, Robert. (2012). *Steel Bridge Design Handbook: Corrosion Protection of Steel Bridges.* FHWA Report No. FHWA-IF-12-052, Federal Highway Administration.

Lee, H., R. D. Cody, A. M. Cody and P. G. Spry (2000). Effects of various deicing chemicals on pavement concrete deterioration. Center for Transportation Research and Education (Ed.), Mid-Continent Transportation Symposium Proceedings, Iowa State University, Ames, USA.

Levelton Consultants Ltd. (2007). *Guidelines for the selection of snow and ice control materials to mitigate environmental impacts. NCHRP REPORT 577.* Washington, D.C.: National Research Council.

Luping, T., L.-O. Nilsson and P. M. Basheer (2011). Modelling of chloride ingress. Resistance of Concrete to Chloride Ingress, CRC Press**:** 75-119.

Lysbakken, K. R. and A. Lalagüe (2013). Accuracy of SOBO-20 in Measurement of Salt on Winter Pavements. Transportation Research Board 92nd Annual Meeting.

Mailvaganam, N.P., and P.G. Collins. (1999). "Effective Installation of Membranes on Parking Garage Decks." *Construction Technology Updates* (Institute for Research in Construction).

MatWeb. (2011). *MatWeb Material Property Data.* Accessed 2014. http://www.matweb.com.

Mindess, Sidney, J. Francis Young, and David Darwin. (2002). *Concrete.* 2nd. New Jersey: Prentice Hall.

Mitchell, G., C. Hunt and W. Richardson (2003). Evaluation of ODOT roadway/weather sensor systems for snow and ice removal operations. Part III: Optimization of salt brine pre-treatment application rates and frequency.

Morcillo, M., B. Chico, I. Diaz, Cano H., and D. de la Fuente. (2013). "Atmospheric corrosion data of weathering steels. A review." *Corrosion Science.*

National Cooperative Highway Research Program. (2012). *Synthesis 425, Waterproofing Membranes for Concrete Bridge Decks.* WASHINGTON, D.C.

Nixon, Wilfrid, George Kochumman, Lin Qiu, Ju Qiu, and Jing Xiong. (2007). "Evaluation of Deicing Materials and Corrosion Reducing Treatments for Deicing Salts." Technical Report, College of Engineering, The University of Iowa.

North Carolina Department of Transportation. (2013). *Safety Tips List.* Accessed 2014. http://www.ncdot.gov/travel/safetytips/.

Organization for Economic Co-operation and Development (2002). Electrochemical Techniques to Detect Corrosion in Concrete Structure in Nuclear Installations. Technical Note.

Pacific Northwest Snowfighters. (2010). "Snow and ice control chemical products specifications and test protocols for the PNS association of British Columbia, Idaho, Montana, Oregon and Washington ."

Pitroda, J. (2013). "Evaluation of Sorptivity and Water Absorption of Concrete with Partial Replacement of Cement by Thermal Industrial Waste (Fly Ash)."

Pitroda, J. (2013). *Evaluation of Sorptivity and Water Absorption of Concrete with Partial Replacement of Cement by Thermal Industrial Waste (Fly Ash).* International Journal of Engineering and Innovative Technology.

Proverbio, E. and F. Carassiti (1997). "Evaluation of chloride content in concrete by X-ray fluorescence." Cement and Concrete Research **27**(8): 1213-1223.

Q-Lab Corporation (2009). Technical Bulletin LF-8144.1, Introduction to Cyclic Corrosion Testing. Cleveland.

SAE International. 1998. "Cosmetic corrosion lab test." SAE J2334.

Shi, P., Y. Liu, M. Mooney, M. Berry, B. Hubbard, L. Fay and A. B. Leonard (2010). Effect of chloride-based deicers on reinforced concrete structures.

SHRP. (1992). *Handbook of Test Methods for Evaluating Chemical Deicers.* Washington, DC: Strategic Highway Research Program.

Smith, Jeffrey, and Yash Virmani. (1996). *Performance of Epoxy-Coated Rebars in Bridge Decks.* Accessed 2014. https://www.fhwa.dot.gov/publications/publicroads/96fall/p96au6.cfm.

Tempest, B. (2004). Measurement of existing chloride exposure in North Carolina and development of chloride diffusion parameters for bridge design modeling. Masters Thesis, University of North Carolina at Charlotte.

Trejo, D., C. Halmen, and K. Reinschmidt. (2009). *Corrosion Performance Tests for Reinforcing Steel in Concrete.* Report No. FHWA/TX-09/0-4825-1 , FHWA.

Vitro Minerals. (2006). "Portland Cement and Pozzolans." Technical Report.

Weather Underground. (2013). *Weather Underground.* Accessed 2013. http://www.wunderground.com/.

Yao, Yuan, Pradeep Kodumuri, and Seung-Kyoung Lee. 2011. *Performance Evaluation of One-Coat Systems for New Steel Bridges.* FHWA Report No. FHWA-HRT-11-046, Federal Highway Administration.

Appendix A Validation of Chloride Detection Methods

A1 Description of the XRF Analyzer

The Delta Handheld X-Ray Fluorescence (XRF) analyzer used in this study was an Innov-X Systems Inc. product that is a handheld energy dispersive X-Ray fluorescence spectrometer, generally referred to as an XRF analyzer. The handheld XRF analyzer is primarily used to determine the elemental composition of a substance and gives an accurate measure of the relative amount of elements present in the substance. Each chemical element has a unique characteristic X-Ray emission wavelength, or energy. The amount of an element present is determined by measuring the intensity or counts detected at its characteristic wavelength. Based on the precision of obtaining the energies of each element, the analyzer has been used extensively for accurate chemical analysis in commercial applications, such as the identification of lead and asbestos limits in buildings and the environment (Innov-X Systems 2010). The analyzer is shown in Figure A.1

The analyzer has many advantages, including the ability to detect concentrations of elements from parts per million (ppm) levels to 100% by weight without destroying the sample. Additionally, the results are often available within less than a minute at a relatively low cost per sample both in the lab and field. The unit presents the results on the screen of the unit and a PDF copy is generated (Figure A.3). The PDF copy of the results shows the ppm or percent results of all the elements detected and also spectra of the elements (Innov-X Systems 2010).

Figure A.1: XRF handheld analyzer

Figure A.2: XRF handheld analyzer attached to the A-020-D test stand

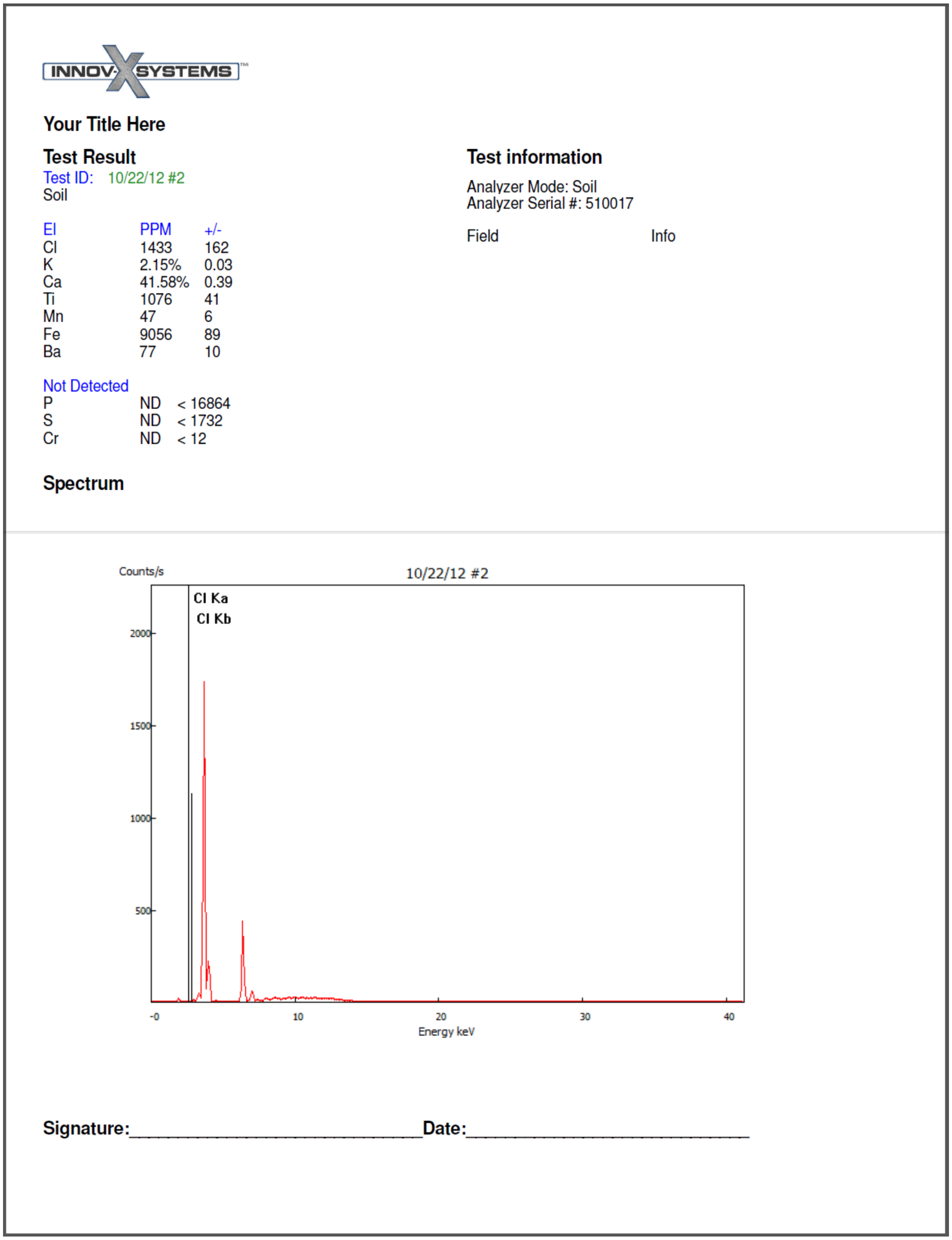

INNOV-X SYSTEMS

Your Title Here

Test Result

Test ID: 10/22/12 #2
Soil

El	PPM	+/-
Cl	1433	162
K	2.15%	0.03
Ca	41.58%	0.39
Ti	1076	41
Mn	47	6
Fe	9056	89
Ba	77	10

Not Detected

P	ND	< 16864
S	ND	< 1732
Cr	ND	< 12

Test information

Analyzer Mode: Soil
Analyzer Serial #: 510017

Field	Info

Spectrum

Signature:______________________________**Date:**_____________________________

Figure A.3: A sample of the XRF handheld analyzer results presented in PDF form.

The analyzer used in this study provides analysis to a limited depth of penetration very close to the surface. Therefore, if a material has been painted, or has received surface treatment, such as epoxy, it may be misidentified. For example, a painted steel piece may show high concentrations of titanium from the paint, and may be misidentified as a titanium alloy (Innov-X Systems 2010).

The unit has five specialized modes available: a soil mode, mining mode, mining plus mode, ROHS mode and the alloy plus mode. For this study, the soil mode was used mostly for measuring low concentrations of chloride depending on the surface material and high concentrations as well. The soil mode uses the Compton normalization algorithm designed for achieving lowest limit of Detection (LOD) possible for samples and the mining plus mode uses the fundamental parameters method. The soil mode used in this study, detects the various elements: K, Ca, S, P, **Cl**, Ti, Cr, Mn, Fe, Ni, Cu, Zn, Hg, As, Pb, Se, Rb, Sr, Zr, Mo, Ag, Cd, Sn, Sb, Ba of which Chloride is of importance in this study (Innov-X Systems 2010).

A2 Validation of the XRF Method for Chloride Determinations in Concrete Powder Samples

For validation of XRF powder measurements, powder samples were collected at ½" depth from the following bridges: NC 62 over I-85 Bridge (10 samples), NC 62 over 421 bridge (10 samples), East Lee Street bridge (10 samples) and Washington Street Bridge (7 samples) in the Greensboro pre-season sampling routine. All powder samples were tested using the handheld XRF analyzer in the XRF test stand and sampling cups. These same powder samples were then tested for chloride concentration by the RCT method. For the purposes of this comparison, the 24 hour results were considered although the five-minute results were used as they better represent the manner in which bridge inspection personnel would typically use the RCT device in the field. For the XRF analysis, the soil (Beam 3-15kV) mode at duration of 60 seconds was used for each sample to maintain consistency with the field sampling protocol.

The XRF analysis of powder samples was plotted against the RCT determination to examine correlation between the two methods (Figure A.4). The plot shows a linear relation between these two methods that provides validity to the XRF analysis. In general, it can be seen that the XRF analyzer consistently provides slightly higher results than the RCT measurement. Linear regression of the data reveals that the XRF analyzer overestimated the chloride concentration on average by a factor of 1.17 compared to the RCT result.

It should be noted that the manufacturer of the RCT instrumentation recommends that an adjustment factor of 1.05 to 1.20 be used to correct five-minute rapid test results to an expected titration result. A prior UNC Charlotte study determined a correction factor of 1.16 when comparing AASHTO titration results to the five-minute RCT digestion readings (Gergely 2004). Consequently, the XRF analyzer may likely provide more accurate results for chloride content (closer to the expected titration result) in the powder samples than obtained by the five-minute RCT results.

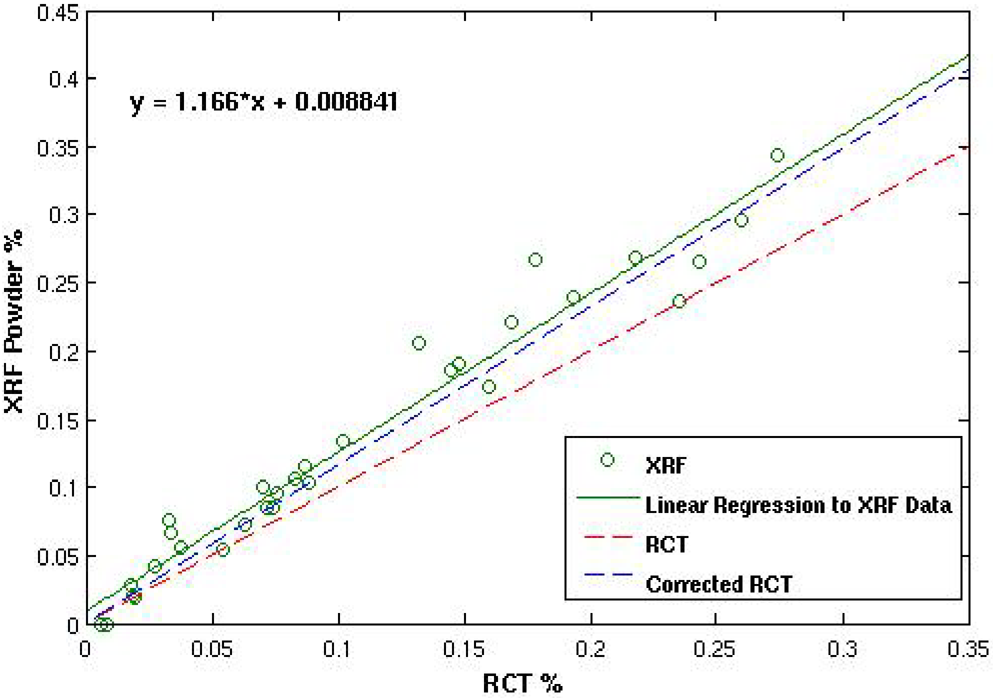

Figure A.4: Plot of XRF analysis of powder samples against RCT results

A3 Validation of XRF Method for Measurement of Surface Chloride Concentrations

The XRF analyzer was used to make in-situ evaluations of chloride concentration at the surface of concrete bridge decks. In contrast to the powder samples obtained at ½” of depth, surface concentrations of chlorides measured on a dry surface were generally not detectable. The chloride levels in the powder samples ranged from 0.005%-0.3% and the highest surface concentration was 0.68% which was found in the cap area of the bridge. There was no correlation in the values obtained on the surface to the powders collected in the same area, which leads to the conclusion that the XRF field analysis is limited to contaminants or elements on the surface of the concrete and not from within the concrete. These experimental observations were the motivation behind developing the surface chloride absorption technique.

Brine solutions of various concentrations were placed on glass surfaces and left to evaporate. After about 24 hours of evaporation, 10ml of deionized water was poured on to the glass surface with the salt particles to determine the rate that recrystallized salt are dissolved into solution. Before the later procedure, the initial surface reading of the glass was taken to determine the concentration of chloride present, if any, before the brine solution was poured. Immediately after the brine solution was poured onto the surface, XRF readings were taken. These readings also showed half the concentration of the theoretical values (Figure A.5). Presented below is a figure of the plot of various readings taking in the soil (Beam 3 -15kV) mode during this process.

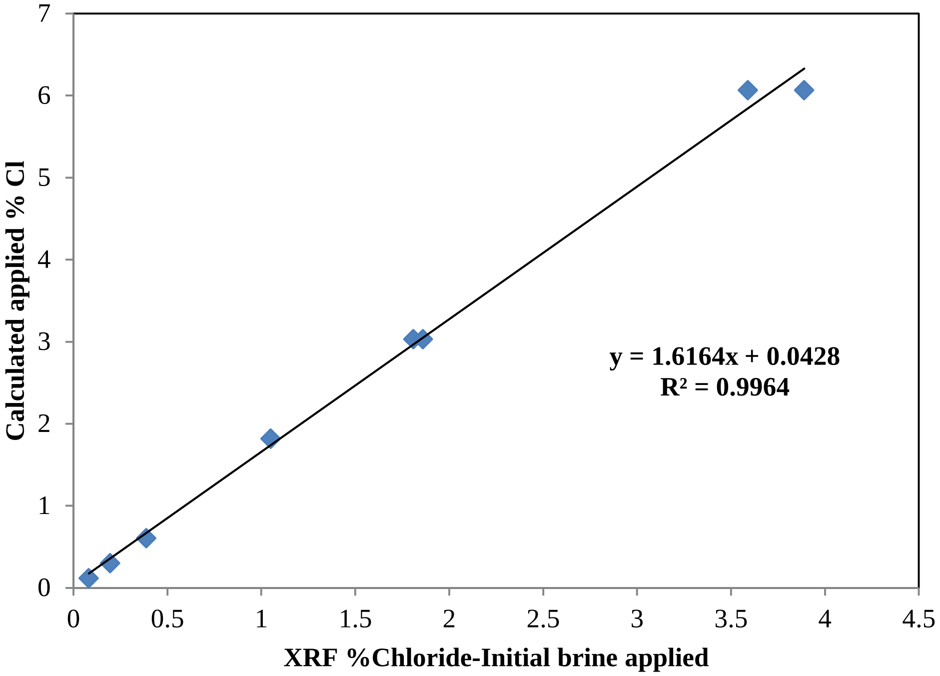

Figure A.5: Soil mode results of glass surface salt application

After the brine solution was poured onto the glass surface (Figure A.6), XRF measurement runs were started in the soil mode (Beam 3-15kV) on the glass surface, then the glass surface was left to enable evaporation of the water to leave residue of the salt particles. Afterwards, 10ml of deionized water was then poured onto the glass surface with the crystallized salt grains. Approximately 10 seconds were given to allow for the crystals to enter solution after which readings were taken at regular time intervals of five minutes. This laboratory validation indicates that it requires approximately twenty minutes for the chloride to fully re-dissolve into solution. In Figure A.7 and Figure A.8 the results obtained after the deionized water was applied are plotted as a percent of the initial chloride concentration registered when the brine solution was poured onto the glass surface. As observed, it took roughly twenty minutes to attain 100% of the initial concentration. Figure A.9 shows the accuracy and linearity of the relationship between the quantity of chloride added to the glass surface and the measurement provided by the XRF analyzer.

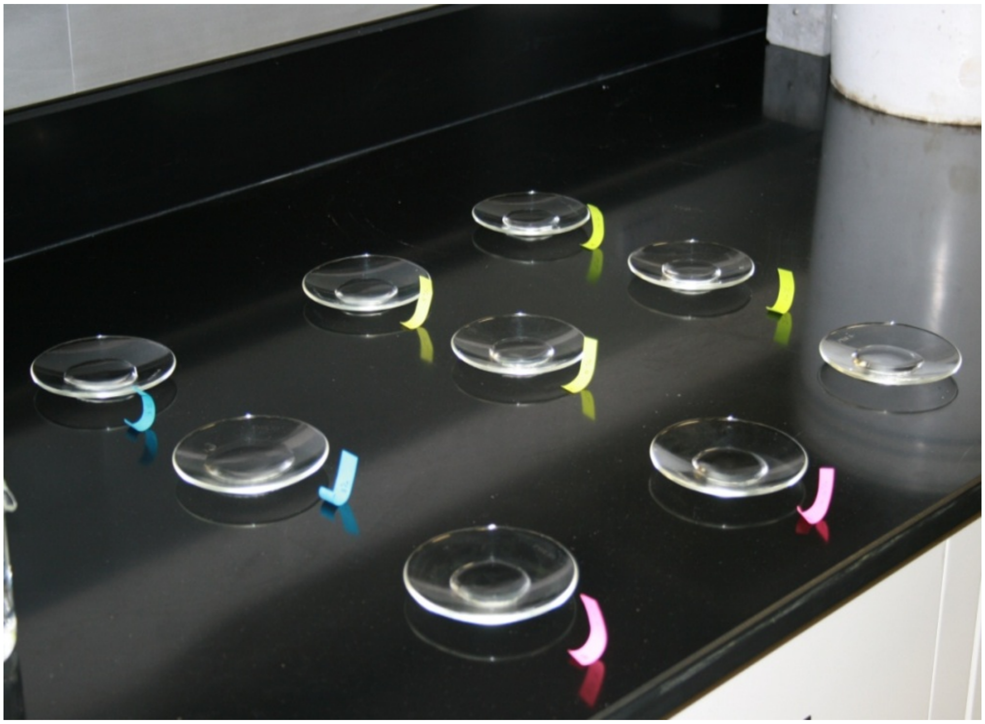

Figure A.6: Brine solutions added to the glass surface

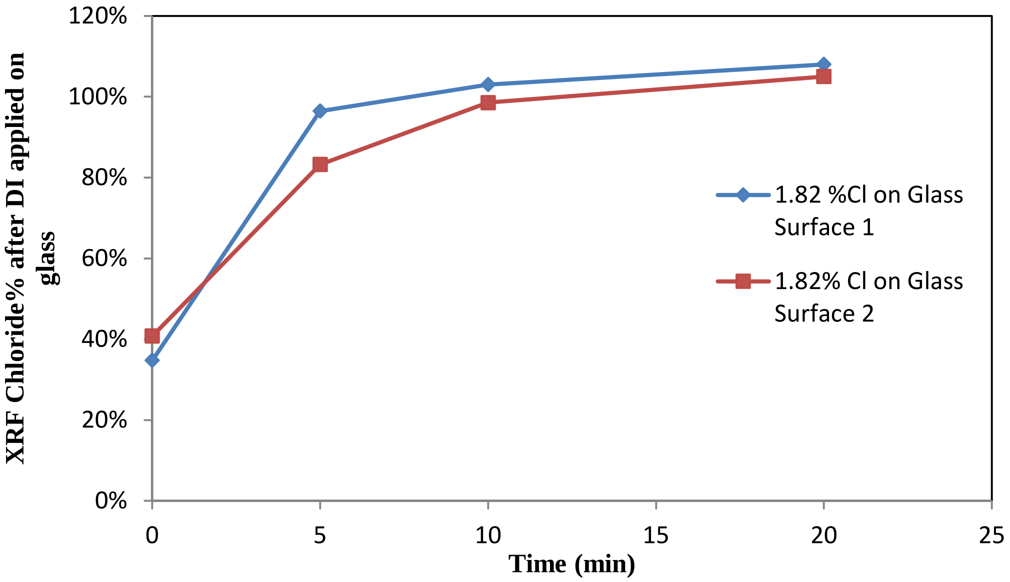

Figure A.7: Increase in chloride concentration after five minute intervals for glass surface, given as percentage of the initial applied concentration

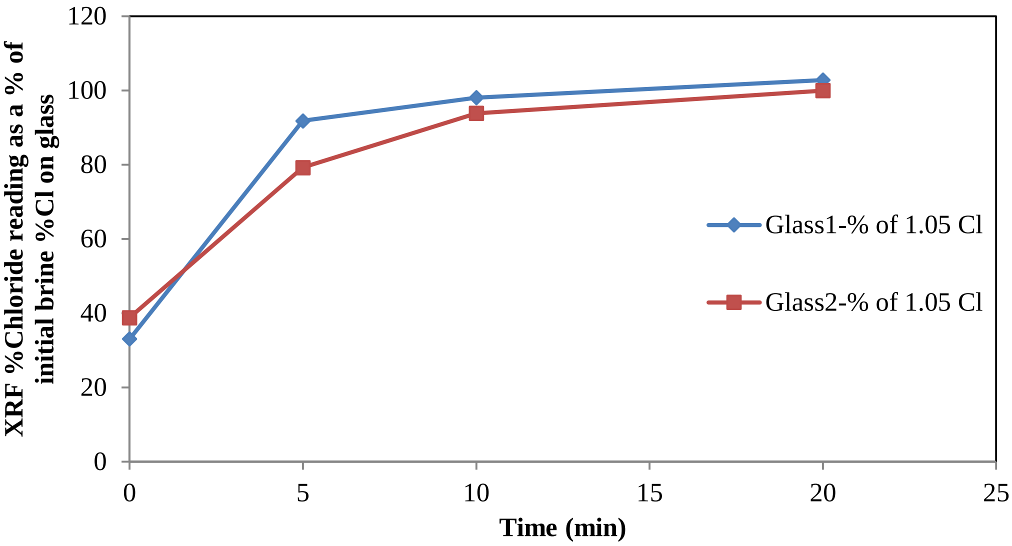

Figure A.8: XRF reading after DI applied as a percent of the initial brine solution measurement over twenty minutes

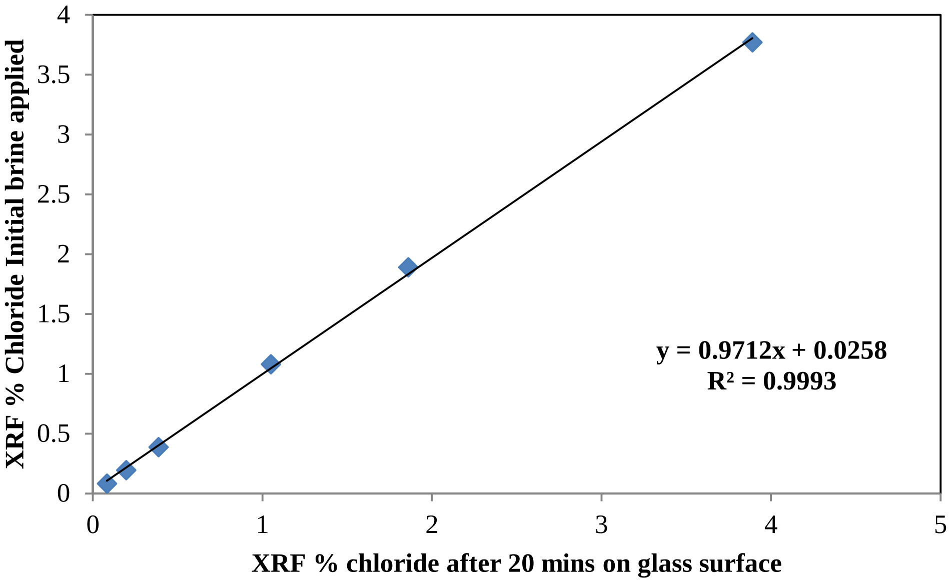

Figure A.9: Linear correlation between the initial applied brine % chloride and the % chloride after 20 min on concrete surface

In order to verify the applicability of the procedure described above to concrete surfaces, the solutions with known chloride concentrations were added to a concrete slab. To keep the brine on the surface area of interest, 3 inch diameter basins were made with hot glue on the concrete slab. Figure A.10 shows the concrete slab with the glue rings.

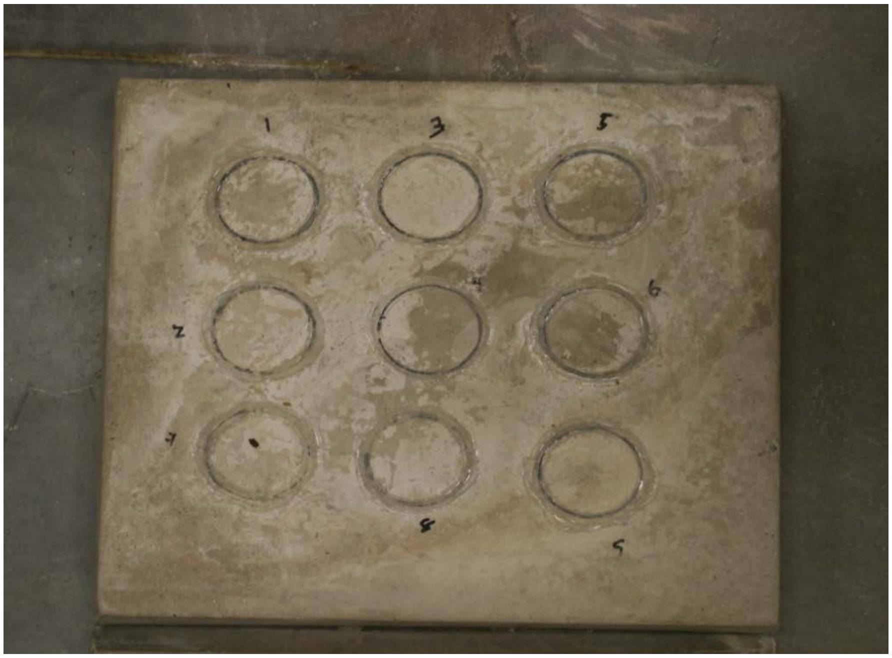

Figure A.10: The concrete slab with glue rings.

Before the glue was applied on to the concrete slab surface, the slab and the glue were tested with the XRF in soil mode (Beam 3-15Kv) to measure any initial chloride concentration.

The glue and concrete spectra showed no measurable chloride content. As with glass surfaces, 10mL of different brine solutions (3%, 5% and 10% NaCl) were poured into the concrete surfaces glue rings and XRF measurements were obtained immediately following application. The solution was allowed to dry by evaporation and absorption into the concrete. After 24 hours, 10 mL deionized water was added to the surface to dissolve the remaining salts. The XRF was used to measure the concentration of chlorides in the solution at five minute intervals. These results are plotted in Figure A.11. The results showed that salts deposited on the concrete surface dissolved more slowly back into solution than from the glass surface. This is expected as there are potential reactions between the chloride ions and concrete that could bind some of the chlorides in the concrete matrix. If bound, they would not be available for dissolution back into solution. Considering the permeability of the concrete, it may be that during the 24hr evaporation period, a very small percentage of the chlorides diffused into the concrete.

Figure A.12 shows the correlation between the measured brine solution on the surface of the concrete slab and the theoretical chloride concentration based on the amount of salt applied. At lower concentrations, the dissolution rate was proportionally slower, however the quantity of salt entering the solution was directly proportional to the initial amount applied to the surface.

The utilization of the surface chloride absorption method was found to provide consistent readings. Based on these observations, it is assumed that field measurements taken after twenty minutes will be representative of the water soluble chloride concentrations that have not bonded with the concrete surface. The measurements collected at the surface must be adjusted as is shown by the regression line in Figure A.12.

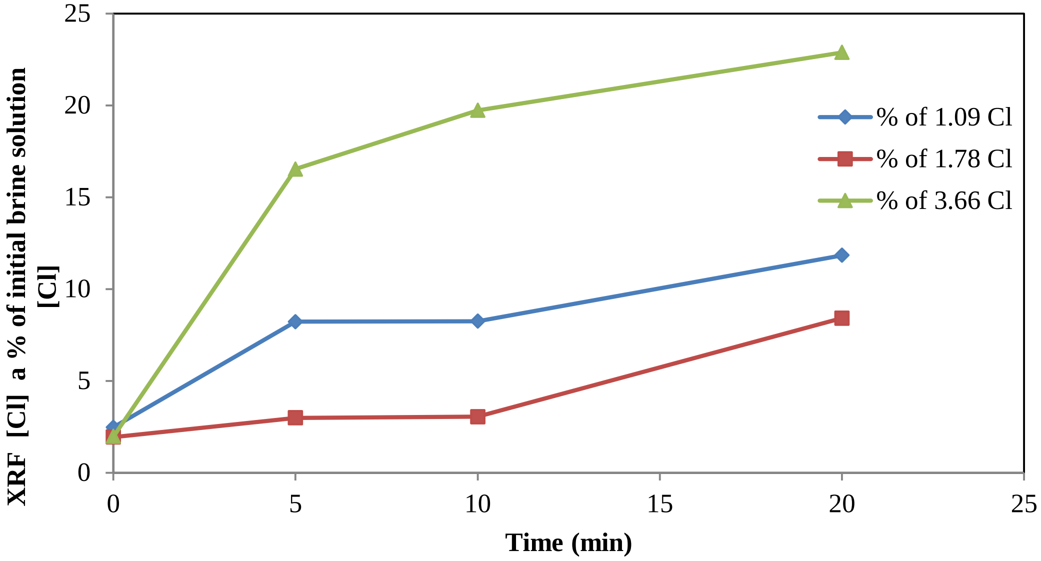

Figure A.11: XRF reading at five minute intervals of extraction time, as a percentage of the initial, applied chloride concentration

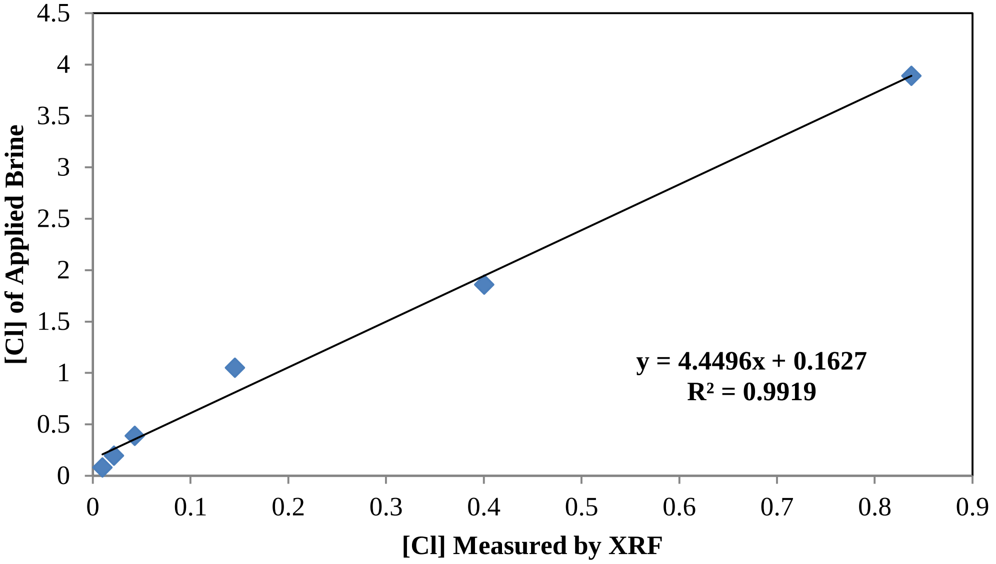

Figure A.12: Linear correlation between the chloride concentration of the applied brine and the measured concentration after 20 minutes of extraction time